ALKYLATION REACTIONS OF AROMATIC COMPOUNDS OVER ALKALINE MOLECULAR SIEVES AND ALKALINE SILICA

A THESIS

submitted to the

UNIVERSITY OF PUNE

for the degree of

DOCTOR OF PHILOSOPHY

in

CHEMISTRY

By

RAJARAM BAL

CATALYSIS DIVISION

NATIONAL CHEMICAL LABORATORY

PUNE - 411 008, INDIA

MAY 2001

DEDICATED TO MY PARENTS

CERTIFICATE

This is to certify that the work incorporated in the thesis, **"Alkylation Reactions of Aromatic Compounds over Alkaline Molecular Sieves and Alkaline Silica"** submitted by **Mr. Rajaram Bal,** for the Degree of ***Doctor of Philosophy,*** was carried out by the candidate under my supervision in the Catalysis Division, National Chemical Laboratory, Pune, INDIA. Such material as has been obtained from other sources has been duly acknowledged in the thesis.

Dr. S. Sivasanker

Research Guide

ACKNOWLEDGMENTS

I am most grateful to my research supervisor, Dr. S. Sivasanker, for his help support and advice through out the course of this investigation. I am expressing my reverence towards him and my sincere regards for him forever.

I am grateful to Dr. A.V. Ramaswamy, Head, Catalysis Division for his encouragement and discussions.

I am also deeply indebted to Dr. D. Srinivas and Dr. S.G. Hegde for their stimulating discussions and constant personal help they rendered throughout the course of investigation.

I wish to express my thanks to Dr. (Mrs.) A.J. Chandwadkar, Dr. B.S. Rao, Dr. C. Gopinath, Ms. M.S. Agashe, Ms. N.E. Jacob, Dr. (Mrs.) A. A. Belhekar, Dr. H.S. Soni, Dr. S.P. Mirajkar, Dr. C.V.V. Satyanarayana, Dr. Rajmohanan, Dr. (Mrs.) V. Ramaswamy, Dr. R. Vetrivel, Dr. (Mrs.) S.V. Awate, Dr. K.J. Waghamare and all other scientific and nonscientific staff in the Catalysis Division, NCL, for their help and cooperation given to me in completing my research work successfully.

I would like to thank my friends Karuna, Tapanda, Mantri, Babu, Subho, Bikash, Pradip, Madhab, Anil, Bivas, Tarasankar, Tapasda, Sumanda, Amiya, Annyt, Chitto, Bennur, Balu, Suresh, Sindhu, Anilda, Priyada, Laha, Dinu, Aditya, Koushik, Mannada and boudi, Manasda, Subarnada, Lahada, Majida, Hazra, Tarun, Sumit, Sarada, Vasu, Abhimunya, Venkat, Suhas, Anand, Shiju, Thomas, Pai, Biju, Sridevi, Sabde, Gore sir and my innumerous friends for their wholehearted help and discussion.

It gives me great pleasure to thank my parents, uncle and aunty, sisters, Madhuri, Manasi, Tapasi, Atasi, my brother in law, Santanuda, my brother Rahul for their love, unfailing support, tremendous patience, trust and encouragement that they have shown to me.

I take this opportunity also to extend my heartfelt thanks to my beloved Arpita. This work would never have received the present shape had it not been backed by her constant encouragement and patience.

Finally, my thanks are due to the Council of Scientific & Industrial Research, New Delhi, for my fellowship award and to Dr. P. Ratnasamy, Director, National Chemical Laboratory, for permitting me to carry out my research work at NCL.

RAJARAM BAL

CONTENTS

CHAPTER - I

INTRODUCTION

1.1 INTRODUCTION

Both acid-catalyzed and base-catalyzed reactions are initiated by acid-base interactions followed by catalytic cycles. In acid catalyzed reactions, reactants act as bases toward catalysts which act as acids. In base-catalyzed reactions, on the contrary, reactants act as acids toward catalysts which act as bases.

Heterogeneous acid catalysis has attracted much attention primarily because of the large volume applications in petroleum refinery operations such as catalytic cracking. Studies of heterogeneous cracking catalysts undertaken in the 1950s revealed that the essential feature of cracking catalysts is acidity, and generation of acidic sites on solids was extensively investigated. Clays and amorphous silica-alumina were used as cracking catalysts in the beginning followed by crystalline aluminoslicates (zeolites).

In contrast to the extensive studies carried out on heterogeneous acidic catalysts, studies on heterogeneous basic catalysts have been far too limited. Pines et al. [1] first reported that sodium metal dispersed on alumina acted as an effective catalyst for double bond migration of alkenes. During the 1970s, Kokes et al. [2,3] reported that hydrogen molecule is adsorbed on zinc oxide by acid-base interactions to form proton (H^+) and hydride (H^-) on the surface. In the same period, Hattori et al. [4] reported that calcium oxide and magnesium oxide were very active in 1-butene isomerization and they recognized this as a base catalyzed reaction. The

catalytic activities of basic zeolites were also reported in early 1970s by Yashima et al. [5].

In addition to the above-mentioned catalysts, a number of materials have been reported to act as heterogeneous basic catalysts. Different types of heterogeneous basic catalysts [6] are listed in Table 1.

Table 1. Types of heterogeneous basic catalysts

Heterogeneous basic catalyst	Examples
1. Single component metal oxides	Alkaline earth oxides,
	Alkali metal oxides,
	Rare earth oxides
	ThO_2, ZrO_2, ZnO, TiO_2
2. Zeolites	Alkali ion-exchanged zeolites,
	Alkali ion-added zeolites
3. Supported alkali metal ions	Alkali metal ions on alumina,
	Alkali metal ions on silica
	Alkali metal on alkaline earth oxides
	Alkali metals and alkali metal hydroxides on alumina
4. Clay minerals	Hydrotalcite,
	Chrysolite,
	Sepiolite
5. Non-oxide	KF supported on alumina,

1.2 BASIC ZEOLITES

Zeolites are hydrated, crystalline, microporous aluminosilicates whose structures are made up of TO_4 tetrahedra (T = tetrahedral atom, e.g. Si, Al), each apical oxygen is shared with an adjacent tetrahedron. The crystallographic unit cell of a zeolite may be represented by the general formula [7]:

$$M_{x/n} [(AlO_2)_x (SiO_2)_y] zH_2O.$$

The net negative charge of the framework is the same as the number of aluminium atoms and is balanced by exchangeable charge compensating cations M of valence n; z is the number of water molecules and x + y represents the total number of tetrahedra present in a unit cell of zeolite. All zeolites have large internal surface areas available for adsorption due to channels or pores, which uniformly penetrate the entire volume of the solid. The external surface of the adsorbant particles contributes to only a small amount of the total available suface area.

Due to the presence of Al in the framework structure, a negative charge is generated. Again, in principle, if the framework Si were to be replaced by a higher valent ion like V^{5+} or P^{5+}, a positive charge should be generated in the framework. The presence of the positive or negative charge determines the acidobasic character of the zeolite. In fact, two main features characterize the acidobasic properties: a purely structural feature resulting from specific connection of TO_4 tetrahedra and a physicochemical feature arising from the chemical composition. It will be seen that

both features may govern the acidobasic characteristics of zeolites. The first feature is linked to the geometry (bond angels, bond lengths, spatial distribution of charges) and the second one to physicochemical properties such as electronegativity, polarizing power of ions, ionicity etc.

Basic properties of zeolites have been investigated mainly in the case of the Si-Al system [8]. The oxygen atom in the Si-O-Al species bears a negative charge, which may generate a basic character. Basicity may also originate from other sites through hydrolysis of metal ions, exchanged oxide clusters, supported metals, or reducing centers. It may also be associated with acidity in acid-base pairs.

The basicity of zeolites may arise from

1. Bronsted sites associated with hydrolysis of metal ions
2. Structural basicity
3. Clusters of oxides and hydroxides
4. Ionic and metal alkali clusters

1.2.1 Bronsted sites

The negatively charged lattice of Si-Al zeolites does not reveal the existance of basic OH^- groups. The OH^- groups reported are linked to extraframework species. For instance, Mg^{2+} or Ce^{3+} in faujasite cages have been shown to generate basicity through hydrolysis [9,10]. They give -OH infrared bands at 3685 cm^{-1} (MgY) and 3675 cm^{-1} (CeY), originating [11] from the reaction:

$$M^{2+} (H_2O) \rightarrow M^{2+} OH^- + H^+.$$

1.2.2 Structural basicity

The framework oxygen bearing the negative charge of the lattice is the structural basic site. In most structures all the oxygen atoms are accessible to adsorbates (faujasite). In less open structures, some oxygen atoms belong to cages, which are too small to be accessed (LTL, mordenite). It follows that only a part of all the existing basic oxygens will interact with adsorbates or be active in these zeolites. Another characteristic of the oxygen sites is that they are fixed between two T atoms. In other words, unlike the protons in acidic zeolites, the oxygen sites are not mobile. While the H^+ ions can move to the reactants, the molecules have to approach the lattice oxygen in a configuration that is favourable for the formation of a reaction intermediate.

The chemical composition of the zeolite and its structure type affect the oxygen basicity. In Si-Al zeolites, the most highly negatively charged oxygen belongs to the AlO_4 tetrahedron [12]. This selects which oxygen sites, among all the existing oxygens of the lattice (i.e. Si-O-Si) are basic. The charge on oxygen, expressing the basic strength, can be calculated theoretically [13,14]. Another factor influencing the oxygen charge is the TOT bond angle. The electronic charge on oxygen (basic strength) increases as the TOT angles are smaller and the TO distances are longer [15,16].

1.2.3 Clusters of oxides or hydroxides

Small oxide particles can be encapsulated in zeolite cages [9,10, 16-21]. Some oxide materials are known as basic catalysts (MgO, CaO, ZnO) [22]. Dispersed in zeolite cages they may form small oxide clusters with basic properties.

Clusters of MgO and M_2O (M = Na, K, Rb and Cs) are prepared in Y and X zeolites by soaking them in solutions of magnesium dimethoxide (alcoholic solutions) or alkali acetates (aqueous solutions) [21]. Strong basic sites are obtained in the Mg case only if the ensamble (Mg and O) forms a MgO lattice, while isolated M_2O species produce strong basicity in the case of the alkali metal oxides [21]. Two general trends are observed in the properties of these materials. Firstly, exchanged zeolites are less basic than those contain additional clusters of oxides. Secondly, carbonates are formed very easily from these oxides with atmospheric CO_2.

1.2.4 Ionic and metal alkali clusters

Interaction of alkali metal vapours with zeolites generates colored products, which often possess basic properties. It was first reported that Na_6^{5+} and Na_4^{3+} paramagnetic centers were formed in alkali X and Y zeolites [23]. In the field of zeolites, the dependence of selectivity in the alkylation of toluene with methanol upon the acidic and non-acidic character of the solid was first mentioned by Sidirenko et al. [24]. This was further studied in detail, and the formation of ethylbenzene and styrene was linked to basic sites in X and Y exchanged with K, Rb and Cs cations. The production of xylenes was related to the acidic character of Li- and Na-zeolites [25]. Hathaway and Davis [26-29] prepared catalysts by impregnation of Na-Cs-X and Cs-Na-Y with cesium acetate followed by thermal decomposition of the acetate into oxide and showed that they act as base catalysts.

Alkaline molecular sieves may be formed by hydroxides or oxides, not only in basic or neutral Si-Al zeolites [7,9,10,16-21, 30-40], but also in mesoporous molecular sieves. While Na-MCM-41 and Cs-MCM-41 (prepared by ion exchange)

are active in the base catalyzed Knovenagel condensation, cesium acetate impregnated MCM-41 is active in Michael addition and appears to be a promising super base catalyst [41]. More generally, one may expect that the chemistry of highly dispersed basic oxides in various porous supports (neutral and basic) will open an expanding field for the generation of tailor made basic catalysts. Both the support and the dispersed oxide may gain new properties. For instance, the impregnation with Cs acetate of previously exchanged Cs-Na-X and Cs-Na-Y generates occluded species, which are more strongly basic when located in Cs-Na-Y [42]. Simultaneously, modified Cs-Na-X zeolites are more thermally stable than modified Cs-Na-Y. Binary, cesium-lanthanum oxide supported MCM-41 is also a very stable heterogeneous catalyst [43]. Tsuji et al. [44] followed the synthesis procedure of Hathaway and Davis and carried out the isomerization of 1-butene over a series of MX (M^+ exchanged X zeolite; M = alkali metal) and M^+ impregnated MX. At 273K, all the ion exchanged zeolites (MX) showed practically no activity, while M^+ loaded MX showed considerable activity. A Cs loaded Cs-X sample showed the highest activity (1.4×10^{-4} mole / g /min). The authors claimed that these materials are solid super bases. The various evidences including ^{133}Cs NMR and temperature programmed desorption (TPD) of carbon dioxide indicate that the active species is nanophase cesium oxide occluded in the supercage of the zeolites [45,46].

1.3 SUPPORTED ALKALI METAL IONS ON SILICA

The oxides of the first group metals (Li, Na, K, Rb and CS) are bases. The oxides of rubidium and cesium have been reported to be super bases, possessing base strengths with a Hammett basicity function (H_) exceeding +26 [47]. Therefore, it is believed that supported oxides of these alkalies also exhibit strong basicity [48]. Sodium was one of the first solid base catalysts studied and was used for the isomerization of olefins [1]. More recently, an aluminium supported sodium catalyst was prepared by treatment of γ- alumina with NaOH and Na metal to give a superbasic solid with H_ > 37 [49]. Other super basic catalysts have been synthesized by supporting one or more alkali elements on basic supports like MgO and CaO [50,51]. Unlike solid superacids, very little work has been done to investigate solid superbases, despite their potential use in many industrial applications as heterogeneous base catalysts [6].

1.4 CHARACTERIZATION OF BASIC SURFACES

The surface properties of heterogeneous basic catalysts have been studied by various methods by which the existence of basic sites has been realized. Different characterization methods give different information about the surface properties. All the properties of the basic sites cannot be measured by any single method. Integration of the results obtained by different characterization methods leads us to understand the structures, reactivities, strengths and amount of the basic sites on the surfaces. These methods are briefly described below:

1.4.1 Indicator method

The strength of the surface sites are expressed by an acidity function (H_) proposed by Paul and Long [52]. The H_ function is defined by the following equation [52, 53]

$$H_ = pK_{BH} + \log [B^-] / [BH]$$

Where [BH] and $[B^-]$ are, respectively, the concentration of the indicator BH and its conjugate base, and pK_{BH} is the logarithm of the dissociation constant of BH. The reaction of the indicator BH with the basic site (B) is

$$BH + B = B^- + BH^+$$

The amount of basic sites of different strengths can be measured by titration with benzoic acid. A sample is suspended in a nonpolar solvent and an indicator is adsorbed on the sample in its conjugated base form. The benzoic acid titer is a measure of the amount of basic sites having a base strength corresponding to the pK_{BH} value of the indicator used.

1.4.2 Temperature programmed desorption (TPD) of carbon dioxide

This method is frequently used to measure the number and strength of basic sites. The strength and amount of basic sites are reflected in the desorption temperature and the peak area, respectively, in a TPD plot. However it is difficult to express the strength in a definite scale and to count the number of sites quantitatively. Relative strengths and relative numbers of basic sites on the different catalysts can be estimated by carrying out the TPD experiments under the same conditions [54].

1.4.3 UV-absorption and luminescence spectroscopies

UV absorption and luminescence spectroscopies give information about the coordination states of the surface sites [55,56]. Luminescence corresponds to the reverse process of UV absorption, and the shape of the luminescence spectrum varies with the excitation light frequency and with the adsorption of the molecules. Emission sites and excitation sites are not necessarily the same. Excitons move on the surface and emit at the ion pair of low coordination numbers where emission efficiency is high. This method is very useful mainly for oxides.

1.4.4. Temperatured programme desorption (TPD) of hydrogen

This method gives information about the co-ordination state of the surface ion pairs when combined with other methods such as UV absorption and luminescence spectroscopies. The number of each ion pair could be counted if TPD is accurately measured with proper calibration. This method has been applied to the MgO surface [57,58].

1.4.5. X-ray photoelectron spectroscopy (XPS)

The XPS binding energy (BE) of oxygen reflects the basic strength of the oxygen. As the O1S BE decreases, electron pair donation becomes stronger. Okamoto et al. [59] studied the effects of zeolite composition and the type of cation on the BE of the constituent elements for X- and Y-zeolites ion-exchanged with a series of alkali cations as well as H-forms of A, X, Y, and mordenite. The O1S BE of a zeolite is directly delineated to the electron density of the framework oxygen. On the basis of XPS features of zeolites, Okamoto et al. [59] also proposed a bonding model of a zeolite as shown in Fig. 1. Configurations I and II are in resonance. In configuration I, extra framework cations form covalent bonds with

framework oxygens, while in configuration II, the cations form fully ionic bondings with the negatively charged zeolite lattice. As the electronegetivity of the cations increases and approaches that of oxygen, the contribution of configuration I increases to reduce the net charge of the lattice. This explains the dependances of O1S BE on the electronegativity of the cation. XPS measurement of a probe molecule (pyrrole) adsorbed on the basic sites gives information about the strength of the basic sites [60].

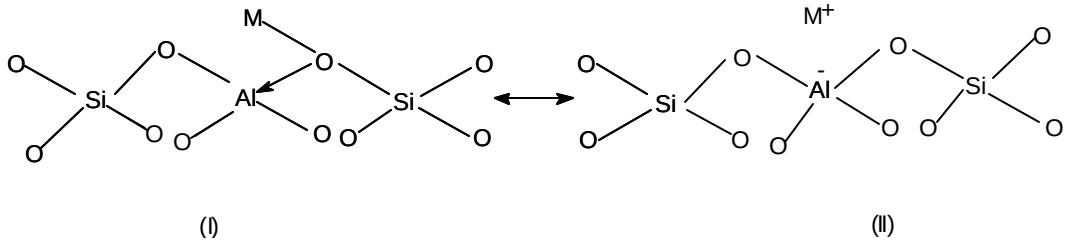

Fig. 1. Schematic bonding model of a zeolite.

1.4.6 IR of adsorbed carbon dioxide

This method gives information about the adsorbed state of CO_2 on the surface. Carbon dioxide interacts strongly with a basic site and, therefore, the surface structure including basic sites is estimated from the adsorbed state of CO_2. Carbon dioxide is adsorbed on heterogeneous basic catalysts in different forms: unidentate, bidentate, bicarbonate etc.

Recently Davis et al. [61] studied the interactions of CO_2 on Rb supported on MgO, TiO_2, Al_2O_3 and SiO_2 by IR spectroscopy. They reported that the strongest basic sites formed by the incorporation of Rb were found on Rb/MgO, which

contain significant carbonate species even after heating to 773K. Carbonates were not present on the other heat-treated Rb catalysts. The least basic support, silica, is thought to react with Rb to form a highly disordered, weakly basic surface silicate. Auroux et al. [62] have studied the acidobasic properties of various oxides. According to them CO_2 molecules can be adsorbed on positive and negative surfaces. The adsorbed CO_2 (carbonates) may then block the surface sites. The different ways CO_2 adsorption occurs on the surface of oxides can be summarized:

a) adsorption on the hydroxyl group with formation of a superficial hydroxycarbonyl ion (Fig. 2(I));
b) adsorption on the metal cation and dissociation of the resulting species (Fig. 2(II));
c) adsorption on the metal ion and the neighbouring oxygen ion and formation of a bidentate carbonate group (Fig. 2(III));
d) adsorption on the oxygen vacancy and formation of a superficial carbonyl group (Fig. 2(IV));
e) adsorption on the metal ions with participation of oxygen in excess and formation of a carbonate (Fig. 2(V) or 2(VI) or 2(VII)).

According to Knozinger et al. [63] the structures of monodentate and bidentate species on metal and oxide surfaces may be Fig. 2(VIII) and Fig. 2(IX), respectively.

1.4.7 IR of pyrrole

Pyrrole has been used as a probe molecule for measurement of strength of basic sites [64]. The IR band ascribed to the N-H stretching vibration shifts to a

lower wave number on interaction of the H atom in pyrrole with a basic site. Barthomeuf measured the shifts of N-H vibration of pyrrole adsorbed on alkali ion exchanged zeolites [65, 66]. The results are given in Table 2. The shift increases when the negative charge on the oxide ion increases.

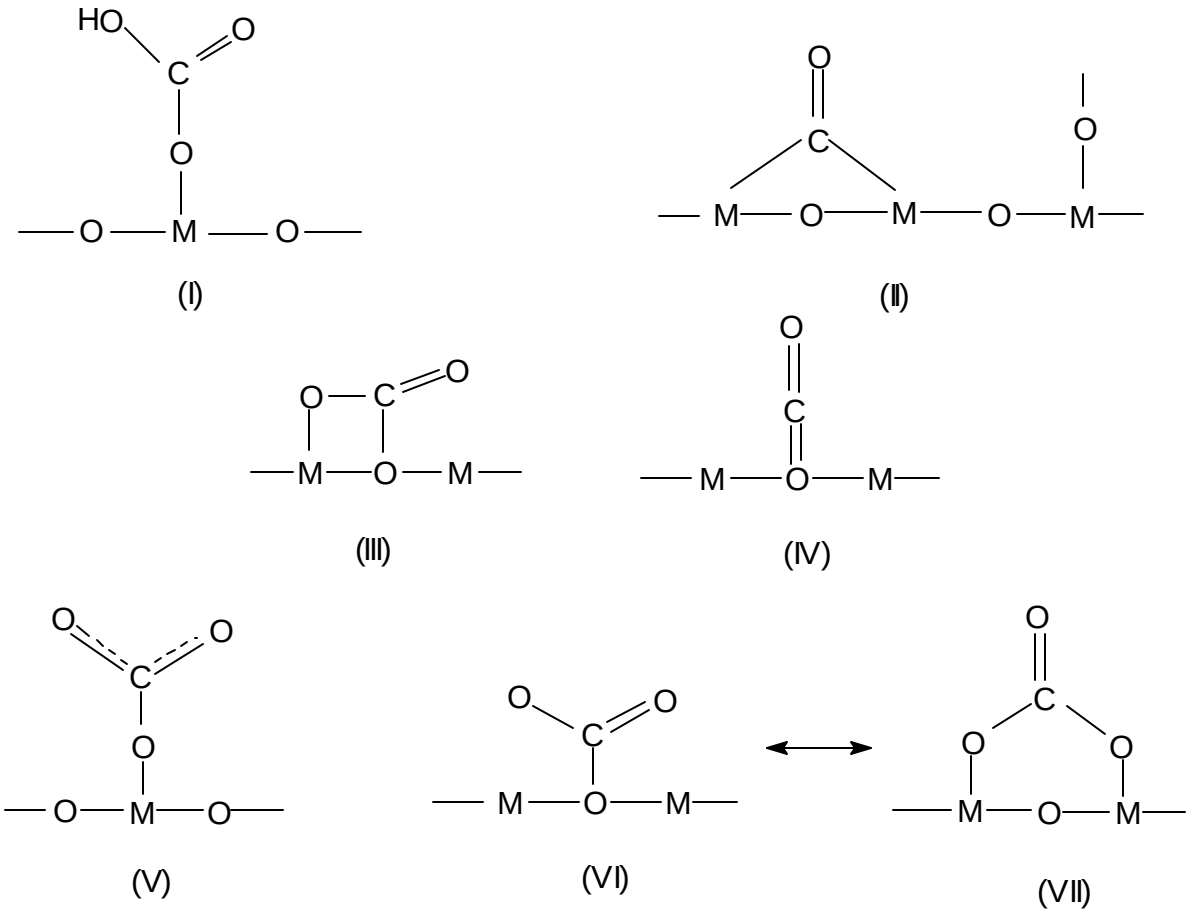

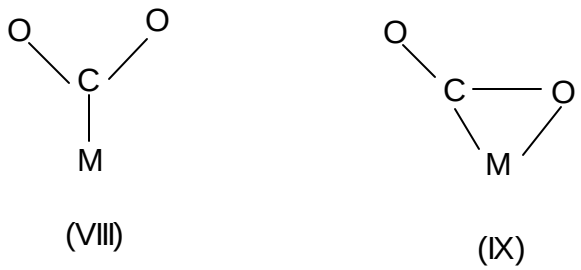

Fig. 2. Adsorbed CO_2 specie on metal oxides and metals

The negative charge is associated closely with the strength of the basic site. The basic strengths of alkali ion exchanged zeolites are in the order: CsX > NaX > KY > NaY, KL, Na-mordenite, Na-beta.

Table 2. Shifts of N-H vibration of pyrrole adsorbed on zeolites

Zeolite	$\Delta\nu_{NH}$[a]
CsX	240
NaY	180
KY	70
NaY	30 – 40
KL	30
Na-mordenire	30
Na-beta	30
Cs-ZSM-5	0
Na-ZSM-5	0

a Shift of N-H from the liquid.

1.5 ALKYLATION REACTION

Alkylation is a major and industrially important process used widely in the synthesis of low and high volume chemicals. Petrochemical industry is a major beneficiary of this class of reactions where a number of alkyl hydrocarbons are synthesized by alkylation reactions. The conventional catalysts used in these reactions are $AlCl_3$, HF, H_2SO_4 and BF_3 though solid acids like zeolites have also

found some recent applications. Many are batch processes using $AlCl_3$ as a soluble acid catalyst. $AlCl_3$ is inexpensive, very reactive and is one of the powerful Lewis acids. $AlCl_3$ and similar metal halides are difficult to handle and get readily hydrolyzed. Very often such catalysts are required in stoichiometric quantities. A large inventory of these materials poses health, safety and storage problems. Furthermore, the traditional route of liquid phase alkylation using mineral acids and $AlCl_3$ suffer from the disadvantages of high capital cost, reactor corrosion, formation of byproducts and difficulty in catalyst regeneration. In recent times, scientists worldwide have been devoting their attention to the development of environmentally friendly catalysts for the production of industrially important chemicals and chemical intermediates.

The use of safe solid catalysts (acidic and basic) in place of traditional acid and base catalysts is becoming very important. Several alkylation reactions of aromatic hydrocarbons have been tried out over oxides, mixed oxides, supported oxides and zeolites. Alkylation is a substitution reaction, where a hydrogen atom is replaced by an alkyl (methyl, ethyl, propyl etc) group. Friedel-Craft alkylation takes place over acidic catalysts. This is an electrophilic substitution reaction; the electrophile is the carbonium ion formed from the alkylating agent, *viz.*,olefins, alcohols, or alkyl halide with the help of acid sites on the catalyst surface. Solid acids, which possess Lewis or Bronsted acid sites function successfully as alkylation catalysts.

1.6 SIDE CHAIN C-ALKYLATION

In general, alkylation of aromatics occurs at a ring position over an acidic catalyst, while side chain aklylation takes place over a basic catalyst. Chemical industry, because of economic considerations, presently favours toluene over benzene as the starting material for many processess [67]. Side chain alkylation is now regarded as one of the synthetic methods for the conversion of methyl groups into vinyl and /or ethyl groups. Side chain alkylation of toluene with methanol results in styrene and/or ethylbenzene. In the production of styrene, this process offers the advantage of lower raw material cost compared to the traditional Friedel-Craft alkylation of benzene and further dehydrogenation.

Side chain alkylation of toluene proceeds on catalysts with basic properties such as basic oxides [68] as well as X and Y zeolites exchanged with alkali cations [24,25]. Alkylation of toluene with methanol over zeolite catalysts [69] can produce ethylbenzene, styrene, and/or xylenes depending upon the acidity of the catalyst and the pore size of the molecular sieves. Medium pore acidic zeolites, e.g. H-ZSM-5, favour ring alkylation [70-72], while large pore basic zeolites e.g. KX favour side chain alkylation [24,25,73]. Over zeolites exchanged with alkali cations, the selectivity for side chain alkylation against benzene ring alkylation increases with the size of the alkali cation (Li < Na < K < Rb < Cs) [24,25,74,75]. Sidorenko et al. [74] suggested that during the side chain alkylation of toluene with methanol, styrene is formed by the reaction of toluene and formaldehyde produced by the dehydrogenation of methanol. Also, some styrene is hydrogenated to ethyl benzene with H_2 produced in methanol dehydrogenation.

Anderson et al. [76] investigated the side chain alkylation of toluene with methanol by solid state ^{13}C NMR aver zeolite-X and concluded that methyl carbocation can be found during the formation of the surface formates. They also reported that CsX plays a crucial role gettering these highly reactive carbocation by binding them as surface bound methyl group. Selectivity for styrene formation can be improved directly by increasing the desired dehydrogenation of methanol. According to Sefick [75] and Unland [77] this can be achieved by post exchange treatment of Cs-X zeolite with borates. This treatment leads to a higher styrene/ethylbenzene ratio by reducing the number or the strength of the excess basic sites of the catalysts. According to Itoh et al. [78] both basic and weak acid sites on the zeolite are required for side chain alkylation. They also reported that slightly stronger acid sites in Rb-X were produced by [78,79] introducing a small amount of Li^+ ions. This hindered the undesired decomposition of formaldehyde formed from methanol. An opposite effect, an increase in ethylbenzene/styrene ratio, was obtained on CsX, CsY, and β-X zeolite catalysts by having Cu and Ag promoters [80]. On the promoted catalysts, the yield of the side chain alkylates increased on using hydrogen as a carrier gas.

On the basis of Laser Raman [81] and diffuse reflectance [82] measurements, Unland and Freeman concluded that reaction selectivity was influenced by the electrostatic field experienced by the aromatic nucleus. This interaction, primarily through perturbation of the π-electrons, increased with loading level in a particular zeolite with increasing cationic size. Infrared studies [83] of the decomposition of methanol and formaldehyde on Na, K, Rb and Cs

forms of X type zeolites have shown that methoxide, carbonate and formate species are formed in varying amounts and types on the different samples. Quantum mechanical calculations [79] have shown that the presence of basic sites is important to the mechanism of side chain alkylation.

The currently accepted reaction scheme [24,79,84] for side chain alkylation is as follows:

1. dehydrogenation of methanol to formaldehyde,

2. attack of formaldehyde at the methyl group of toluene to form styrene and

3. hydrogenation of styrene to ethylbenzene by H_2 produced during the methanol dehydrogenation.

$$CH_3OH \rightarrow HCHO + H_2$$

$$C_6H_5CH_3 + HCHO \rightarrow C_6H_5CH{=}CH_2 + H_2O$$

$$C_6H_5CH{=}CH_2 + H_2 \rightarrow C_6H_5CH_2CH_3$$

Over all reaction: $C_6H_5CH_3 + CH_3OH \rightarrow C_6H_5CH_2CH_3 + H_2O$

In *situ* infrared study of toluene methylation with methanol on alkali exchanged zeolites [85] reveals the actual structures of the surface species and their function in the alkylation process. Side chain alkylation of toluene with isopropanol and methanol over alkali (Li, Na, K and Cs) exchanged zeolites (X, β and ZSM-5) was reported by Vasanthy et al. [86]. Over Li exchange zeolites, isopropylation takes place exclusively at the nucleus, producing cymenes while methylation gives xylenes and ethylbenzene, the former being the major product. According to them

the side chain alkylation of toluene is a cooperative action of both acidic and basic sites.

Huang et al. [87] reported the side chain alkylation of ethylbenzene with methanol over alkali exchanged X type zeolites to yield isopropylbenzene as the major product. They reported that with KX (at 773K) alkylation and dealkylation proceeded respectively via carbanion and carbonium ion mechanisms, whereas dehydrogenation and demethylation occurred via free radical mechanisms.

1.7 ALKYLATION OF PHENOL

Alkylation of phenol is another important industrial reaction that has been studied in detail. O-alkylated products (aryl alkyl ethers) of which anisole is the simplest member, are important industrial chemicals and are extensively used as starting materials for the production of dyes and agrochemicals, as antioxidants for oils and grease and as stabilizers for plastics. The O-alkylation of phenol yielding anisole is a reaction of potential interest in the upgrading of phenolic compounds derived from lignin. It has been shown that methyl aryl ethers (MAE) are good organic octane improves. Long range tests have shown that MAE blended at 5 volume percent with commercial gasoline is a superior fuel not only in terms of octane quality but also in terms of fuel economy, performance and engine durability [88].

Conventionally, these can be obtained by Williamson ether synthesis, which requires a methyl halide and a stoichiometric amount of sodium hydroxide. They can also be synthesized with phenol and methyl halide in the presence of sodium

hydride in tetrahydrofuran at room temperature [89, 90]. In these methods, the toxic and corrosive properties of the halides or the sulphates cause problems. Therefore, special care is necessary in handling them. Besides, expensive materials may be needed for the reactors and tedious procedures are required for the disposal of the waste material.

The O-alkyation of phenol over zeolites was first reported by Balsama et al. [89] over various X, Y and ZSM-5 zeolites. After that, many research groups have carried out the alkylation over ZSM-5 [91-94], $AlPO_4$ and SAPO [95] molecular sieves. SAPO catalyzes only the formation of anisole, whereas on other molecular sieves, cresols and anisoles are simultaneously produced. Over SAPO and $AlPO_4$ molecular sieves, cracking products are also observed. The selectivities are generally determined by the Bronsted acidity of the molecular sieves and factors such as pore size and geometry. Various oxides and supported oxides [96] yield mainly 2,6-xylenol as the major product. Catalysts like γ-Al_2O_3, Nafion-H, silica-alumina and phosphoric acid have also been tested for this reaction [97]. While γ-Al_2O_3 contains strong Lewis acid sites, Nafion -H contains strong Bronsted acid sites and silica-alumina contains both Bronsted and Lewis acid sites of medium and weak strengths. On the basis of this, different mechanisms have been proposed for the formation of the product. For example, over Nafion-H, the two types of mechanisms proposed are: a) A dual site mechanism in which an acid site is strongly bound to the oxygen of methanol (or of alkylating agents) to form a alkylcarbocation, while another acid site directly interacts with the aromatic ring

b) A Rideal mechanism according to which the reaction occurs between the molecules of the adsorbed alkylating agent and the aromatic nucleus from the vapour phase. This mechanism does not exclude the possibility of horizontal adsorption of aromatic nucleus on the acid sites which is responsible for coke formation.

Mn_3O_4 is a good catalyst for phenol alkylation [98] in the vapour phase in a fixed bed reactor. Oxide catalysts are more selective for the synthesis of 2,6-xylenol than zeolites, because of absence of pore constraints. It is also suggested that the presence of basic sites on the oxide surface enables phenol alkylation to proceed on a pair of acid and base sites. Ono et al. [99] reported the selective O-methylation of phenol with dimethylcarbonate (DMC) over X-zeolites. A 76% yield of anisole was obtained with 93% selectivity over Na-X at 553 K. The mechanism proposed by them for anisole formation (base catalyzed scheme) may be expressed as follows:

$$PhOH + BZ \Rightarrow PhO^- + H^+BZ^-$$

$$PhO^- + DMC \Rightarrow PhOCH_3 + CO_2 + CH_3O^-$$

$$CH_3O^- + H^+BZ^- \Rightarrow CH_3OH + BZ$$

Here, BZ denotes a basic site on the zeolite surface. The basic site interacts with phenol molecules to form PhO^- ions, which in turn react with DMC molecules to generate CH_3O^- ions. The CH_3O^- ions react with protons to produce methanol and to regenerate the basic sites.

Samolada et al. [100] reported the selective O-methylation of phenol over sulphates supported on γ-Al_2O_3. Potassium (3wt%) in the form of K_2SO_4

supported on γ-Al_2O_3 was found to be the most promising catalyst. The reaction temperature and the potassium content of the catalyst were found to be the most important factors affecting the selectivity towards the O-alkylation of phenol. An empirical equation expressing the reactor output as a function of the reaction temperature and the potassium content of the catalyst, within the range of the parameters considered, has been proposed. A catalyst prepared with γ-Al_2O_3, K_2SO_4 and $KAl(SO_4)_2$ (with a potassium content of 3 wt%) and characterized by a low acidity (22×10^{-4} mmole/ m^2) was found to be suitable for the successful production of methyl aryl ethers. Its optimum performance, marked by MAE selectivity of 98% and phenol conversion of 65 wt%, remained constant over a wide temperature range (563 K - 603 K). The impregnation of γ-Al_2O_3 with potassium sulphate results in the appearance of acid sites of medium strength ($+1.5 < H_0 \leq 4.8$), the presence of which is essential for the O-alkylation of phenol. Xu et al. studied [101] the O-alkylation of phenol with methanol on H-beta zeolite.

Bentel et al. [102] reported the spectroscopic and kinetic study of the alkylation of phenol with dimethyl carbonate over NaX zeolite. They concluded that at room temperature, phenol is preferentially adsorbed by hydrogen bonding to basic oxygen atoms of NaX. Moreover phenol is partially deprotonated over the basic site to form zeolitic hydroxyl groups and phenolate ions ligated to Na^+ ions (NaOPh). The zeolitic hydroxyl group formed is likely to interact with the π- electron system of phenolate ions and are able to form surface ether, O_zPh, with phenol. DMC forms two types of surface complexes with Na^+ ions at room

temperature; a chelating complex via the two carbonyl oxygen atoms and a monodentate complex via a single carbonyl oxygen atom. The chelating complex reacts with Na----O_z acid-base sites to form dimethyl ether and CO_2. The decomposition of DMC proceeds stepwise via formation of monomethyl carbonate, Na bonded methoxy groups, $NaOCH_3$, and lattice oxygen bonded methyl groups, O_xCH_3.

Phenol inhibits the formation of chelating DMC, thus retarding the decomposition of DMC. The formation of anisole proceeds presumably via nucleophilic attack at the methyl carbon of DMC by the oxygen of phenol. This reaction supposedly takes place on a Na----O_z acid base site, where DMC is activated on a Lewis acid site by its carbonyl oxygen and phenol on an adjacent Lewis base site by H-bonding. This reaction sets in at *ca*. 423 K and yields anisole, H-bonded methanol and CO_2. Bautista et al. [103] reported the alkylation of phenol with DMC over $AlPO_4$, Al_2O_3 and $AlPO_4$-Al_2O_3 catalysts. According to them, at low reaction temperatures anisole was formed and as the reaction temperature was increased, cresols and methyl and dimethyl anisoles were increasingly produced. Moreover, Al_2O_3 showed low activity while basic oxides (MgO and ZnO) showed negligible activity because these oxides are easily poisoned by carbon dioxide. They suggest the participation of combined acidic and basic sites for the alkylation of phenol with DMC over $AlPO_4$-Al_2O_3 catalysts.

Lee et al. [104] reported the O-alkylation of phenol derivatives over basic zeolites. The substrates selected were phenol, 4-nitrophenol, 4-aminophenol and

4-chlorophenol. The activity of the catalyst increased with basicity of the loaded metal and there was no difference in catalytic activity between ion exchanged Cs^+ and Cs oxide particles. The high selectivity to anisole over basic Cs-ion exchanged zeolite was no more a function of conversion.

Ono et al. [105-107] reported the selective O-alkylation of catechol over alumina, alkali hydroxide loaded alumina and potassium nitrate loaded alumina. Over alumina, DMC is a much more efficient methylating agent than methanol in the methylation of catechol. The main product was guaiacol, the selectivity for it being *ca*. 70%. Addition of water to the feed considerably increased the catalytic activity and the yield of guaiacol. Over alumina loaded with alkali hydroxide, catechol was converted only to guaiacol. $LiOH/Al_2O_3$ was found to be a selective catalyst for the O-methylation of catechol with DMC to yield guaiacol. A guaiacol yield of 84% was obtained at a catechol conversion of 100% at 583 K. Over alumina loaded with potassium nitrate, catechol gave selectively veratrole with dimethylcarbonate. KNO_3/Al_2O_3 showed a very high catalytic activity and selectivity for the O-methylation of catechol to give veratrole [99]. A veratrole yield of 97% was obtained at a catechol conversion of 99% at 583 K with DMC/catechol ratio of 4. Catechol yielded guaiacol and catechol carbonate. The further reaction of these primary products with DMC resulted in the formation of veratrole.

1.8 ALKYLATION OF ANILINE

Aniline alkylation is an industrially important reaction due to the fact that many valuable bulk intermediates and fine chemicals can be prepared from alkylanilines. Alkylanilines form the basic raw materials for the synthesis of organic chemicals and chemical intermediates (or additives) in dyes, synthetic rubbers, explosives, herbicides, and pharmaceuticals [108]. However, when common alkylating agents (alkyl halides) are used, the reaction is less useful for synthetic purposes due to poor selectivity for any single alkylated product. The high nucleophilicity of the amine nitrogen results in the formation of mixtures of secondary and tertiary amines along with the corresponding ammonium salt [109]. Dialkyl amines may be prepared directly from corresponding amines by heating the latter with trialkyl phosphates. But this procedure has many disadvantages like environmental problems, waste and need for much precaution during the reaction.

Due to these problems, vapour phase aniline alkylation over environmentally safe solid catalysts is an answer to the conventional method of producing alkylamines using mineral acids and Friedel-Craft type catalysts [110]. The traditional route also presents the disadvantages of high capital cost, reactor corrosion, and formation of byproducts that cannot be recycled. Several types of catalysts based on oxides and supported oxides [111-119], zeolites [120-132] and microporous aluminophosphates [132-134] have been tested for aniline methylation. The main factors influencing activity and selectivity (N- and/or C-alkylation) are acid-base properties (number and strength) and shape selectivity

in the solid acid catalyst as well as reaction conditions (temperature, composition and feed rate). Rao et al. [133] reported the mechanism of aniline alkylation with methanol over $AlPO_4$-5 molecular sieve. They observed that in aniline methylation, N-methylaniline appears to be favoured at low temperatures (less than 598K). This is subsequently converted to N,N-dimethylaniline (NNDMA), which itself isomerises to N-methyl toluidine. As the temperature is increased above 598K, isomerisation occurs in large measure by the carbocation mechanism, as demonstrated by studying the reaction of NNDMA. Ono et al. [135,136] reported the alkylation of aniline with methanol and dimethyl carbonate (DMC) over faujasite X and Y. They showed that faujasite (X and Y) was a better catalyst than ZSM-5, KL and Na-mordenite with regard to activity and selectivity. In particular, at the experimental conditions used (453 K), KY was a very good catalyst giving up to 99.6% conversion with 93.5% N-methylaniline (NMA) selectivity, the other product being mainly N,N-dimethyl aniline (NNDMA). DMC was a better methylating agent than methanol.

Barthomeuf et al. [137,138] studied the selectivity to mono or dialkylation in the reaction of aniline with dimethylcarbonate on alkaline faujasite, EMT and beta zeolites. They concluded that K-EMT was as selective as KY for the formation of NMA from aniline and DMC. EMT zeolite exchanged with K or other cations was also a good catalyst for alkylation of other compounds. Alkaline X-zeolites were the best catalysts for the production of NNDMA. The experimental conditions (space velocity, reactant ratio) could be optimized to improve the performance in the formation of NMA or NNDMA. Park et al.

[128] reported the selective alkylation of aniline with methanol over metallosilicates. According to their observation the selectivity for NNDMA is higher when metallosilicates possess larger amount of medium acid sites (567 - 673 K). Barthomeuf et al. [129,130] also reported the alkylation of aniline with methanol. They investigated changes in selectivity with acidobasicity of faujasite catalysts and also compared the acid base properties of faujasite, and MOR (Na form) in benzene adsorption and alkylation of aniline with methanol. They concluded that the alkylation of aniline by methanol involved the participation of acid (cations) and basic (anions) sites of the faujasites. NNDMA was produced mainly over X-zeolites. The more basic zeolites (X and Y exchanged with K, Rb and Cs) favoured the production of N-alkylated anilines. The zeolites with the more acidic cations, Li and Na, gave rise to C-alkylation. C-alkylation which requires acid sites could be limited by more basic ions, like in KY or RbY. The considerable aging observed in the more basic zeolites might result from an anionic polymerization which poisons the active sites. They also concluded that the most active zeolites are NaX, NaY and NaEMT. This probably was due to both a strong oxygen basicity (NaX, NaY) responsible for formation of N-alkylates and a higher number of accessible Na^+ ions leading to C-alkylation. The most selective zeolites were Na-L and Na-MOR which very likely did not have enough accessible cations i.e. acid sites, for C-alkylation to prevail. The deactivation, suggested to arise from an anionic polymerization involving aniline with methanol, was favoured on zeolites with

acessible basic sites. In addition to the participation of acid (cations) and basic (oxygen) sites, the reaction involved parameters specific to each structure.

Selva et al. [139] reported the monomethylation of primary amines by DMC over X and Y type zeolites. According to them the unusual mono N-alkyl selectivity observed was likely to be due to synergistic effects between the double reactivity of DMC (acting both as a methylating and as a reversible methoxy carboxylating agent) and the dual acid base properties of zeolites along with the steric demand by their cavities. Besides, the high selectivity which allows high purity mono NMA to be prepared, the reaction also has remarkable environmentally benign features: it uses the non toxic DMC, no inorganic wastes are produced and no solvent is required.

Campelo et al. [140-145] reported the N-alkylation of aniline with methanol over $CrPO_4$ and $CrPO_4$-$AlPO_4$ (15-50 wt% $AlPO_4$) catalysts. According to them, N-alkylated products result in selectivity of over 90 mole% throughout the 573-673 K temperature range. Varying the feed rates indicated that low contact time and low temperature promote the N-mono methylation reaction. Moreover, N,N-dimethyltoluidines (p- > o-) are only present in very small quantities at the highest temperatures and/or contact times. On the other hand, the addition of $AlPO_4$ to $CrPO_4$ did not cause any significant change in the selectivity pattern exhibited by the $CrPO_4$ catalyst. This behaviour could indicate that similar adsorbed active species are formed on $CrPO_4$ and $CrPO_4$-$AlPO_4$ catalyst. Furthermore, there is no simple relationship between aniline alkylation activity and surface acidity measured by pyridine and 2,6-dimethylpyridine adsorption at

573 - 673K. They also examined $AlPO_4$, metal oxide (Al_2O_3, TiO_2 and ZrO_2), SAPO-5 and a commercial silica alumina catayst [142]. They found $CrPO_4$, and $CrPO_4$-$AlPO_4$ catalyst to be less active, but more selective for the N-monomethylation process yielding N-methylaniline at similar conversion levels.

Murugesan et al. [143] reported aniline methylation over AFI and AEL type molecular sieves. According to them due to the presence of strong acidic sites, CoAPO-5 and ZAPO-5 gave a considerable amount of N-methyltoluidine (NMT) apart from NMA and NNDMA. Although CoAPO-11 and ZnAPO-11 possessed strong acid sites, these two catalysts did not produce NMT. The reason for the absence of NMT over these two catalysts (CoAPO-11, ZnAPO-11) was attributed to the smaller pore size, which may not be sufficient for the formation of NMT. They concluded that weak acid and moderate acid sites are sufficient for N-alkylation, whereas strong acid sites are mandatory for C-alkylation and the increase of NMT with the simultaneous decrease of NMA over CoAPO-5 and ZnAPO-5 with increase in contact time was due to further C-alkylation of NMA.

Bautista et al. [141] also reported that N-alkylated products (NMA and NNDMA) are formed by the stepwise first order reaction processes. Moreover, strong acid sites were not required for N-methylation of aniline whereas weak to moderate acid sites seem to be responsible for the reaction. Furthermore, there was no catalyst deactivation by coke deposition, whereas the addition of pyridine or dimethyl pyridine deactivated the catalyst. Narayanan et al. [144,145] reported aniline alkylation with ethanol over zeolites and vanadium modified

zeolites prepared by solid state exchange method. According to them, in addition to the acid base properties, geometric effects characteristic of each zeolite govern aniline alkylation. Three dimensional and mildly acidic zeolites (HZSM-5, HY and HY) were more active than widepore unidimensional and strongly acidic H-mordenite. Vanadium addition improved the activity by i) blocking the strong acid sites and ii) by creating V^{4+} species due to vanadium-zeolite interaction, which acted as active sites for alkylation. V^{4+} species may also act as carbonium ioncreating sites, thereby helping aniline alkylation and only weak /moderate acid sites may be required to trigger the reaction. They also reported that template free zeolites (SiO_2 / Al_2O_3 = 28, synthesis duration = 168 h) gave more aniline conversion compared to HZSM-5 synthesized with template. Recently Rao et al. [146,147] studied N-alkylation over $Zn_{1-x}Ni_xFe_2O_4$ (x = 0, 0.2, 0.5, 0.8, 1) types of catalysts and over Zn-Co-Fe ternary spinel system. According to them $Zn_{1-x}Ni_xFe_2O_4$ (x = 0, 0.2, 0.5, 0.8 and 1) can efficiently alkylate aniline to give N-methylaniline selectively (~99%). Even at low concentration of methanol in the feed, these catalysts exhibited high activity. They suggested that DMC produced both NMA and NNDMA and MeOH was a better alkylating agent than DMC over these catalysts.

1.9 OBJECTIVES OF THE THESIS

A survey of the literature reported above reveals that solid bases such as alkali exchanged zeolites and alkali loaded oxides are interesting catalysts in that they catalyze alkylation at C-, O- and N-. Though much research has been

carried out on many catalysts, alkali dopped SiO_2 has not been sufficiently investigated. Besides, C-alkylation reactions over alkali exchanged zeolite X has not been investigated to any significant extent using dimethyl carbonate, a very safe and active alkylating agent. It was therefore decided to carry out detailed investigations on C-, O- and N-alkylation properties of alkali exchanged zeolites, MCM-41 and alkali loaded silica. Again, correlations between measured basicities and catalytic activities have not been clearly established in many of the published catalyst-reaction systems. It was also, therefore proposed to measure the basicities of the catalysts and relate them to their catalytic activities. The specifics of the research undertaken are presented below.

1) Synthesis of zeolite-X, KL, ferrierite, silicalite-1 and mesoporous MCM-41. Introducing allkali metal ions (K and Cs) by ion exchanging or impregnation methods.

2) Preparation of alkali (Li, Na, K, Cs) loaded silica.

3) Characterization of the zeolites and alkali loaded silica by physicochemical and spectroscopic methods such as XRD, N_2 sorption, TPD of CO_2 , IR of adsorbed CO_2 and MAS-NMR.

4) Evaluation of the catalytic activity of alkali exchanged X in the side chain C-alkylation of toluene and ethylbenzene with dimethylcarbonate in the vapour phase.

5) Study the catalytic activity of alkali loaded silica and Cs loaded MCM-41 in the O-alkylation of hydroxyaromatic compounds such as phenol, cresols (ortho,

meta and para), catechol, resorcinol, hydroquinone and 2-naphthol with methanol in the vapour phase.

6) Examination of the catalytic activity of Cs loaded X, L, ferrierite, silicalite-1 and MCM-41 in the N-alkylation of aniline with methanol and dimethylcarbonate in the vapour phase.

1.10 REFERENCES

1. H. Pines, J.A. Vaseley and V.N. Ipatieff, *J. Am. Chem. Soc*. **77**, 6314 (1955).
2. R.J. Kokes, A.L. Dent, *Advan. Catal*. **22**, 1 (1972).
3. R.J. Kokes, Proceedings of the 5th International Congress on Catalysis, Miami Beach, FL, 1972; p.1.
4. H. Hattori, N. Yoshii and K. Tanabe, Proceedings of the 5th International Congress on Catalysis, Miami Beach, FL, 1972, p. 233.
5. T. Yashima, K. Sato; T. Hayasaka and N. Hara, *J. Catal*. **26**, 303 (1972).
6. H. Hattori, *Chem. Rev*. **95**, 537, (1995).
7. D. W. Breck, in "Zeolite Molecular Sieves", Willey, New York, p.460, 1974.
8. D. Barthomeuf, *Cat. Rev. Sci .& Eng*. **38(4)**, 521 (1996).
9. C. Mirodatos, P. Pichat and D. Barthomeuf, *J. Phys. Chem*. **80**, 1335 (1976).
10. C. Mirodatos, A. Abou Kais, J. C. Vedrine, P. Pichat and D.

Barthomeuf, *J. Phys. Chem.* **80,** 2366 (1976).

11. C.J. Planck, 3rd Proc. Int. Congress on Catalysis, Amsterdam, 1964, Vol.1, p. 727.
12. R.A. Van Santen, B.W.H.Van Beest and A.J.M. de Man, in "Guidelines for Mastering the Properties of Molecular Sieves" (D. Barthomeuf, E.G. Derouane, and W. Holdrich, eds.) NATO ASI series, Plenum Press, New York, 1990, Ser. B: Physics, Vol. 221, p. 201.
13. R.T. Sanderson, "Chemical Bonds and Bond Energy", Academic Press, New York, 1976.
14. R.T. Sanderson, *J. Am. Chem. Soc*. **105**, 2259 (1983).
15. G.V. Gibbs, E.P. Meagher, J.V. Smith and J. J. Pluth, *ACS Symp. Ser*. **40**, 19 (1977).
16. A. Abou-Kais, C. Mirodatos, J. Massardier, D. Barthomeuf and J. C. Vedrine, *J. Phys. Chem.* **81**, 397 (1977).
17. P. E. Hathway and M. E. Davis, *J. Catal.* **116**, 263 (1989).
18. P.E. Hathway and M. E. Davis, *J. Catal.* **116**, 279 (1989).
19. T. Turk, F. Sabin, and A. Vogler, *Mater. Res. Bull*. **27**, 1003 (1992).
20. M. Lasperas, H. Cambon, D. Brunel, I. Rodriguez, and P. Geneste, *Microp. Mater*. **1**, 343 (1993).
21. H. Tsuji, F. Yagi, H. Hattori and K. Kita, Proc. 10th Inter. Cong. Catal. Budapest (L. Guczi,, F. Solymosi, and P. Tetenyi, eds.) *Akademiai Kiado, Budapest*, **B**, 1171 (1993).
22. K Tanabe, "Solid Acids and Bases", Kodansha, Tokyo, 1970.

23. J. A. Rabo, C. L. Angell, P. H. Kasai, and V. Schomarker, *J. Faraday. Soc*. **4**, 328 (1966).

24. Y. N. Sidorenko, P. N. Galich and V. S. Gutyrya, V. G. II' in and I. E. Neimak, *Dokl. Akad. Nauk, SSSR* **173**, 132 (1967).

25. T. Yashima, K. Sato, H.T. Hayasaka and N. Hara, *J. Catal.* **26**, 303 (1972).

26. P.E. Hathaway and M.E. Davis, *J. Catal.* **116**, 263 (1988).

27. P.E. Hathaway and M.E. Davis, *J. Catal.* **119**, 497 (1988).

28. P.E. Hathaway and M.E. Davis, *J. Catal.* **116,** 279 (1988).

29. J.C. Kim, H.-X. Li, C.-Y. Chen and M. Davis, *Micropor. Mater.* **2,** 413 (1994).

30. J. Ward, in "Zeolite Chemistry and Catalysis" (J. Rabo. Eds.), *ACS Monograph* **171**, 233 (1976).

31. J. Engelhardt, J. Szanyi and B. Jover, *Acta Symp Ibero-Amer, Catal, 9th* **2**, 1435 (1984).

32. C. Lacroix, A. Deluzarche, A. Kiennemann, and A. Boyer, *J. Chem. Phys*. 81, 473, 481, 486 (1984).

33. D. Barthomeuf and V. Barbarin, French Patent, 2,623,423 (1989).

34. D. Archier, G. Coudurier and C. Naccache, Proc. 9th Int. Zeol. Conf., Montreal (R. Van Ballmoos, J.B. Higgins and M.M.J. Treacy, eds.), Butterworth-Heinemann, Boston, **II**, 525 (1993).

35. S. Kawi, J.R. Chang and B.C. Gates, *J. Catal*. **142**, 585 (1993).

36. J. M. Graces, G.E. Vrieland, S.I. Bates and F.M. Scheidt, *Stud. Surf.*

Sci. Catal. **20**, 67 (1985).

37. J.C. Kim, H.X. Li and M.E. Davis, *Sym. New. Catal. Chim., Div. Petrol. Chem.* 206th *National Meeting, Am. Chem. Soc., Chicago* **38**, 776 (1993), J.C. Kim, H.X. Li, C.Y.Chen, and M.E.Davis, *Microp. Mater*. **2**, 413 (1994).

38. I. Rodriguez, H. Cambon, D. Drunel, M. Lasperas and P. Geneste, *Stud. Surf. Sci. Catal.* **78**, 623 (1993).

39. Rodriguez, H. Cambon, D. Brunel, M. Lasperas and P. Geneste, Europacat, Montpellier, 1993, Book of Abstracts, I, p. 164.

40. R. M. Dessau, *Zeolites*, **10**, 205 (1990).

41. K.R. Kloestra and H. Van Bekkum, *J. Chem. Soc., Chem. Commun*. 1005, (1995).

42. M. Lasperas, I. Rodriguez, D. Brunel, H. Cambon and P. Geneste, *Stud. Surf. Sci. Catal.* **97**, 319 (1995).

43. K.R. Kloetstra, M. Van Laven and H. Van. Bekkum, *J. Chem. Soc., Faraday Trans.* **93(6)**, 1211 (1997).

44. H. Tsuji, F. Yagi. and H. Hattori, *Chem. Lett*. 1881 (1991).

45. M. Lasperas, H. Combon, D. Brunel, I. Rodriguez and P. Geneste, *Microp. Mater.* **1(5)**, 343 (1993).

46. M. Lasperas, H. Combon, D. Brunel, I. Rodriguez and P. Geneste, *Microp. Mater.* **7**, 61 (1996).

47. S. Tsuchiya, S. Takase and H. Imamura, *Chem. Lett*. 661 (1984).

48. K. Tanabe, M. Misono, Y. Ono and H. Hattori, "New Solid Acids and

Bases", Kodansha, Tokyo, 1989.

49. G. Suzukamo, M. Fukao and M. Minobe, *Chem. Lett*. 585 (1987).

50. E. Ruckenstein and A.Z. Khan, *J. Catal*. **141**, 628 (1993).

51. E. Ruckenstein and A.Z. Khan, *J. Chem. Soc., Chem. Commun*. 1290 (1993).

52. M. A. Paul and F.A. Long, *Chem. Rev*. **57**, 1 (1957).

53. L. P. Hammett, "Physical Organic Chemistry"; McGraw-Hill: New York, 1940; Chapter IX.

54. J. Take, N. Kikuchi and Y. Yoneda, *J. Catal*. **21,** 164 (1971).

55. R.L. Nelson and J.W. Hale, *Disc. Faraday Soc*. **52,** 77 (1958).

56. A.J. Tench and G.T. Pott, *Chem. Phys. Lett*. **26,** 590 (1974).

57. T. Ito, M. Kuramoto, M. Yoshida and T. Tokuda, *J. Phys. Chem*. **87,** 4411 (1983).

58. T. Ito, T. Murakami and T. Tokuda, *J. Chem. Soc. Trans. Faraday I* **79,** 913 (1983).

59. Y. Okamoto, M. Ogawa, A. Maezawa and T. Imanaka, *J. Catal*. **112**, 427 (1988).

60. M. Huang, A. Adnot and S. Kaliaguine, *J. Catal*. **137**, 322 (1992).

61. E.J. Doscocil, S.V. Bordawekar and R.J. Davis, *J. Catal*. **169**, 327 (1997).

62. A. Auroux and A. Gervasini, *J. Phys. Chem*. **94,** 6371 (1990).

63. F. Solymosi and H. Knozinger, *J. Catal*. **122**, 166 (1990).

64. H. Tsuji, F. Yagi and H. Hattori, *Chem. Lett*. 1881 (1991).

65. D. Barthomeuf, *J. Phys. Chem.* **55**, 138 (1978).

66. D. Barthomeuf, *Stud. Surf. Sci. Catal*. **65**, 157 (1991).

67. A. M. Brownstein, in "Catalysis of Organic Reactions" (W.R. Moser, Ed.), p. 3 Dekker, New York, 1981.

68. K. Tanabe, O. Takahashi and H. Hattori, *Reac. Kinet. Catal. Lett.* **7**, 347 (1977).

69. W. Holderich, M. Hesse and F. Navmann, *Angew. Chem. Int. Ed. Engl.* **27**, 226 (1998).

70. W.W. Kaeding, C. Chu, L.B. Young, B. Weinstein and S.A. Butter, *J. Catal.* **67**, 159 (1981).

71. J. Datka, Z. Piwowarska, J. Rakoczy and B. Sulikowski, *Zeolites* **8**, 199 (1988).

72. Y.S. Bhat, A.B. Halgeri, T.S.R. Prasada Rao, *Ind. Eng. Chem. Res.* **28**, 890 (1989).

73. J. Engelhardt, J. Szanyi and J.Valyon, *J. Catal.* **107**, 296 (1987).

74. Y. N. Sidorenko and P.N. Galich, *Dokl. Acad. Nauk. SSSR* **174**, 1234 (1968).

75. M.D. Sefcik, *J. Am. Chem. Soc*. **101**, 2164 (1979).

76. A. Philippou and M.W. Anderson, *J. Am. Chem. Soc.* **116,** 5774 (1994).

77. M. L. Unland, and G. E. Barkar, in "Catalysis of Organic Reactions", (W.R. Moser, Ed.) p. 51, Dekker, New York, 1981.

78. H. Itoh, T. Hattori, K. Suzuki and Y. Murakami, *J. Catal.* **79**, 21

(1983).

79. H. Itoh. A. Miyamoto and Y. Murakami, *J. Catal*. **64**, 284 (1980).

80. C. Lacroix, A. Deluzarche, A. Kienneman and A. Bayer, *Zeolites* **4,** 109 (1984).

81. J. J. Freeman and M. L. Unland, *J. Catal*. **54**, 183 (1978).

82. M.L. Unland and J. J. Freeman, *J. Phys. Chem.* **82**, 1036 (1978).

83. M. L. Unland, *J. Phys. Chem.* **82**, 580 (1978).

84. Y.N. Sidorenko and P.N. Gallich, *Ukr. Khim. Zh.* **36**, 1234 (1970).

85. S.T. King and J. M. Graces, *J. Catal.* **104**, 59 (1987).

86. B. K. Vasanthy, M. Palanichamy and V. Krishnaswamy, *Appl. Catal. A: Gen.* **148**, 51 (1996).

87. C.S. Haung and A. -N. Ko, *Catalysis Lett.* **19**, 319 (1993).

88. G. M. Singerman, "Methyl Aryl Ethers from Coal Liquids as Gasoline Extenders and Octane Improvers" Dept. of energy, CE 5022-1, Washington, 1980.

89. A. Matsukuma, I. Takagishi and K. Yoshido, Patent. Japan, Kokai 7357935.

90. A.S. Barbara and N. Leo Benoiton, *Tetrahedron Lett*. **1**, 21 (1973).

91. S. Balsama, P. Beltrame, P.L. Beltrame, P. Carniti, L. Forni and G. Zuretti, *Appl. Catal.* **13**, 161 (1984).

92. P.D. Chantal, S. Kaliaguine and J.L. Grandmaison, *Appl. Catal.* **10**, 317 (1984).

93. P. D. Chantal, S. Kaliaguine and J.L. Grandmaison, *Appl. Catal*. **18**,

133 (1985).

94. M. Renaud, P.D. Chantal and S. Kaliaguine, *Can. J. Chem. Eng.* **64**, 787 (1986).

95. V. Durgakumari, S. Narayanan and L. Guczi, *Catal. Lett*. **5**, 377 (1990).

96. V. Venkata Rao, K.V.R. Chary, V.Durgakumari and S. Narayanan, *Appl. Catal*. **61**, 89 (1990).

97. E. Santacesaria, D. Grasso, D. Gelosa and S. Carra, *Appl. Catal*. **64**, 83 (1990).

98. C. Bezouhanova and M.A. Al-Zihari, *Appl. Catal. A: Gen*. **83**, 45 (1992).

99. Zi - Hua Fu and Y. Ono, *Catal. Lett*. **21**, 43 (1993).

100. M.C. Samolada, E. Grigoriadou, Z. Kiparissides and I.A. Vasalos, *J. Catal.* **152**, 52 (1995).

101. J. Xu, A.Z. Yan and Q. H. Xu, *Reac. Kinet. Catal. Lett*. **62(1)**, 71 (1997).

102. T. Beutel, *J. Chem. Soc., Faraday Trans.* **94(7)**, 985 (1998).

103. F. M. Bautista, J. M. Campelo, A. Garcia, D. Luna, J.M. Marinas and A.A. Romeo, *Reac. Kine. Catal. Lett.* **63(2)**, 261 (1998).

104. S.C. Lee, S.W. Lee, K.S. Kim, T.J. Lee, D.H. Kim, J.C. Kim, *Catal. Today* **44**, 253 (1998).

105. Y. Fu, T. Baba and Y. Ono, *Appl. Catal. A: Gen.* **166**, 419 (1998).

106. Y. Fu, T. Baba and Y. Ono, *Appl. Catal. A: Gen*. **166**, 425 (1998).

107. Y. Fu, T. Baba and Y. Ono, *Appl. Catal. A: Gen.* **176**, 201 (1999).

108. Kirk-Othmer, in "Encyclopodia of Chemical Technology", Wiley, New York, 3rd edn., 2, 309 (1978).

109. J. March, in "Advanced Organic Chemistry", Wiley, New York, 4th edn. 1991.

110. A. K. Bhattacharya and D.K. Nandi, *Ind. Eng. Chem. Prod. Res. Dev.* **14**, 162 (1975).

111. A.G. Hill, J.H. Shipp and A.J. Hill, *Ind. Eng. Chem.* **43**, 1579 (1951).

112. T. H. Evans and A.N.Bourns, *Can. J. Tech*. **29**, 1 (1951).

113. J.M. Parera, A. Gonzalez and A. Barral, *Ind. Eng. Chem. Prod. Res.* Dev. **7**, 259 (1968).

114. C. M. Naccache and Y.B. Taarit, *J. Catal.* **22**, 171 (1971).

115. N. Takamiya, Y. Koinuma, K. Ando and S. Murai, *Nippon Kagaku Kaishi,* 1452 (1979).

116. N. Kakamiya, H. Yamabe, K. Ando and S. Murai, *Nippon Kagaku Kaishi,* 1316 (1980).

117. L.K. Doraiswamy, G.R.V. Krishnan and S.P. Mukherjee, *Chem. Eng.* **88**, 78 (1981).

118. H. Matsuhashi and K. Arata, *Bull. Chem. Soc. Jp*. **64**, 2605 (1991).

119. A. N. Ko, C. L. Yang, W. Zhu and H. Lin, *Appl. Catal. A: Gen.* **134**, 53 (1996).

120. M. Onaka, K. Ishikawa and Y. Izumi, *Chem. Lett*. 1783 (1982).

121. O. Mokoto, I. Koji and I. Yusuke, *J. Inclusion Phenom.* **2**, 359 (1984).

122. G.O. Chivadze and L.Z. Chkheidze, *Iz. Akad. Nauk. Gruz. SSR, Ser. Khim.* **10,** 232 (1984).

123. P.Y. Chen, M.C. Chen, H.Y. Chu, N.S. Chang and T.K. Chuang, in "New Developments in Zeolite Science and Technology" (Y. Murakami, A. Iijima and J.W. Ward, Eds.), p. 739, Elsevier, Amsterdam.

124. K.G. Ione and O.V. Kikhtyanin, in "Zeolites: Facts, Figure, Fiture" (P.A. Jacobs and R.A. van Santen, Eds.), p. 1073, Elsevier, Amsterdam, 1989.

125. S.I. Woo, J.K. Lee, S.B. Hong, Y.K. Park and Y.S. Hu, in "Zeolites: Facts, Figure, Fiture" (P.A. Jacobs and R.A. van Santen, Eds.), p. 1095, Elsevier, Amsterdam, 1989.

126. P.Y. Chem, S.J. Chu, N.S. Chuang and T.K. Chuang, in "Zeolites: Facts, Figure, Fiture" (P.A. Jacobs and R.A. van Santen, Eds.), p. 1105, Elsevier, Amsterdam, 1989.

127. O.V. Kikhtyanin, K.G. Ione, L.V. Malysheva and A.V. Toktarev, in " Chemistry of Microcrystals" (T. Inui, S. Namba and T. Tatsumi, Eds.), p. 319, Elsvier, Amsterdam, 1991.

128. Y.K. Park, K.Y. Park and S. I. Woo. *Catal. Lett*. **26**, 169 (1994).

129. B.L.Su and D. Barthomeuf, *Appl. Catal. A: Gen.* **124**, 73 (1995).

130. B.L.Su and D. Barthomeuf, *Appl. Catal*. *A: Gen*. **124**, 81 (1995).

131. P.R.H.P. Rao, P. Massiani and D. Barthomeuf, in "Zeolite Science 1994: Recent Progress and Discussions (H.G. Karge and J. Weitkamp,

Eds.), p. 287, Elsvier, Amsterdam, 1985.

132. P.S. Sing, R. Bandyopadhyay an1d B.S. Rao, *Appl. Catal. A* **136,** 177(1996).

133. S. Prasad and B.S. Rao, *J. Mol. Catal.* **62**, L17 (1990).

134. S.M. Yang and T.W. Pan, *J. Chin. Chem. Soc.* **42,** 935 (1995).

135. Z.H. Fu and Y. Ono, C*atal. Lett.* **18**, 59 (1993).

136. Z.H. Fu and Y. Ono, *Catal. Lett.* **22**, 277 (1993).

137. P. R. Hariprasad Rao, P. Massiani and D. Barthomeuf, *Stud. Surf. Sci. Catal*. **84**, 1449 (1994).

138. P. R. Hariprasad Rao, P. Massiani and D. Barthomeuf, *Catal. Lett.* **31**, 115 (1995).

139. M. Selva, A. Bomben and P. Tuldo, *J. Chem. Soc., Perkin. Trans*. **1**, 1041 (1999).

140. F. M. Bautista, J. M. Campelo, A. Garcia, D. Luna, J. M. Marina, A.A. Romero and M.R. Urbano, *J. Catal.* **172**, 103 (1997).

141. F. M. Bautista, J. M. Campelo, A. Garcia, D. Luna, J. M. Marina and A.A. Romero, *Appl. Catal. A: Gen.* **166**, 39 (1998).

142. F. M. Bautista, J. M. Campelo, A. Garcia, D. Luna, J.M. Marinas and A.A. Romero, *Stud. Surf. Sci. Catal*. **108**,123 (1997).

143. S.P. Elangoven, C. Kannan, B. Arabindo and V. Murugesan, *Appl. Catal. A: Gen.* **174**, 213 (1998).

144. S. Narayanan and A. Sultana, *Appl. Catal. A: Gen.* **167**, 103 (1998).

145. S. Narayanan and K Deshpande, *Appl. Catal. A: Gen.*, **199**, 1 (2000).

146. K. Sreekumar, T. Raja, B.P. Kiran, S. Sugunan and B.S. Rao, *Appl. Catal.A: Gen*. **182**, 327 (1999).

147. K. Sreekumar, T. Mathew, S.P. Mirajkar, S. Sugunan and B.S. Rao, *Appl. Catal. A: Gen*. **201**, L1 (2000).

CHAPTER - II

EXPERIMENTAL AND CHARACTERIZATION

2.1 INTRODUCTION

Zeolites possess cations in extra framework positions, which can be exchanged with H^+ (protons) to generate Bronsted acid sites. Pure Si analogues of zeolites (silicalites) are almost neutral. It is reported that as synthesized X and L are slightly basic. Basic zeolites can be prepared by exchanging the extra framework cations by cations of alkali metals like K, Rb, Cs etc. or by impregnating with alkali metal salts (acetate / hydroxide) followed by calcination. Basic sites can be generated in neutral oxides like SiO_2 by loading alkali metal oxides. Just as the acidity of solids can be characterized by adsorption and temperature programmed desorption (TPD) of basic compounds like NH_3 and amines, basic materials can be characterized by adsorption / desorption of weakly acidic gases like CO_2 or compounds like pyrrole. In this chapter, the procedures adopted for the preparation of the various basic zeolite and oxide catalysts are described. The various methods used in the characterization of the catalysts and the physicochemical characteristics of the catalysts are presented. Detailed characterization of the basicity of the catalysts has been carried out by TPD and FTIR spectra of adsorbed CO_2.

2.2 PREPARATION OF CATALYSTS

2.2.1 Synthesis of molecular sieves

2.2.1.1 Synthesis of zeolite -X

Zeolite-X was synthesized using the gel composition in terms of oxides:

$4.54\ Na_2O : 3.44\ SiO_2 : Al_2O_3 : 180 H_2O$.

Sodium silicate (28.6 % SiO_2, 8.88 % Na_2O and 62.6% H_2O) was used as the silica (SiO_2) source and $NaAlO_2$ was used as the alumina (Al_2O_3) source. In a typical synthesis [1], 18.6 g sodium silicate was taken in a beaker and a mixture of 5.9 g sodium aluminate, 3.9 g sodium hydroxide and 70 g water was added to it. The mixture was stirred for 2 h, transferred into an autoclave, aged for 24 h at room temperature and then heated for six hour at 373K. The product was filtered, washed with distilled water and dried at ambient temperature.

2.2.1.2 Synthesis of zeolite-L

Zeolite-L was synthesized using the gel composition in terms of oxides:

2.62 K_2O : 10 SiO_2 : Al_2O_3 : 158H_2O.

Fumed silica was used as the silica source and pseudoboehmite (Catapal-B) was used as the alumina source. In a typical synthesis [2], 9 g KOH and 1.55 g pseudoboehmite (Catapal-B) were dissolved in 45 g water and fumed silica was added to it. The mixture was stirred for 2 h and transferred into an autoclave. The gel was heated at 415K for 108h. The product was filtered, washed with distilled water and dried at ambient temperature.

2.2.1.3 Synthesis of Si-MCM-41

Si-MCM-41 samples were prepared hydrothermally using a gel with the following molar composition in terms of oxides [3]:

SiO_2 : 0.27 $(CTMA)_2O$: 0.13 $(TMA)_2O$: 60 H_2O.

Sodium silicate (28.48% SiO_2, 9.03% Na_2O, 62.5% H_2O), cetyltrimethylammonium bromide (99%, Aldrich), tetramethylammonium

hydroxide (TMAOH, 25% aqueous solution, Aldrich), and fumed silica (Cab-O-Sil, 99%, Fluka) were used in the synthesis.

In a typical synthesis, 18.9 g TMAOH was added to 16.9 g sodium silicate diluted with 100 g water. In another beaker, 19.7 g CTMABr was dissolved in 50 g water and 30 g ethanol and 1.9 g aqueous ammonia solution was added to it (solution A). Solution A was added to the above mixture of sodium silicate and TMAOH and then 7.1 g fumed silica was added to it. The combined mixture was stirred for 1h. The gel formed (pH = 11.5-12) was then transferred to an autoclave and heated at 373K for 5 days. The product was filtered, washed with distilled water and dried at ambient temperature. The sample was calcined at 813K in nitrogen flow for 1h and then in air for 6h.

2.2.1.4 Synthesis of silicalite -1

The silicalite-1 sample was prepared hydrothermally using a gel with the following molar composition [4]:

0.99TPABr : 0.026 Na_2O : SiO_2 : 24.8 H_2O.

Tetramethyl ammoniumsilicate was the silica source. Tetrapropyl ammonium bromide was used as the template. In a typical synthesis, 26.6 g TPABr was dissolved in 25 g H_2O and then 0.21 g NaOH dissolved in 20 g H_2O was added to it. The mixture was stirred for 1h and then 10.6 g tetramethyl ammoniumsilicate was added to it. The mixture was stirred further for 1h. The gel formed (pH = 11.5-12) was then transferred to an autoclave and heated at 445K for 72 h. The product was filtered, washed with distilled water and dried at ambient temperature. The sample was calcined at 813K in nitrogen flow for 1h and then in air for 6h.

2.2.1.5 Synthesis of ferrierite

The ferrierite sample was prepared hydrothermally using a gel with the following composition in term of oxides:

27.2 Na_2O : 32 Py : 50 SiO_2 : 5 H_2SO_4 : 1798 H_2O.

Sodium silicate (28.48% SiO_2, 9.03% Na_2O, 62.5% H_2O), pyrrolidine and H_2SO_4 were used in the synthesis. In a typical synthesis [5], 52.5 g sodium silicate was dissolved in 70 g H_2O and 1.8 g H_2SO_4 (98%, S.D. Fine-chem Ltd., India) in 10 g H_2O was added to it. After stirring for 1h, 10 g pyrrolidine was added to it. The mixture was transferred into an autoclave and heated at 433K for 40 h. The product was filtered, washed with distilled water and dried at ambient temperature. The sample was calcined at 813K in nitrogen flow for 1h and then in air for 6h.

2.2.2 Modification of supports

2.2.2.1 Ion exchange

Ion exchange of zeolite-X was carried out using both hydroxide and chloride solutions (1M) of K and Cs. Ion exchange was carried out at 353K using 50 ml of solution per g of sample (6h duration). The exchange procedure was repeated six times. The ion exchanged zeolites were washed with deionised water and dried at 383K for 12h. The degree of ion exchange was estimated by flame photometry and atomic adsorption spectroscopy.

Ion exchange of zeolite L was carried out using 1M cesium hydroxide solution. 50 ml / g of the sample was used for each exchange. Six exchanges were carried out at 353K. The ion exchanged zeolites were washed with deionised water and dried at 383K for 12h.

2.2.2.2 Impregnation

2.2.2.2.1 Preparation of Cs-MCM-41

Samples of Cs loaded MCM-41 were prepared by stirring 5 g of MCM-41 in a solution containing the appropriate amount of cesium acetate in 30 g methanol for 3 h at 333K. The solvent was removed quickly under vacuum in a rotary evaporator and the materials were subsequently dried at 383K for 6 h and then calcined at 813K for 8 h in air. The amounts of cesium acetate used per g of Si-MCM-41 to prepare the different catalysts are given in Table 1.1.

2.2.2.2.2 Preparation of alkaline silica

Fumed silica (Cab-osil, Surface area = 166 m^2 / g) was used as a support for alkali (Li, Na, K and Cs) oxides. The different alkali loaded catalysts were prepared by an impregnation procedure using minimum amount of metal hydroxide / acetate. In this method, the required amount of M-OAc (M = Li, Na, K and Cs) was dissolved in 50 ml water, then 10 g fumed silica was added to it with constant stirring at 353K. The mixture was evaporated to dryness at 333K and further dried at 383K for 6 h. It was then calcined at 813K in air. The amount of metal salts used per g of silica to prepare the different catalysts are presented in Table 2.2.

2.2.2.2.3 Preparation of Cs-silicalite and Cs-ferrierite

Samples of Cs-loaded silicalite-1 and ferrierite were prepared by taking 10 g of silicalite-1 / ferrierite in a solution containing an appropriate amount (3 wt% Cs) of cesium acetate in 50 g methanol. The solution was stirred for 3h at 333K. The solvent was removed quickly under vacuum in a rotary evaporator and the materials were subsequently dried at 383K for 6 h and then calcined at 813K for 8 h in air.

Table 2.1 Amount of Cs acetate used to prepare the different catalysts

Sample name [a]	Cesium aetate (g)[b]
Cs(0.075) MCM-41	0.014
Cs(0.15) MCM-41	0.028
Cs(0.225) MCM-41	0.043

[a] The number in brackets denotes the mmole of alkali metal loaded per g of Si-MCM-41; [b] Amount used per g of MCM-41.

Table 2.2 Amount of metal salts taken as acetate / hydroxide for preparing the different catalysts

Sample[a]	M-acetate[b] (g)	M-hydroxide[b] (g)
Li (1.5)SiO_2	0.099	0.036
Li (2.25)SiO_2	0.148	0.054
Na (1.5)SiO_2	0.123	0.06
Na(2.25)SiO_2	0.184	0.09
K(1.5)SiO_2	0.147	0.084
K (2.25)SiO_2	0.22	0.13
Cs(0.075)SiO_2	0.014	0.011
Cs(0.375)SiO_2	0.072	0.056
Cs(0.75)SiO_2	0.145	0.112
Cs(1.5)SiO_2	0.29	0.225
Cs(2.25)SiO_2	0.43	0.337

[a] The number within brackets denotes the mmole of alkali metal loaded per g of SiO_2;

[b] M = Li, Na K and Cs; amount used per g of silica

2.3 CHARACTERIZATION

2.3.1 X-ray diffraction (XRD)

X-ray diffraction measurements were carried out using Ni-filtered CuKα radiation (Rigaku, D/MAX-VC). X, L, ferrierite, silicalite-1 and MCM-41 were all highly crystalline materials. For X and L, a decrease in peak intensities of the samples with increasing size of the exchanging cations was noticed. For zeolite X, the peaks were slightly less intense when exchanged with hydroxide solutions, than when exchanged with chloride solutions. Similar results were earlier reported by Englehardt et al. [6].

For Cs-loaded ferrierite, silicalite-1 and MCM- 41 samples, the peak intensities were almost the same as those of the parent samples. The XRD figures of some of the samples are given in Fig. 2.1.

XRD revealed all the alkali (Li, Na, K and Cs) loaded silica samples to be amorphous.

2.3.2 Surface area

The surface areas of the samples were calculated from N_2 sorption isotherms using the BET procedure. The surface areas of the various samples are presented in Table 2.3. The surface areas decrease on exchange with heavier metal atoms. For silicalite and ferrierite samples, surface area decreases with Cs-loading. The results are presented in Table 2.4. For MCM-41, surface area also decreases with Cs-loading. The average pore diameter also decreases with metal loading. The results are given in Table 2.5. The decrease in pore diameter is probably due to the large diameter of the Cs ions (3.34Å; ionic) narrowing the dimensions of the pores.

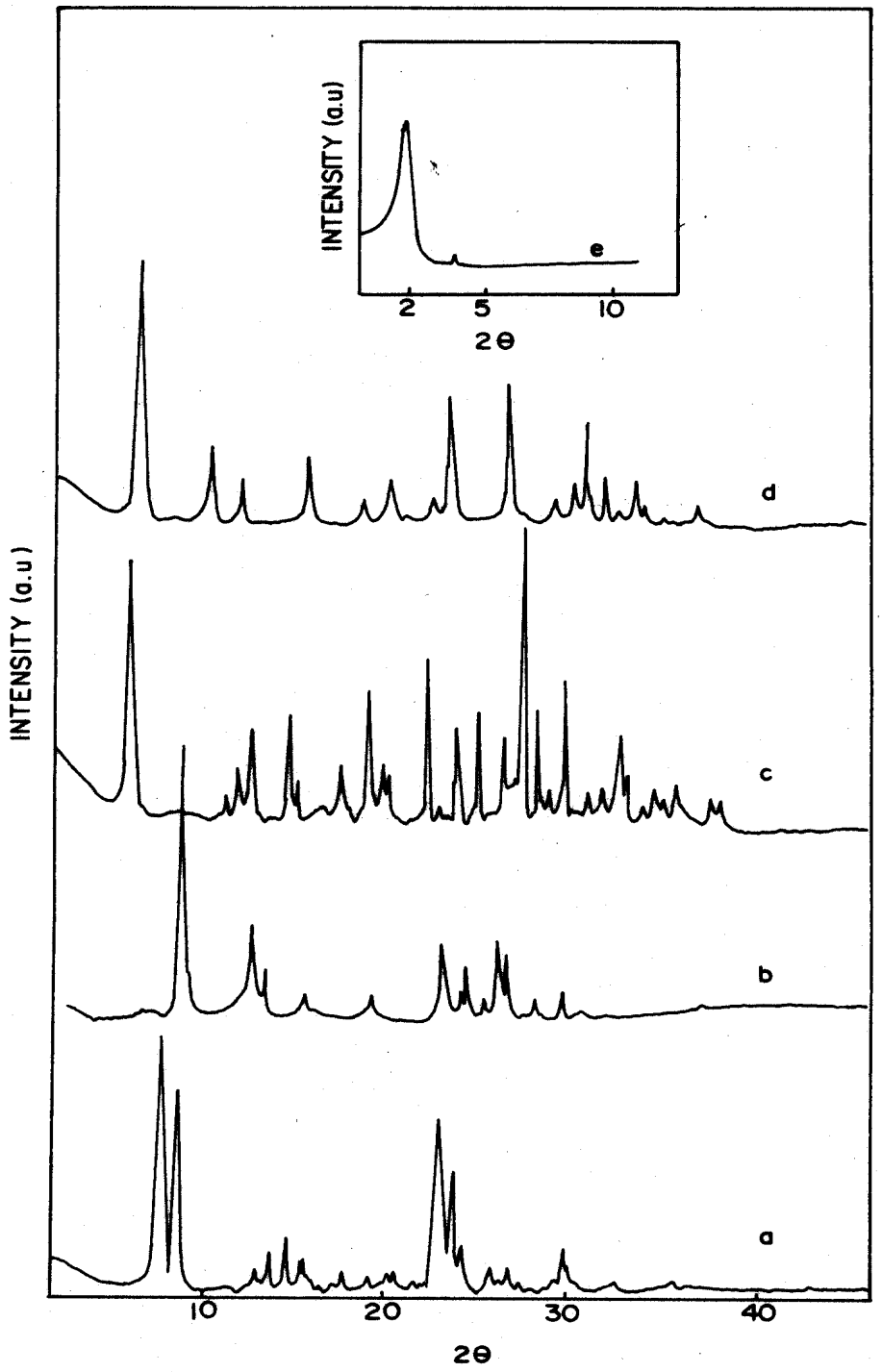

Fig. 2.1 XRD patterns of the samples: (a) Cs-Silicalite-1; (b) Cs-Ferrierite; (c) CsL; (d) CsX(OH) and (e) Cs(0.225)MCM-41.

Table 2.3 Composition and surface area of ion exchanged X and L zeolites

Catalyst	Si / Al	% Na	% K	% Cs	BET surface area (m^2/ g)
NaX	1.34	100	-	-	712
KX(Cl)	1.34	18	82	-	624
KX(OH)	1.34	12	88	-	600
CsX(Cl)	1.34	49	-	51	572
CsX(OH)	1.34	48	-	52	550
KL	3.5	-	100	-	416
CsL	3.5	-	36	64	352

Table 2.4 Surface areas of silicalite and ferrierite samples

Sample	Si / Al	Surface area (m^2 / g)
Silicalite-1	α	432
Cs(0.225)-silicalite-1	α	379
Ferrierite	α	381
Cs(0.225)-ferrierite	α	331

Table 2.5 Surface areas and average pore diameters of MCM-41 samples

Sample	Surface area (m^2 / g)	Pore diameter (Å)
Si-MCM-41	1049	28
Cs(0.075) MCM-41	837	22
Cs(0.15) MCM-41	771	20
Cs(0.225) MCM-41	625	17.5

For alkali loaded silica samples the surface area decreases with metal loading. The surface area also decreases with increase in basicity of the metal atom. As part of the observed decrease in area is due to the large amount of deposited alkali oxides, surface areas were calculated on alkali free basis also. These values are given in Table 2.6. These values are also lower than that of pure SiO_2. The decrease in surface area is attributed to the dissolution of the surface by the alkali during impregnation, fusion of SiO_2 particles and pore filling by the alkali oxides. However, except in the case of samples containing large amounts of Cs ($\geq$ 0.75 mmole/g) and K (2.25 mmole/g), the decrease in area is small (< 10%) suggesting that the deposited oxide covers the SiO_2 surface reasonably uniformly without causing much pore blockage.

Table 2.6 Surface areas of alkali loaded silica samples.

Catalyst[a]	Metal loading as oxide (wt%)	S. Area[b] (m^2/g)	S. Area[c] (m^2/g).
SiO_2	-	166	166
$Li(1.5)SiO_2$	2.25	104	161
$Li(2.25)SiO_2$	3.37	98	160
$Na(1.5)SiO_2$	4.65	99	158
$Na(2.25)SiO_2$	6.97	89	154
$K(1.5)SiO_2$	7.05	91	156
$K(2.25)SiO_2$	10.57	82	148
$Cs(0.075)SiO_2$	1.06	149	164
$Cs(0.375)SiO_2$	5.28	121	157
$Cs(0.75)SiO_2$	10.5	102	149
$Cs(1.5)SiO_2$	21.1	70	133
$Cs(2.25)SiO_2$	31.7	56	113

[a] The number in brackets denotes the mmole of alkali metal loaded per g of SiO_2; [b] Measured by N_2 adsorption (BET method); [c] normalized to 100% silica.

2.3.3 Intermediate electronegativity (S_{int})

The intermediate electronegativity (S_{int}) of zeolite X was calculated on the basis of Sanderson's intermediate electronegativity principle [7]. These values are given in Table 2.7 along with those for alkali loaded silica samples. With increase in basicity of the exchanged (or deposited) ion, the S_{int} value decreases.

Table 2.7 Intermediate electronegativity (S_{int}) values

Sample	Intermediate electronegativity (S_{int})	Average charge on the O atom
NaX	3.28	-0.41
KX(Cl)	3.10	-0.44
KX(OH)	3.09	-0.45
CsX(Cl)	3.08	-0.45
CsX(OH)	3.07	-0.45
SiO_2	4.25	-0.20
$Li(1.5)SiO_2$	3.98	-0.26
$Na(1.5)SiO_2$	3.96	-0.26
$K(1.5)SiO_2$	3.92	-0.27
$Cs(0.075)SiO_2$	4.22	-0.21
$Cs(0.375)SiO_2$	4.18	-0.22
$Cs(0.75)SiO_2$	4.09	-0.23
$Cs(1.5)SiO_2$	3.91	-0.27
$Cs(2.25)SiO_2$	3.69	-0.32

2.3.4 Temperature programmed desorption (TPD) of carbon dioxide

Temperature programmed desorption (TPD) of CO_2 was carried out with 0.25 g of dried sample in each experiment. The sample was activated at 673 K in a flow of He at the rate of 30 ml/min and cooled to room temperature. Ultra high purity CO_2 was passed for 1h at room temperature at a flow rate of 25 ml/min,

then flushed with He for 90 min (30 ml/min) and the temperature raised to 723K at the rate of 5K / min in He flow (30 ml/min). The evolved CO_2 was estimated using a TCD (Zeton Altamira AM1-200) to obtain the TPD curves.

The results of temperature programmed desorption (TPD) of adsorbed CO_2 of alkali loaded silica and MCM-41 samples are presented in Tables 2.8 and 2.9. The TPD plots of various alkali metal (Li, Na, K and Cs) loaded silica samples are shown in Fig. 2.2. The plots for Cs loaded silica and MCM-41 samples are shown in Fig. 2.3 and Fig. 2.4, respectively. It was found that most of the CO_2 desorbed from the samples below 500K with desorption peak maxima in the range 375 – 425K. Though CO_2 adsorbs weakly and desorbs easily from the catalysts, the TPD data do reveal some information concerning the basicity of the samples. At constant metal loading (1.5 mmole / g of catalyst), the amount of adsorbed (actually desorbed) CO_2 increases with increasing basicity of the metal (Li to Cs). An increase in CO_2 adsorption is noticed also with an increase in Cs_2O loading both for Cs loaded silica and MCM-41 samples (Tables 2.8 and 2.9). However, the number of moles of CO_2 adsorbed per mole of alkali metal decreases with increase in Cs_2O loading. This is due to lower dispersion and cluster formation in samples containing higher amount of Cs_2O. The basicity trend obtained from TPD of CO_2 matches the trend of intermediate electronegativity ($S_{int.}$) values calculated [7] on the basis of Sanderson's intermediate electronegativity principle (Table 2.7).

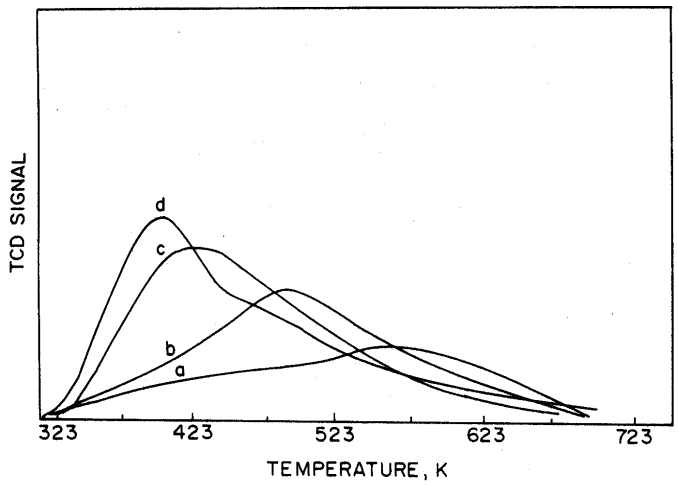

Fig. 2.2 TPD plots of CO_2 adsorbed on different alkali metal loaded samples: (a) $Li(1.5)SiO_2$; (b) $Na(1.5)SiO_2$; (c) $K(1.5)SiO_2$ and (d) $Cs(1.5)SiO_2$.

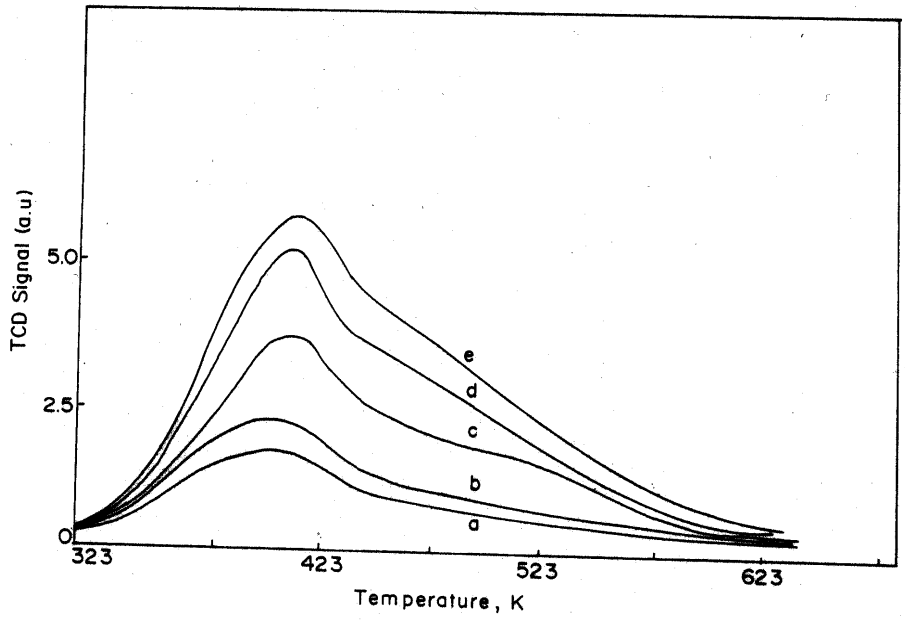

Fig. 2.3 TPD plots of CO_2 adsorbed on different Cs loaded samples: a, b, c, d and e refer to samples with Cs loading of 0.075, 0.375, 0.75, 1.5 and 2.25 mmolee/g silica, respectively.

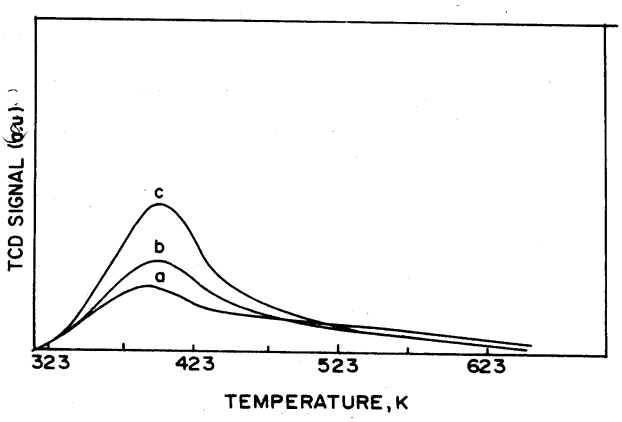

Fig. 2.4 TPD of CO_2 adsorbed on different Cs loaded MCM-41 samples: (a), (b) and (c) refer to samples with Cs loading of 0.075, 0.15 and 0.225 mmole/g of Si-MCM-41, respectively.

Table 2.8 Amount of CO_2 desorbed during TPD measurements over different SiO_2 catalysts

Sample[a]	TPD of CO_2	
	mmole/g[b]	mole /mole metal[c]
Li(1.5)SiO_2	0.062	0.041
Na(1.5)SiO_2	0.071	0.047
K(1.5)SiO_2	0.078	0.052
Cs(0.075)SiO_2	0.031	0.41
Cs(0.375)SiO_2	0.049	0.13
Cs(0.75)SiO_2	0.061	0.081
Cs(1.5)SiO_2	0.079	0.053
Cs(2.25)SiO_2	0.082	0.036

[a] The number in brackets denotes the mmole of alkali metal loaded per g of SiO_2 ;

[b] mmole CO_2 desorbed / g of catalyst and

[c] moles of CO_2 desorbed / mole of alkali metal in the catalyst.

Table 2.9 Amount of CO_2 desorbed during TPD measurements over different MCM-41 catalysts

Sample[a]	TPD of CO_2	
	mmole/g[b]	mole /mole Cs[c]
Cs(0.075) MCM-41	0.032	0.42
Cs(0.15) MCM-41	0.044	0.29
Cs(0.225) MCM-41	0.068	0.30

[a] The number in brackets denotes the mmole of alkali metal loaded per g of SiO_2 ;
[b] mmole CO_2 desorbed / g of catalyst and [c] moles of CO_2 desorbed / mole of alkali metal in the catalyst.

2.3.5 Infrared spectra of adsorbed carbon dioxide

FT-IR spectra of the samples in the region of structural vibrations were recorded using KBr pellets. For spectra of adsorbed CO_2, self-supported wafers were used. The sample was pressed into thin wafers (5-6 mg/cm^2), evacuated (10^{-5} torr) at 673 K and cooled to 298K to record the spectrum of the pure sample. Ultra pure CO_2 (99.999 %, Linde Air) was then adsorbed on the sample at 5 mm equilibrium pressure for 1h and another spectrum was recorded. Then part of the CO_2 gas was pumped out to maintain an equilibrium pressure of 0.4 mm and the spectrum was recorded again. All the spectra were recorded using a Nicolet 60 SXB spectrometer with 2 cm^{-1} resolution, averaging over 500 scans.

2.3.5.1 Silica supported samples

FT-IR spectrum of pure silica shows strong bands due to tetrahedral framework vibrations of Si-O-Si linkages at 1106 and 807 cm^{-1}. As the Cs_2O loading increases these characteristic bands shift systematically to lower wave numbers as can be noticed in Fig. 2.5. The bands at 1106 cm^{-1} and 807 cm^{-1} in pure SiO_2 shift (respectively) to 1097 and 794 cm^{-1} in $Cs(2.25)SiO_2$ (31.7 % Cs_2O) sample. In the case of cesium silicate, they appear, respectively, at 1041 and 787 cm^{-1}. The shift indicates that Si-O-Si bonds are perturbed by the formation of Si-O-Cs linkages in the framework indicating the formation of cesium silicate type of species at the surface. Doscosil et al. [8] have identified such alkali silicate phase in the case of Rb_2O/SiO_2 system from X-ray absorption studies.

CO_2 being amphoteric in nature can be used to monitor both Lewis acid centers and Lewis base centers on metal oxides and zeolite surfaces. It is a linear molecule having $D_{\alpha v}$ symmetry and three fundamental vibrations, one stretching vibration ν_1, which is Raman active appearing as a doublet at 1285 and 1388 cm^{-1} and two other IR active vibrations, doubly degenerate deformation ν_2 at 667 cm^{-1} and the antisymmetric stretch ν_3 at 2349 cm^{-1} [9]. The IR spectrum of adsorbed CO_2 varies distinctly from the gas phase spectrum and three types of adsorption have been distinguished.

a) On unreactive surfaces, the infrared spectrum of adsorbed CO_2 shows mostly the ν_3 vibration near 2349 cm^{-1}. b) The adsorption of CO_2 on reactive surfaces may give rise to several adsorbed species, such as carbonate, bicarbonate and formate which exhibit characteristics adsorption bands [10-12].

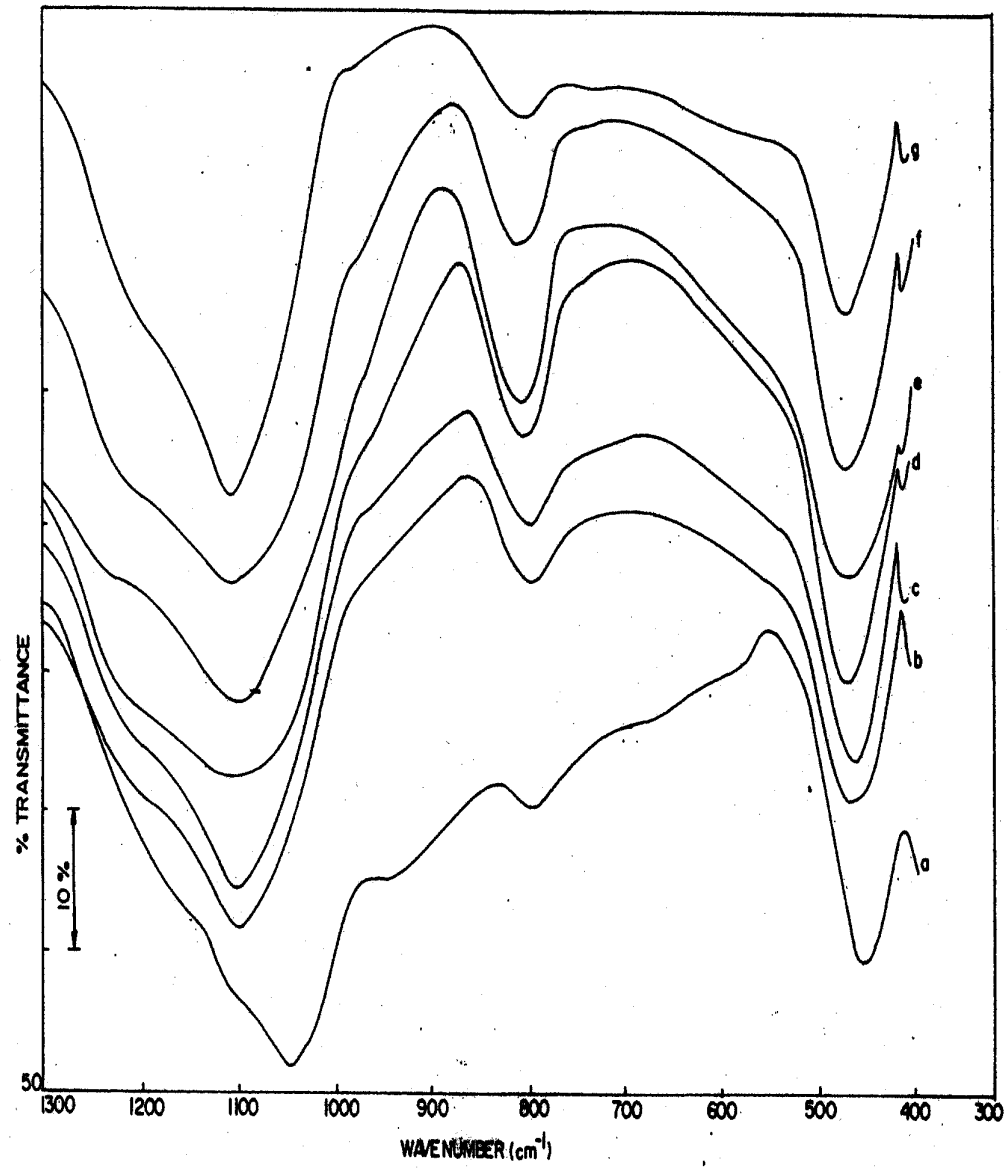

Fig. 2.5 FTIR spectra (298K) of Cs_2O-SiO_2 samples in the framework region: a) Cesium silicate and b, c, d, e, f refer to samples with Cs loading of 2.25, 1.5, 0.75, 0.375, 0.075 mmolee/g of silica, respectively and g) SiO_2.

c) O_2 can also function as a ligand in different complexes of transition metals as highly perturbed structures. These CO_2 species have a characteristic pair of absorption bands in the region 1200 – 1700 cm^{-1}. This type of bond is formed when electrons are donated to CO_2 molecule and CO_2^- anion is formed. But such an anion is stable only at low temperatures.

Adsorption of CO_2 on pure SiO_2 shows a band only due to molecularly adsorbed CO_2 (ν_3, type 1) at 2349 cm^{-1} associated with changes in the band shapes of the hydroxyl groups on SiO_2. The hydroxyl groups on pure silica exhibit a sharp band at 3745 cm^{-1} and a broad band centered around 3550 cm^{-1} which are perturbed by the adsorption of CO_2 (not shown). These hydroxyl groups are centers of CO_2 adsorption. No bands are observed in the carbonate region, 1200 – 2000 cm^{-1}. Similar reports have earlier been made by many workers [8,13 –15]. CO_2 was completely desorbed on evacuating the sample.

IR spectra of adsorbed CO_2 on alkali metal modified silica are shown in Figs. 2.6, 2.7 and 2.8. In the Fig. 2.6, bands due to antisymmetric stretching ν_3 vibrations of physisorbed CO_2 on Li_2O, Na_2O, K_2O and Cs_2O modified SiO_2 are seen; they appear, respectively, at 2348, 2346, 2342 and 2340 cm^{-1}. As the ionic radius of the alkali metal cation and the metal – oxygen bond length increases, the electron donating ability (to adsorbed CO_2) increases and hence the ν_3 frequency shifts to lower wave number, in accordance with the basicity of the alkali metal. In Fig. 2.7, the corresponding FTIR spectra in the region of carbonate vibrations (1275 – 1975 cm^{-1}) are presented. Adsorption of CO_2 produced two sets of bands.

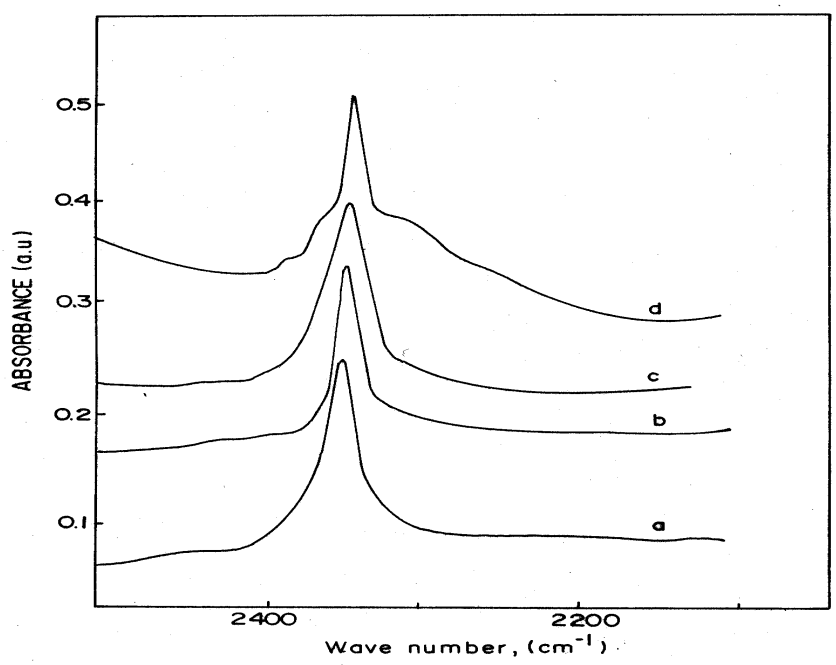

Fig. 2.6 FTIR spectra (298K) of adsorbed CO_2 (5 mm equilibrium pressure of CO_2) in the region of anti-symmetric stretching on alkali metal (1.5 mmolee/g) loaded silica: (a) Li_2O-SiO_2; (b) Na_2O-SiO_2; (c) K_2O-SiO_2 and (d) Cs_2O-SiO_2.

Each set consists of bands due to one anti-symmetric and one symmetric stretching vibration. The frequencies of these bands for Li_2O, Na_2O, K_2O and Cs_2O loaded SiO_2 (1.5 mmole/g loading) are presented in Table 2.10. The intensity of these bands decreases with decrease (Table 2.11) in equilibrium pressure but persists even after evacuation. It is clear that the supported alkali metal changes the adsorptive property of SiO_2. The frequencies of these bands of adsorbed carbonate species decrease as the basicity of the alkali metal increases. The difference between the high and the low frequency bands varies

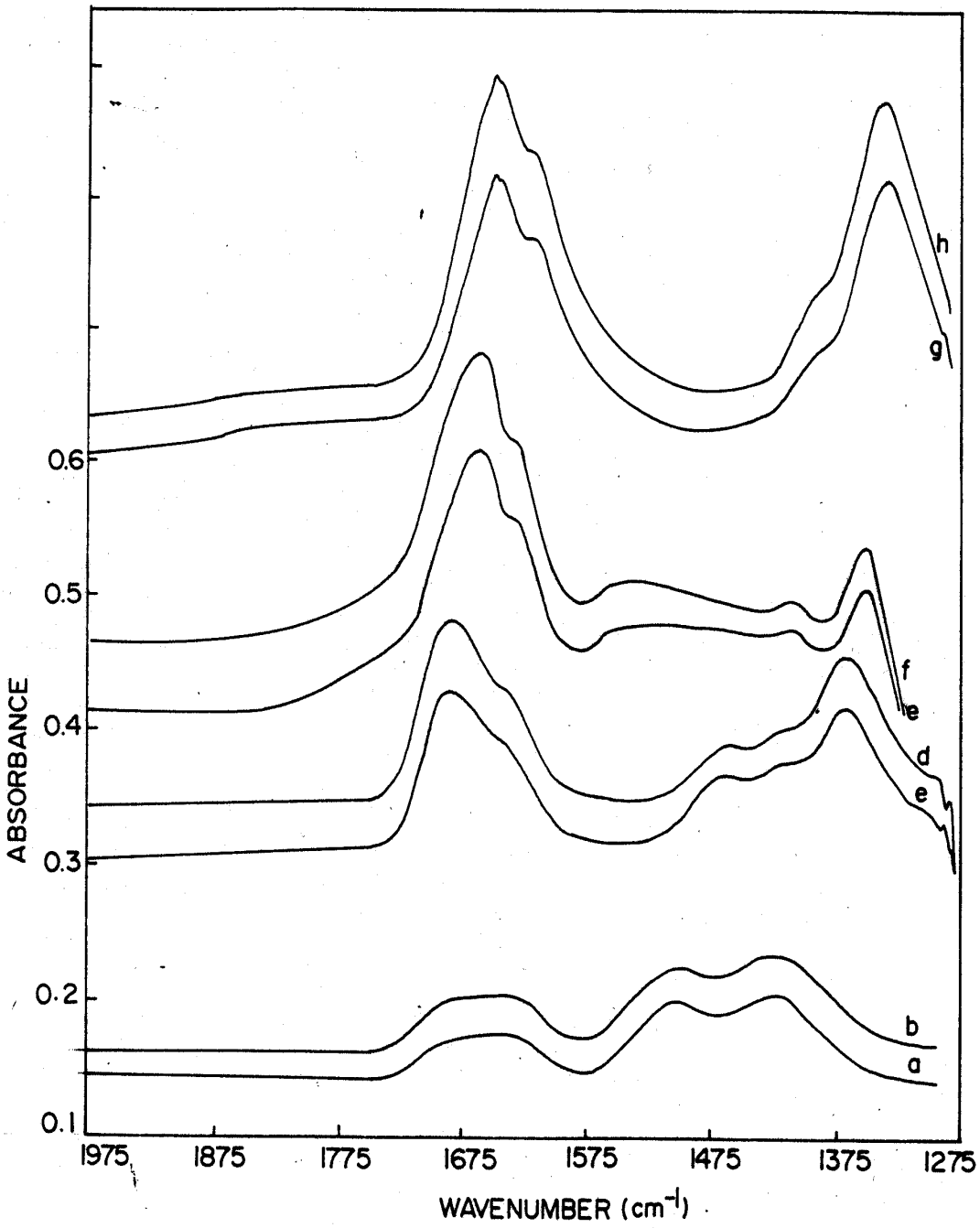

Fig. 2.7 FTIR spectra (298K) of adsorbed CO_2 on alkali metal (1.5 mmole/g) loaded silica: a,b) Li-SiO_2; c,d) Na-SiO_2; e,f) K-SiO_2; g,h) Cs-SiO_2. (a, c, e, g, I at 0.4 mm and b, d, f, h, j at 5 mm equilibrium pressure of CO_2, respectively.

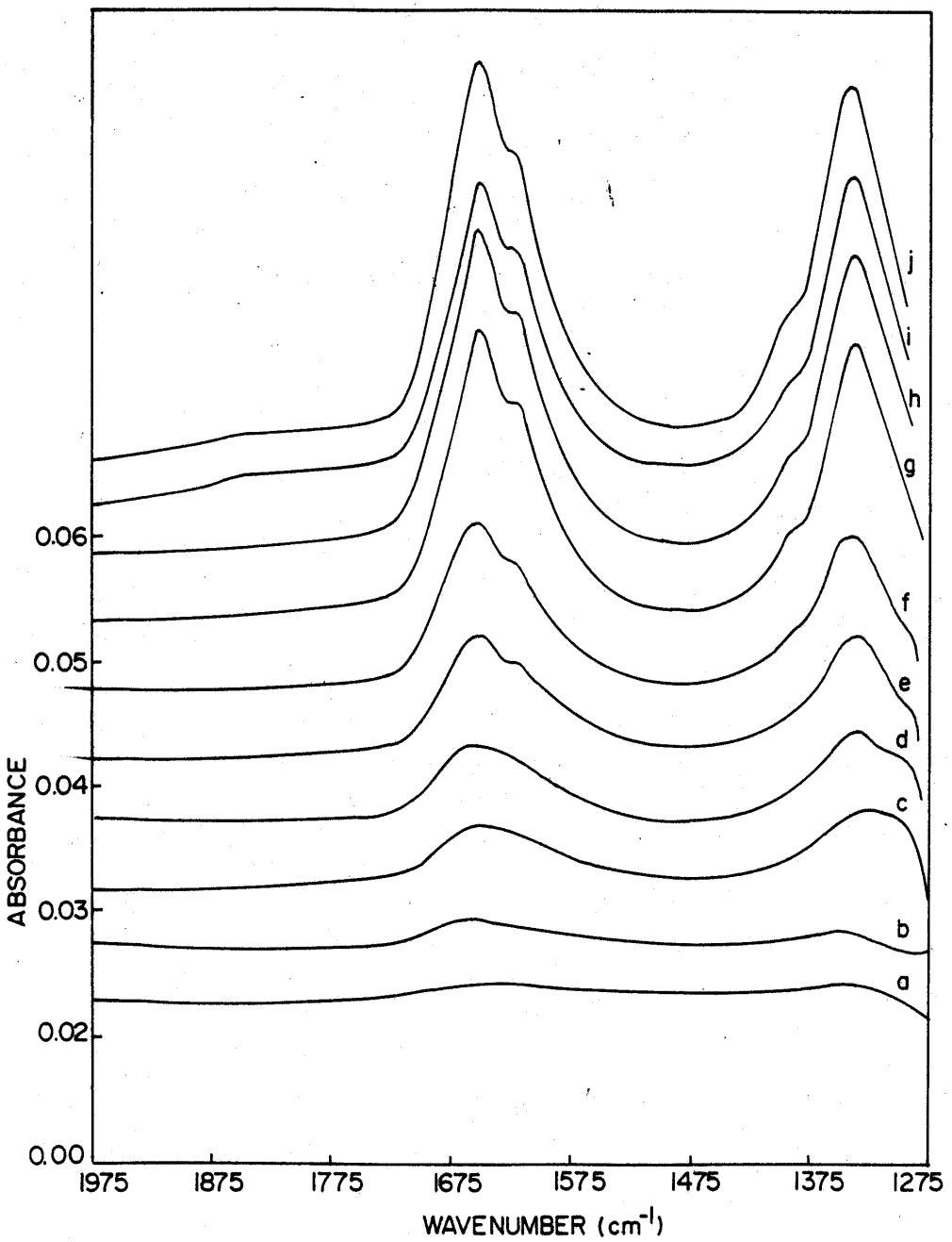

Fig. 2.8 FTIR spectra (298K) of adsorbed CO_2 in the CO_3 vibration region on Cs_2O-SiO_2 samples with Cs loading of 0.075, 0.375, 0.75, 1.5 and 2.25 mmolee/g: a, c, e, g, i at 0.4 mm and b, d, f, h, j at 5mm equilibrium pressure of CO_2, respectively.

from 258 to 319 cm^{-1} for anti-symmetric stretch and 154 to 234 cm^{-1} for symmetric stretch vibrations for different metal oxide loaded samples. For samples containing different amounts of Cs_2O, the frequency variations are much less (Table 2.10). The assignment of these absorption bands is based on characteristic vibrations reported previously for CO_2 adsorption on metal oxides and some alkali metal modified metal oxides [11, 12].

Carbon dioxide is believed to adsorb on metals and basic oxides in many forms, the symmetrical, monodentate, bidentate and bridged forms [12] The interaction of CO_2 is believed to be through transfer of electronic charge to CO_2 molecule from alkali metal oxide which increases with the size of the metal ion. Besides, the simultaneous interaction of alkali cation and O^{2-} anion on adsorbed CO_2 may also be taking place. The increasing shift in the high and low frequency bands and increasing frequency difference between the bands on going from Li^+ to Cs^+ cation modified SiO_2 samples indicate increasing interaction with CO_2. Solymosi and Knozinger [12] have proposed $\Delta\nu$ values of 0, 100, 300 and >400 for symmetrical, monodentate, bidentate and bridged confirmation for adsorbed CO_2 species, respectively, on interacting surfaces. Going by this concept, the $\Delta\nu$ values observed for CO_2 on Li^+, Na^+, K^+ and Cs^+ modified SiO_2 surface indicate the presence of mainly monodentate and bidentate types of adsorbed species (described in chapter I). The concentration of bidentate species increases with the basicity of the alkali metal.

2.3.5.2 Zeolite and molecular sieve samples

In Cs-MCM-41, Cs-silicalite and Cs-ferrierite, basicity is induced by encapsulating Cs_2O in the intrinsic pores of different sizes. Considering the possible cation distribution on different crystallographic sites in X and L type zeolites under our ion exchange conditions most of Cs cations should be located in the supercages of zeolite-X samples whereas in the case of silicalites and MCM-41, which do not have cation sites, Cs_2O is occluded in the pores. CO_2 has a kinetic diameter of 3.3 Å, it can not enter the sodalite cages in X type and cancrinite cages in L type zeolites; so, it can only interact with cations in supercages. In the case of porous silicalites, CO_2 can interact with basic sites present in the 10 MR pore system. It forms the complex M…O=C=O giving rise to absorption bands due to antisymmetric stretching vibrations, v_3 mode. In Fig. 2.9 (curves a - c) FTIR spectra in this region of CO_2 adsorbed on zeolites NaX, CsX(OH), and Cs-L are presented.

Similar spectra for Cs-MCM-41, Cs-silicalite and Cs-ferririte samples are presented in Fig. 2.10. In Table 2.12 the corresponding band positions are given of which the most intense and dominating band positions are underlined. From the data presented above and to be presented later, it appears that adsorption of CO_2 on the zeolite samples studied involves both physical and chemical interactions because all modes of vibrations are observed in the spectra. For convenience, the adsorption of CO_2 on cation modified X and L type zeolite (Table2.12) is considered separately from others, because they have anionic framework oxygens due to isomorphous substitution of Al^{3+} by Si^{4+} in

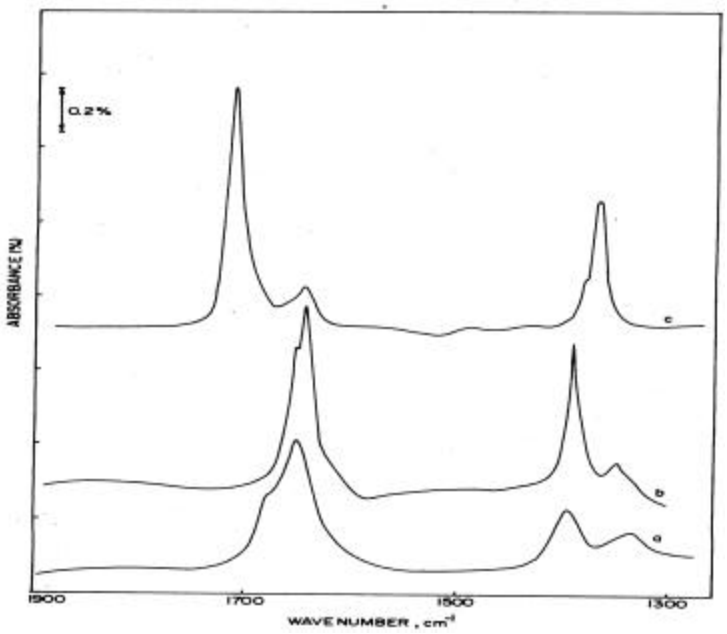

Fig. 2.9 FTIR spectra (298K) of adsorbed CO_2 in the CO_3 vibration region on: (a) CsL; (b) CsX (OH) and (c) NaX at 5 mm equilibrium pressure of CO_2.

the SiO_2 polymorph. MCM-41, silicalite and ferrierite are pure silica polymorphs of different micro and mesoporous morphology, whose frameworks are electrically neutral. Due to the large size of the Cs ions and the partial exchange (~ 50%), most of the Cs cations are expected to be located only in the supercages. Also, the large CO_2 molecules (3.3 Å size) cannot enter into the small (6MR) cages, in the two zeolites and hence mainly Cs cations are available for adsorption. As a result, the prominent ν_3 mode vibrational band at 2353 cm^{-1} is shifted to 2342 cm^{-1} for NaX. The very weak side bands at 2341 and 2340 cm^{-1} can be seen for NaX. They become invisible on Cs cation exchange, instead, weak side bands at higher frequency at 2350 and 2349 cm^{-1} are observed (Fig. 2.11). In the literature, different values between 2351 and

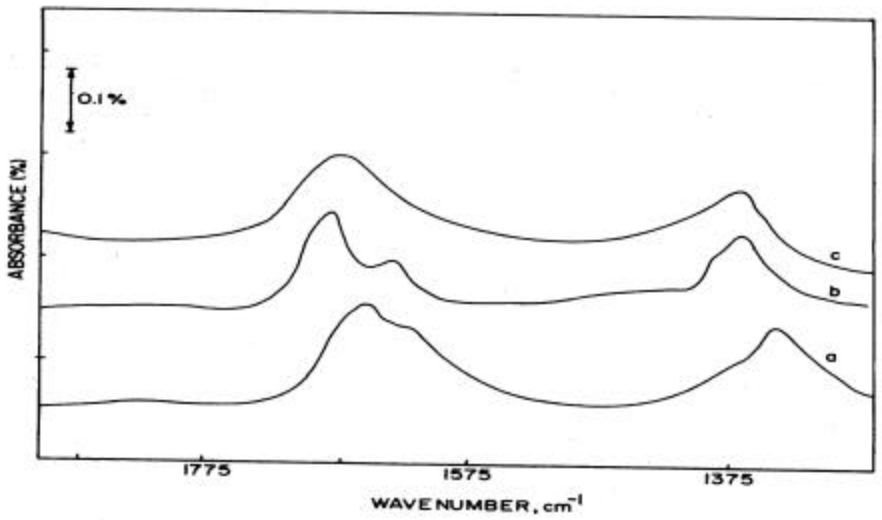

Fig. 2.10 FTIR spectra (298K) of adsorbed CO_2 in the CO_3 vibration region on (a) Cs(0.225)MCM-41; (b) Cs-Silicalite-1 and (c) Cs-Ferrierite at 5 mm equilibrium pressure of CO_2.

2355 cm^{-1} have been reported [16] for ν_3 mode of adsorbed CO_2 on NaX; a value of 2342 cm^{-1} has been reported in the case of CsX(OH). The experimental values are consistent with these reported values and are attributed to the adsorption of CO_2 on Na and Cs cations, respectively that are available in the supercages. The minor side bands at 2341 and 2351 cm^{-1} are due to the presence of less accessible Na and residual Na cations respectively.

The other set of samples, silicalite, ferrierite and MCM-41, are all pure silica polymorphs and do not possess cation exchange capacity and have different pore dimensions. Silicalite, ferrierite and MCM-41 have 5.6, 7.2 and 28Å pore openings. These samples possess mostly Cs though Na may be ppm level present as impurity (analysis not done). The prominent ν_3 mode bands are

observed for these samples at 2343, 2342 and 2341 cm^{-1} respectively, for Cs-silicalite, Cs-ferrierite and Cs-MCM-41 (Fig. 2.12). These bands are due to interaction of CO_2 with Cs cations. The regular variation from 2343 to 2341 cm^{-1} may be attributed to the systematic increase in the pore sizes and the diminishing influence of the nearby framework. The side bands at higher frequency at around 2360 cm^{-1} may be due to the impurity Na cations present. The side band at lower frequency may be due to some inaccessible Cs cations.

In summary, the data of Table 2.12 indicate that micro and mesoporous zeolites possess active sites for CO_2 adsorption on the surface of the framework and in the bulk of the intrapore volume. The topology of the surface and the intrapore volume determine the energetics of CO_2 adsorption and the v_3 mode band positions.

Of all the arguments developed for explaining the FTIR spectra of adsorbed CO_2 on alkali modified zeolite surfaces, those of Bonelli et al. [17] are very important. From FTIR, adsorption microcalorimetry and quantum chemical calculations they concluded that cation-CO_2 interaction alone can not account for the nature of the spectra of CO_2 adsorbed on alkali metal cation incorporated zeolite samples and the presence of nearby framework anionic O_2^- should also be considered. Their calculations show that in the series from Li^+ to Cs^+, the cation becomes progressively weaker Lewis acid for CO_2 adsorption; simultaneously the adjacent anionic framework surface becomes progressively stronger base causing internal compensation. This observation shows that different adsorption sites can not be treated as distinctly independent, but they

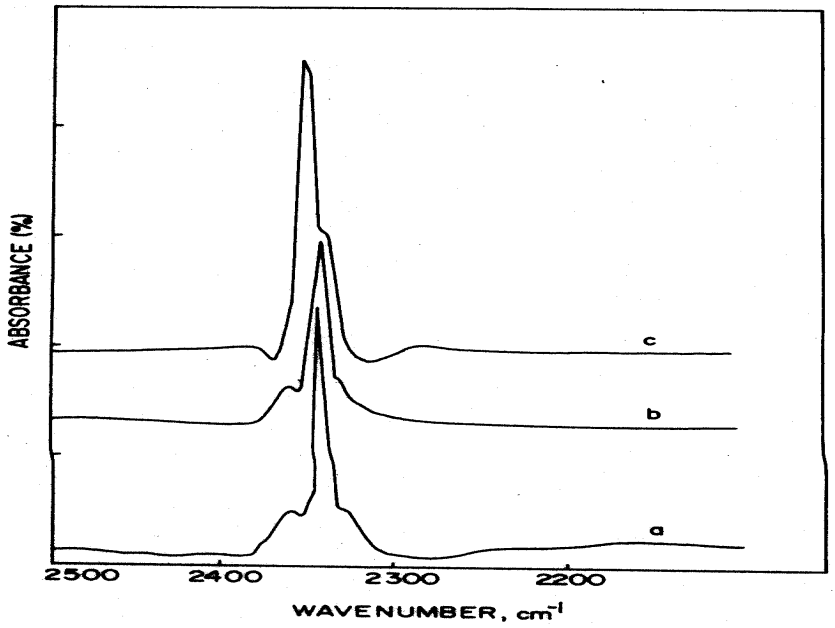

Fig. 2.11 FTIR spectra (298K) of adsorbed CO_2 (5 mm equilibrium pressure of CO_2) in the region of antisymmetric stretching on: (a) CsL; (b) CsX(OH) and (c) NaX.

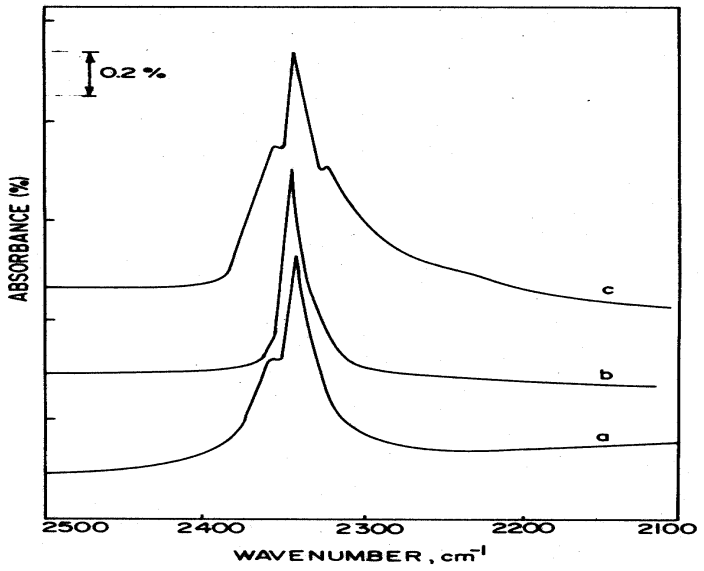

Fig. 2.12 FTIR spectra (298K) of adsorbed CO_2 (5 mm equilibrium pressure of CO_2) in the region of antisymmetric stretching on: (a) Cs-ferrierite; (b) Cssilicalite-1 and (c) Cs(0.225)MCM-41.

are influenced by each other. Hence the concept of surface and bulk adsorption sites gains relevance. So, on the basic metal sites nearest to the porous surface metal cation can coordinate one CO_2 molecule as $[Na(CO_2)]^+$, where as on the metal clusters in the bulk two CO_2 molecules can coordinate as $[Na(CO_2)_2]^+$. On the reactive surfaces of metal oxides, CO_2 can form many types of carbonate species like monodentate, bidentate and bridging bidentate carbonates, carboxylate, bicarbonate and formate. In the spectrum, the carbonate specie is characterized by a pair of bands for both symmetric and asymmetric stretching vibrations of C-O bond. These bands are located between 1850 and 1250 cm^{-1}. The splitting in these pair of bands are reported to be around 300 cm^{-1} for bidendate, 100 cm^{-1} for monodentate and less than 100 cm^{-1} for symmetric carbonate species and entirely depends on the basicity of the adsorbate.

In Table 2.13, the band positions for all the samples in this region are presented. CO_2 adsorption on cation exchanged X type zeolites develops bands at 1711,1680(sh), 1480, 1425, 1378 and 1363 cm^{-1} for Na^+ form and at 1653,1639,1386 and 1343 cm^{-1} for Cs^+ form respectively (Fig. 2. 9). These are consistent with the reported values [17]. The differences between the two high frequency bands around 1700 cm^{-1} and two low frequency bands around 1380 cm^{-1} in both of them indicate the presence of bidentate type species. Corresponding bands for CsL are observed at 1675,1647,1389 and 1343 cm^{-1} (Fig. 2.9). These bands are also consistent with the reported results and can be ascribed to bidentate type of species

.

Table 2.10 $\Delta\nu$ for different forms of carbonate specie adsorbed on alkaline-silica catalysts

Sample[a]	Type-I			Type-II		
	cm^{-1}	cm^{-1}	$\Delta\nu$	cm^{-1}	cm^{-1}	$\Delta\nu_3$
Li(1.5) SiO_2	1679	1421	258	1652	1498	154
Na(1.5) SiO_2	1683	1365	318	1643	1462	181
K(1.5) SiO_2	1663	1347	316	1633	1407	226
Cs(0.375) SiO_2	1652	1336	316	1617	1390	227
Cs(0.75) SiO_2	1651	1333	318	1619	1387	232
Cs(1.5) SiO_2	1648	1329	319	1618	1384	234
Cs(2.25) SiO_2	1645	1331	314	1617	1383	234

[a] The number in brackets denotes the mmolee alkali metal loaded per g of SiO_2.

Table 2.11 Relative basicity of alkaline samples from FTIR studies

Sample[a]	Intensity of IR spectra of CO_2	
	FTIR (0.4)[b]	FTIR (5)[c]
Li(1.5)SiO_2	92	102
Na(1.5)SiO_2	132	140
K(1.5)SiO_2	153	180
Cs(0.075)SiO_2	19	24
Cs(0.375)SiO_2	88	96
Cs(0.75)SiO_2	120	168
Cs(1.5)SiO_2	216	229
Cs(2.25)SiO_2	262	281
NaX	139	179
CsX(OH)	182	218
CsL	130	166
Cs-MCM-41	83	122
Cs-silicalite	64	80
Cs-ferrierite	49	55

[a] The number in brackets denotes the mmolee of alkali metal loaded per g of SiO_2. [b, & c] Relative band intensity of adsorbed CO_2 in FTIR spectra (1200 - 1750 cm^{-1}) at 0.4 and 5 mm equilibrium pressure, respectively.

Table 2.12 FTIR spectral bands (ν_3 vibration mode) of physisorbed CO_2 on alkaline molecular sieves

Sample			
NaX	2353	2341	
CsX(OH)	2350	2342	
CsL	2359	2343	2332
Cs-MCM-41	2359	2341	2322
Cs-silicalite	2360	2343	2331
Cs-ferrierite	2359	2342	2331

Table 2.13 FTIR spectral bands of adsorbed CO_2 in carbonate region in alkaline molecular sieves

Sample						
NaX	1711	1680	1480	1425	1378	1363
CsX(OH)	1653	1639	1620		1386	1343
CsL	1675	1647			1389	1343
Cs-ferrierite	1648				1326	
Cs-silicalite	1674	1632			1388	1366
Cs-MCM-41	1648	1630			1383	1340

2.3.6 Nuclear Magnetic Resonance Spectra (NMR)

2.3.6.1 ^{133}Cs NMR spectra

Solid state ^{133}Cs NMR spectra were obtained on a Bruker MSL 400 spectrometer operating at a ^{133}Cs frequency of 52.481 MHz. Samples for NMR measurements were prepared by packing the materials in 7 mm zirconia rotors with boron nitride caps. Experiments were carried out at room temperature. The spectra were obtained by single π / 12 pulses (2.5μsec) with a recycle delay of 1 sec. The spectral width was 125 kHz and the spinning rate was 2 to 5 kHz. The FID was processed by Bruker WIN NMR software by applying 100 Hz line broadening. An aqueous solution of Cs_2SO_4 was used as a reference (δ = 0).

The ^{133}Cs spectra of Cs-SiO_2 and Cs-MCM-41 samples are presented in Fig. 2.13 and 2.14. The relevent spectral data are presented in Table 2.14. ^{133}Cs is a quadrupolar nucleus and hence the line broadening arises from chemical shift anisotropy (CSA) and quadrupolar interaction. The CSA is small for Cs loaded MCM-41 samples (weak side bands), whereas, it is mostly absent over the Cs loaded pure silica samples. It is clearly observed from the table that the chemical shift changes from high field to low field with increasing Cs loading for both MCM-41 and pure silica samples. This suggests that the Cs nuclei become more and more mobile and isotropic with Cs loading. This is probably due to weaker interaction between the support and Cs_2O specie at higher loading. The increasing mobility (isotropic nature) of the Cs species over Cs-MCM-41 at higher loading is probably also responsible for the narrowing of the lines with Cs loading. The broadening observed (Table 2.14) in the case of Cs loaded pure silica samples is

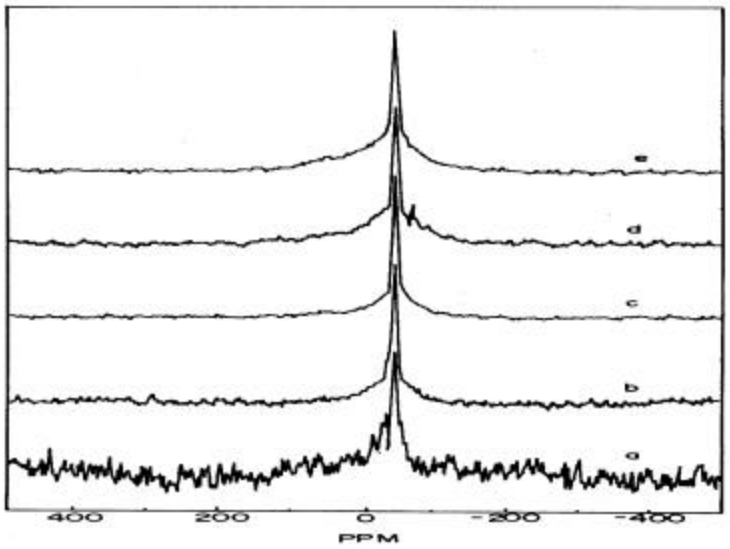

Fig. 2.13 ^{133} Cs NMR spectra of Cs-SiO_2 samples: (a) Cs(0.075)SiO_2; (b) Cs(0.375)SiO_2; (c) Cs(0.75)SiO_2; (d) Cs(1.5)SiO_2 and (e) Cs(2.250SiO_2.

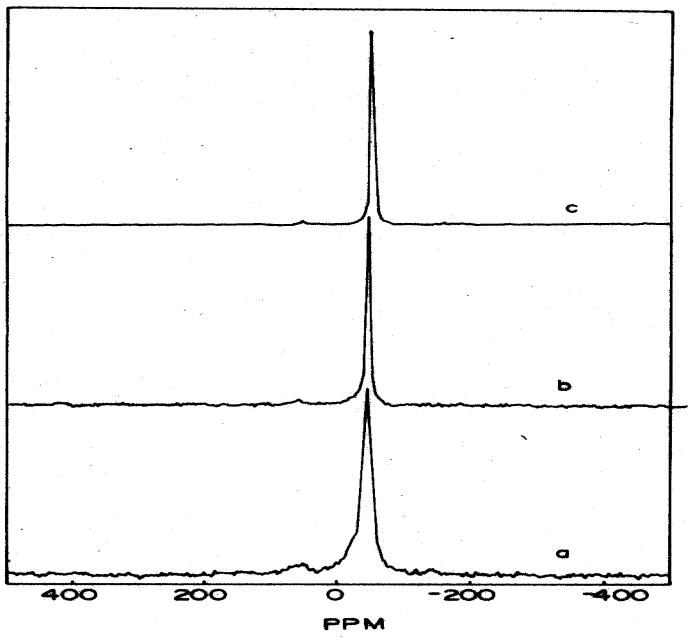

Fig. 2.14 ^{133}Cs NMR spectra of Cs-MCM-41 samples: (a) Cs(0.075)MCM-41; (b) Cs(0.15)MCM-41 and (c) Cs(0.225)MCM-41.

Table 2.14 ^{133}Cs NMR spectral data of Cs-MCM-41 and Cs-SiO_2 samples

Sample	Spinning speed (kHz)	Chemical shift of isotropic line (ppm)	Line width at half height of the central line (Hz)
Cs(0.075) MCM-41	5	-46.38	694
Cs(0.15) MCM-41	5	-39.4	305
Cs(0.225) MCM-41	5	-37.07	244
Cs(0.075)SiO_2	2.5	-47.54	366
Cs(0.375)SiO_2	5	-44.05	366
Cs(0.75)SiO_2	5	-32.42	366
Cs(1.5)SiO_2	5	-19.04	397
Cs(2.25)SiO_2	5	-19.04	488

probably due to quadrupolar interaction. It may also be due to the overlap of many closely spaced Cs lines from different Cs_2O specie present on the surface at higher loadings.

2.3.6.2 ^{29}Si MAS NMR

The ^{29}Si MAS NMR spectra were recorded on a Bruker MSL 300 spectrometer. For magic-angle spinning (MAS) NMR studies, the finely powdered samples were loaded in 7.0-mm-o.d. zirconia rotors and spun at 2.5-3.3 kHz. Experiments were carried out at room temperature (298K).

The ^{29}Si MAS NMR spectra of Cs-MCM-41 are presented in Fig. 2.15. The different environments and large range of T-O-T angles in the amorphous silica samples results in ^{29}Si NMR spectra with broad peaks for the Cs-SiO_2 samples. For Cs loaded MCM-41 with higher

Cs loading, the Q_3 / Q_4 (Q_3 from -98 to -103 ppm and Q_4 from -105 to -114 ppm) ratio becomes small suggesting the loss of silanol (-SiOH) groups through formation of Si-O-Cs specie.

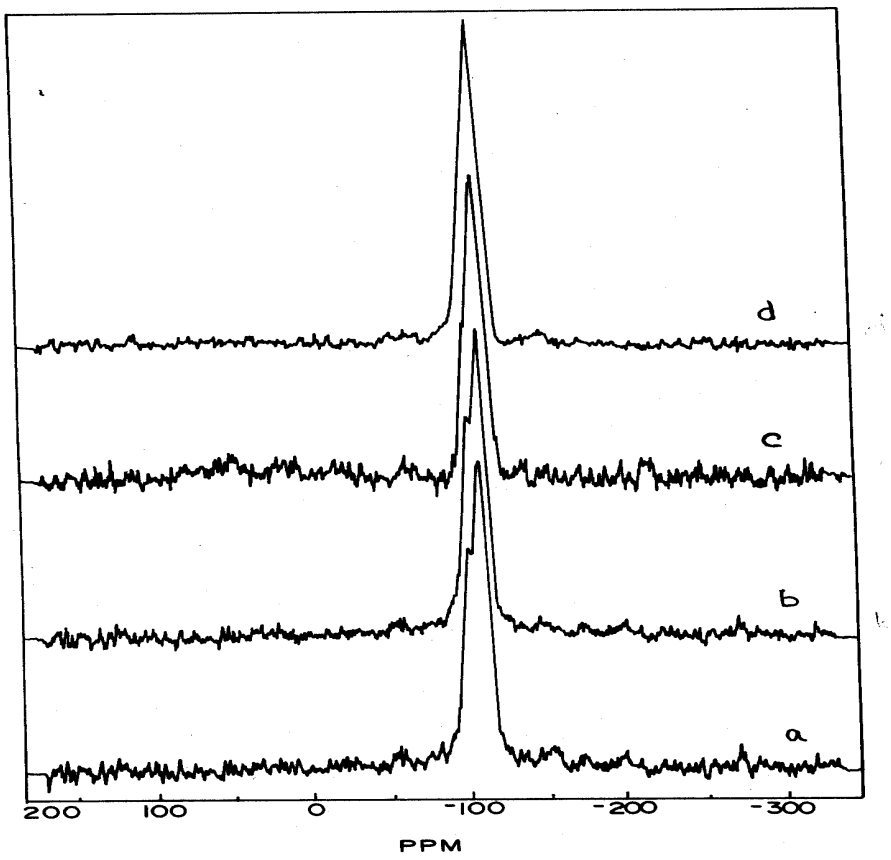

Fig. 2.15 ^{29}Si MAS NMR spectra of CS-MCM-41 samples: (a) $Cs(0.075)SiO_2$; (b) Cs(0.15)MCM-41 and (c) Cs(0.225)MCM-41.

2.3.7 Electron Spectroscopy for Chemical Analysis (ESCA)

Photoemission spectra were recorded on a VG Microtech Multilab ESCA 3000 spectrometer equipped with a twin anode of Al and Mg. All measurements were made at room temperature using non-monochromatized Mg K_α x-ray source ($h\nu$ = 1253.6 eV) on powder samples. Base pressure in the analysis chamber was maintained at 3-6 x 10^{-10} Torr range. The energy resolution of the spectrometer was measured from the full width at half maximum of metallic gold surface and the value obtained is better than 0.8 eV with MgKα radiation at pass energy of 20 eV. Binding energy calibration was performed with Au $4f_{7/2}$ core level (83.9 eV). Binding energy of adventitious carbon (284.9 eV) was utilized for charge correction with all the samples.

The X-ray photoelectron spectra of different Cs loaded SiO_2 samples did not reveal any significant change in the Cs or O binding energies with Cs loading. The relative Cs / Si contents at the surface of different Cs loaded samples were calculated from electron counts of the respective peaks for the elements (Si2p and $Cs3d_{5/2}$) and photoionisation cross sections. The Cs/Si (relative) ratios obtained for different Cs-SiO_2 catalysts are presented in Fig. 2.16. It is found that the ratio increases rapidly with Cs loading upto 1.5 mmole / g beyond which the increase is very small. This may be attributed to the presence of substantially large Cs_2O particles at higher Cs loading and saturation of Cs at the surface.

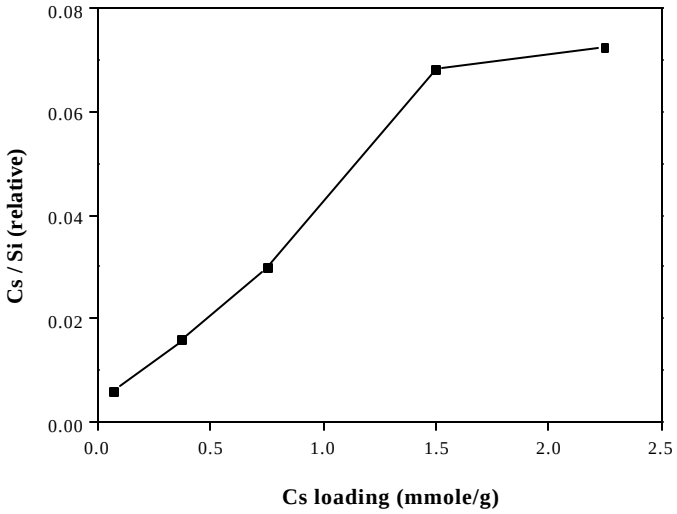

Fig. 2.16 Influence of Cs loading on surface Cs / Si ratio.

2.4 CONCLUSIONS

Alkali metal (Na, K and Cs) exchanged zeolite-X, Cs-exchanged zeolite L, Cs-impregnated fumed silica, Si-MCM-41, silicalite-1 and ferrierite samples are moderately basic. Their surface areas decrease on loading with alkali ions. The basicity of the catalysts can be estimated by temperature-programmed desorption of carbon dioxide and IR spectra of adsorbed carbon dioxide. The basicity of the catalysts increases in the order: Li < Na < K < Cs.

2.5 REFERENCES

1. F. Polak, *Int. Chem. Eng.* **11,** 449 (1971).

2. S. Sharma, Ph. D. Thesis, NCL, Pune, India (1997).

3. K. Chaudhari, T.K. Das, A.J. Chandwadkar and S. Sivasanker, *J. Catal.* **186,** 81(1999).

4. R.W. Grose and E.M. Flanigen, U.S. Patent, 4,061,721 (1977).

5. S. Shevade, Ph. D. Thesis, NCL, Pune, India (2000).

6. J. Engelhardt, J. Szanyi and J. Valyon, *J. Catal.* **107,** 296 (1987).

7. W.J. Mortier, *J. Catal.* **55,** 138 (1978).

8. E.J. Doskocil, S.V. Bordawekar and R.J. Davis, *J. Catal.* **169,** 327 (1997).

9. G. Hertzberg, " Infrared and Raman Spectra of Polyatomic Molecules", p 178, Van Nostrand, New York, 1945.

10. K. Nakamoto, "Infrared and Raman Spectra of Inorganic and Co-ordination Compounds", 3rd Edn., p243, Wiley, New York, 1978.

11. G. Busca and V. Lorenzeli, *Mater. Chem.* **7,** 89 (1982).

12. F. Solymosi and H. Knozinger, *J. Catal.* **122,** 166 (1990).

13. A. Ueno and C.O. Bennett, *J. Catal.* **54,** 31 (1978).

14. J.L. Falconer and A.E. Zagli, *J. Catal.* **62,** 280 (1980).

15. R.P. Eischens and W.A. Plisken, *Adv. Catal*. **9,** 662 (1952).

16. P.A. Jacobs, F.H. Cavwelaert and E.F. Vansant, *J. Chem. Soc., Faraday Trans.1* **69,** 2130 (1973).

17. B. Bonelli, B. Civalleri, B. Fubini, P. Ugliengo, C. Otero Arean and E. Garrone, *J. Phys. Chem. B* **104,** 10978 (2000).

CHAPTER - III

SIDE CHAIN C-ALKYLATION

SIDE CHAIN ALKYLATION OF ETHYLBENZENE AND TOLUENE WITH DIMETHYL CARBONATE

3. 1 INTRODUCTION

Side chain methylation of toluene by methanol is an important reaction, considering the usefulness of the products, particularly ethyl benzene and styrene. Alkali ion exchanged zeolites have been used as basic catalysts, the most common choice being Na-X zeolite exchanged with cesium, rubidium or potassium [1-6]. Often such basic catalysts have been modified by addition of B or P [7]; B and Cu or Ag [8]; B, P, Cu or other metals [9]; KOH or CsOH [10] or CsOAc [11]. Wang et al. [12] reported a comparison of X and ZSM-5, exchanged with K and modified with B and alkali metal hydroxides. It was found that ZSM-5, even if exchanged with strongly basic metals like Cs, catalyzed only the ring methylation of toluene [13], while the basic X-zeolite catalyzed side chain alkylation [14]. Beltrame et al. [15] studied the kinetics of side chain alkylation of toluene by methanol over basic zeolites and concluded that CsX was a good catalyst for side chain alkylation.

Side chain alkylation of toluene with isopropanol and methanol over alkali (Li, Na, K and Cs) exchanged zeolites (X, β and ZSM-5) was reported by Vasanthy et al. [16]. Isopropylation takes place exclusively at the nucleus (over Li exchange zeolites) resulting in cymenes while methylation gives xylenes and ethylbenzene, the former being the major products. According to them, side chain alkylation of toluene takes place by a cooperative action of both acidic and basic sites. Sefcik [17] investigated the zeolite catalyzed alkylation of toluene using ^{13}C NMR and suggested that the alkali cations in the X-type zeolites affect the alkylation of toluene by chemically controlling the formation of reactive intermediates

and byproducts and by sterically influencing the transition state geometry. Anderson et al. [18] investigated the side chain alkylation of toluene with methanol by solid state ^{13}C NMR over zeolite-X and concluded that methyl carbocation can be found during the formation of the surface formates. They also reported that CsX plays a crucial role, gettering these highly reactive carbocation by binding them as surface bound methyl group. Quantum mechanical calculations [19] have shown that the presence of basic sites is important to the mechanism of side chain alkylation. It was suggested that specific configurations of acidic and basic sites was crucial to the formation of reaction complexes on zeolite surfaces. Further, Raman and UV spectroscopic studies [20,21] on the interaction of aromatic molecules with alkali metal cations showed that the increase in the electrostatic field within the supercages, for large cations, leads to an increase in the interaction with the cation. This interaction is through the π-electron cloud and influence of the electrostatic field has been correlated with the selectivity of these catalysts for side chain alkylation. In situ infrared study of toluene methylation with methanol on alkali exchanged zeolites has revealed the actual structures of the surface specie and their functions in the alkylation process [22].

Huang et al. [23] reported the side chain alkylation of ethylbenzene with methanol over alkali exchanged X type zeolites to get isopropylbenzene as a major product. They reported that with KX at 773 K alkylation and dealkylation proceeded, respectively *via* carbanion and carbonium ion mechanisms, whereas dehydrogenation and demethylation occurred *via* free radical mechanisms.

The accepted reaction scheme [19, 24, 25] for side chain alkylation of toluene is as follows: (1) dehydrogenation of methanol to formaldehyde; (2) attack of formaldehyde at the methyl group of toluene to form styrene and (3) hydrogenation of styrene to ethyl benzene by

H_2 produced during methanol dehydrogenation. The side chain alkylation reactions investigated in this work are shown in Scheme 1.

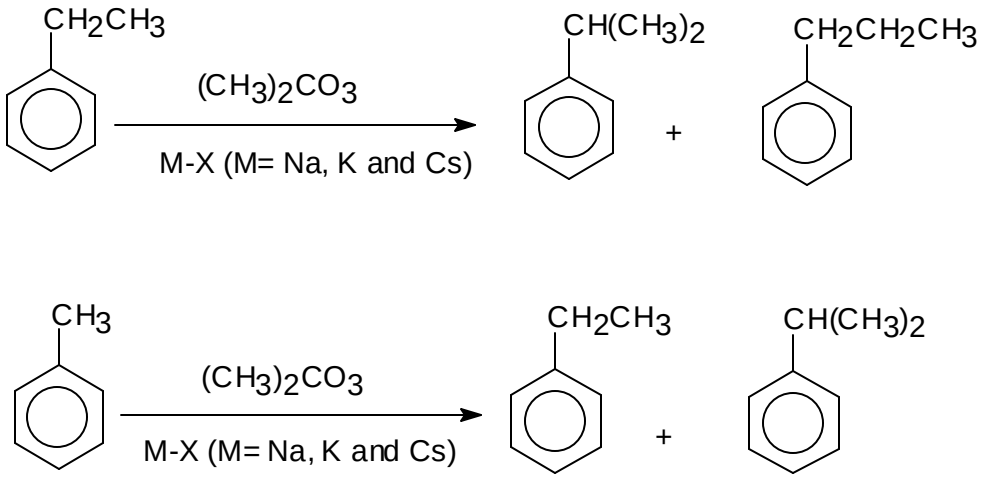

Scheme 1. Side chain C-alkylation reactions investigated in this work.

3. 2 EXPERIMENTAL

3. 2.1 Materials and catalysts

Ethylbenzene (EB; > 99% purity), toluene (> 99% purity) and dimethyl carbonate (DMC; > 99% purity) were obtained from Aldrich, USA. Ion exchanged forms of zeolite X, namely NaX, KX(Cl), KX(OH), CsX(Cl), CsX(OH) were used in the reaction. Their preparation has been reported in Chapter II.

3.2. 2 Reaction procedure

The reactions were carried out in a fixed bed down flow glass reactor (i.d. = 15 mm) at atmospheric pressure using a 2 g charge of catalyst. The zeolite powders were pelleted without any binder, crushed and sized (8-14 mesh) and were activated at 773K for 12h in air and 3h in N_2 before reaction. The mixture of EB or toluene and DMC was then feed into the reactor using a syringe pump. The liquid products were cooled in an ice trap and were collected periodically for analysis. Analysis of the gas and liquid products was carried out by gas chromatography (HP5880A) using a methyl-silicone gum capillary column (0.2 mm x 50m) with FID. The gaseous products were analyzed separately in a gas analyzer (HP5880A) with multiple packed columns. CO_2 in the outlet gas was also estimated by absorption in NaOH.

3.3 RESULTS AND DISCUSSION

3.3.1 Alkylation of EB with DMC

The reaction of DMC with ethylbenzene can be written as:

a) $2C_6H_5CH_2CH_3 + (CH_3)_2CO_3 \Rightarrow C_6H_5CH_2CH_2CH_3 + C_6H_5CH(CH_3)_2 + CO_2 + H_2O$

b) $C_6H_5CH_2CH_3 + (CH_3)_2CO_3 \Rightarrow C_6H_5CH_2CH_2CH_3 + CH_3OH + CO_2$.

In the temperature range (673 - 773K) used in these studies, all the DMC in the feed was found to have decomposed. Besides, the methanol content in the product was small (1.5 to 4% between 733- 773K), which further decreased at higher temperatures (~ 1.5% at 773K). Very little C-alkylation products (ethyl toluenes) were noticed (< 1.0 % at 733K). Carbon oxides were also found in the products and these were estimated in some experiments to calculate mass balances. The data reported in the following sections are the major hydrocarbon components estimated by gas chromatography. Detailed carbon balances carried out for some of the representative experiments were in the range 94 – 98%. Experiments were carried out in the temperature range 673 - 773K at different feed rates and feed compositions over all the catalysts listed in Table 3.1. The influence of the various reaction parameters on conversion of EB and product distribution are presented in the following sections.

3.3.1.1 Influence of process time

The activity of the catalysts increased slightly upto about 2h and then decreased continuously with process time (studied upto 6 h; Fig. 3.1 (a)). The reason for the initial increase in activities of the catalysts is not clear. The changes in yields of the different products are also similar (Fig. 3.1(b)) suggesting that the phenomenon (activation / deactivation) is related to changes occurring in the

Table 3. 1. Activity and product distribution over the catalysts

Catalyst	Conv. of EB (wt%)	Product yield (wt%)							Deactivation	
		Bz	Tol	Xy	Styrene	i-PrBz	n-PrBz	Methane	$(C_1 - C_6)^a$	Rate[b]
NaX	12	0.37	0.49	2.18	0.92	2.63	2.8	2.61	3.7	0.15
KX(Cl)	17	0.45	0.53	3.09	1.69	3.78	4.03	3.43	4.4	0.06
KX(OH)	19.4	0.56	0.68	3.48	1.78	4.1	4.7	4.09	6.1	0.07
CsX(Cl)	22.6	0.68	0.79	4.19	2.08	4.8	5.1	4.96	6.2	0.06
CsX(OH)	24.5	0.75	0.96	4.4	2.16	5.43	5.57	5.45	6.9	0.06

Conditions: Temperature = 733K, EB/DMC (mole ratio) = 5, W/F = 60 g.h.mole^{-1}, N_2/F (mole) = 5, Time on steam = 2h.

Bz = Benzene; Tol = Toluene; Xy = Xylene; i-PrBz = iso-propylbenzene; n-PrBz = n-propylbenzene.

a: $(C_1 - C_6)$ = % Conversion at 1st hour - % Conversion at 6th hour. b: Rate = $2(C_1 - C_6)/ 5(C_1 + C_6)$; conversion loss per hour per unit conversion.

catalyst. Earlier workers have also reported this behaviour during the side chain alkylation of toluene and attributed it to coke deposition and occurrence of side reactions [1]. Examining the overall activity loss over a 5h period (1h to 6h), it appears that the more basic catalysts deactivate more rapidly (Table 1; C_1 - C_6). However, when we examine the deactivation rate normalized to unit conversion (Table 1; rate, [h^{-1}.conv.$^{-1}$]), all the catalysts except NaX deactivate at nearly the same rate

3.3.1.2 Influence of basicity of the catalyst

The activities of the different catalysts at various temperatures in the alkylation of EB with DMC are presented in Fig. 3.2 (a). The product break up (at 733K) is given in Fig. 3.2 (b). The activities of the catalysts (based on EB conversion) increase with increase in basicity (decrease in intermediate electronegetivity, S_{int}) as found by earlier workers in the alkylation of toluene [10]. The yields of the side chain alkylation products (n- and i-propyl benzenes) also increase with increasing basicity. The increase in conversion and side chain alkylation activity appears to be disproportionate to the decrease in S_{int} values (comparing KX and CsX). This could be because the S_{int} values were calculated based on the overall cation contents (Na, K or Cs) eventhough the reaction may be catalyzed preferentially by the more basic Cs sites. This probably also suggests the requirement of a threshold basicity for the reaction. Styrene, which is formed by the dehydrogenation of EB over basic sites also, increases in the same manner. o-Xylene is found in much larger quantities (o-xylene, 86%, m-xylene, 7%, p-xylene, 7%) than the other xylenes suggesting that it a primary product and is probably

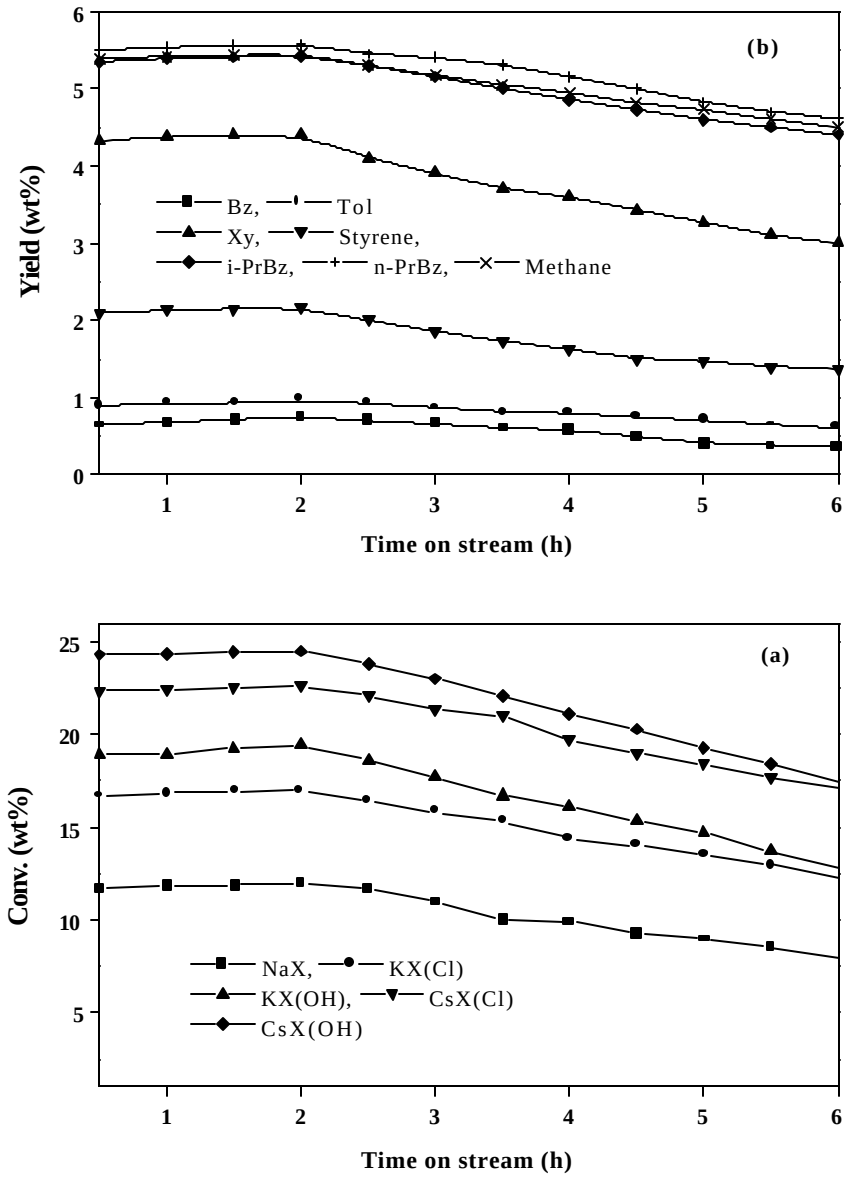

Fig. 3.1 Influence of time on stream on: (a) EB conversion over different catalysts; (b) product yields over CsX(OH). (Conditions: Temp. = 733K, EB/DMC (mole) = 5, W/F (g.h.mole^{-1}) = 60, N_2/F (mole) = 5).

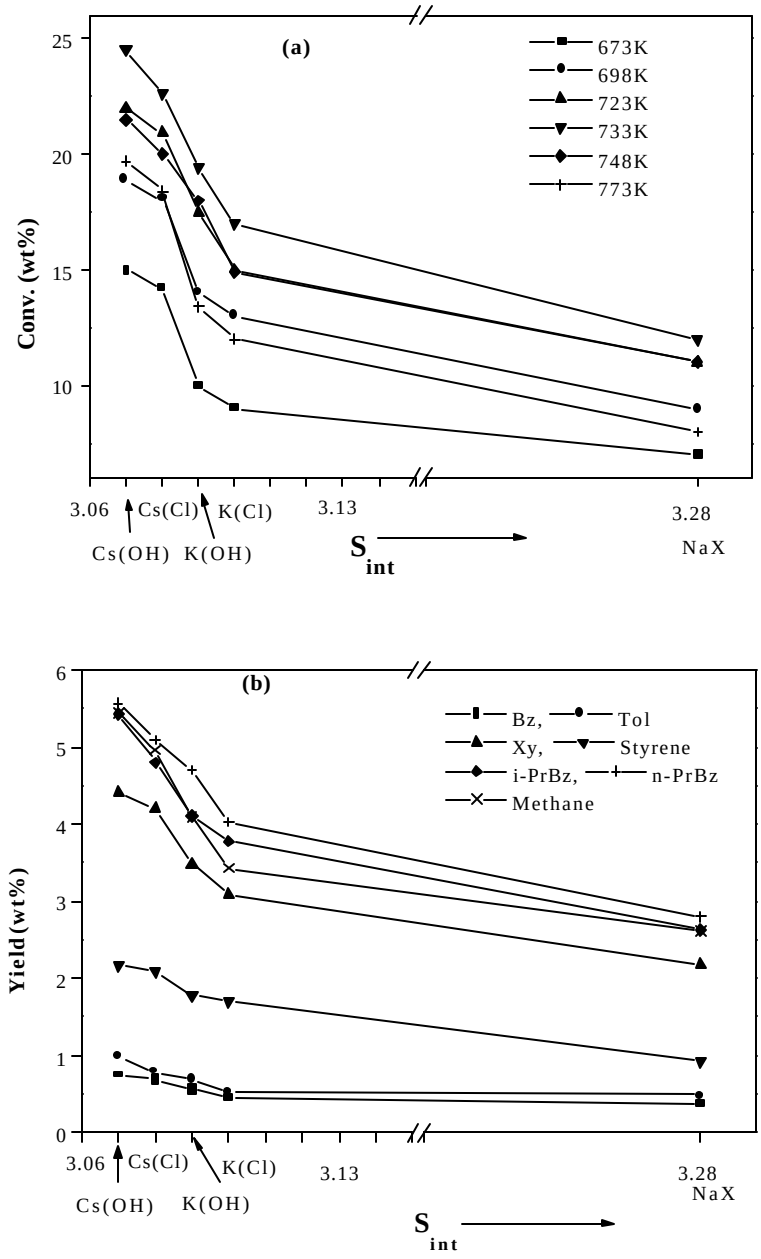

Fig. 3.2 Influence of basicity of the catalysts on: (a) EB conversion at different temperatures; (b) product yields over CsX(OH) at 733K (Conditions: EB/DMC (mole) = 5, W/F (g.h.mole^{-1}) = 60, N_2/F (mole) = 5, Process time = 2h).

formed from EB directly. The absence of strong acidity prevents the equilibration of the xylenes through carbocations and this explains the low yields of m- and p-xylenes. Small amounts of toluene and benzene are also produced presumably through dealkylation and intermolecular reactions. Higher yields of the side chain alkylation products (propylbenzenes) are obtained as reported by the earlier workers [10] on catalysts ion-exchanged with hydroxide solutions than chloride solutions. This may be due to the presence of small clusters of Cs_2O trapped inside the zeolite cages in catalysts exchanged with CsOH. Such catalysts have been reported to be highly basic by earlier workers [11,26-28]. Both conversion and activity for side chain alkylation increase in the order: NaX < KX (Cl) < KX (OH) < CsX (Cl) < CsX (OH).

3.3.1.3 Influence of temperature

Conversion is found to go through a maximum (~ 733K) with temperature over all the catalysts (Fig. 3.3 (a)). Many factors such as equilibrium constraints, changes in the nature of the catalyst with temperature, changes in adsorption coefficients of the reactants and rapid decomposition of the alkylating agent at higher temperatures could be responsible for the observed behaviour. Earlier workers have also reported a similar behaviour in the alkylation of toluene (with methanol) over similar catalysts and have attributed it to decomposition of the alkylating agent [1] and passivation of the active center [29]. We believe that the rapid decomposition of the alkylating agent (DMC) and lower adsorption coefficient of the active alkylating species at higher temperatures are probably responsible for the observed lower conversions at higher temperatures. The yields of the different

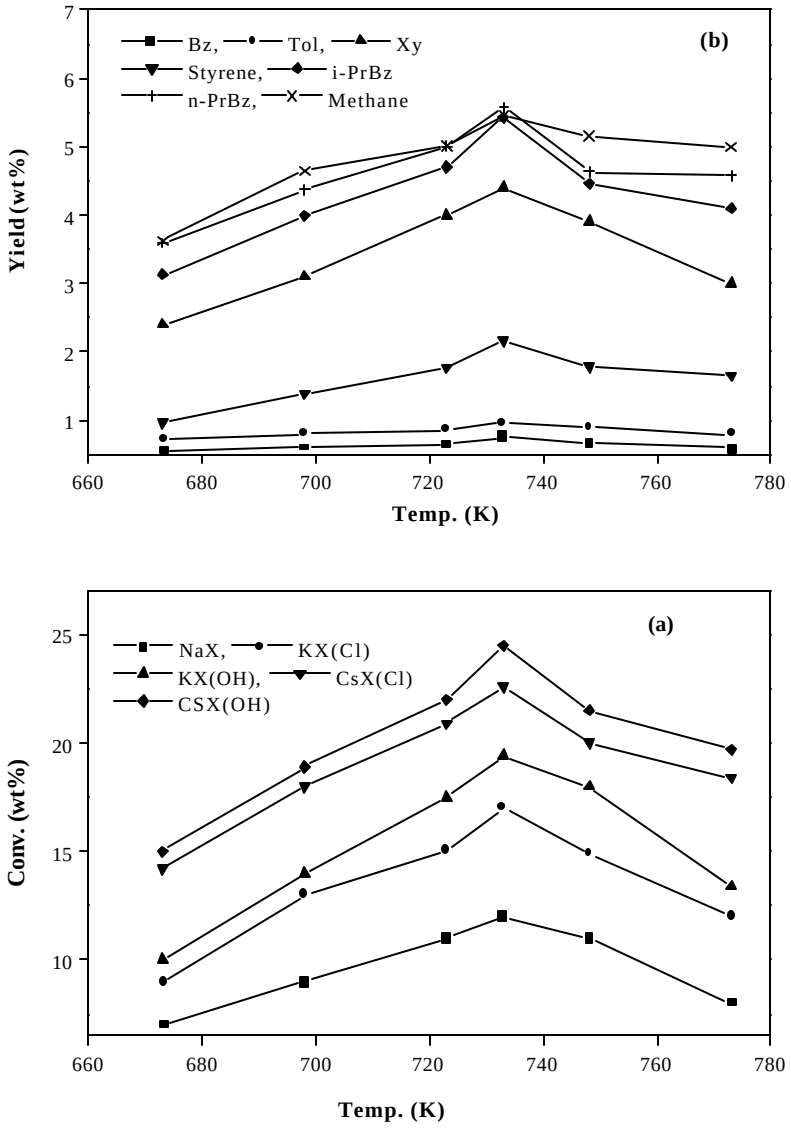

Fig. 3.3 Influence of temperature on: (a) EB conversion over different catalysts; (b) product yields over CsX (OH) (Conditions: EB/DMC (mole) = 5, W/F (g.h.mole^{-1}) = 60, N_2/F (mole) = 5, Process time = 2h).

products also go through a similar maxima at 733K (Fig. 3.3 (b)). It appears that the trend is not due to equilibrium constraints as even benzene goes through a maximum at a similar temperature range; one would expect benzene yields to increase continuously with temperature. Besides the xylenes are not present in equilibrium amounts.

3 3.1.4 Influence of contact time

The influence of contact time (W/F; g.h.mole^{-1}; W = catalyst wt., g; F = feed rate, mole h^{1}) on the reaction is presented in Fig. 3.4 (a). An increase in contact time increases conversion and product yield over all the catalysts. The product distributions obtained at different W/F values are presented in Fig. 3.4 (b) for CsX(OH). The influence of contact time on the activity of CsX(OH) at different temperatures is presented in Fig. 3.4 (c). The results show that the activities of the catalysts increase with contact time at all the temperatures investigated and go through a maximum (at 733K) at all the contact times investigated. Plots of product yields over CsX(OH) as a function of conversion are presented in Fig. 3.4 (d). It is noticed that the yields of the propylbenzenes, xylenes and methane can be extrapolated to origin suggesting these to be the primary products.

3.3.1.5 Influence of molar ratios of reactants

Increasing the EB/DMC molar ratio increases EB conversion over all the catalysts (Fig. 3.5 (a)). This increase suggests a positive order for the reaction with respect to EB. The effect is less beyond EB/DMC = 1 due to the diminished availability of the alkylating agent at the surface. The yields of the primary products (propyl benzenes and methane) increase more rapidly with increase in the EB / DMC ratio than the other products (Fig. 3.5 (b)).

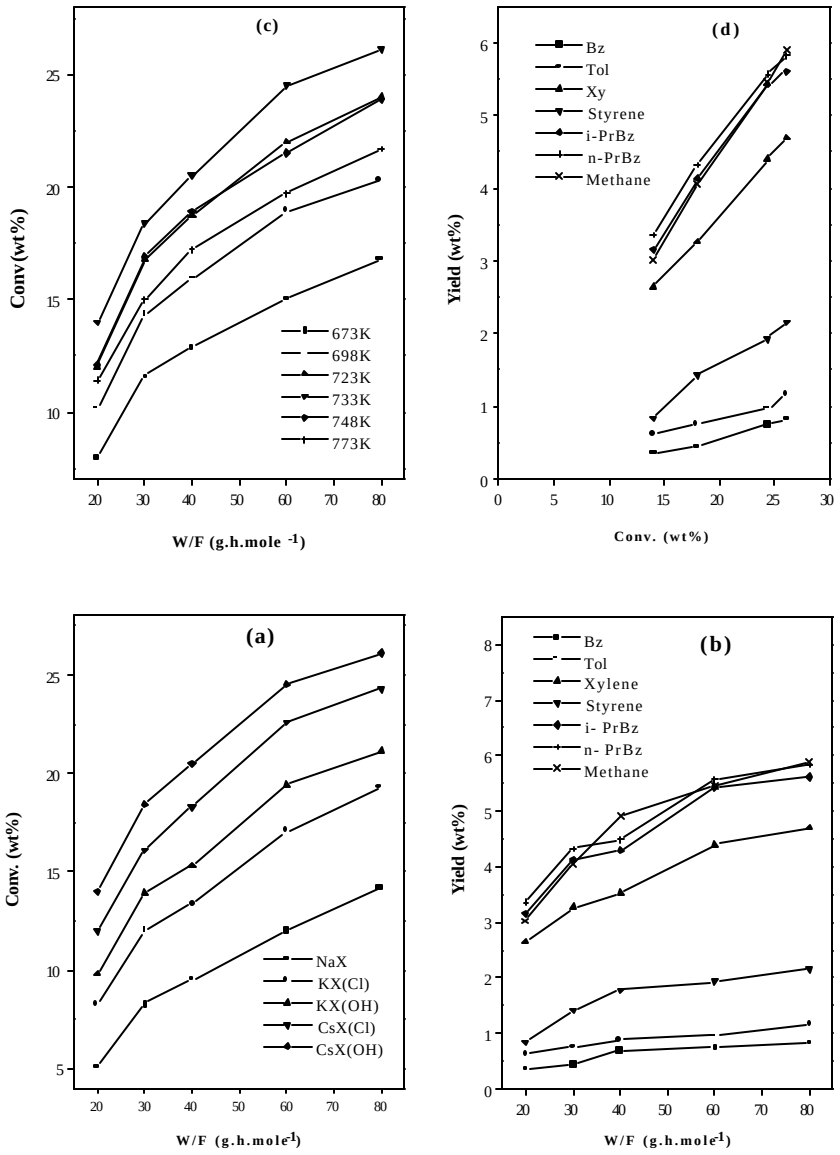

Fig. 3.4 Influence of contact time on: (a) EB conversion over different catalysts at 733K; (b) product yields over CsX(OH); (c) EB conversion at different temperatures over CsX(OH); (d) product yields at different conversions over CsX(OH) at 733K (Conditions: EB/DMC (mole) = 5, N_2/F (mole) = 5, process time = 2h).

3.3.1.6 Influence of carrier gas (N_2)

The carrier gas (N_2) has a substantial effect on the conversion of EB. The effect of carrier gas on conversion and product yields is presented in Fig. 3.6(a) and (b), respectively. The reason for the increase in conversion observed with increase in N_2 flow rate (N_2/F) is not clear. It is probably due to desorption of strongly adsorbed CO_2 (formed from DMC decomposition) from the surface of the catalyst.

3.3.1.7 Reaction mechanism

The side chain alkylation of toluene by methanol has been suggested to occur over basic sites in alkali exchanged zeolites [1, 3, 15]. Some workers have also proposed a cooperative action of acidic and basic sites in side chain alkylation, the basic site activating the side chain and the acidic site adsorbing the benzene ring [9]. While alkylation using methanol has been suggested to take place through the intermediate HCHO, DMC has been reported to alkylate through CH_3^+ [17]. Based on the suggestions of the earlier workers and the results of the present studies, the formation of the major products during the alkylation of EB with DMC can be rationalized as shown below

1. Activation of EB on a basic site:

$C_6H_5CH_2CH_3 + B^- \Rightarrow C_6H_5CH_2CH_2^- + BH$ (B^- = Basic site)

$C_6H_5CH_2CH_2^- \Leftrightarrow C_6H_5CH^-CH_3$

2. Formation of propylbenzenes:

$C_6H_5CH_2CH_2^- + (CH_3)_2CO_3 + BH \Rightarrow C_6H_5CH_2\,CH_2\,CH_3 + CH_3OH + CO_2 + B^-$

$C_6H_5CH^-CH_3 + (CH_3)_2CO_3 + BH \Rightarrow C_6H_5CH_2\,(CH_2)_2 + CH_3OH + CO_2 + B^-$

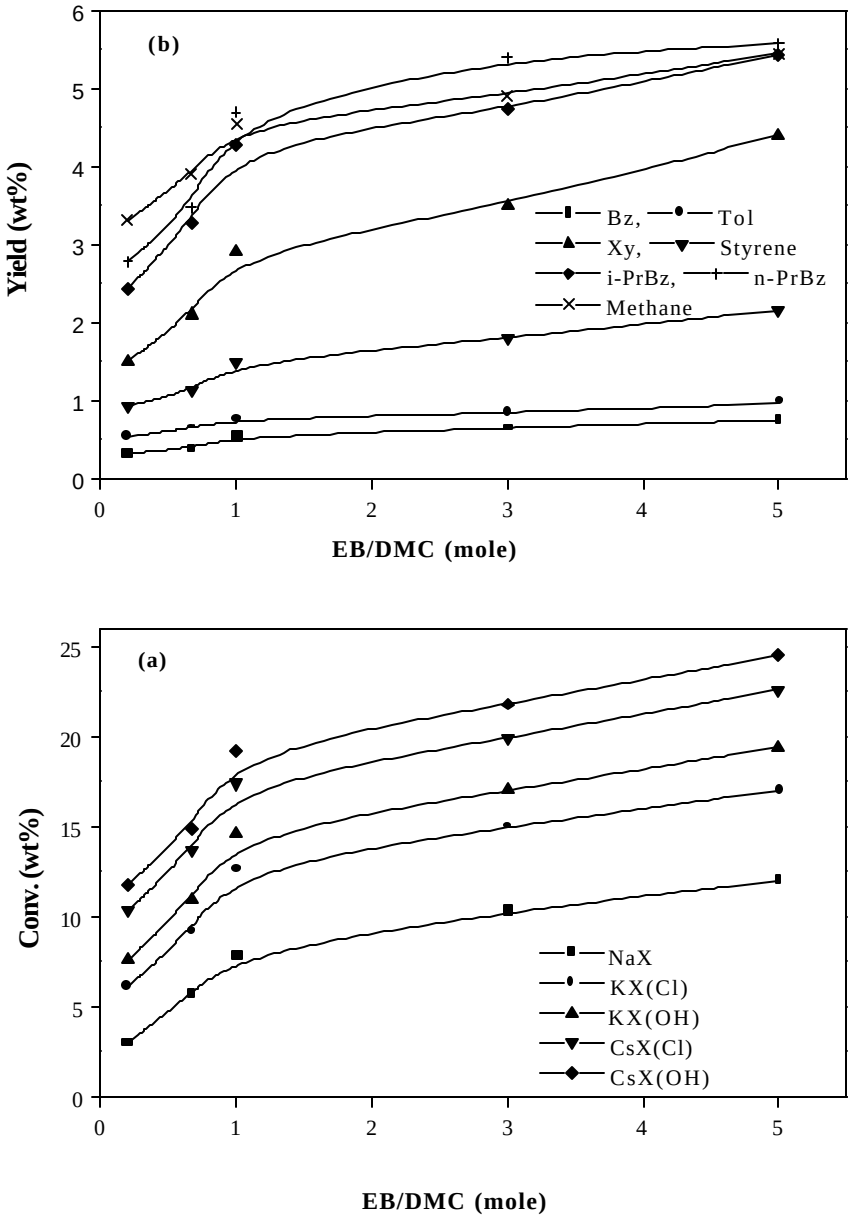

Fig. 3.5 Influence of EB/DMC mole ratio on: (a) EB conversion over the different catalysts; (b) product yields over CsX(OH) (Conditions: Temperature = 733K, W/F (g.h.mole^{-1}) = 60, N_2/F (mole) = 5, Process time = 2h).

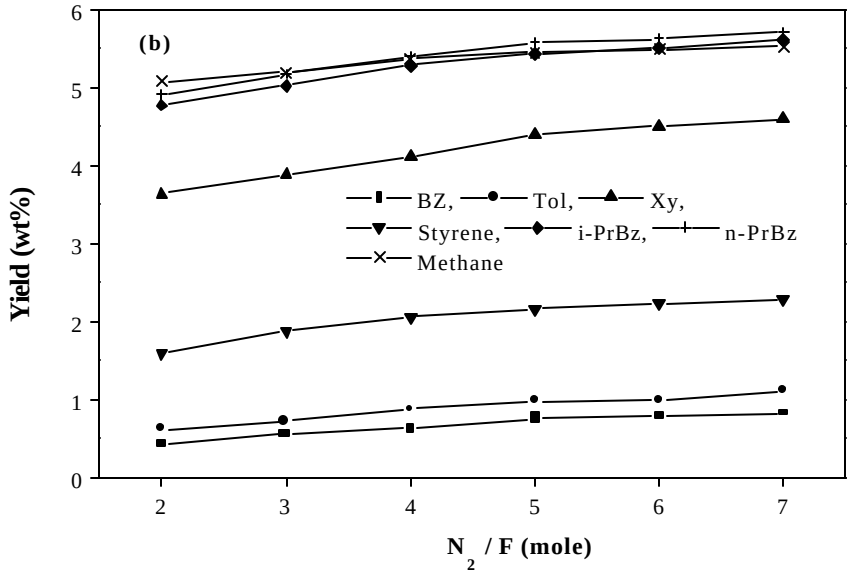

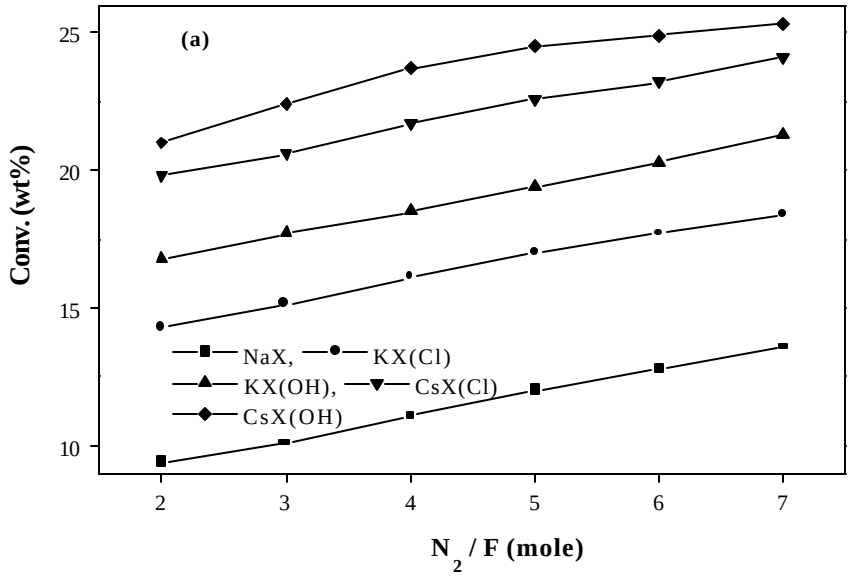

Fig. 3.6 Influence of carrier gas on: (a) EB conversion over different catalysts; (b) product yields over CsX(OH) (Conditions: Temperature = 733K, time on stream = 2h, contact time ($g.h.mole^{-1}$) = 60, EB / DMC (mole) = 5).

n-propylbenzene is a little more likely to be produced (as observed) as the primary carbanion is more stable due to resonance with the phenyl group.

3. Formation of o-xylene and styrene:

$(CH_3)_2CO_3 \Rightarrow CH_3^+ + CO_2 + CH_3OH$

$C_6H_5CH_2CH_3 + CH_3^+ \Rightarrow CH_4 + C_6H_5CH^+CH_3$

$C_6H_5CH^+CH_3 \Leftrightarrow CH_3C_6H_4CH_2^+$

$CH_3C_6H_4CH_2^+ + C_6H_5CH_2CH_3 \Rightarrow CH_3C_6H_4CH_3$ (o-Xylene) $+ C_6H_5CH^+CH_3$

$C_6H_5CH^+CH_3 + C_6H_5CH_2CH_2^- \Rightarrow C_6H_5CH{=}CH_2 + C_6H_5CH_2CH_3$

3.3.2 Side chain alkylation of toluene with dimethyl carbonate

The reaction of DMC with toluene can be written as:

a) $C_6H_5CH_3 + (CH_3)_2CO_3 \Rightarrow C_6H_5CH_2CH_3 + CH_5OH + CO_2$

b) $C_6H_5CH_2CH_3 + CH_3OH \Rightarrow C_6H_5CH(CH_3)_2 + H_2O.$

In the temperature range (673 - 773K) used in the studies, not only all the DMC was found to have decomposed, the methanol content in the product was also small (1.0 to 3% between 698 - 773K). Very little C-alkylation products (xylenes) were noticed. Experiments were carried out in the temperature range 673 - 773K at different feed rates and feed compositions over all the catalysts listed in Table 3. 2. The influence of various process parameters on conversion of EB and product distribution are presented in the following sections.

3.3.2.1 Influence of process time

The activity of the catalysts increased slightly upto about 2h and then decreased continuously with process time (studied upto 6 h; Fig. 3.7 (a)). The reason for the initial increase in activities of the catalysts is not clear. The changes in yields of the different products are also similar suggesting that the

phenomenon (activation / deactivation) is probably related to changes in the catalyst. Earlier workers have also reported this behaviour during the side chain alkylation of toluene with methanol and attributed it to deactivation of catalyst and occurrence of side reaction [1]. The average deactivation rate per unit conversion calculated over a six hour period for all the catalysts are reported in Table 3.2. The results reveal, as observed in the case of EB alkylation, that the less basic catalysts deactivate more rapidly.

3.3.2.2 Influence of basicity of the catalyst

The activities of the different catalysts at various temperatures in the alkylation of toluene with DMC are presented in Fig. 3.8 (a). The product break up (at 698K) is given in Fig. 3.8 (b). The activities of the catalysts (based on toluene conversion) increase with increase in basicity (decrease in intermediate electronegetivity, S_{int}) as found by earlier workers [10]. The yields of the side chain alkylation products (ethylbenzene and i-propyl benzene) also increase with increasing basicity. A small amount of benzene was also produced presumably through dealkylation and intermolecular reactions. Higher yields of the side chain alkylation products (ethylbenzene and i-propyl benzene) are obtained on catalysts ion-exchanged with hydroxide solutions [3] than chloride solutions. Both conversion and activity for side chain alkylation increase in the order: NaX < KX (Cl) < KX (OH) < CsX (Cl) < CsX (OH).

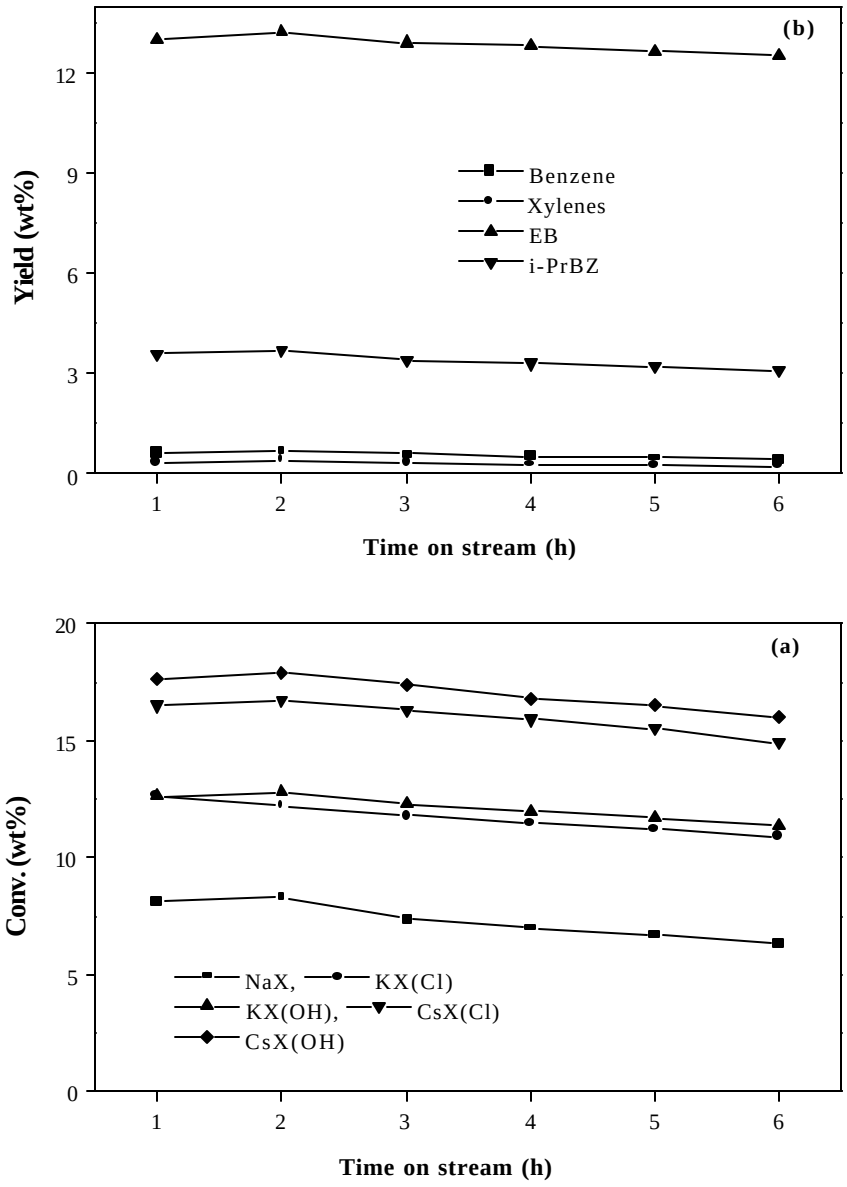

Fiig. 3.7 Influence of process time on: (a) toluene conversion over different catalysts; (b) product yields over CsX(OH) (Conditions: Temp. = 698K, toluene / DMC (mole) = 5, W/F (g.h.mole $^{-1}$) = 30, N_2/F (mole) = 5).

Table 3. 2 Activity and product distribution over the catalysts

Catalyst	Conv.	Yield (wt%)				Deactivation	
	(wt %)	Benzene	Xylenes	EB	i-PrBz	$(C_1 - C_6)^a$	Rate[b]
NaX	8.31	0.41	0.19	5.92	1.79	1.8	0.05
KX(Cl)	12.57	0.47	0.28	9.17	2.65	1.7	0.03
KX(OH)	13.17	0.53	0.31	9.51	2.82	1.2	0.02
CsX(Cl)	16.72	0.59	0.36	12.38	3.39	1.6	0.02
CsX(OH)	17.94	0.68	0.41	13.18	3.67	1.6	0.02

Conditions: Temperature = 698K, Toluene / DMC (mole) = 5, W/F ($g.h.mole^{-1}$) = 30, N_2/F (mole) = 5, Time on steam = 2h.
a: $(C_1 - C_6)$ = % Conversion at 1st hour - % Conversion at 6th hour. b: Rate = $2(C_1 - C_6)/ 5(C_1 + C_6)$; conversion loss per hour per unit conversion.

3.3.2.3 Influence of temperature

Conversion goes through a maximum (~ 698K) with temperature over all the catalysts (Fig. 3.9 (a)). Many factors such as equilibrium constraints, changes in the nature of the catalyst with temperature, changes in adsorption coefficients of the reactants and rapid decomposition of the alkylating agent at higher temperatures could be responsible for the observed behaviour. We believe that the rapid decomposition of the alkylating agent and lower adsorption coefficient of the active alkylating species at higher temperatures are probably responsible for the observed deactivation behaviour which has also been reported by earlier workers in the alkylation of toluene with methanol [1]. The yields of the different products also go through similar maxima at 698K (Fig. 3.9 (b)).

3.3.2.4 Influence of contact time

The influence of contact time (W/F; g.h.mole^{-1}; W = catalyst wt., g ; F = feed rate, mole h^{-1}) on the reaction is presented in Fig. 3.10 (a). An increase in contact time increases conversion and product yields over all the catalysts. The product distribution at different W/F values is presented in Fig. 3.10 (b) for CsX(OH). Plots of product yields over CsX(OH) as a function of conversion are presented in 3.10 (c). It is noticed that the yields of EB and isopropylbenzene are extrapolatable to origin suggesting these to be the primary products. It appears that both EB and i-propylbenzene are formed from the same adsorbed intermediate as shown below:

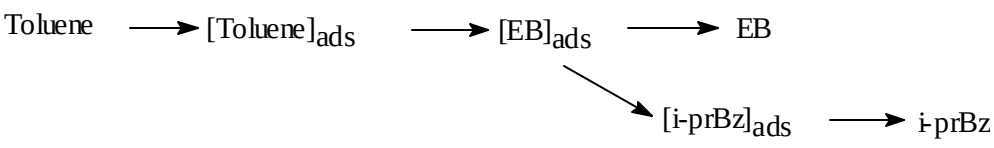

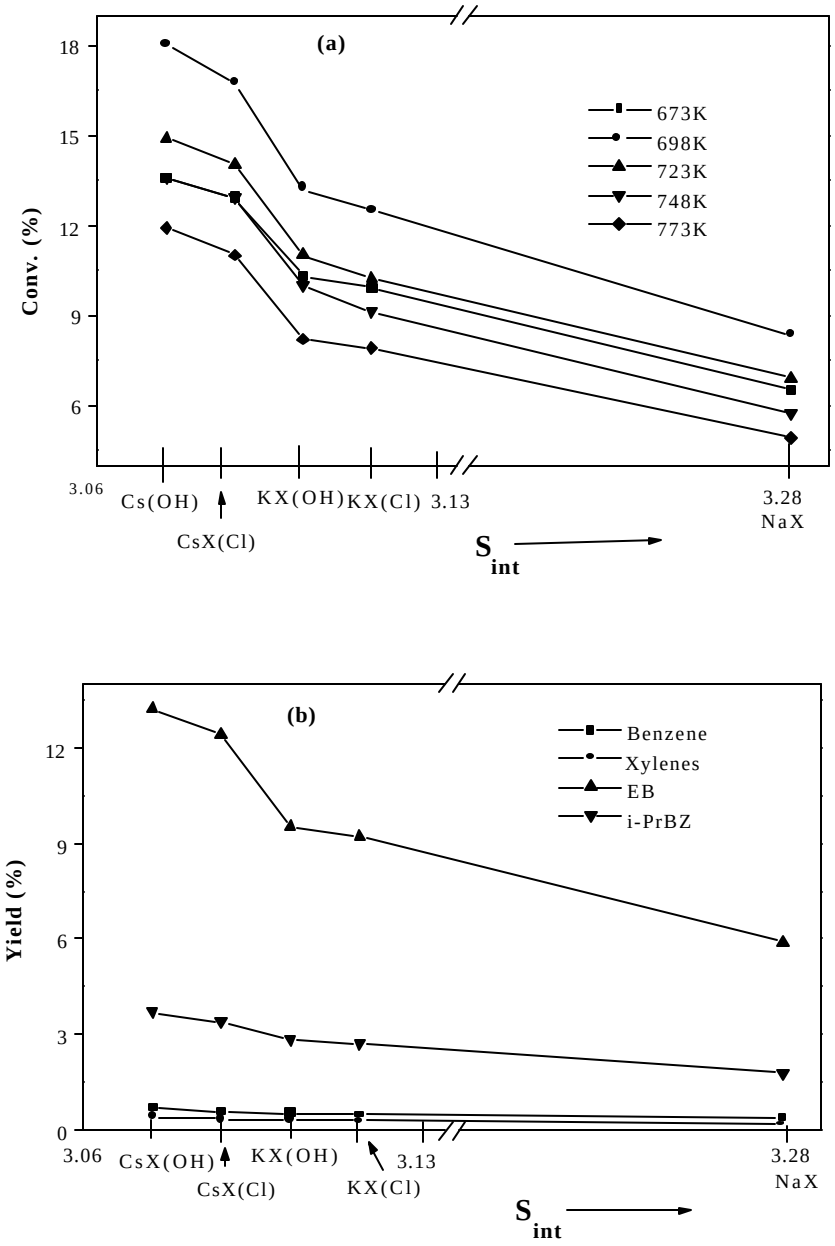

Fig. 3.8 Influence of basicity of the catalysts on: (a) toluene conversion at different temperatures; (b) product yields over CsX(OH) at 698K (Conditions: Toluene / DMC (mole) = 5, W/F (g.h.mole^{-1}) = 30, N_2/F (mole) = 5, Process time = 2h).

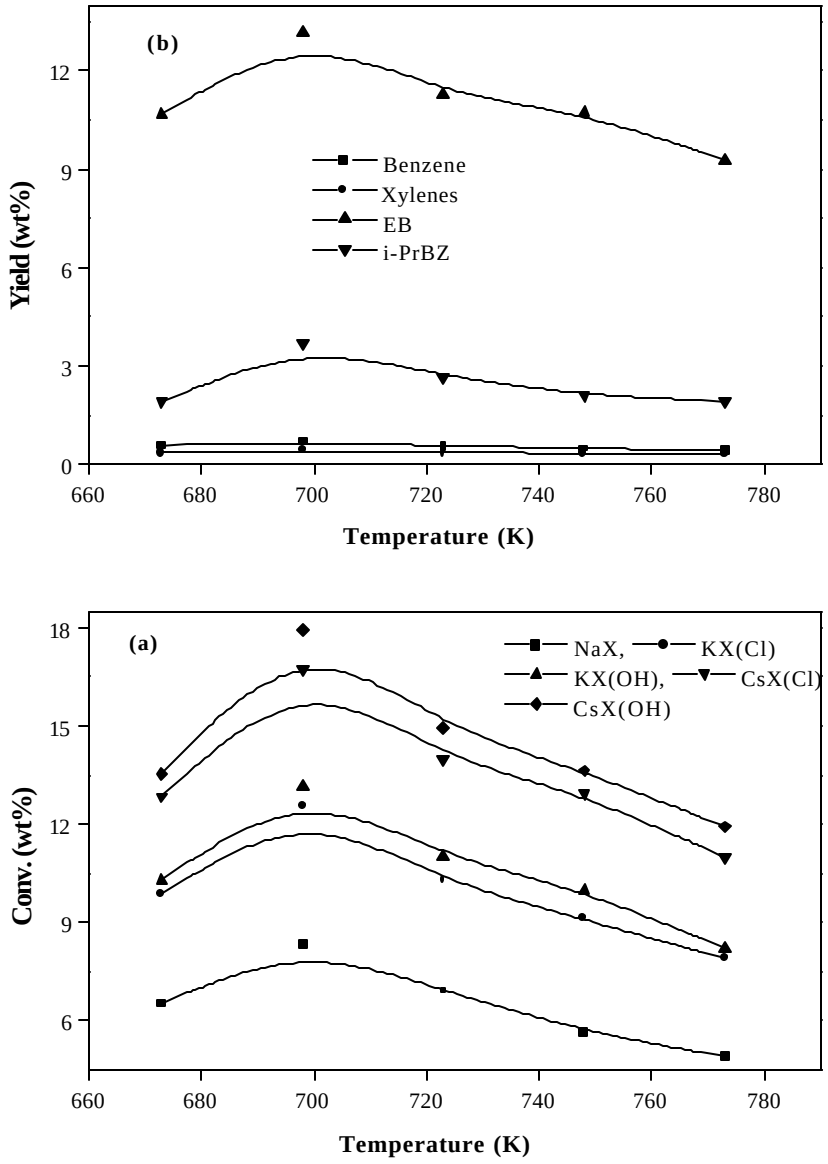

Fig. 3.9 Influence of temperature on: (a) toluene conversion over different catalysts; (b) product yields over CsX (OH) (Conditions: Toluene / DMC (mole) = 5, W/F ($g.h.mole^{-1}$) = 30, N_2/F (mole) = 5, Process time = 2h).

3.3.2.5 Influence of molar ratios of reactants

Increasing the toluene/DMC molar ratio increases toluene conversion over all the catalysts (Fig. 3.11 (a)). This increase suggests a positive order for the reaction with respect to toluene. The effect is less beyond toluene/DMC = 1 due to the diminished availability of the alkylating agent at the surface. The yields of the primary products (ethyl and propylbenzenes) increase more rapidly with increase in the toluene / DMC ratio than the other products (Fig. 3.11 (b)).

3.3.2.6 Reaction mechanism

The side chain alkylation of toluene by methanol has been suggested to occur over basic sites in alkali exchanged zeolites [1, 3, 14]. Some workers have also proposed a cooperative action of acidic and basic sites in side chain alkylation, the basic site activating the side chain and the acidic site adsorbing the benzene ring [9]. While alkylation using methanol has been suggested to take place through the intermediate HCHO, DMC has been reported to alkylate through CH_3^+ [15].

The alkylation of toluene to EB with DMC is shown below

$$C_6H_5CH_3 + (CH_3)_2CO_3 \rightarrow C_6H_5C_2H_5 + CH_3OH + CO_2.$$

The formation of i-propylbenzene probably occurs by the reaction of EB with methanol as shown below [24]

$$CH_3OH \rightarrow HCHO + H_2$$

$$C_6H_5C_2H_5 + HCHO \rightarrow C_6H_5C(CH_3)=CH_2 + H_2O$$

$$C_6H_5C(CH_3)=CH_2 + H_2 \rightarrow C_6H_5CH(CH_3)_2$$

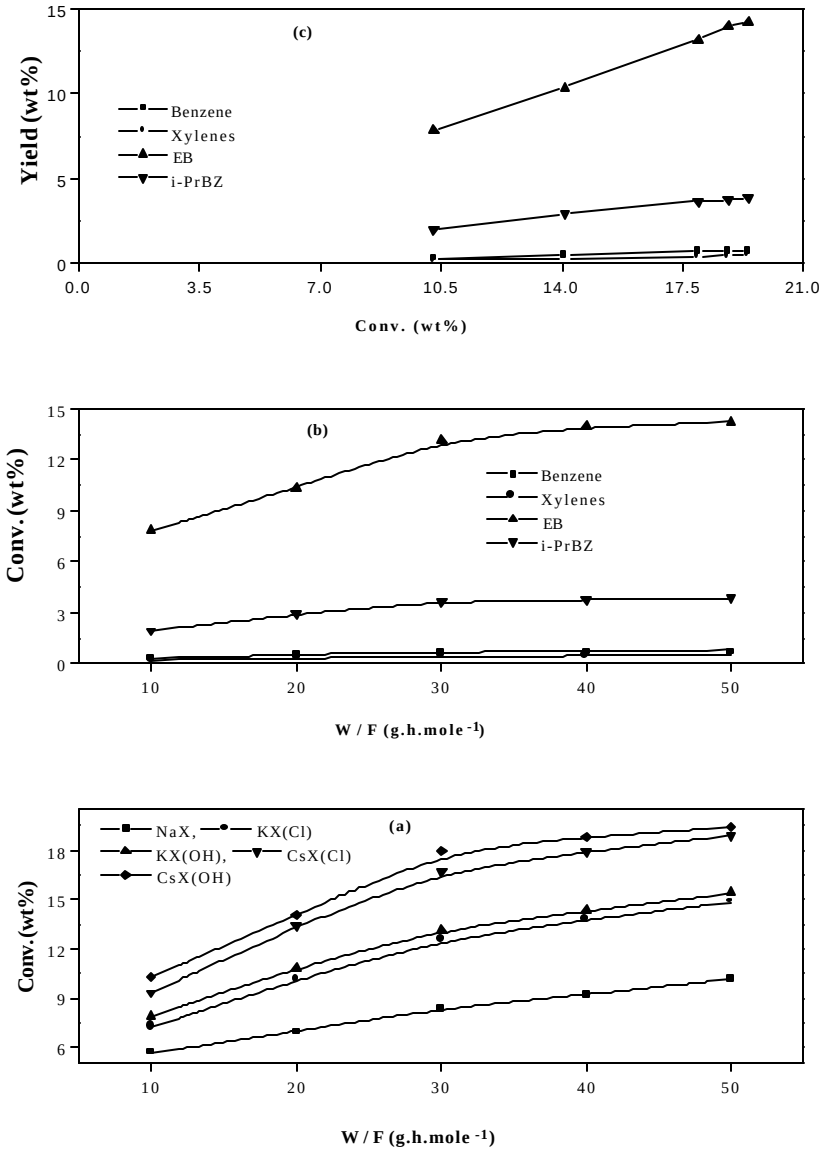

Fig. 3.10 Influence of contact time on: (a) toluene conversion over different catalysts at 698K; (b) product distribution over CsX(OH); (c) product yields at different conversions over CsX(OH) (Conditions: Temperature = 698K, toluene / DMC (mole) = 5, N_2/F (mole) = 5, process time = 2h).

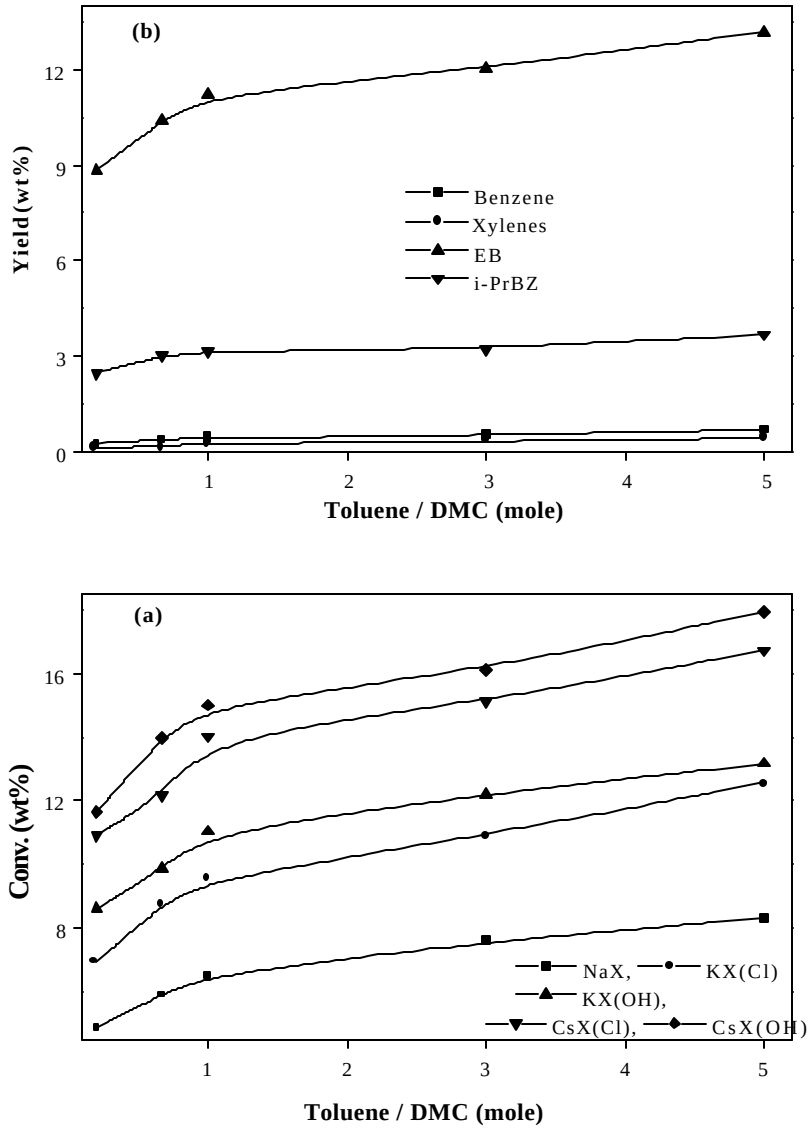

Fig. 3.11 Influence of toluene / DMC mole ratio on: (a) toluene conversion over the different catalysts; (b) product yields over CsX(OH) (Conditions: Temperature = 698K, W/F (g.h.mole^{-1}) = 30, N_2/F (mole) = 5, Process time = 2h).

3. 4 CONCLUSIONS

Alkylation of ethylbenzene (EB) and toluene with dimethylcarbonate (DMC) is promoted by alkali exchanged zeolite-X. Propylbenzenes (n- and i-) are the major products besides styrene and o-xylene in the alkylation of ethyl benzene. In the case of toluene alkylation, ethylbenzene is the major product besides i-propylbenzene, which is the doubly methylated product. Side chain alkylation activity increases with increasing basicity of the exchanging cation. The catalysts prepared by exchanging with alkali hydroxides were more active than those prepared from chlorides. Conversion of EB (or toluene) and the yield of the products are maximum at a process time of 2 h. Maximum EB conversion and side chain alkylation product formation are observed at ~733K at an EB/DMC mole ratio of 5 and a W/F ($g.h.mole^{-1}$) of 60. Maximum toluene conversion and side chain alkylation product formation are observed at ~698K at toluene/DMC mole ratio of 5 and a W/F ($g.h.mole^{-1}$) of 30.

3. 5 REFERENCES

1. T. Yashima, K. Sato, T. Hayasaka and N. Hara, *J. Catal*. **26,** 303 (1972).
2. H. Itoh., T. Hattori, K. Suzuki and Y. Murakami, *J. Catal*. **79**, 21 (1983).
3. C.H. Liu (Exxon), U. S. Pat. 1984, 4,463,204.
4. J.M. Garces, G.E. Vrieland, S.I. Bates, F.M. Scheidt and F.M. Basico, *Stud. Surf. Sci. Catal*. **20,** 67 (1985).
5. N. Giordano, L. Pino, S. Cavallaro, P. Vitarelly and B. S. Rao. *Zeolites* **7,** 131 (1987).
6. S. Zheng, J. Cai, D. Liu, *Proceedings of the Ninth International Congress on*

Catalysis; Chemical Institute of Canada: Ottawa **1,** 476 (1988).

7. M. L. Unland and G. E. Barker, (Monsanto) Zeolite Catalyst. U.S. Pat. 4,115,424 (1978).
8. C. Lacroix, A. Deluzarche, A. Keinnemann and A. Boyer, *J. Chim. Phys.* **b,** 81, 473, 481, 487 (1984).
9. H.C. Liu and R.J. Spohn, U.S. Patent. 4,483,936, 1984.
10. J. Engelhardt, J. Szanyi and J. Valyon., *J. Catal.* **107**, 296 (1987).
11. P. E. Hathaway and M. E. Davis, *J. Catal* **116**, 263 (1989).
12. X. Wang, G. Wang, D. Shen, C. Fu and M. Wei, *Zeolites* **11,** 254 (1991).
13. C. Yang and Z. Meng, *Appl. Catal.* **71,** 45 (1991).
14. H. Vinek, M. Derewinski, G. Mirth and J. A. Lercher, *Appl. Catal.* **68,** 277 (1991).
15. P. Beltrame, P. Fumagalli and G. Zeretti, *Ind. Eng. Chem. Res.* **32,** 26 (1993).
16. B.K. Vasanthy, M. Palanichamy and V. Krishnaswamy, *Appl. Catal.A: Gen.* **148,** 51 (1996).
17. M. D. Sefcik, *J. Am. Chem. Soc.* **101**, 2164 (1979).
18. A. Philippou and M.W. Anderson, *J. Am. Chem. Soc.* **116,** 5774 (1994).
19. H. Itoh, A. Miyamoto and Y. Murakami, *J. Catal.* **64**, 284 (1980).
20. J. J. Freeman and M. L. Unland, *J. Catal.* **54**, 183 (1978).
21. M. L. Unland and J. J. Freeman , *J. Phys. Chem.* **82**, 1036 (1978).
22. S.T. King and J.M. Graces, *J. Catal.* **104,** 59 (1987).
23. C.S. Huang and A.-N. Ko, *Catal. Lett.* **19,** 319 (1993).
24. Y. N. Sidorenko, P. N. Galich and V.S. Gutyrya, II' in V.G., Neimark, I.E. *Dokl. Akad. Nauk SSSR* **173,** 132 (1967).
25. Y.N. Sidorenko and P. N. Gallich, *Ukr. Khim. Zr.* **36,** 1234 (1970).

26. P.E. Hathaway and M.E. Davis, *J. Catal*. **116,** 279 (1988).

27. P.E. Hathaway and M.E. Davis, *J. Catal*. **119,** 497 (1988).

28. J.C. Kim, H.-X. Li, C.-Y. Chen and M. Davis, *Microporous Mater*. **2,** 413 (1994).

29. A.N. Vasiliev and A.A. Galinsky, *React. Kinet. Catal. Lett*. **51,** 253 (1993).

CHAPTER - IV

0-ALKYLATION

ALKYLATION REACTIONS OF HYDROXY AROMATIC COMPOUNDS OVER ALKALI LOADED SILICA

4. 1 INTRODUCTION

The large E-factors (kg waste / kg product) [1] of most processes used at present in the fine chemicals industry make the development of environmentally clean and economical processes based on solid catalysts highly relevant. Though liquid acids have been replaced by solids such as zeolites in numerous reactions, the application of solid bases in fine chemical production is not yet common. Many inorganic solid bases like alkali modified zeolites, either through ion exchange or by decomposition of alkali salts in the zeolite cages have recently been found useful in the production of fine chemicals [2-13].

O-alkylated products of phenol, the aryl alkyl ethers, of which anisole is the simplest member, are important industrial chemicals that are extensively used as starting materials in the production of dyes and agrochemicals, as antioxidants for oils and grease and as stabilizers for plastics. Conventionally, alkyl aryl ethers can be prepared by Williamson ether synthesis, which requires an alkyl halide and a stoichiometric amount of sodium hydroxide. Conventional processes are atom inefficient and generate waste. For example, if one were to alkylate cresol stoichiometrically with dimethyl sulfate and neutralize the H_2SO_4 with sodium carbonate, the atom efficiency (AE) would be just 0.58 [1]. On the other hand, the direct methylation with methanol will have an AE of 0.87, the only byproduct being water. Besides methanol is far cheaper and easier to handle than methyl sulfate.

The vapour phase methylation of phenol with methanol using metal oxide, sulphate, phosphate and zeolite catalysts has been extensively studied [14-23]. The products are usually mixtures of anisole (product of O-methylation) and cresols and xylenols (products of ring methylation), the selectivity being strongly dependent on the catalyst. The O-alkyation of phenol over zeolites was reported by Balsama et al. [24] over X, Y and ZSM-5. O-alkylations have also been carried out over ZSM-5 [25-27], $AlPO_4$ and SAPO [28] molecular sieves. SAPO produced only anisole and both cresols and anisoles were produced over the other molecular sieves. The selectivities, generally determined by the Bronsted acidity of the molecular sieves, are also affected by factors such as pore size and pore geometry. Ono et al. [29] reported the selective O-methylation of phenol with dimethylcarbonate (DMC) over X-zeolites. Samolada et al. [30] reported the selective O-methylation of phenol over sulphates supported on γ-Al_2O_3. Xu et al. studied [31] the O-alkylation of phenol with methanol on H-beta zeolite. Beutel et al. [32] reported spectroscopic and kinetic studies of the alkylation of phenol with dimethyl carbonate over NaX. Bautista et al. [33] reported the alkylation of phenol with DMC over $AlPO_4$, Al_2O_3 and $AlPO_4$-Al_2O_3 catalysts. Lee et al. [34] reported the O-alkylation of phenol derivatives over basic zeolites. The substrates investigated by them were phenol, 4-nitrophenol, 4-aminophenol and 4-chlorophenol; the activity of the catalyst increased with basicity of the loaded metal and there was no difference in catalytic activity between Cs cation exchanged and Cs oxide loaded zeolites.

O-methylated hydroxy benzenes are important synthetic intermediates in the production of fine chemicals and pharmaceuticals [35]. Guaiacol (O-

methoxy phenol) is an important intermediate for the production of flavorings, fragrances and pharmaceuticals. Ono et al. [36-38] reported the selective O-alkylation of catechol over alumina, alkali hydroxide loaded alumina and potassium nitrate loaded alumina. DMC was a much more efficient methylating agent than methanol in the methylation of catechol over alumina. The main product was guaiacol, the selectivity for it being ca. 70%. Addition of water to the feed considerably increased the catalytic activity and the yield of guaiacol. Similarly, over alumina loaded with alkali hydroxides, catechol was methylated mainly into guaiacol [37]. A guaiacol yield of 84% was obtained at a catechol conversion of 100% at 583 K over $LiOH/Al_2O_3$ with DMC as the alkylating agent. Over alumina loaded with potassium nitrate, catechol produced selectively veratrole with dimethylcarbonate [38]. A veratrole yield of 97% was obtained at a catechol conversion of 99% at 583 K and a DMC/catechol ratio of 4.

The various O-alkylation reactions investigated and described in this chapter are shown in Scheme 1.

4. 2 EXPERIMENTAL

4.2.1 Materials and catalysts

The chemicals used in the O-alkylation reactions, their purity and source are presented in Table 4.1. The catalysts used in the studies are presented in Table 4.2. The details of the preparation of all the catalysts have been presented in Chapter II. Their physicochemical characteristics are also presented in Chapter II.

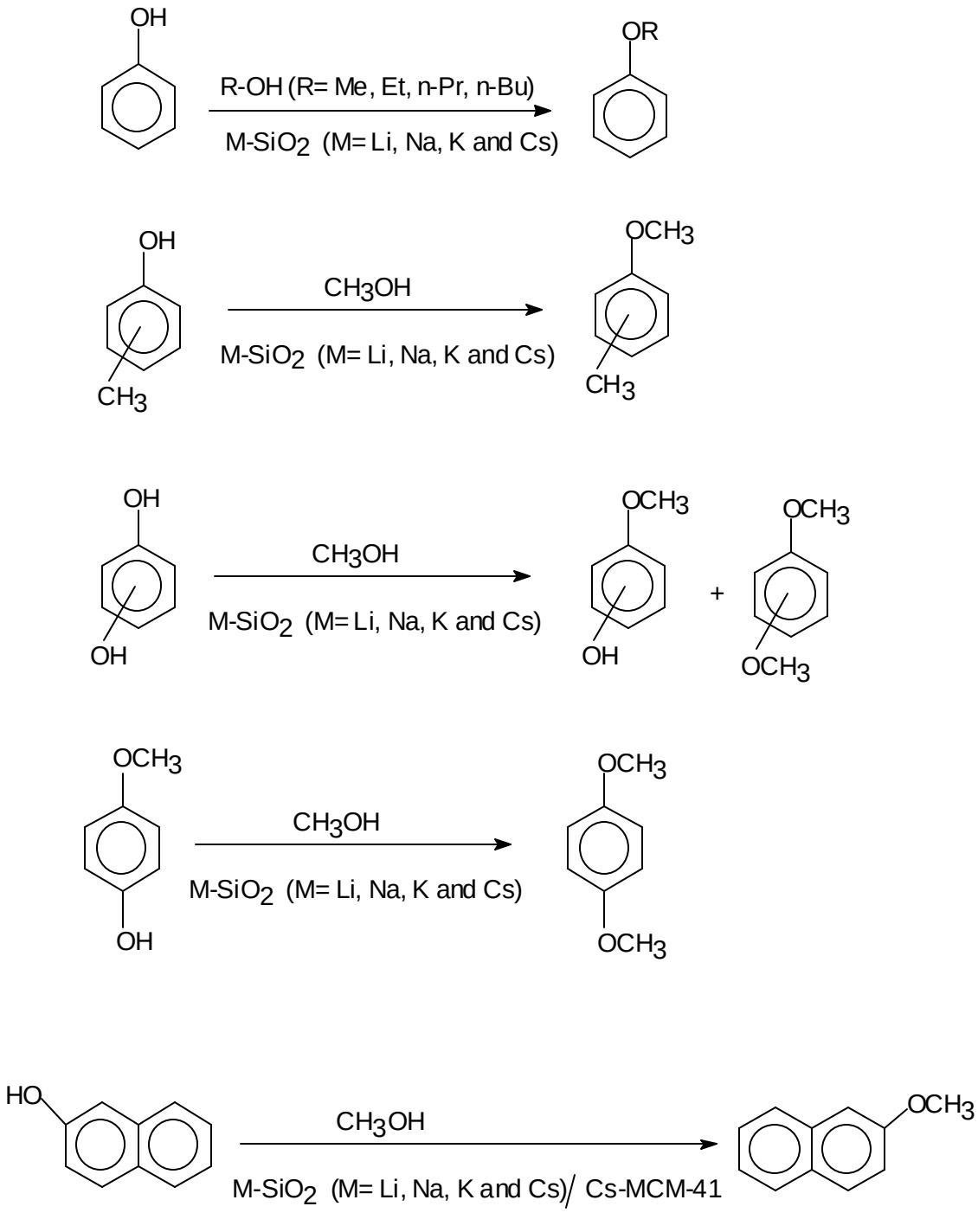

Scheme 1. The O-alkylation reactions investigated in this work.

Table 4.1 Chemicals used in this study

Name	Purity	Source
Phenol	> 99%	S.D. Fine-chem Ltd., INDIA
o-Cresol	99%	Aldrich, USA
m-Cresol	99%	Aldrich, USA
p-Cresol	99%	Aldrich, USA
Catechol	99%	S.D. Fine-chem Ltd., INDIA
Resorcinol	99%	Loba Chemie Pvt. Ltd., INDIA
Hydroquinone	99%	Loba Chemie Pvt. Ltd., INDIA
p-Methoxy phenol	99%	Loba Chemie Pvt. Ltd., INDIA
2-Naphthol	99%	S.D. Fine-chem Ltd., INDIA
Methanol	> 99.5%	S.D. Fine-chem Ltd., INDIA
Ethanol	> 99.5%	S.D. Fine-chem Ltd., INDIA
n-Propanol	> 99.5%	S.D. Fine-chem Ltd., INDIA
n-Butanol	> 99.5%	S.D. Fine-chem Ltd., INDIA

4.2.2 Reaction procedure

The catalytic experiments were carried out in a vertical down-flow glass reactor (15mm i.d.). The catalyst (2g) was used in the form of granules (10-22 mesh) prepared by pelleting of the powders and crushing into the desire size.

Table 4.2 Catalysts used in the different reactions

Catalysts	Reactions
SiO_2; $Li(1.5)SiO_2$; $Na(1.5)SiO_2$; $K(1.5)SiO_2$; $Cs(0.075)SiO_2$; $Cs(0.375)SiO_2$; $Cs(0.75)SiO_2$; $Cs(1.5)SiO_2$; $Cs(2.25)SiO_2$	O-alkylation of phenol
SiO_2; $Li(1.5)SiO_2$; $Na(1.5)SiO_2$; $K(1.5)SiO_2$; $Cs(0.075)SiO_2$; $Cs(0.375)SiO_2$; $Cs(0.75)SiO_2$; $Cs(1.5)SiO_2$; $Cs(2.25)SiO_2$	O-methylation of cresols
SiO_2; $Li(1.5)SiO_2$; $Na(1.5)SiO_2$; $K(1.5)SiO_2$; $Cs(0.075)SiO_2$; $Cs(0.375)SiO_2$; $Cs(0.75)SiO_2$; $Cs(1.5)SiO_2$; $Cs(2.25)SiO_2$	O-methylation of dihydroxy benzenes
SiO_2; $Li(1.5)SiO_2$; $Na(1.5)SiO_2$; $K(1.5)SiO_2$; $Cs(1.5)SiO_2$;	O-methylation p-methoxy phenol
SiO_2; $Li(1.5)SiO_2$; $Na(1.5)SiO_2$; $K(1.5)SiO_2$; $Cs(0.075)SiO_2$; $Cs(0.375)SiO_2$; $Cs(0.75)SiO_2$; $Cs(1.5)SiO_2$; $Cs(2.25)SiO_2$; MCM-41; Cs(0.075) MCM-41; Cs(0.15) MCM-41; Cs(0.225) MCM-41	O-methylation of 2-naphthol

The reactor was placed inside a temperature controlled furnace (Geomecanique, France) with a thermocouple placed at the center of the catalyst bed for measuring the reaction temperature. The catalyst was activated in flowing air (20 ml. min^{-1}) at 773K for 3h prior to flushing in N_2 and adjustment of temperature for start of the experiment. The feed (mixture of the desired phenol and alcohol) was passed using a syringe pump (Braun, Germany) along with N_2 gas (18ml / min). The product was cooled in a water-cooled (ice-cold) condenser, collected in a receiver and analyzed in a gas chromatograph (HP5880A; capillary column HP1, 50m X 0.2mm; FID detector). Product identification was done by GC-MS and GC-IR.

4.3 RESULTS AND DISCUSSION

4.3.1 O-alkylation of phenol

4.3.1.1 Activities of the catalysts

Catalytic activities of different alkali loaded silica samples are presented in Table 4.3. Pure SiO_2 has little O-alkylation activity, but alkali loaded silica is catalytically active. For a given molar loading (1.5 mmole/g) of the alkali ions, activity of the catalysts (in the case of all the alkylations) is in the order $Cs(1.5)SiO_2$ > $K(1.5)SiO_2$ > $Na(1.5)SiO_2$ > $Li(1.5)SiO_2$. Table 4.3. also reveals that the activity of the catalysts increases with increasing Cs content (basicity). Detailed carbon balances carried out for many of the experiments were in the range 94-98%. Assuming the absence of boundary, inter- and intraparticle diffusion effects, phenol conversion (X_p) can be fitted into the first order rate equation,

$$\ln [1/ (1- X_p)] = k (W/F) \quad \ldots\ldots\ldots (1),$$

where W = weight of the catalyst and F = feed rate in mole/sec.

Runs were performed at four feed rates in the range 1.5 – 6.5 x 10^{-5} mole sec^{-1} and at reaction temperatures in the range 573 K – 673 K. The ln [1/ (1- X_p)] versus W/F plots according to Eq. [1] are almost linear (at low conversions) passing through the origin indicating a reasonable fit of the data to Eq. (1). The slope of the straight line yields the value of the reaction rate constant (k) in mole $g^{-1}sec^{-1}$. The values obtained at various temperatures for different catalysts, at a time on stream of 1h are presented in Table 4.4. The basicities of the catalysts calculated from Sanderson's electronegativity (S_{int}) and FTIR intensities of adsorbed CO_2 are also presented in the table. Though there is a relationship between basicity (FTIR intensity) and rate constants, no linear correlation is found. Similarly, though the activity increased with decreasing S_{int}, the relationship is not linear. The data do confirm that though the activity of the catalyst is related to its basicity, simple linear relationships may not be present.

4.3.1.2 Reactivities of the alcohols

The relative activities of the alcohols are in the order: n-butanol < n-propanol < ethanol < methanol. The reason for this reactivity trend may be the difference in their adsorption coefficients over the catalytic surfaces. The acidity order of the alcohols is: n-butanol < n-propanol < ethanol < methanol. It is probable that the higher acidity of methanol causes it to adsorb in sufficient amount (in competition with the more acidic phenol) on the basic surface. The mechanism of the reaction probably involves the formation of a phenolate

Table 4.3 Activities of the catalysts in phenol alkylation

Catalyst[a]	Methylation		Ethylation		n-Propylation		n-Butylation	
	Conv.[b]	Sel.[c]	Conv.[b]	Sel.[c]	Conv.[b]	Sel.[c]	Conv[b]	Sel.[c]
SiO_2	3.4	6.9	2.2	3.3	1.7	2.2	-	
$Li(1.5)SiO_2$	1.2	100	-		-		-	
$Na(1.5)SiO_2$	12.3	100	9.9	100	2.6	100	2.0	100
$K(1.5)SiO_2$	30.1	100	13.3	100	8.7	100	4.5	100
$Cs(0.075)SiO_2$	33.2	100	20.2	100	15.1	100	14.7	100
$Cs(0.375)SiO_2$	59.8	100	41.6	100	38.3	100	30.5	100
$Cs(0.75)SiO_2$	69.7	100	51.2	100	42.8	100	37.7	100
$Cs(1.5)SiO_2$	91.4	100	61.5	100	44.9	100	39.2	100
$Cs(2.25)SiO_2$	92.8	100	63.0	100	49.1	100	41.4	100

[a] The number in brackets denotes the mmole of alkali metal loaded per g of SiO_2; b: Conv. = conversion (wt%) of phenol; c = selectivity for O-alkylated product (moles of O-alkylated product X 100 / moles of all the products) (Conditions: Temperature = 673 K, contact time (1/WHSV) = 0.38h, time on stream = 1h, alcohol / phenol (mole) = 5, N_2 = 18 ml/min).

Table 4.4. Rate constants (k x 10^{-3} mole $g^{-1}sec^{-1}$) for different alkali loaded catalysts in phenol methylation and bsicity data

Catalyst	Basicity		573 K	608 K	640 K	673 K
	S_{int}	FTIR				
Li(1.5)SiO_2	3.98	92	-	-	0.01	0.01
Na(1.5)SiO_2	3.96	132	0.01	0.08	0.07	0.09
K(1.5)SiO_2	3.92	153	0.05	0.11	0.19	0.26
Cs(0.075)SiO_2	4.22	19	0.01	0.05	0.08	0.19
Cs(0.375)SiO_2	4.18	88	0.02	0.17	0.31	0.65
Cs(0.75)SiO_2	4.09	120	0.13	0.27	0.45	0.86
Cs(1.5)SiO_2	3.91	216	0.22	0.44	0.75	1.77
Cs(2.25)SiO_2	3.69	262	0.28	0.49	0.79	1.86

[a] The number in brackets denotes the mmole of alkali metal loaded per g of SiO_2. (Conditions: contact time (1/WHSV) = 0.38h, time on stream = 1h, alcohol / phenol (mole) = 5, N_2 = 18 ml/min). S_{int}: Calculated from Sanderson's electronegativity principle; FTIR: relative band intensity of adsorbed CO_2 in FTIR spectra in 1200 cm^{-1} to 1750 cm^{-1} region at 0.4 mm equilibrium pressure.

species on the basic O^{2-} site on the surface of alkali loaded silica as shown below:

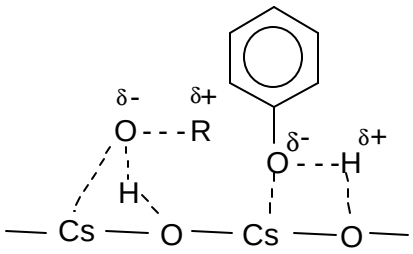

(R = CH_3, C_2H_5, n-C_3H_7 and n-C_4H_9)

4.3.1.3 Influence of time on stream

The influence of duration of run on the conversion of phenol with alcohols is presented in Fig. 4.1(a). The catalyst investigated was $Cs(1.5)SiO_2$. The influence of time on stream on the conversion of phenol with methanol over different alkali (Li, Na, K and Cs) loaded catalysts is presented in Fig. 4.1(b). It is observed that the catalyst deactivates with time on stream in the case of all the alcohols. Deactivation probably arises from coke deposition on the catalysts. At higher temperatures, the deactivation of the catalysts is more due to rapid coke formation. Studies on other alkali loaded catalysts reveal (data not reported) that the catalysts deactivate to different extent depending on the alkali metal and alkylating agents. A parameter called the average deactivation rate is used to compare the different catalysts and alcohols. The average deactivation rate is defined as the average activity loss per hour during the experimental period divided by the average conversion during this period. The parameter defines the activity loss per unit conversion in unit time and is therefore useful for comparing different catalysts with different intrinsic activities. The deactivation

rate for different alkali (Li, Na, K and Cs) loaded catalysts are plotted in Fig. 4.2 (a). The deactivation rate for different Cs-loaded catalysts are plotted in Fig. 4.2(b). Methanol deactivates the catalyst much more than the other alkylating agents and deactivation decreases with increasing basicity of the catalysts. The greater deactivation of the catalyst by methanol may be due to its stronger adsorption compared to other alcohols. The decrease in deactivation rate with basicity may be related to the mode of adsorption of the phenol. Over the more acidic catalysts, phenol molecule may adsorb by interaction of its π electron cloud, while on a more basic catalyst, it may adsorb by the -OH group. One would expect greater deactivation when the molecule is adsorbed flat on the surface as ring condensation reactions that lead to coke are more likely in this adsorption mode.

4.3.1.4 Effect of temperature

Conversions obtained with different alkylating agents at different temperatures (573 - 673 K) are presented in Fig. 4.3 (a). The catalyst investigated was $Cs(1.5)SiO_2$. Conversion is found to increase with temperature in all the cases. The influence of temperature on methylation over different alkali loaded silica samples is presented in Fig. 4.3 (b). Though the activity (as expected) increases from Li to Cs, the activity of the Cs catalyst is much larger than the other catalysts (Fig. 4.3 (b)). The decrease in activity of the catalyst with time on stream at different temperatures in the methylation of phenol over $Cs(1.5)SiO_2$ is presented in Fig. 4.4. It is seen from the data of Fig. 4.4 that the catalyst deactivates faster at higher temperatures. The activity loss per hour calculated from the above data are 1%, 0.9%, 0.8% and 0.8%, respectively at 613K, 598K, 583K and 573K.

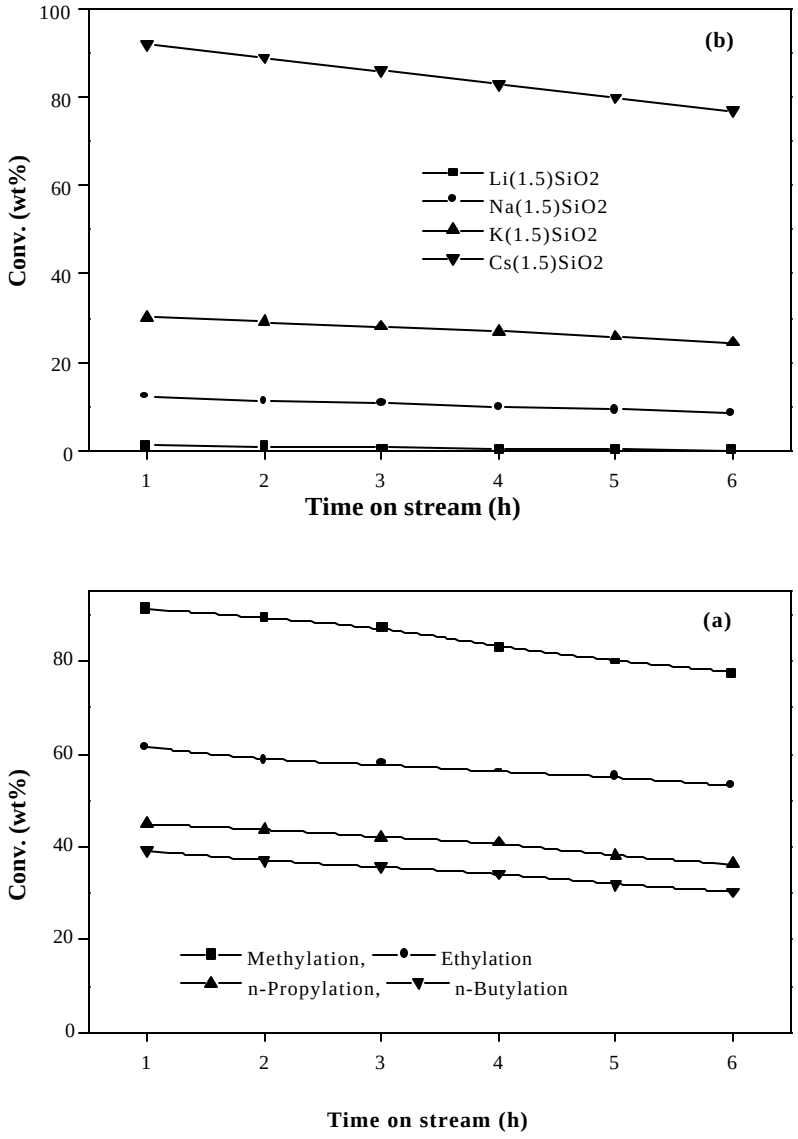

Fig. 4.1 Influence of duration of run on conversion: (a) over $Cs(1.5)SiO_2$; (b) methylation over different catalysts (Conditions: Temperature = 673K, contact time (h) = 0.38, alcohol / phenol (mole) = 5, N_2 = 18 ml/min).

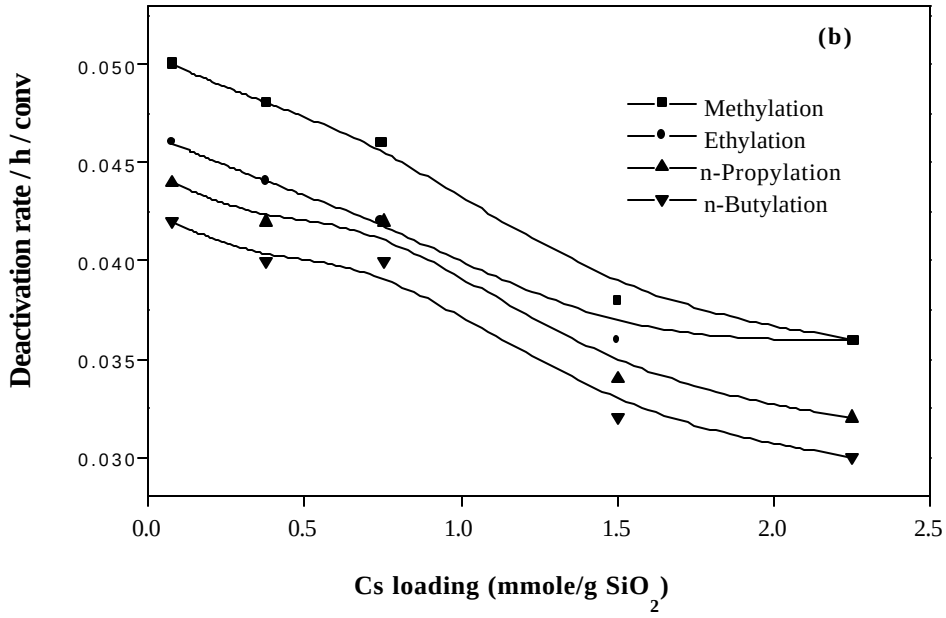

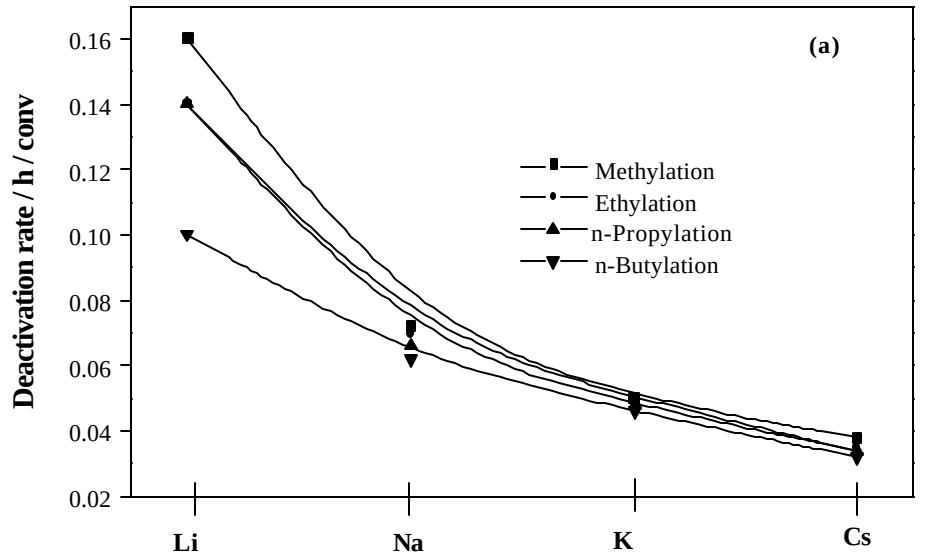

Fig. 4.2 Influence of substrate on catalyst deactivation rate: (a) over different alkali loaded catalysts; (b) over various Cs loaded catalysts (deactivation rate / h = $2(C_1 - C_6) / 5(C_1 + C_6)$, where C_1 and C_6 are conversions at 1h and 6h respectively) (Conditions: Temperature = 673K, contact time (h) = 0.38, alcohol / phenol (mole) = 5, N_2 = 18 ml/min).

4.3.1.5 Effect of contact time

Conversion increases with increase in contact time (studied from 0.19 h to 0.75 h at 673 K) for all the alcohols (Fig. 4.5(a)) over $Cs(1.5)SiO_2$. At all contact times, conversion is higher for methylation followed by ethylation, n-propylation and n-butylation. For all the alkylations, conversion increases rapidly with contact time initially (< 0.36h) and then levels off. The influence of contact time on methylation over different catalysts is presented in Fig. 4.5(b). For methylation, the conversion increases with contact time for all the catalysts but the Cs loaded catalyst is more reactive than other alkali loaded catalysts (Fig. 4.5(b)). The influence of time on stream on activity of $Cs(1.5)SiO_2$ at different contact times is presented in Fig. 4.6. Going by the slopes of the conversion vs. time on stream plots (Fig. 4.6), the deactivation rates appear to be nearly similar at the different contact times.

4.3.1.6 Effect of methanol / phenol mole ratio (methylation of phenol)

The conversion of phenol decreases as the methanol to phenol mole ratio decreases. The conversion decreases to almost one third as the methanol to phenol mole ratio decreases from 5 to 1. The influence of MeOH partial pressure in the feed (including N_2) on conversion is presented in Fig. 4.7(a). The corresponding MeOH / phenol (mole) ratios are also presented in the figure. At higher methanol to phenol mole ratio, the catalyst deactivation is more compared to deactivation at lower mole ratios (Fig. 4.7(b)). The deactivation per hour is 3.6%, 2.3% and 1.9%, respectively at mole ratios of 5, 2.5 and 1.

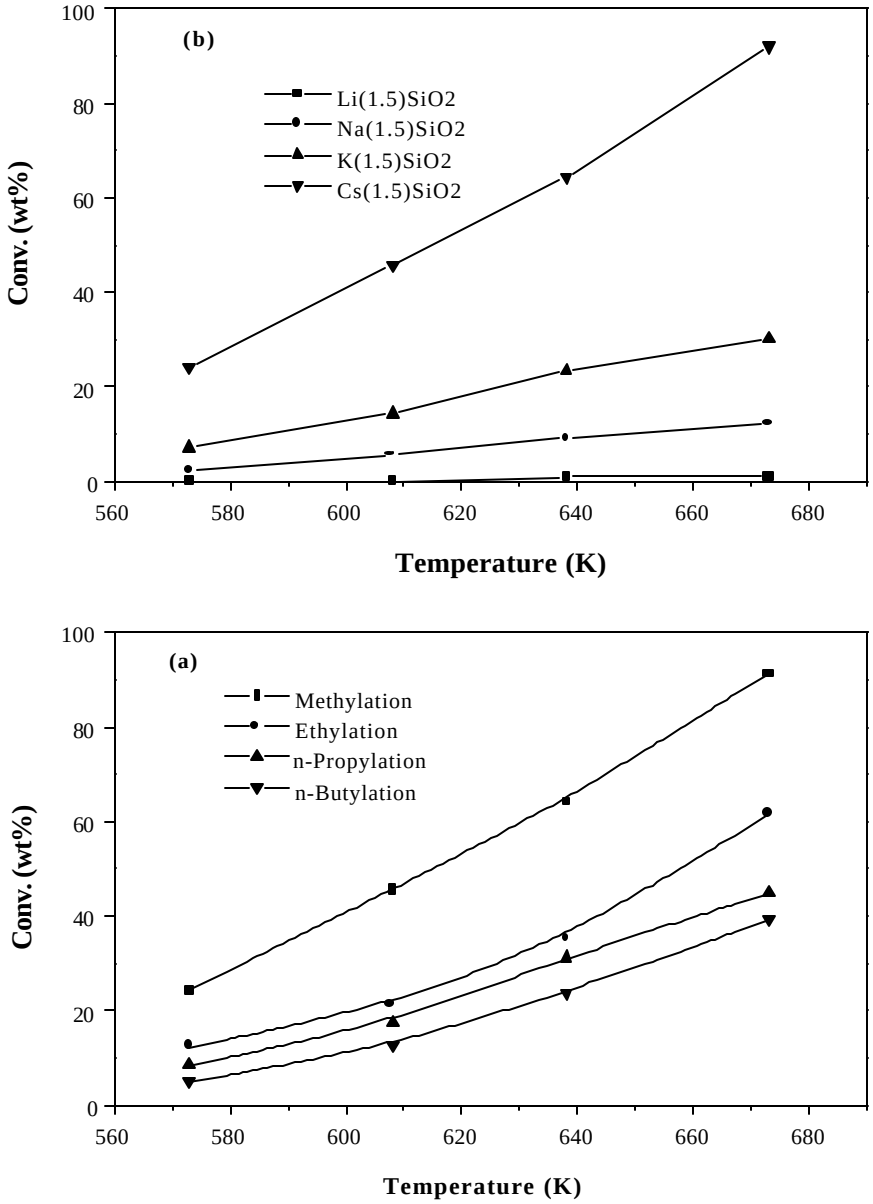

Fig. 4.3 Effect of temperature on conversion: (a) Over $Cs(1.5)SiO_2$; (b) methylation over different catalysts (Conditions: Time on stream = 1h, contact time (h) = 0.38, alcohol / phenol (mole) = 5, N_2 = 18 ml/min).

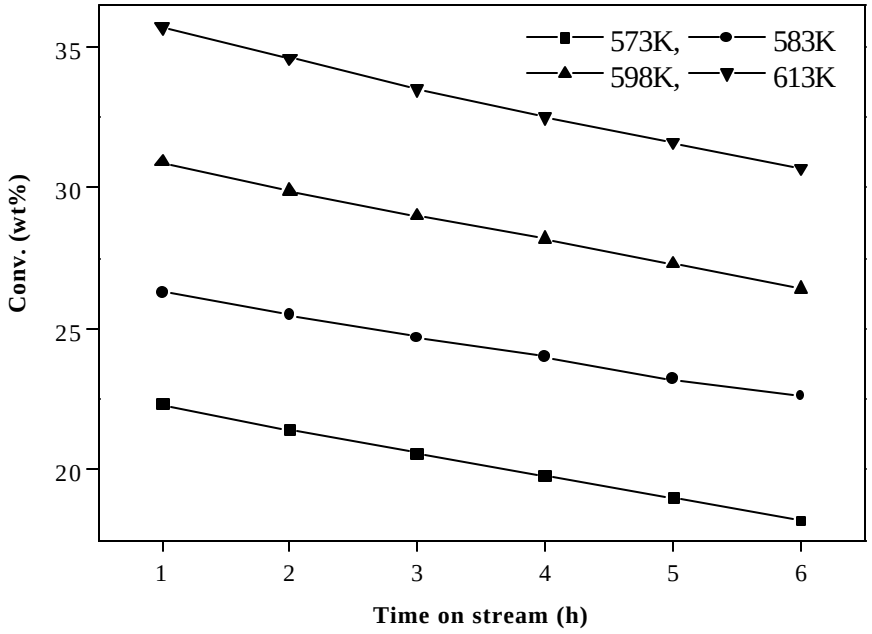

Fig. 4.4 Influence of time on stream on conversion at different temperatures (Conditions: Contact time (h) = 0.38, methanol / phenol (mole) = 5, N_2 = 18 ml/min).

4.3.1.7 Studies on catalyst deactivation

The results of the studies indicate that though high O-alkylation selectivity is achieved over alkali loaded SiO_2 catalysts, deactivation of catalysts is rather substantial. For a given conversion, the most basic catalyst (Cs-SiO_2) deactivates the least. Again, deactivation rate is lower at lower temperature and lower methanol / phenol mole ratios at which the conversions are also lower. It was therefore decided to look at other ways of decreasing catalyst deactivation. These experiments (A to D) are described below. The deactivation rates (normalized for conversions) are presented in Fig. 4.8.

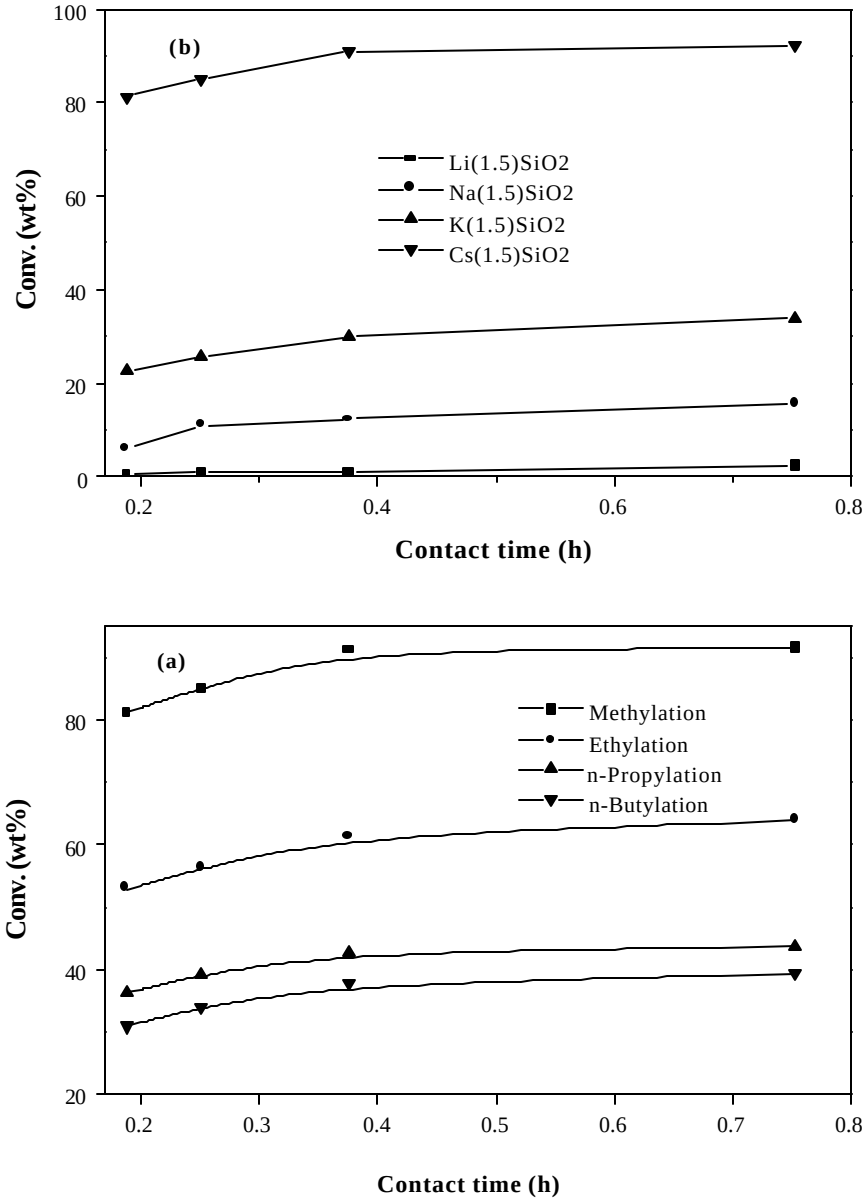

Fig. 4.5 Effect of contact time on conversion: (a) over $Cs(1.5)SiO_2$; (b) methylation over different catalysts (Conditions: Time on stream = 1h, temperature = 673K, alcohol / phenol mole) = 5, N_2 = 18 ml/min).

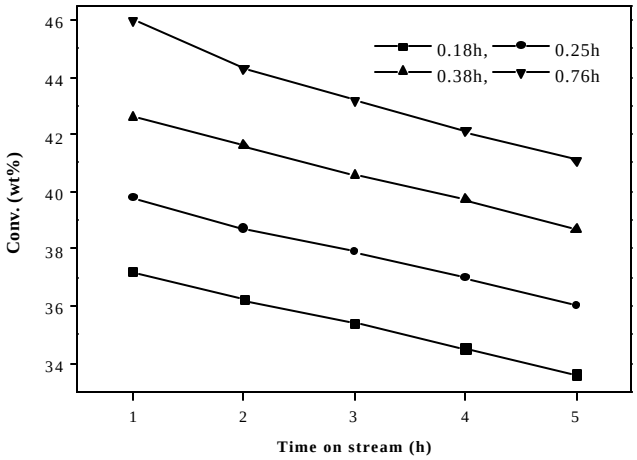

Fig. 4.6 Effect of time on stream on conversion at different contact times (1/WHSV) over $Cs(1.5)SiO_2$ (Conditions: Temperature = 598K, methanol / phenol (mole) = 5, N_2 = 18 ml/min).

Expt. A:

This is a normal experiment over $Cs(1.5)SiO_2$ at 598K, contact time (h) = 0.38 and MeOH / phenol (mole) = 2.5. N_2 is used as diluent gas. The conversion is 30.9% and the deactivation rate (% loss $h^{-1}conv^{-1}$) is 0.03.

Expt. B:

The conditions of the experiment were the same as in Expt. A. However, H_2 was used instead of N_2. There is a small decrease in conversion (28.5% in H_2 and 30.9% in N_2), and a larger decrease in deactivation rate (0.024 in H_2 and 0.03 in N_2). This suggests that H_2 probably hydrogenates and desorbs the coke precursors causing deactivation.

Expt. C:

In this experiment a $Cs\ (1.5)SiO_2$ catalyst loaded with 0.01wt% Pt was used as the catalyst. The experimental conditions (including N_2 gas) were the same as in Expt. A. A sharp decrease in deactivation rate (0.03 to 0.016) is seen. A small conversion decrease is also noticed (26.3 in the presence of Pt).

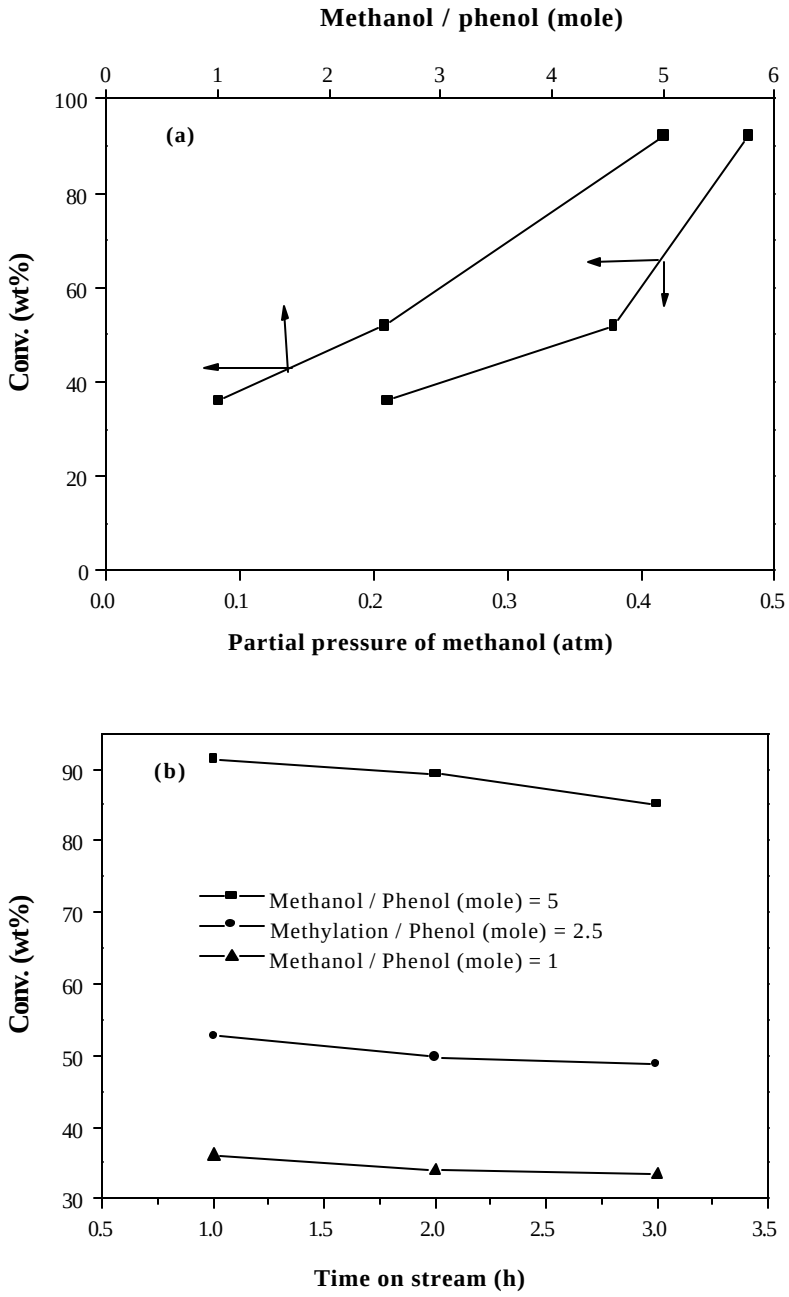

Fig. 4.7 (a) Effect of feed mole ratios on conversion over $Cs(1.5)SiO_2$ (Temperature = 673K, time on stream = 1h, contact time (h) = 0.38, N_2 = 18ml/min); (b) Effect of time on stream on conversion for different mole ratios over $Cs(1.5)SiO_2$ (Temperature = 673K, contact time (h) = 0.38, N_2 = 18ml/min).

The experiment suggests that Pt even when present in small amount is able to hydrogenate the coke precursors and suppress the deactivation. The H_2 for the hydrogenation of the coke precursors probably comes from MeOH dehydrogenation, which is known to occur on basic catalysts.

Expt. D:

This experiment was similar to C, but H_2 was used instead of N_2. The deactivation rate is decreased further to 0.012. Again a small loss in conversion is observed (23.8%).

The experiments suggest that one way of decreasing catalyst deactivation is by hydrogenating the coke precursors. However, during the process, a small conversion loss also occurs. The reason for the loss of alkylation activity in H_2 is not clear.

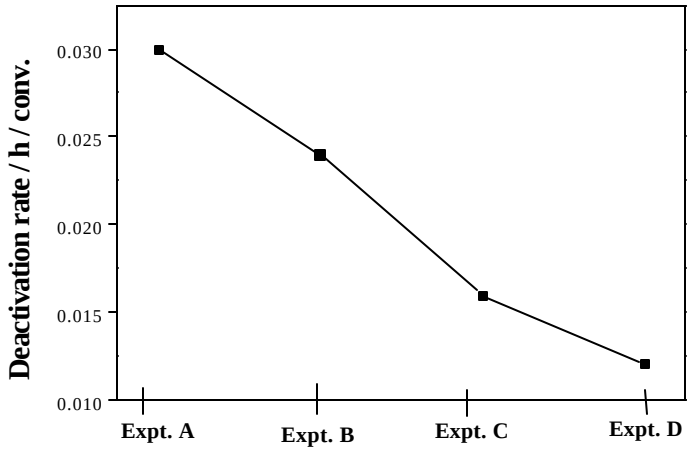

Fig. 4.8 Catalyst deactivation studies: Expt. A = $Cs(1.5)SiO_2$, N_2 = 18ml/min; Expt. B = $Cs(1.5)SiO_2$, H_2 = 18ml/min; Expt. C = $Cs(1.5)SiO_2$ + 0.01 wt% Pt, N_2 = 18ml/min; Expt. D = $Cs(1.5)SiO_2$ + 0.01 wt% Pt, H_2 = 18ml/min (Conditions: Temperature = 598K, contact time (h) = 0.38, methanol / phenol (mole) = 2.5).

4.3.2 O-Methylation of cresols

4.3.2.1 Activities of the catalysts

The catalytic activities of different alkali loaded silica samples are presented in Table 4.5. Pure SiO_2 has little O-methylation activity; alkali (Li, Na, K and Cs) loaded silica is catalytically active. For a given molar loading (1.5 mmol/g) of the alkali ions, activity of the catalysts (in the case of all the three substrates) is in the order, $Cs(1.5)SiO_2$ > $K(1.5)SiO_2$ > $Na(1.5)SiO_2$ > $Li(1.5)SiO_2$. Table 4.5. reveals that the activity of the catalysts also increases with increasing Cs content (basicity).

4.3.2.2 Influence of time on stream (TOS)

The influence of duration of run on the conversion of cresols with methanol is presented in Fig. 4.9. The catalyst investigated was $Cs(1.5)SiO_2$. The influence of TOS on the conversion of cresols with methanol over different alkali (Li, Na, K and Cs) loaded catalysts is presented in Fig. 4.10(a), Fig. 4.10(b) and Fig. 4.10(c), respectively for o-cresol, m-cresol and p-cresol. It is observed that the catalyst deactivates with time on stream in the case of all the substrates (o-cresol, m-cresol and p-cresol). Deactivation arises probably due to coke formation over the catalyst. Studies on the various alkali metal (Li, Na, K and Cs) loaded catalysts reveal that the catalysts deactivate to different extents depending on the alkali metals and the feed cresol. The average deactivation rate (defined as the average hourly loss in conversion during the first to sixth hour divided by the average conversion during that period) decreases with increasing basicity of the catalysts (Fig. 4.11).

Table 4. 5 Activities of different catalysts in the methylation of cresols

Catalyst[a]	o-Cresol		m-Cresol		p-Cresol	
	Conv.[b] (wt %)	Sel.[c] (wt %)	Conv.[b] (wt %)	Sel.[c] (wt %)	Conv.[b] (wt %)	Sel.[c] (wt %)
SiO_2	1.3	7.9	1.4	8.2	1.4	8.5
$Li(1.5)SiO_2$	6.6	>99	7.4	>99	9.1	>99
$Na(1.5)SiO_2$	7.4	>99	8.1	>99	9.8	>99
$K(1.5)SiO_2$	32.5	>99	36.6	>99	38.6	>99
$Cs(0.075)SiO_2$	22.9	>99	31.8	>99	13.9	>99
$Cs(0.375)SiO_2$	52.3	>99	68.8	>99	58.2	>99
$Cs(0.75)SiO_2$	64.5	>99	72.5	>99	77.2	>99
$Cs(1.5)SiO_2$	79.0	>99	81.9	>99	88.5	>99
$Cs(2.25)SiO_2$	84.5	>99	88.0	>99	94.0	>99

a: The number in brackets denotes the wt% of Cs loaded on SiO_2; b: Conversion of the cresol; c: Selectivity = (moles of the O-methylated product / moles of all products) x 100 (Conditions: temperature = 673K; time on stream = 1h; contact time (h) = 0.376h; N_2 flow = 18 ml/min).

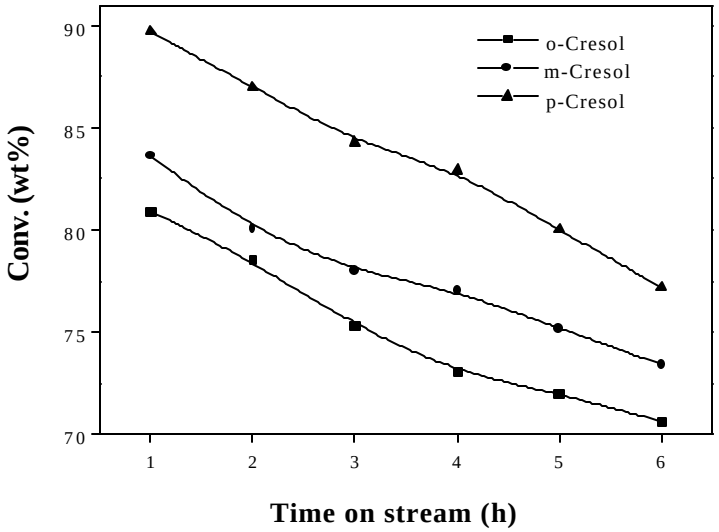

Fig. 4.9 Effect of time on stream on conversion over $Cs(1.5)SiO_2$ (Conditions: Temperature = 673K, contact time (h) = 0.38, methanol / substrate (mole) = 5, N_2 = 18 ml/min).

The deactivation rate is more for o-cresol and least for p-cresol. As already described in the case of phenol, the relative occurrence of different modes of adsorption (by the –OH group or aromatic ring) for the different substrate - catalyst combinations may be determining the deactivation rate (Fig. 4.11).

4.3.2.3 Reactivities of cresols

The relative reactivities of the three cresols are in the order: o-cresol < m-cresol ≤ p-cresol (Fig. 4.12 (a) to (d)). The relative acidities of the cresols are in the order: mcresol > p-cresol ~ o-cresol. As the catalyst is basic, one would expect the strengths of adsorption by the –OH group to be in the same order as above for the three cresols. The reason for the lower reactivity of o-cresol is

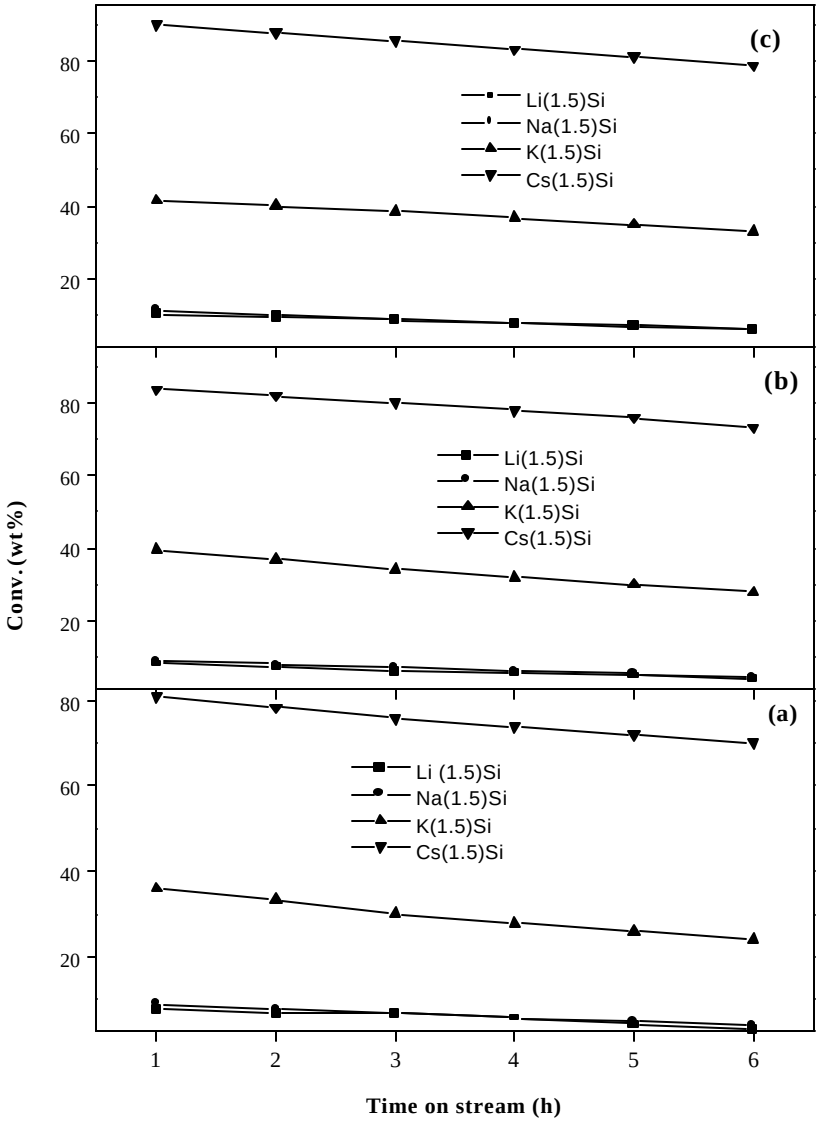

Fig. 4.10 Effect of time on stream on conversion over different alkali loaded catalysts: (a) o-cresol; (b) m-cresol; (c) p-cresol (Conditions: Temperature = 673K, contact time (h) = 0.38, methanol / substrate (mole) = 5, N_2 = 18ml/min).

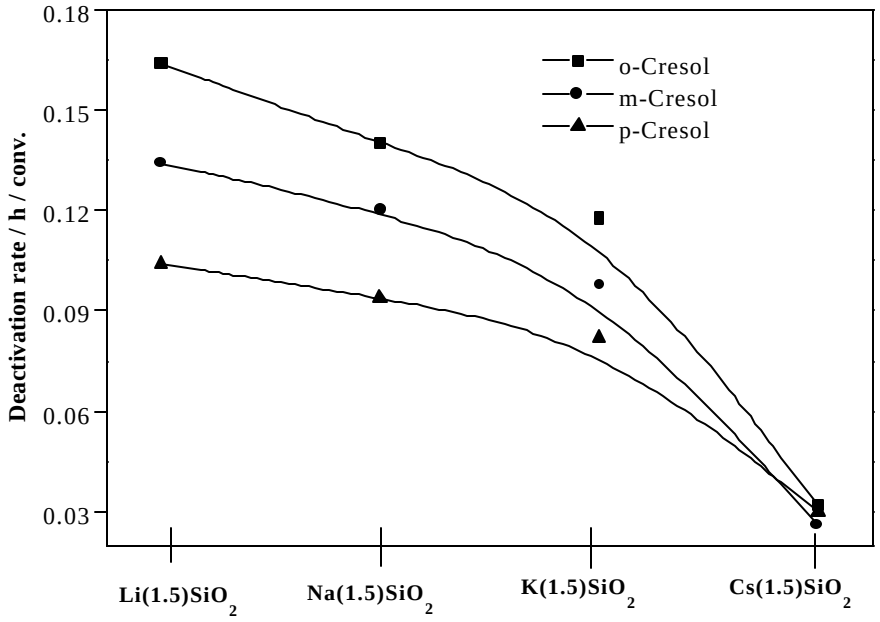

Fig. 4.11 Influence of substrate on deactivation rate (deactivation rate = $2(C_1 - C_6) / 5(C_1 + C_6)$, where C_1 and C_6 are conversions at 1h and 6h respectively) (Conditions: Temperature = 673K, contact time (h) = 0.38, methanol / substrate (mole) = 5, N_2 = 18 ml/min).

probably steric hindrance from the –Me group at the o-position (to adsorption by the –OH group; see section 4.3.1.2). It is noticed that though o-cresol is less reactive over all the catalysts (with different basicities), m- and p-cresols possess nearly similar reactivities over Na and K catalysts, while p-cresol is more reactive over the most basic $Cs(1.5)SiO_2$ (at higher temperatures) and least basic $Li(1.5)SiO_2$. The observations cannot be explained on the basis of adsorption strengths, catalyst basicity or substrate acidity. Though the exact reasons for the observed trends in reactivities of m- and p-cresols are nor clear, it is presumed that the relative reactivities arise from an interplay of steric, electronic and acidity-basicity effects.

4.3.2.4 Effect of temperature

The reactivities of the three cresols at different temperatures (573K – 673K) over the different catalysts are presented in Fig. 4.13 (a) to (d). Conversion increases with temperature for all the three cresols over all the catalysts. Activity increases (as expected) from Li to Cs for all the substrates at all the temperatures investigated.

4.3.2.5 Effect of contact time

Conversion increases with increase in contact time (studied from 0.188 h to 0.752 h) for all the three substrates and catalysts. The results obtained over $Cs(1.5)SiO_2$ are presented in Fig. 4.14. Again, it is noticed that the reactivity of p-cresol is more than those of o- and m-cresols at all the contact times investigated, the reactivity differences being smaller at lowerer contact times. The influence of contact time in the methylation of cresols over different alkali metal (Li, Na, K and Cs) loaded catalysts is presented in Fig. 4.15(a), 4.15(b) and 4.15(c), respectively for o-cresol, m-cresol and p-cresol.

4.3.3 O-Methylation of dihydroxy benzenes

4.3.3.1 Activities of the catalysts

The catalytic activities of different alkali loaded silica samples are presented in Table 4.6 and Fig. 4.16 (a). Pure SiO_2 has little O-methylation activity; alkali (Li, Na, K and Cs) loaded silica is catalytically active. For a given molar loading (1.5 mmol/g) of the alkali ions, activity of the catalysts (in the case of all the three substrates) is in the order, $Cs(1.5)SiO_2$ > $K(1.5)SiO_2$ > $Na(1.5)SiO_2$ > $Li(1.5)SiO_2$. Fig. 4.16 (a) reveals that the activity of the catalysts also increases with increasing Cs content (basicity).

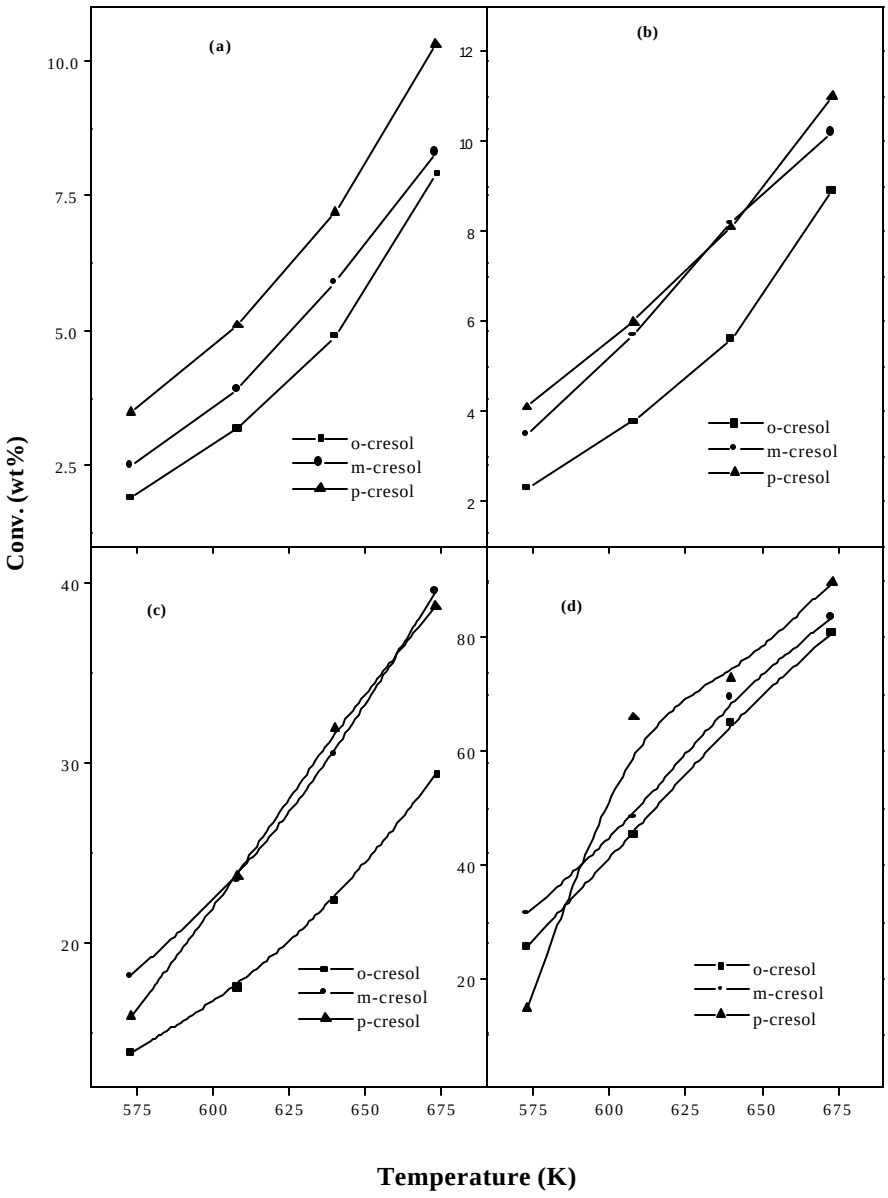

Fig. 4.12 Effect of temperture on conversion over different alkali loaded catalysts: (a) $Li(1.5)SiO_2$; (b) $Na(1.5)SiO_2$; (c) $K(1.5)SiO_2$; (d) $Cs(1.5)SiO_2$ (Conditions: Time on stream = 1h, contact time (h) = 0.38, methanol / substrate (mole) = 5, N_2 = 18 ml/min).

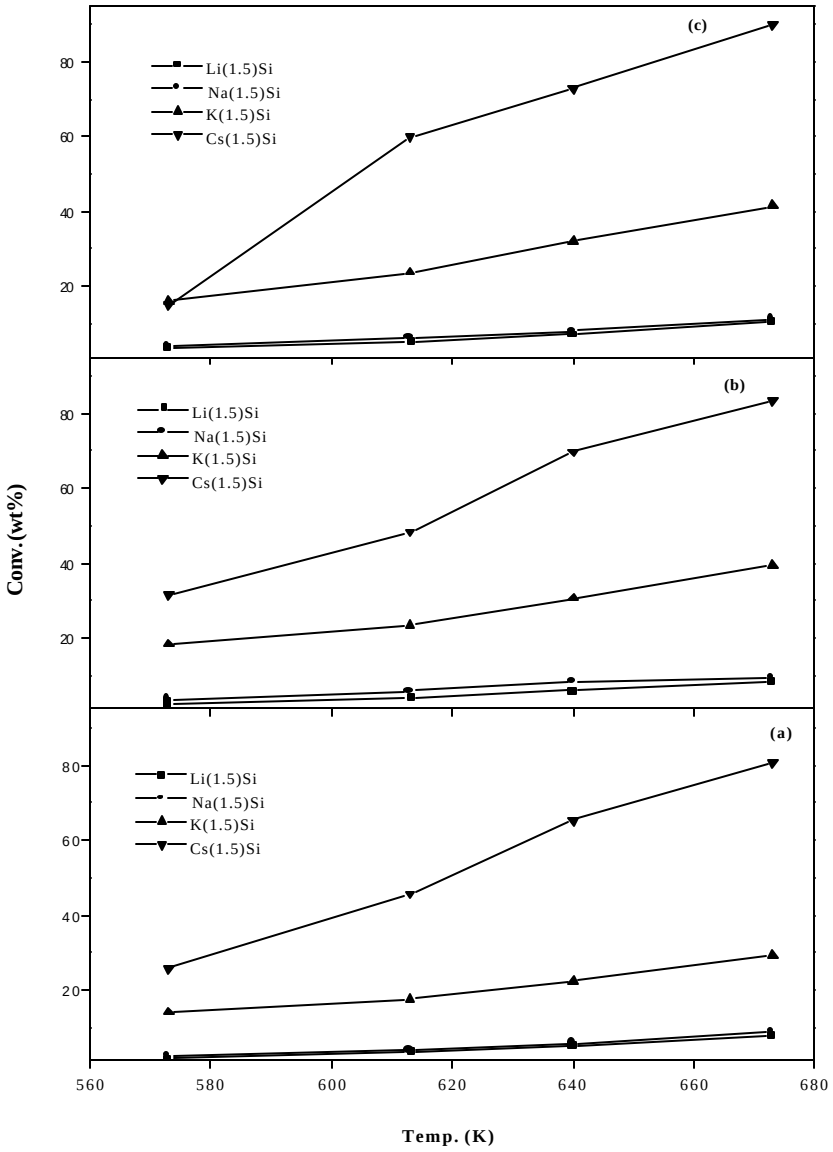

Fig. 4.13 Effect of temperature on conversion over different alkali loaded catalysts: (a) o-cresol; (b) m-cresol; (c) p-cresol (Conditions: Time on stream = 1h, contact time (h) = 0.38, methanol / substrate (mole) = 5, N_2 = 18 ml/min).

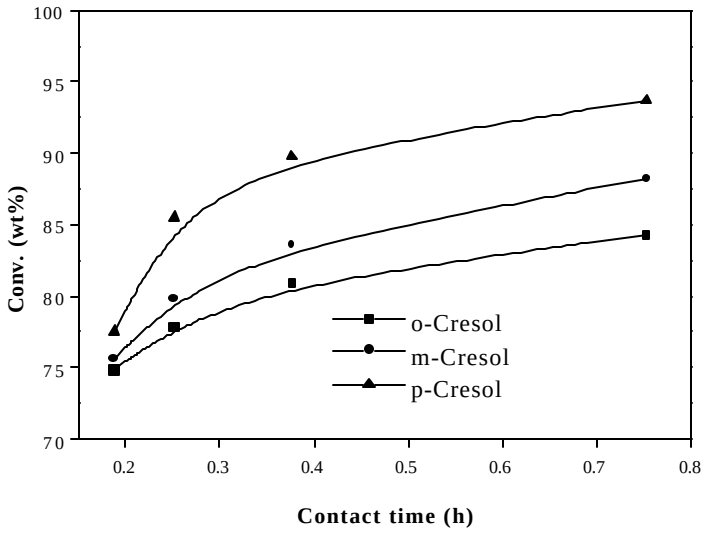

Fig. 4.14 Effect of contact time on conversion of cresols over $Cs(1.5)SiO_2$ (Conditions: Temperature = 673K, time on stream = 1h, methanol / substrate (mole) = 5, N_2 = 18 ml/min).

The relationship between basicity of the catalysts as estimated by TPD of CO_2 and FTIR spectroscopy of CO_2 and Cs loading are presented in Fig. 4.17 (b) and (c). The conversions of different substrates over the catalysts are presented in Fig. 4.17 (d). A similarity of conversion trends is seen with basicity of the catalysts. There is in general a rapid increase in activity (or basicity) with increasing Cs content, which then slows down after a Cs loading of about 1.5 mmol / g of catalyst. This trend is also similar to the Cs / Si ratio obtained by ESCA (electron spectroscopy for chemical analysis) (Fig. 4.17 (a)). This suggests that coverage of SiO_2 surface increases rapidly to saturation (about 1.5 mmole / g) beyond which further coverage is not possible. The trends of observed basicities and conversions may be explained to be due to attainment of

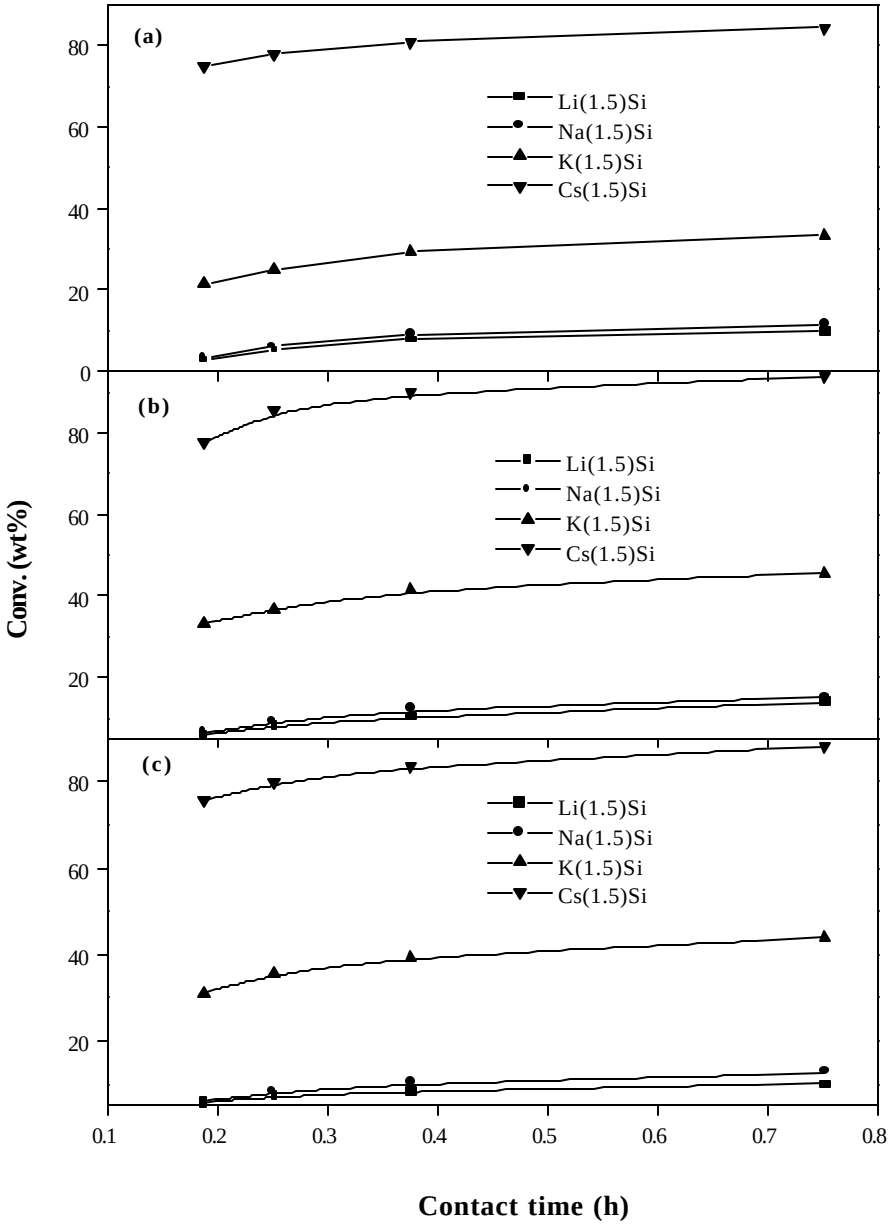

Fig. 4.15 Effect of contact time on conversion over different alkali loaded catalysts: (a) o-cresol; (b) m-cresol; (c) p-cresol (Conditions: Temperature = 673K, time on stream = 1h, methanol / substrate (mole) = 5, N_2 = 18 ml/min).

saturation surface coverage (which implies a saturation inavailability of Cs sites for reaction) beyond 1.5 mmol / g.

The influence of duration of run on the conversion of dihydroxy benzenes and distribution of products is presented in Fig. 4.18. The catalyst investigated was $Cs(1.5)SiO_2$. It is observed that the catalyst deactivates with duration of run in the case of all the substrates. Interestingly, it is noticed that monomethoxy product formation decreases more with time than the dimethoxy isomer.

Studies on other alkali loaded catalysts reveal (data not reported) that the catalysts deactivate to different extents depending on the alkali metal and the substrate. The results on deactivation observed over the different catalysts and substrates are summarized in Fig. 4.19 in which the average deactivation rates (per hour per unit conversion) calculated over a three hour period for different alkali loaded catalysts for the three dihydroxy benzenes are presented. Catechol deactivates all the catalysts except $Li(1.5)SiO_2$ more than the other two compounds and deactivation decreases with increasing basicity of the catalyst from Li to Cs (Fig. 4.19(a)). The greater deactivation observed for catechol may be due to its stronger adsorption on the catalyst through the two adjacent -OH groups. Decrease in deactivation with basicity may also be related to the mode of adsorption of the compound. Over a more acidic catalyst, the molecule may adsorb by interaction of its π-electron system, while on a more basic catalyst, it may adsorb by the -OH group as shown in scheme 1. Increasing the basicity of the catalyst by increasing Cs loading causes a decrease in deactivation rate for catechol and resorcinol (Fig. 4.19(b)).

Table 4.6 Activities of different catalysts in the methylation of dihydroxy benzenes.

Catalyst[a]	Catechol			Resorcinol			Hydroquinone		
	Conv. (wt%)	Sel.[b] (wt%)	Sel.[c] (wt%)	Conv. (wt%)	Sel.[d] (wt%)	Sel.[e] (wt%)	Conv. (wt%)	Sel.[f] (wt%)	Sel.[g] (wt%)
SiO_2	3.5	-	-	4.2	-	-	4.8	-	-
$Li(1.5)SiO_2$	5.2	75.1	15.7	30.9	36.9	44.3	27.1	59.1	14.0
$Na(1.5)SiO_2$	10.3	71.3	22.5	45.3	33.8	52.1	44.2	47.7	31.0
$K(1.5)SiO_2$	17.3	63.3	31.5	65.7	22.6	64.7	49.1	45.8	41.0
$Cs(0.075)\ SiO_2$	21.8	60.0	40.0	68.5	24.3	75.7	54.1	45.0	55.0
$Cs(0.375)\ SiO_2$	30.2	55.5	44.1	77.2	20.2	79.8	67.6	38.4	61.6
$Cs(0.75)\ SiO_2$	43.3	51.0	49.0	82.1	16.9	83.1	71.2	32.8	67.2
$Cs(1.5)\ SiO_2$	57.2	47.0	53.0	87.4	10.7	89.3	87.9	24.8	75.2
$Cs(2.25)\ SiO_2$	67.6	44.3	55.7	95.5	7.2	92.8	96.7	22.3	77.7

[a] The number in brackets denotes the mmole/g of alkali metal loaded on SiO_2. [b] 2-methoxy phenol, [c] 1,2-dimethoxy benzene, [d] 3-methoxy phenol, [e] 1,3-dimethoxy benzene, [f] 4-methoxy phenol, [g] 1,4-dimethoxy benzene. Conditions: Temperature = 673K, time on stream = 1h, Contact time (h) = 0.376, N_2 = 18 ml/min.

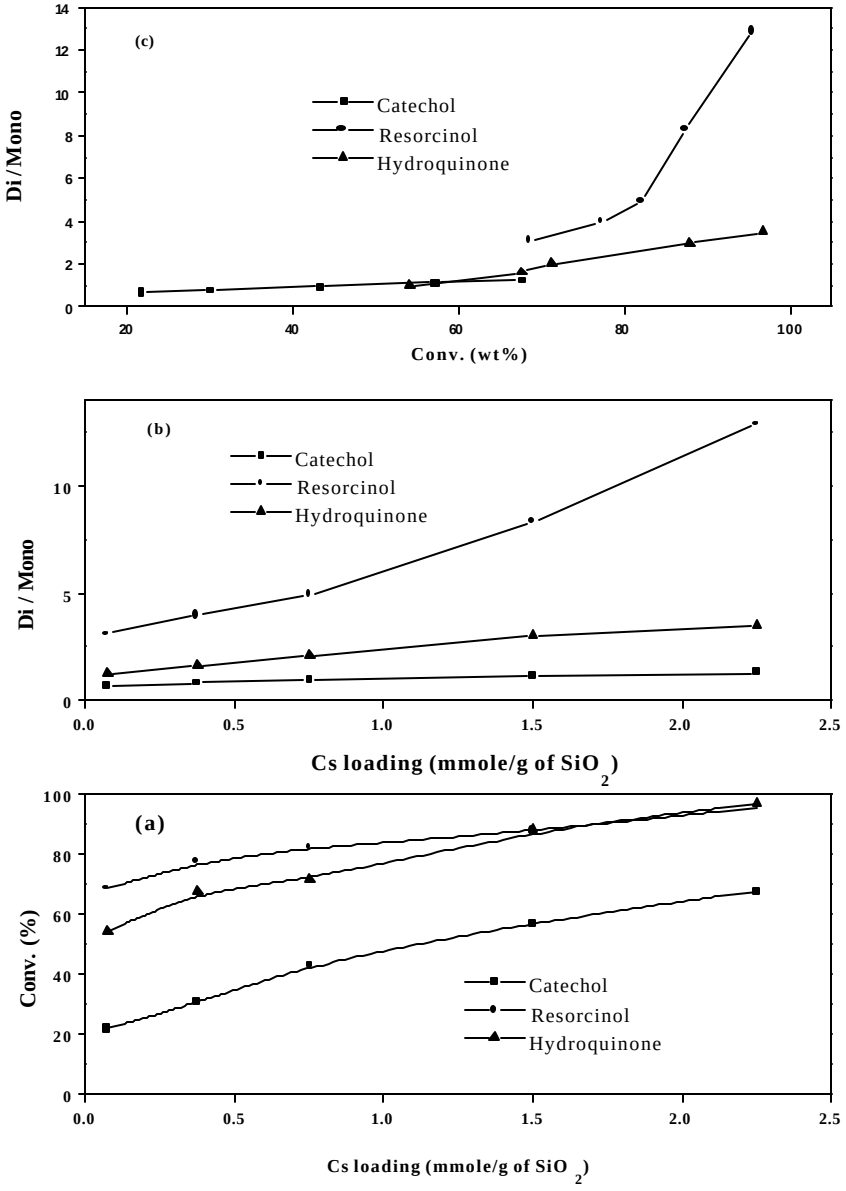

Fig. 4.16 (a) Influence of Cs content of catalyst on conversions of dihydroxy benzenes; (b) Influence of Cs content on dimethoxy / monomethoxy ratios and (c) Relationship between conversion and Di/Mono ratios (Conditions: Temperature = 673K; time on stream (TOS) = 1h; contact time (h) = 0.376; N_2 = 18 ml/min; methanol / substrate (mole) = 5).

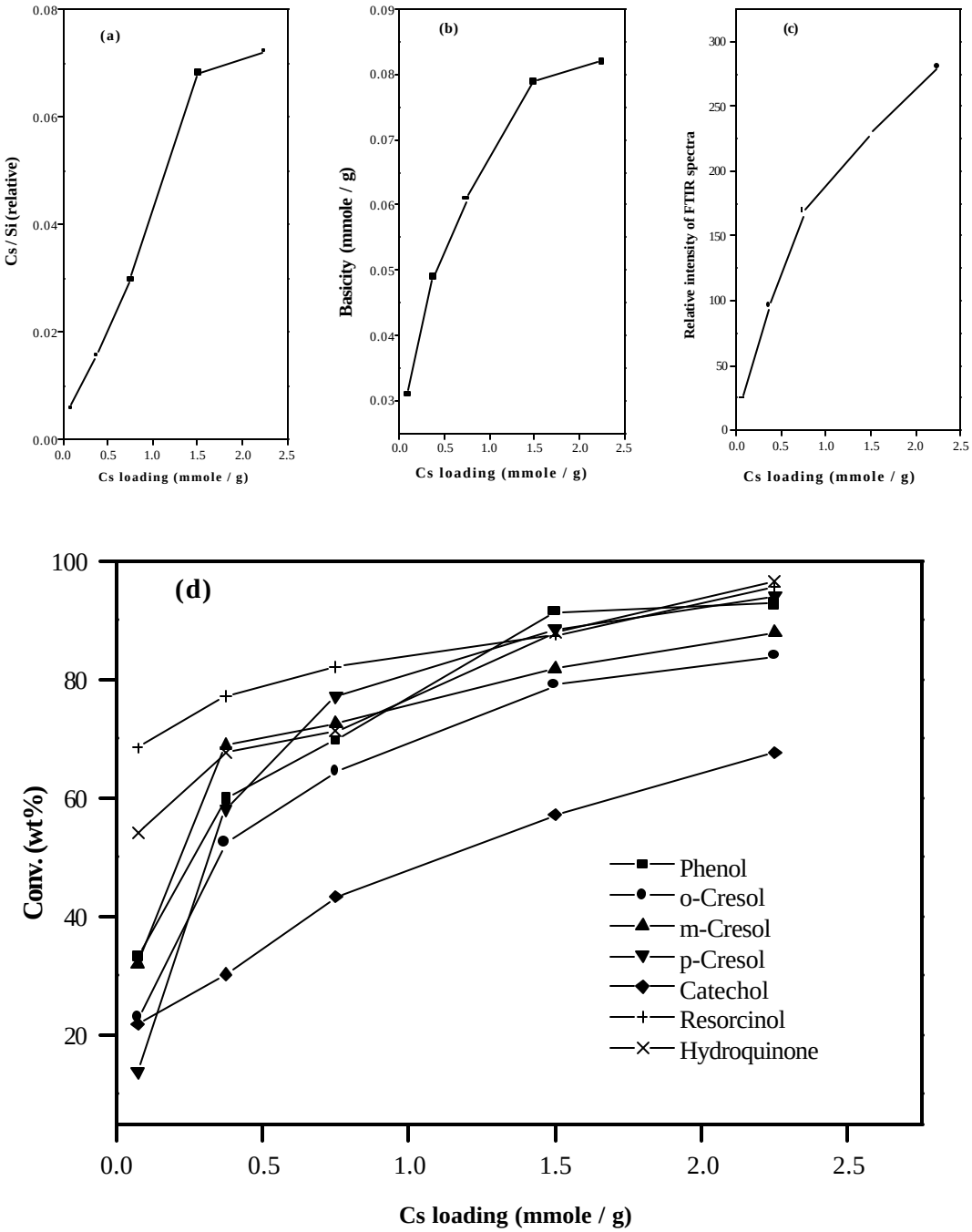

Fig. 4.17 Inter relationship between Cs at the surface, basicity, catalytic activity and Cs loading: (a) results from ESCA; (b) basicity from TPD of CO_2; (c) basicity from FTIR; (d) conversions of various substrates (Conditions: Temperature = 673K, contact time (h) = 0.38, time on stream = 1h, methanol / substrate (mole) = 5).

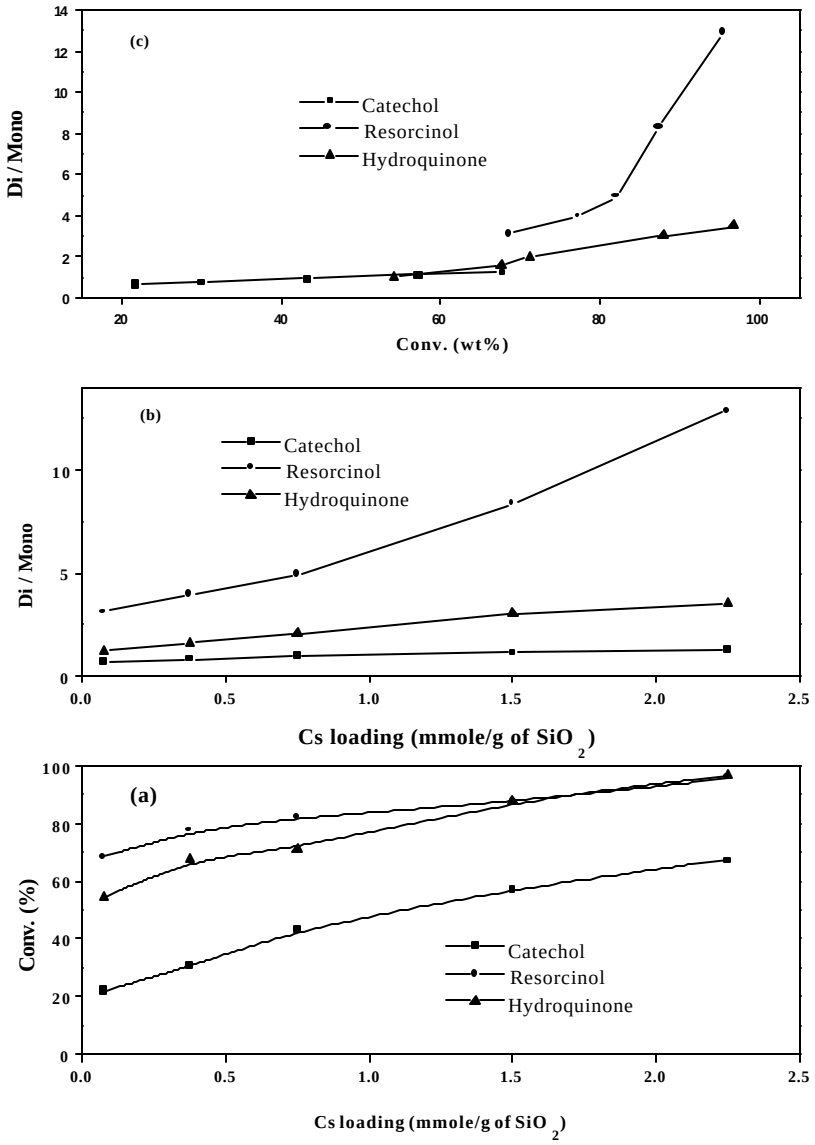

Fig. 4.18 Effect of time on stream on conversions of dihydroxy benzenes and product distribution over $Cs(1.5)SiO_2$: (a) catechol; (b) resorcinol; (c) hydroquinone (Conditions: Contact time (h) = 0.376; temperature = 673K; methanol / substrate (mole) = 5; N_2 = 18 ml / min).

However, the deactivation rate goes through a maximum in the case of hydroquinone. The reasons for this behaviour of hydroquinone are not clear.

4.3.3.2 Reactivities of the dihydroxy benzenes

If we examine the relative activities of the three dihydroxy compounds, catechol, resorcinol and hydroquinone, we find that their reactivity increases in the order catechol < hydroquinone < resorcinol. The reason for this reactivity trend is probably the difference in the acidities of the three compounds and ease of formation of the likely surface intermediate (shown below) on the catalyst.

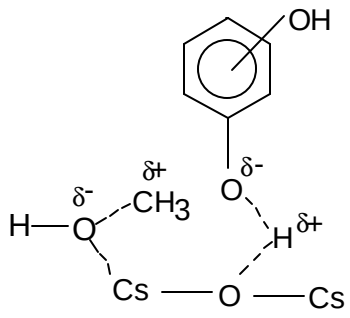

The reactivity trend exactly matches the acidity of the three dihydroxy compounds (catechol < hydroquinone < resorcinol) and electron density trends at the o-, m- and p- positions of phenol. The +M effect of the -OH group trends to cause a lower electron density at the m-position in the case of resorcinol and favours the formation of $[HO\text{-}C_6H_4\text{-}O^{\delta-}]$ adsorbed species (Scheme above). On the other hand, in the case of catechol and hydroquinone, the higher electron densities at the o- and p- positions will destabilize the above transition state. Besides, steric effects may also be responsible for the lower reactivity of catechol.

Selectivity for O-methylation (sum of mono and di methoxy products) also increases in the same order: catechol < hydroquinone < resorcinol. A decrease in monomethoxy products is noticed with increasing basicity in the case of all the three substrates due to increase in dimethoxy product formation (Table 4.6). This is due to faster conversion of the mono methoxy phenols compared to the dihydroxy compounds with increasing catalyst basicity.

Examining the dimethoxy / monomethoxy product (Di / Mono) ratios of the three substrates over different Cs-SiO_2 catalysts (Fig 4.16(b)), one finds that the increase with basicity is small for catechol and HQ while it is large for resorcinol. When Di/Mono ratios are plotted vs. conversion (Fig. 4.16(c)), it is noticed that in the case of HQ and catechol, the increase is slow (both falling on a nearly common curve) while it is very rapid for resorcinol. This suggests a much greater reactivity of m-methoxy phenol than the o- and p-methoxy isomers. The greater reactivity of the monomethoxy phenols than the dihydroxy compounds is probably due to differences in the electronic effects of the -OCH_3 and -OH groups.

4.3.3.3 Effect of temperature

The reactivities of the three substrates over Cs(1.5)SiO_2 at different temperatures (573K - 673K) are presented in Fig. 4.20(a). Conversion increases with temperature for all the substrates. Both mono and di O-methylated products increase with temperature. For catechol, the increase is less compared to resorcinol and hydroquinone. The influence of temperature in the methylation of HQ over different alkali loaded catalysts is presented in Fig. 4.21(a) and 4.21(b). Though activity (as expected) increases from Li to Cs, the activity of the Cs catalyst is much larger than those of the other catalysts.

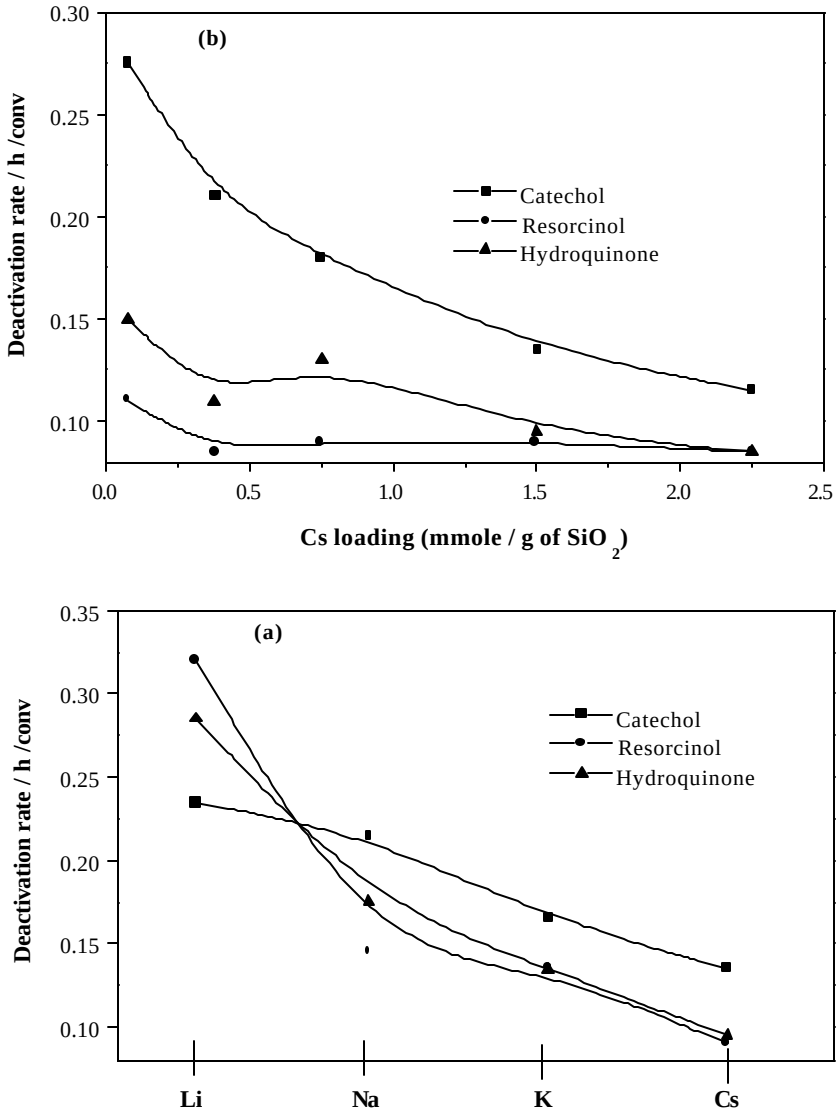

Fig. 4.19 Influence of substrate on catalyst deactivation rate: (a) over different alkali loaded catalysts; (b) Various Cs-loaded catalysts (Conditions: Temperature = 673K, contact time (h) = 0.38, methanol / substrate (mole) = 5, N_2 = 18 ml/min; deactivation rate = $2(C_1 - C_3) / 2(C_1 + C_3)$, where C_1 and C_3 are conversions at 1h and 3h respectively).

Small amount of the dehydroxylated products, phenol and anisole were also formed over $Li(1.5)SiO_2$, $Na(1.5)SiO_2$ and $K(1.5)SiO_2$ at higher temperatures. The Di/Mono ratios observed at different temperatures for the three substrates and the different catalysts are presented in Fig. 4.20 (b) and 4.21 (b). It is noticed that the Di/Mono ratios also increase with temperature suggesting more rapid conversions of the monomethoxy product at higher temperatures. The Di/Mono ratios are much larger for resorcinol than for the other two substrates (Fig. 4.20 (b)). Similarly, the ratios are much larger over the Cs catalyst than over the other three catalysts (Fig. 4.21 (b)).

4.3.3.4 Effect of contact time

Conversion increases with increase in contact time (studied from 0.188 h to 0.752 h at 673K) for all the substrates (Fig. 4.22(a)). Though the reactivities of resorcinol and HQ are similar, the reactivity of catechol is much lower. Conversions of all the three compounds increase with increase in contact time. Examining the influence of contact time on Di/Mono ratio (Fig. 4.22(b)), it is seen that the ratio is larger and increases more rapidly with contact time for resorcinol than for the other two. The influence of contact time on conversion of HQ and Di/Mono ratios over the different alkali loaded catalysts is presented in Fig. 4.23 (a) and Fig. 4.23 (b), respectively. As already reported, the Cs catalyst is much more active than the other three catalysts at all the contact times investigated. Similarly, the Di/Mono ratio also increases more rapidly over the Cs catalysts than over the others. Though both Fig. 4.22 and Fig. 4.23 reveal an increase in conversion with contact time, the increase is more rapid in the lower contact time region (< 0.36 h) than at higher contact times.

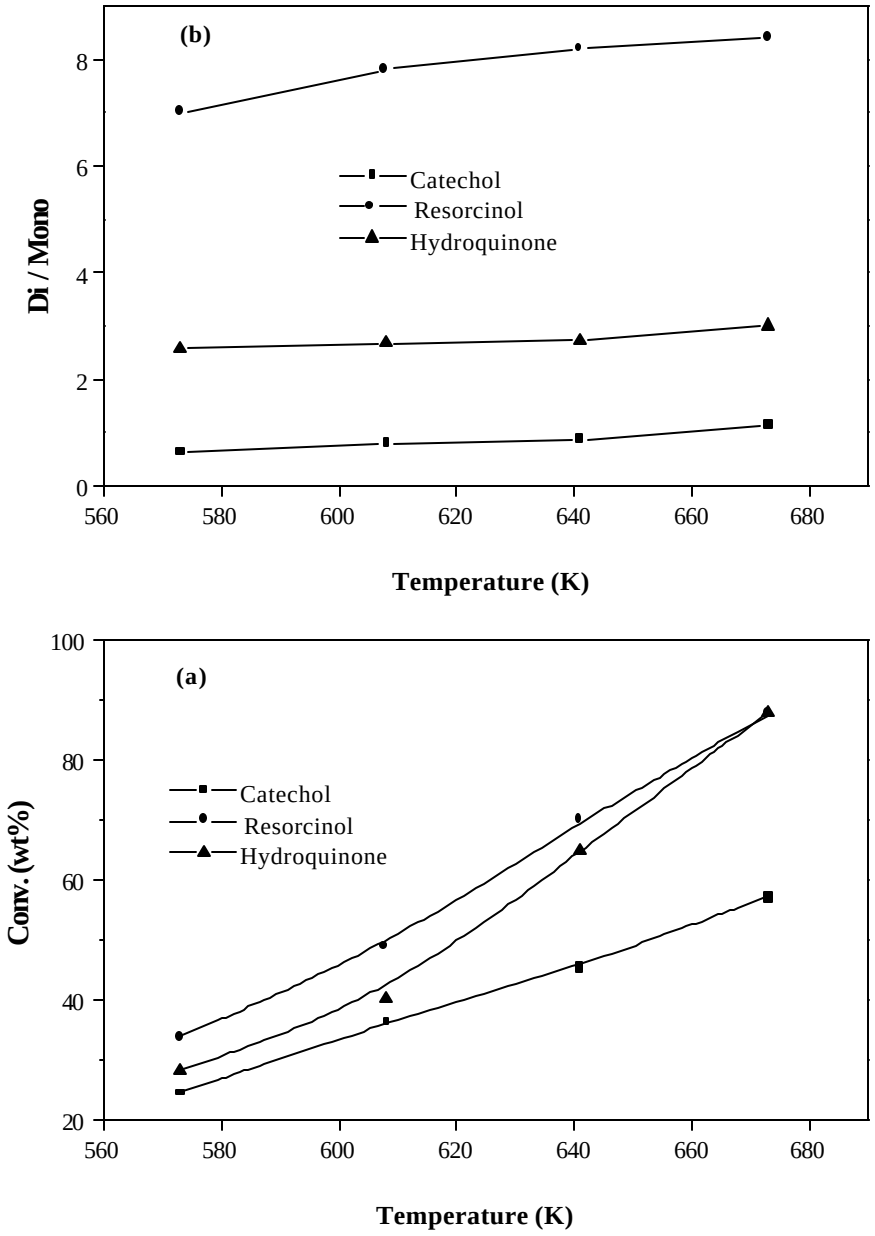

Fig. 4.20 Effect of temperature on conversion of dihydroxy benzenes and dimethoxy benzene / monomethoxy phenol ratios: (a) Conversion; (b) Dimethoxy / monomethoxy (Di / Mono) ratios (Conditions: TOS = 1h; contact time (h) = 0.376; N_2 = 18 ml/min; methanol / substrate (mole) = 5).

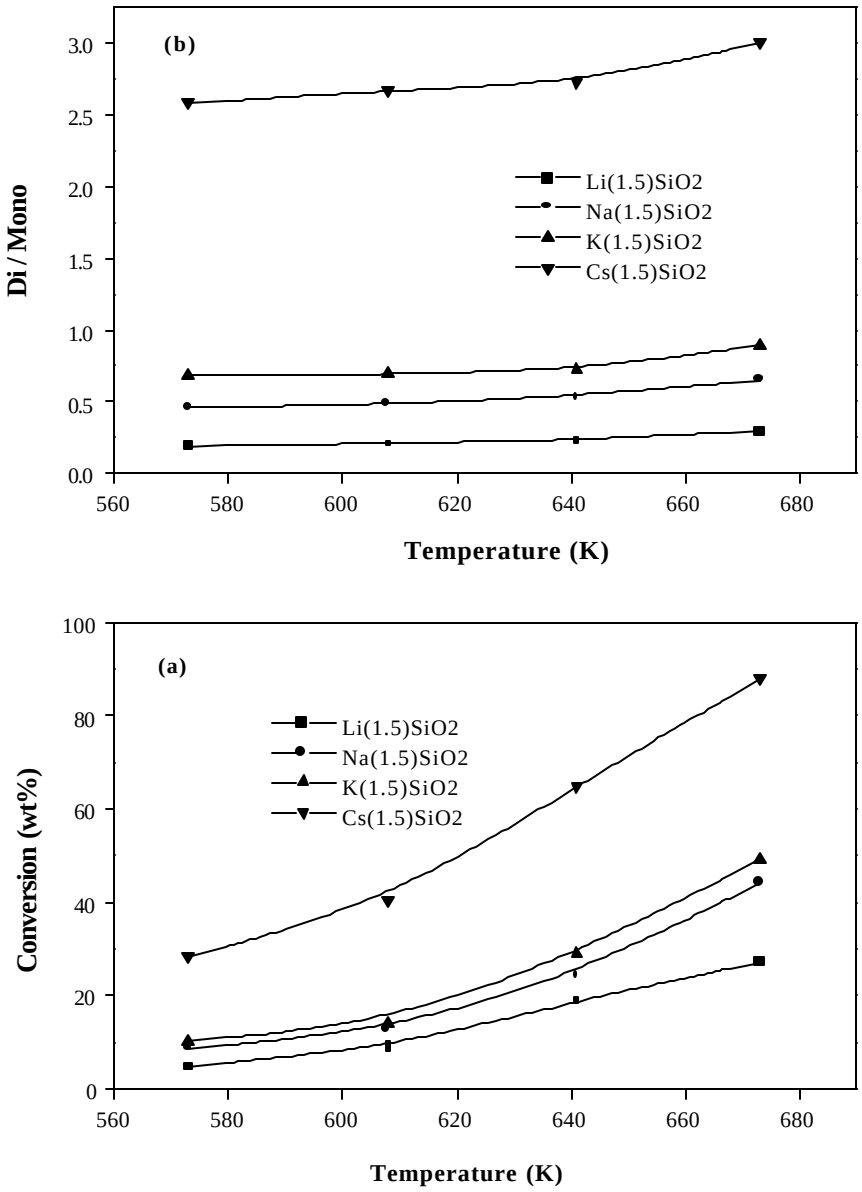

Fig. 4.21 Effect of temperature on conversion of hydroquinone over different alkali silica catalysts and dimethoxy benzene / monomethoxy phenol ratios: (a) Conversion; (b) Dimethoxy / monomethoxy (Di / Mono) ratios (Conditions: TOS = 1h; contact time (h) = 0.376; methanol / hydroquinone (mole) = 5; N_2 = 18 ml / min).

The influence of contact time on the distribution of mono and dialkylated products for the three substrates over $Cs(1.5)SiO_2$ is presented in Fig. 4.24. At the conditions of the study, the yield of the dialkylated product is more than the monoalkylated product due to high conversions in the case of resorcinol and HQ. A crossover of the curves for the di and mono substituted

products is seen for catechol. However, in all the cases, concentration maxima for the intermediate monoalkylated product (expected for consecutive reactions) is not observed. This is mainly due to the second methylation step being faster than the first one ($k_2 > k_1$ in the sequence of reactions shown below) and the maximum being reached at lower contact times (lower conversions) than those used in this study.

$$\text{Dihydroxy benzenes} \xrightarrow{(k_1)} \text{Monomethyl phenols} \xrightarrow{(k_2)} \text{Dimethoxy benzenes.}$$

4.3.4 O-Methylation of p-methoxy phenol

4.3.4.1 Reactivity of p-methoxy phenol (PMP)

The relative activities of alkali loaded SiO_2 in the methylation of PMP and hydroquinone (HQ) with methanol are presented in Table 4.7. As expected, activity for methylation of both PMP and HQ increases with increasing basicity of the catalyst. Similarly, O-methylation selectivity also increases with catalyst basicity for both substrates. Byproduct (C-alkylates) formation is found to be more in the case of HQ than PMP for Li, Na and K loaded catalysts. The selectivity is nearly 100% for both substrates over Cs-SiO_2.

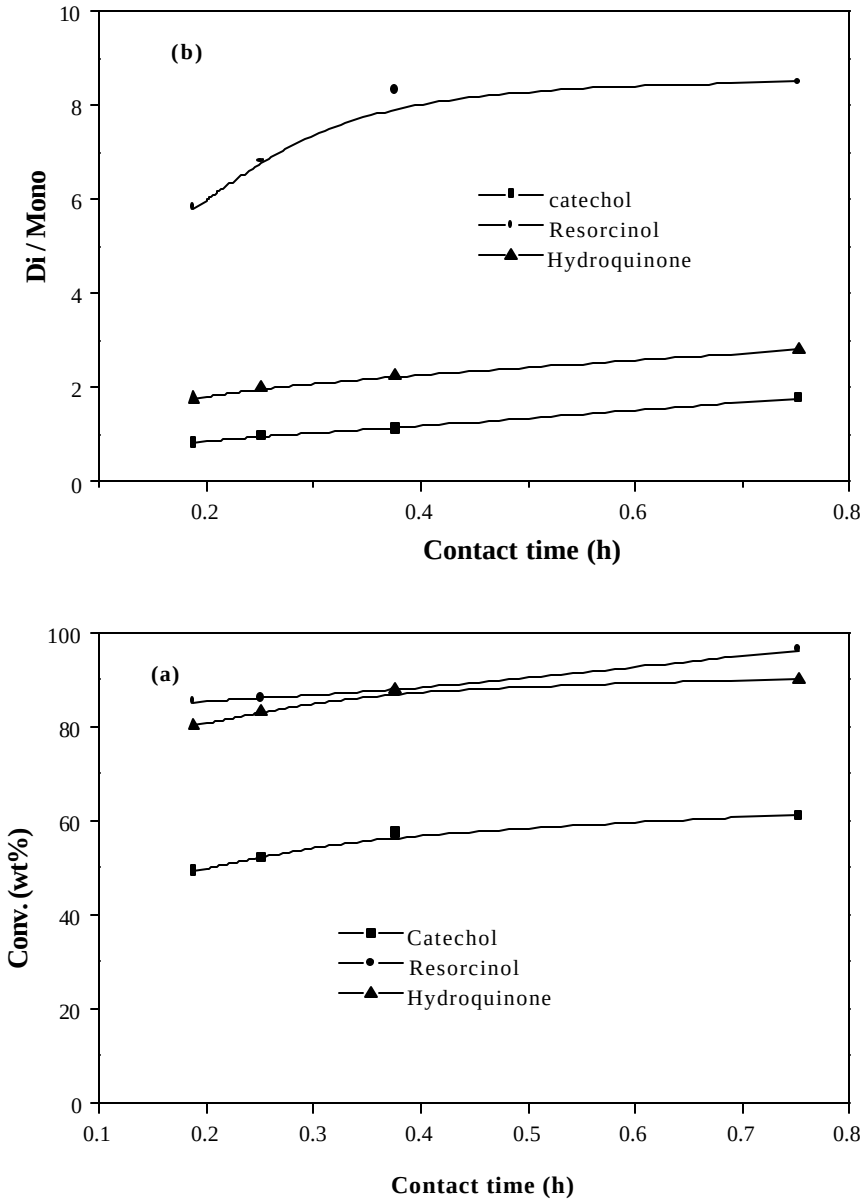

Fig. 4.22 Effect of contact time on conversion of dihydroxy benzenes and dimethoxy benzene / monomethoxy phenol ratios over $Cs(1.5)SiO_2$: (a) Conversions of dihydroxy benzenes; (b) Dimethoxy / monomethoxy (Di / Mono) ratios (Conditions: TOS = 1h; temperature = 673K; N_2 = 18 ml/min; methanol / substrate (mole) = 5).

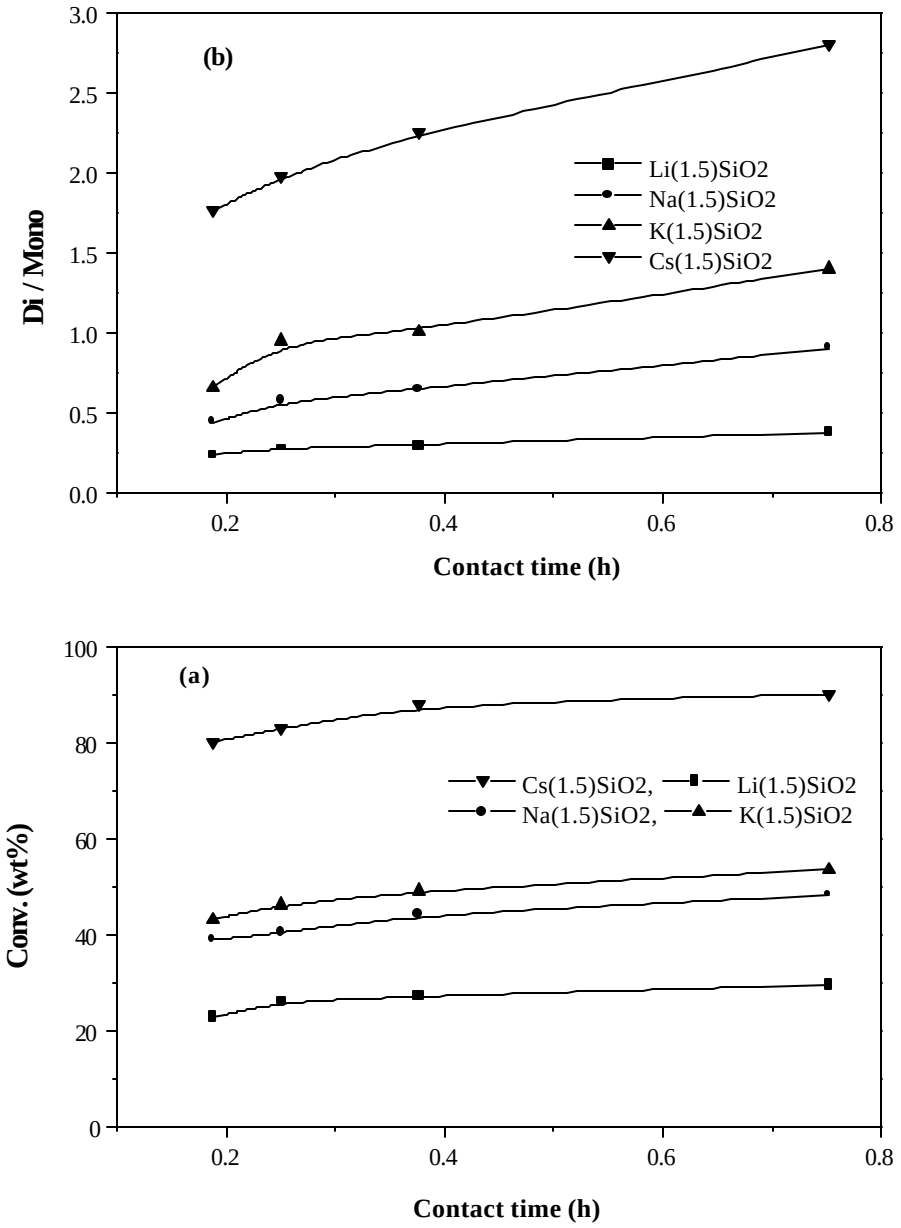

Fig. 4.23 Effect of contact time on conversion of hydroquinone and dimethoxy benzene / monomethoxy phenol ratios over alkali loaded silica: (a) Conversion; (b) Dimethoxy / monomethoxy (Di / Mono) ratios (Conditions: TOS = 1h; temperature = 673K; methanol / hydroquinone (mole) = 5; N_2 = 18 ml / min).

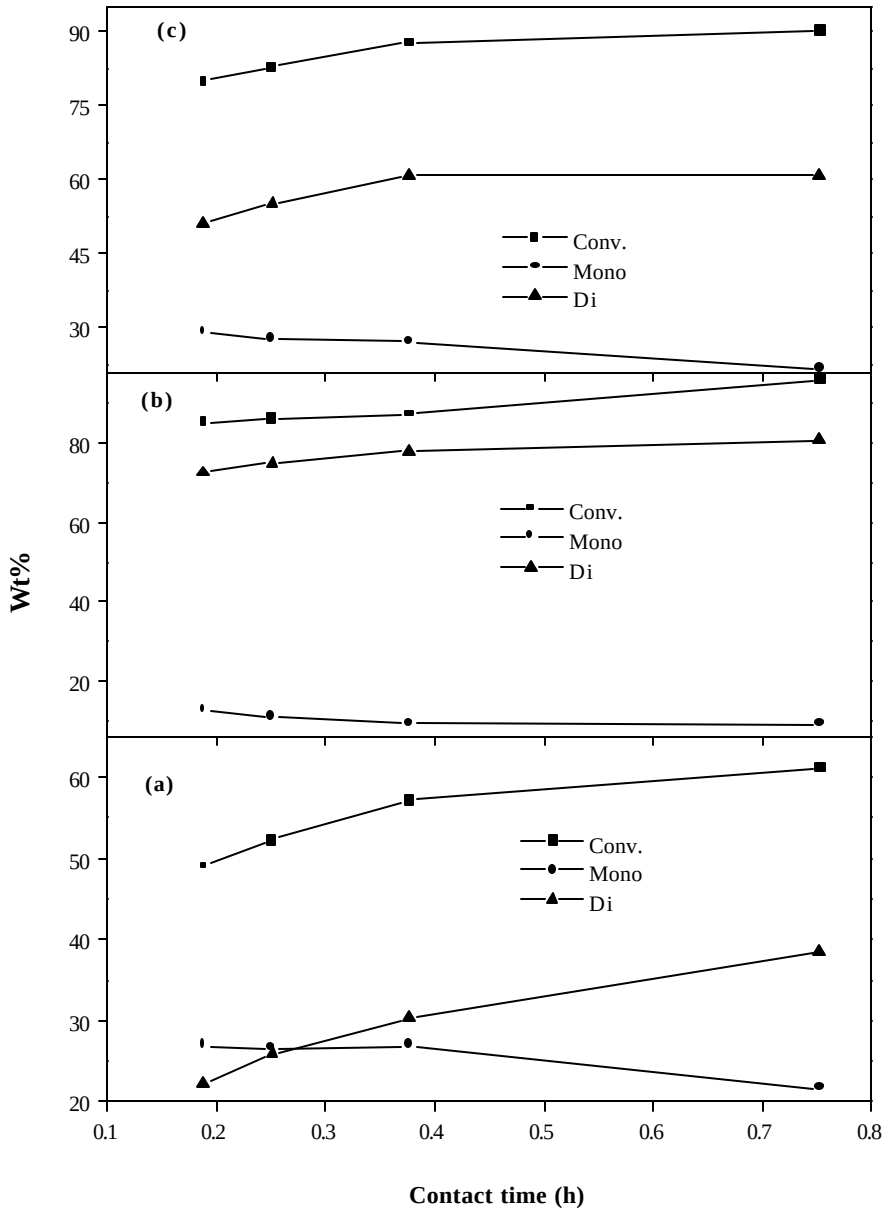

Fig. 4.24 Effect of contact time on conversion and product distribution over $Cs(1.5)SiO_2$: (a) catechol; (b) resorcinol; (c) hydroquinone (Conditions: TOS = 1h; temperature = 673K; methanol / substrate (mole) = 5; N_2 = 18 ml / min).

Comparing the reactivities of the two substrates, it is noticed that PMP is more reactive than HQ over all the catalysts, the reactivity difference decreasing with catalyst basicity. The relative reactivities of the catalysts for the two substrates (Conv. of PMP / Conv. of HQ) is 1.8, 1.4, 1.5 and 1.1 for Li, Na, K and Cs-loaded catalysts. The reason for the greater reactivity of PMP compared to HQ may be due to differences in the electronic effects of the substituent groups in the two molecules and also their modes of adsorption on the catalyst surface. It is expected that $-OCH_3$ group in the p-position will destabilize the adsorbed phenoxy intermediate (shown in section 4.3.3.2. on methylation of dihydroxy benzenes) to a lesser extent than an -OH group.

4.3.4.2 Influence of time on stream

The influence of time on stream on the conversion of PMP and HQ over different alkali loaded catalysts is presented in Fig. 4. 25. It is seen that catalyst activity is relatively more stable with PMP than with HQ as the feed. This is so inspite of the higher conversions obtained for PMP than for HQ. The values of average deactivation rates (per h per unit conversion) are presented in Table 4. 7 for both HQ and PMP. It is seen that the deactivation rates are lower for PMP over all the catalysts. Also, the differences in deactivation rates between the different catalysts are also smaller in the case of PMP.

4.3.4.3 Influence of process parameters

The influence of temperature on conversion of PMP over different alkali loaded SiO_2 samples is presented in Fig. 4. 26. For comparison, the data obtained using HQ are also presented. It is seen that PMP is more reactive

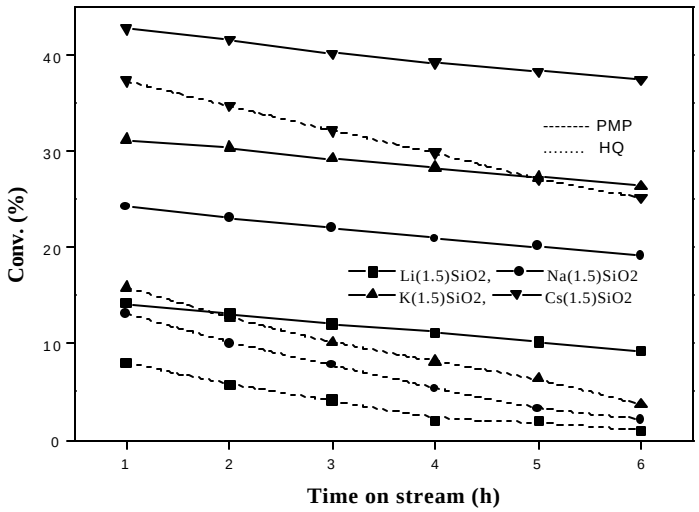

Fig. 4.25 Influence of time on stream on conversion of p-methoxy phenol over different alkali loaded SiO_2 catalysts (data of HQ also shown for comparison) (Conditions: Temperature = 598K, contact time (h) = 0.38, methanol / p-methoxy phenol or hydroquinone (mole) = 5, N_2 = 18 ml/min).

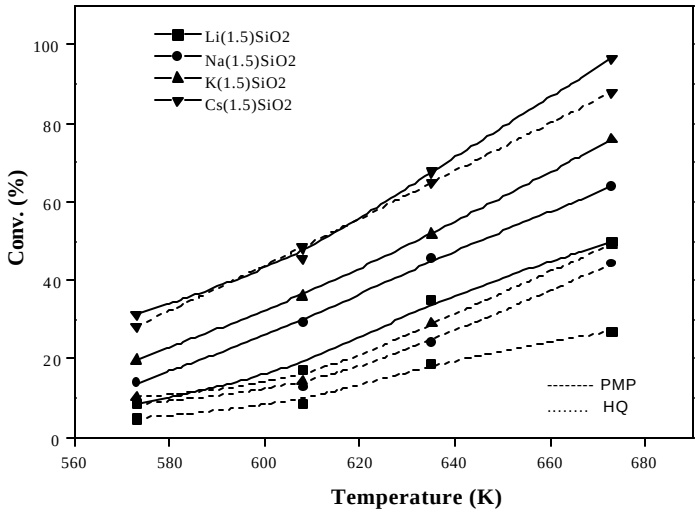

Fig. 4.26 Influence of temperature on conversion of p-methoxy phenol over different alkali loaded SiO_2 catalysts (data of HQ also shown for comparison) (Conditions: Time on stream = 1h, contact time (h) = 0.38, methanol / p-methoxy phenol or hydroquinone (mole) = 5, N_2 = 18 ml/min).

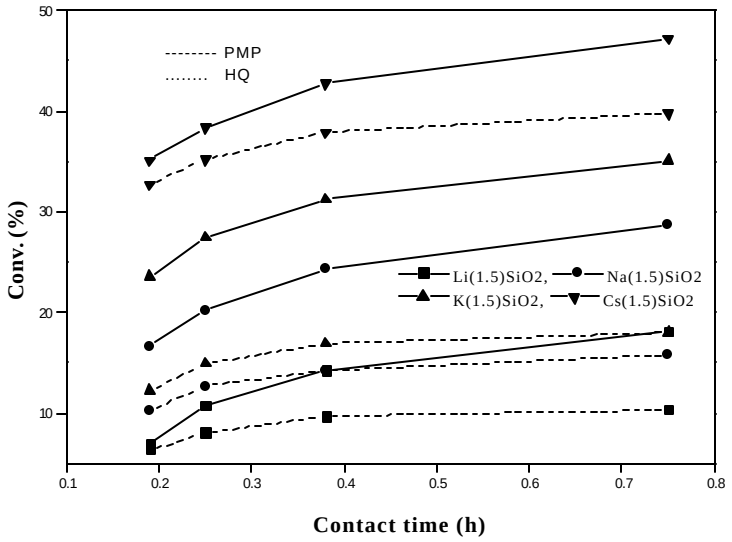

Fig. 4.27 Influence of contact time on the conversion of p-methoxy phenol over different alkali loaded SiO_2 catalysts (data of HQ also shown for comparison) (Conditions: Temperature = 598K, time on stream = 1h, methanol / p-methoxy phenol (mole) = 5, N_2 = 18 ml/min).

than HQ over all the catalysts at all the temperatures studied. As already seen, the more basic catalyst (Cs-SiO_2) is also the most active one at all the temperatures for the conversion of PMP (and HQ).

The influence of contact time on conversion of PMP over different alkali loaded catalysts is presented in Fig. 4. 27. As already found in the case of the other substrates (and as expected) conversion increases with increase in contact

time. The results obtained with HQ are also plotted in the same figure. Interestingly, compared to HQ, the influence of contact time on conversion of PMP is significant even at contact times > 0.4 h, whereas it is small in the case of HQ. This trend is noticed for all the four catalysts investigated

Table 4.7. Activities of the catalysts in methylation of p-methoxy phenol (PMP) and hydroquinone (HQ)

Catalyst[a]	Conv. (wt%)[b]		Selectivity (O-methylation)[c]		Deactivation rate (% conv loss $h^{-1}.conv^{-1}$)	
	PMP	HQ	DMB	PMP + DMB	PMP	HQ
SiO_2	4.5	4.9	5.3	-	-	-
$Li(1.5)SiO_2$	49.7	27.1	100	86.2	0.259	0.285
$Na(1.5)SiO_2$	63.8	44.1	100	91.9	0.156	0.175
$K(1.5)SiO_2$	75.8	49.1	100	94.9	0.102	0.135
$Cs(1.5)SiO_2$	96.4	87.9	100	100	.083	0.095

a: The number in brackets denotes the wt% of Cs loaded on SiO_2;b: Conversion based on p-methoxy phenol or hydroquinone; c: Selectivity difined as (mole O-methylated product / mole all the products) x 100 (Conditions: temperature = 673K; time on stream = 1h; contact time (h) = 0.376h; N_2 flow = 18 ml/min). PMP = p-Methoxy phenol; HQ = Hydroquinone; DMB = p-Dimethoxy benzene.

4.3.5 O-Methylation of 2-naphthol

4.3.5.1 Comparison of catalysts

The catalytic activities of silica samples loaded with different alkali metals and MCM-41 with different amount of Cs in the O-methylation of 2-naphthol at 673K are presented in Table 4. 8. The different products formed in the reaction are presented in Scheme 2. SiO_2 and MCM-41 have low activities, both of them producing mainly the C-alkylated products. 2-Methoxynaphthalene was not detected over these catalysts. The introduction of alkali ions increases dramatically the activity and O-alkylation selectivity of the catalysts. Conversion and selectivity (for O-methylation) increase with metal loading and basicity of the alkali metal (Cs> K> Na >Li; Table 4.8). As Cs/SiO_2 was found to be the most active catalyst, more experiments were carried out at different Cs-loadings. A general trend of increasing activity with increasing Cs loading is noticed. The yield of the C-methylated products, 1-methyl-2-hydroxynaphthalene (II) and 1-methyl-2-methoxynaphthalene (III) decrease with increasing basicity of the alkali ion (Li > Na > K > Cs; Table 4.8). Though the yield of II decreases rapidly and is not at all present in the product from Cs/SiO_2 (Table 4.8), the yield of III decreases only marginally and is formed even over the Cs catalyst. Usually C-alkylation is believed to be catalyzed by acidic sites. The formation of this compound (III) even over the most basic catalyst (Cs/SiO_2) is a result of the 1-

position being highly activated by the substituent in the 2-position. 1-Methyl-2-methoxynaphthalene (III) can be formed from 1-methyl-2-hydroxynaphthalene (II) or from 2-methoxynaphthalene (I). The absence of II in the products from Cs

catalysts suggests that III is probably formed mainly from I over Cs catalysts. This is supported by contact time studies over $Cs(1.5)SiO_2$ (Table 4.8) which reveal an increase in III with increasing contact time, due to further reaction of compound I; concomitantly, the yield of I decreases with contact time. In the case of the other alkali loaded catalysts, 1-methyl-2-hydroxynaphthalene (II) is present in substantial amount due to C-alkylation of 2-naphthol over these catalysts.

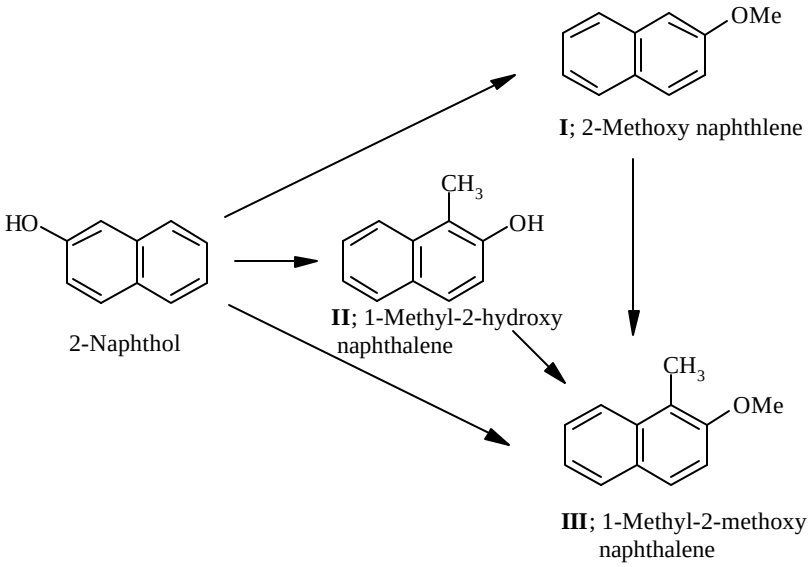

Scheme 2. Products of methylation of 2-hydroxynaphthalene (2-naphthol)

4.3.5.2 Influence of time on stream (TOS)

The influence of duration of run (time on stream, TOS) on conversion and product distribution in the case of Cs-loaded MCM-41 is presented in Fig. 28(a). It is seen that all the catalysts deactivate with time, a conversion loss of ~20% occurring in about 4h (98.9% at 1h and 76.1% at 4h) for Cs(0.225)-MCM-41. The yield of 2-methoxy naphthalene also decreases from 95.7% to 71.5% during the above period (Fig. 4.28(b)). The yield of the C-alkylated product is slightly larger, being 3.2% at

1h and 4.6% at 4h, suggesting a preferential deactivation of the O-alkylation activity. The results for alkali (Li, Na, K and Cs) loaded catalysts are presented in Fig. 4.29(a). It is noticed (again) that Cs-SiO_2 is much more active than the other catalysts. The influence of Cs content on activity of Cs-SiO_2 is presented in Fig. 4.29(b). Though there is an increase

Table 4.8. Activities of alkali loaded catalysts in the methylation of 2-naphthol

Catalyst[a]	Conv. (wt%)	Yield of products (wt%)			
		2-methoxy-naphthalene (I)	1-Methyl-2-methoxy-naphthalene (III)	1-methyl-2-hydroxy-naphthalene (II)	Others
SiO_2	9.2	-	-	6.7	2.5
Li(1.5)SiO_2	45.2	23.9	8.5	12.8	-
Na(1.5)SiO_2	53.0	38.6	9.2	5.2	-
K(1.5)SiO_2	57.1	41.7	9.9	5.5	-
Cs(1.5)SiO_2	100	89.1	10.9	-	-
MCM-41	4.7	--	-	3.8	0.9
Cs(0.075) MCM-41	88.3	70.9	13	4.4	-
Cs(0.15) MCM-41	95.7	87.8	8.9	-	-
Cs(0.225) MCM-41	98.9	95.7	3.2	-	-

[a] The number in brackets denotes the mmole of alkali metal loaded on 1 g of SiO_2 and MCM-41. Conditions: Temperature = 673K, Time on stream = 1h, methanol / 2-naphthol (mole) = 1:10, contact time (h) = 0.43, N_2 = 45 ml/min.

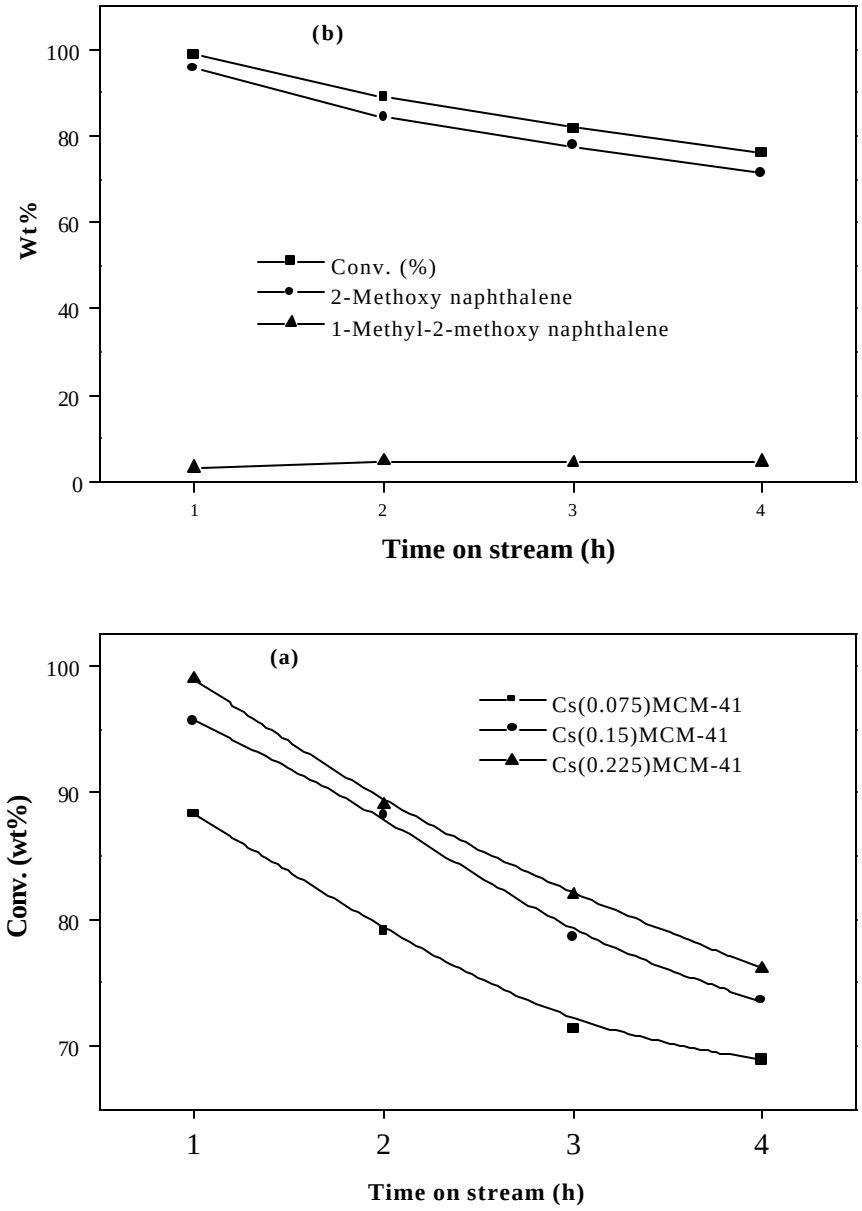

Fig. 4.28 Effect of time on stream on: (a) conversion and (b) product yields from 2-naphthol methylation over Cs(0.225)MCM-41 (Conditions: Temperature = 673K, contact time (h) = 0.43, methanol / 2-naphthol (mole) = 10, N_2 = 45 ml/min).

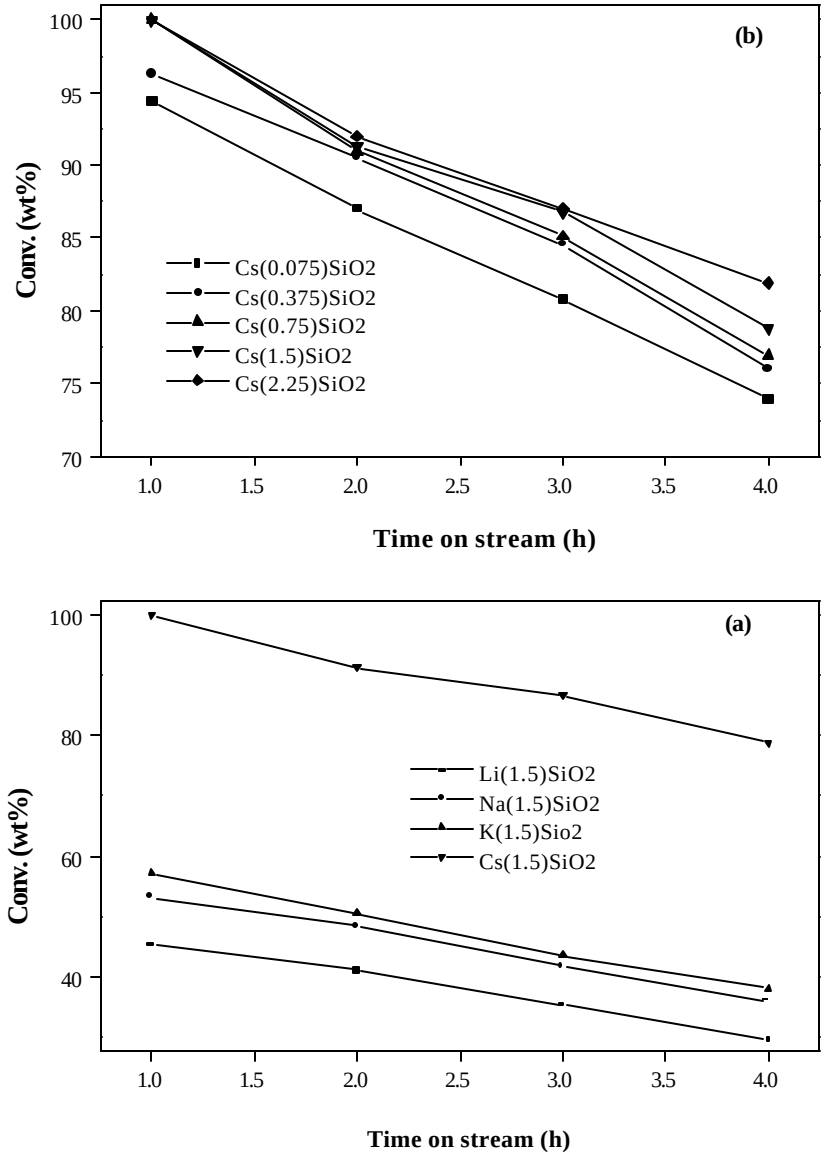

Fig. 4.29 Influence of time on stream on conversion over different catalysts: (a) alkali loaded SiO_2 and (b) Cs-SiO_2 with different Cs contents (Conditions: Temperature = 673K, contact time (h) = 0.43, methanol / 2-naphthol (mole) = 10, N_2 = 45 ml/min).

in conversion with Cs content, the effect becomes small at higher Cs loading. A similar trend is also seen in the case of Cs-MCM-41 samples (Fig. 4.28(a)).

4.3.5.3 Influence of temperature

The influence of temperature on conversion is presented in Fig. 4.30(a) and Fig. 4.31(a), respectively for Cs loaded MCM-41 and alkali (Li, Na, K and Cs) loaded silica. The influence of Cs content on activity at different temperatures is presented in Fig. 4.31(b). Fumed silica and MCM-41 possess negligible activity under the reaction conditions (Table 4.8). The influence of temperature on activity and product yields is presented in Fig. 4.30(b) in the case of Cs(0.225)-MCM-41. Along with increasing conversion, C-alkylation activity also increases slowly as seen from the yields of compound III, (1-methyl-2-methoxy naphthalene).

4.3.5.4 Influence of contact time

Conversion increases with increase in contact time (studied from 0.22 h to 0.88 h at 673K) for all the catalysts. Again as already noted, an increase in contact time favors C-alkylation (Fig. 4. 32 and Fig. 4. 33). Over Cs-SiO_2 catalysts 1-methyl-2-hydroxy naphthalene formation was not observed at all the contact times investigated. But for other alkali (Li, Na and K) loaded silica catalysts and Cs-loaded MCM-41 the formation of C-alkylated product, 1-methyl-2-hydroxy naphthalene increases slowly with contact time. For all the catalysts, the increase in conversion is more at lower contact times than at higher contact times. In the case of Cs-loaded MCM-41, a small amount of 6-methyl-2-hydroxy naphthalene was found at large contact times (data not presented).

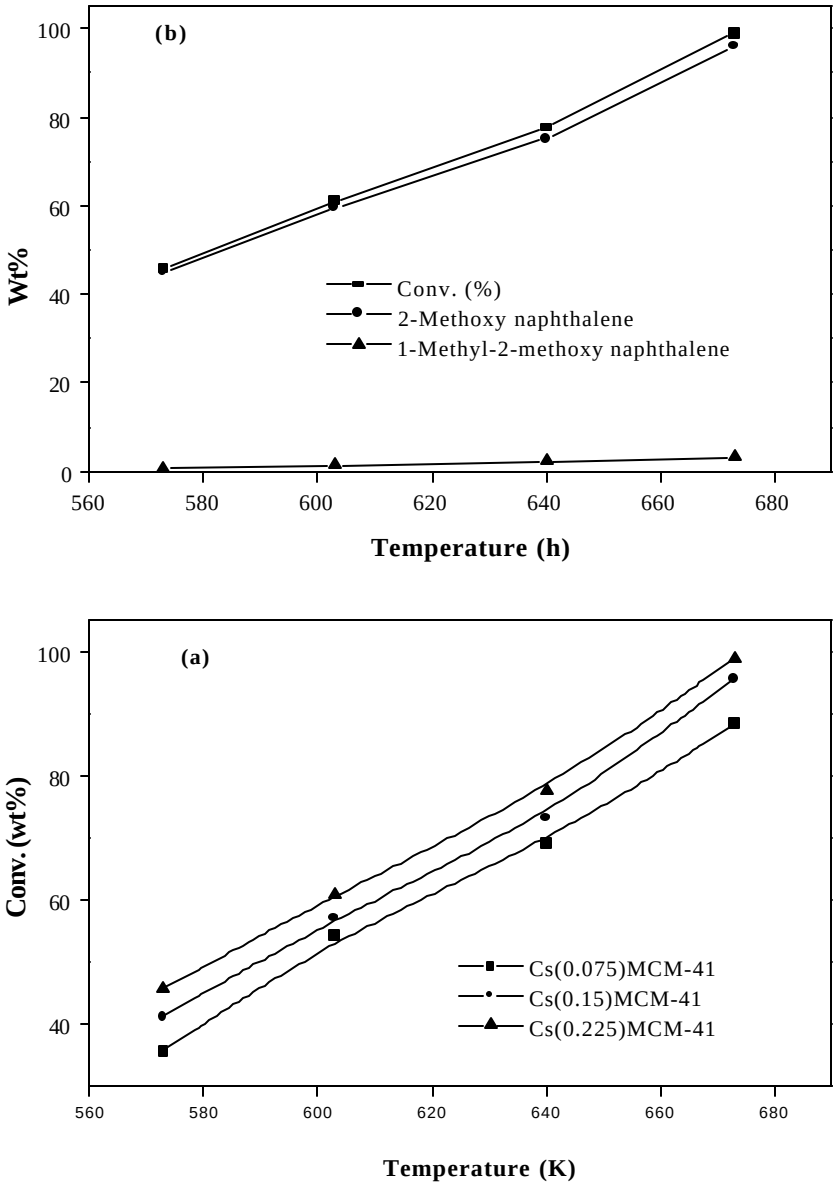

Fig. 4.30 Effect of temperature on: (a) conversion; (b) product yields from 2-naphthol methylation over Cs(0.225)MCM-41 (Conditions: Time on stream = 1h, contact time (h) = 0.43, methanol / 2-naphthol (mole) = 10, N_2 = 45 ml/min).

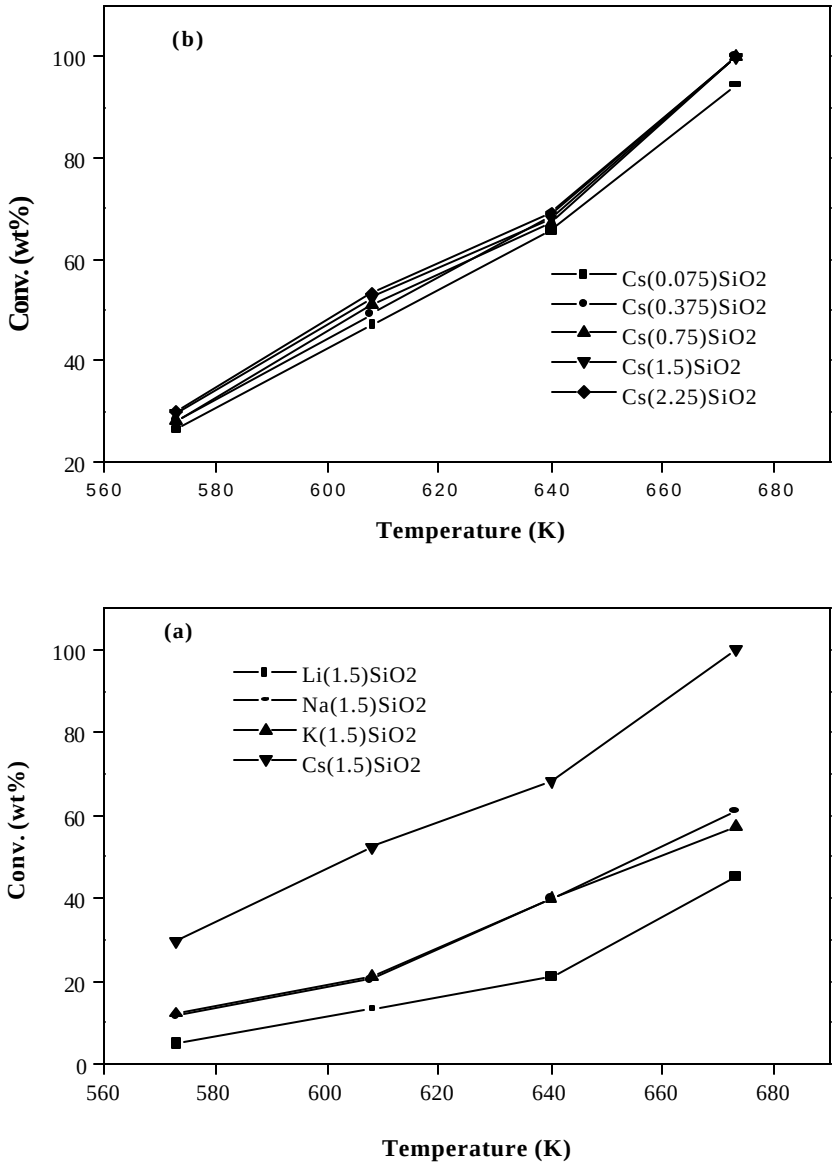

Fig. 4.31 Influence of temperature on conversion over different catalysts (a) alkali loaded SiO_2 and (b) Cs-SiO_2 with different Cs contents (Conditions: Time on stream = 1h, contact time (h) = 0.43, methanol / 2-naphthol (mole) = 10, N_2 = 45 ml/min).

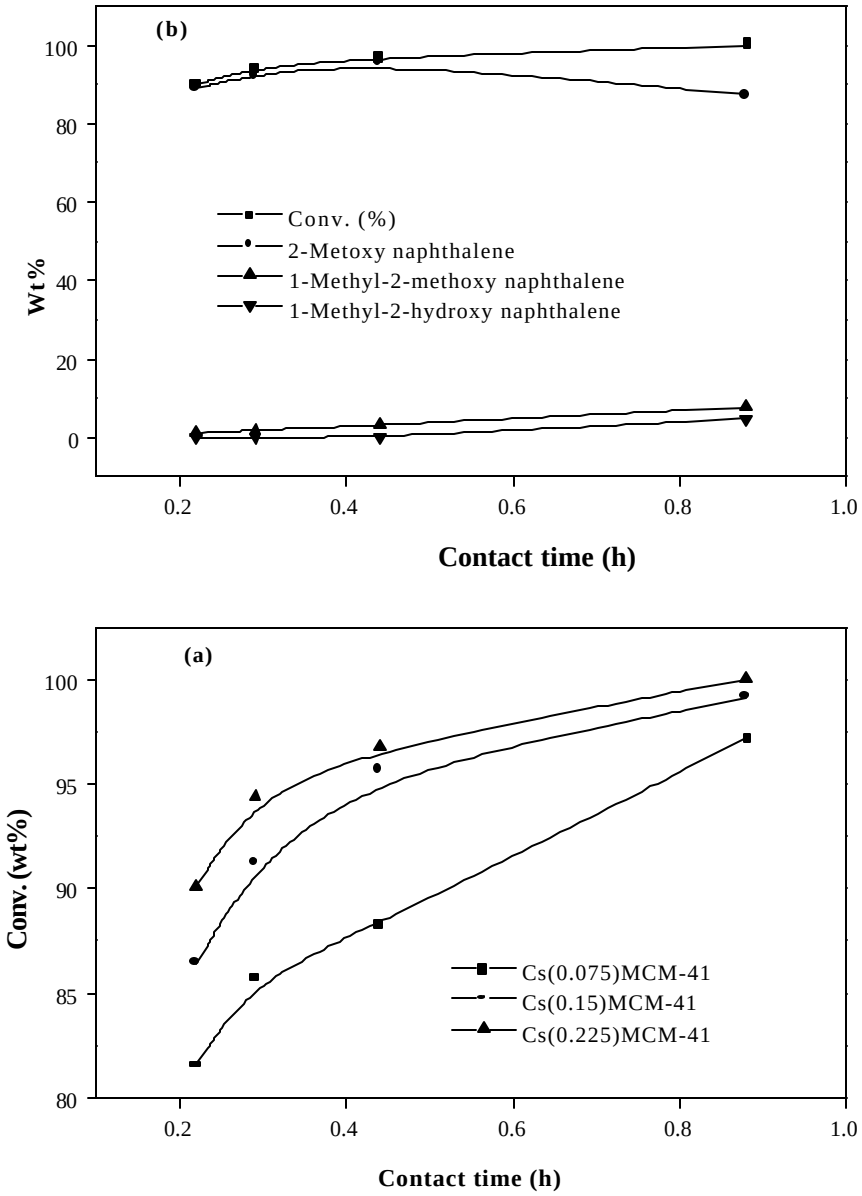

Fig. 4.32 Effect of contact time on (a) conversion and (b) product yields from 2-naphthol methylation over Cs(0.225)MCM-41 (Conditions: Time on stream = 1h, temperature = 673K, methanol / 2-naphthol (mole) = 10, N_2 = 45 ml/min).

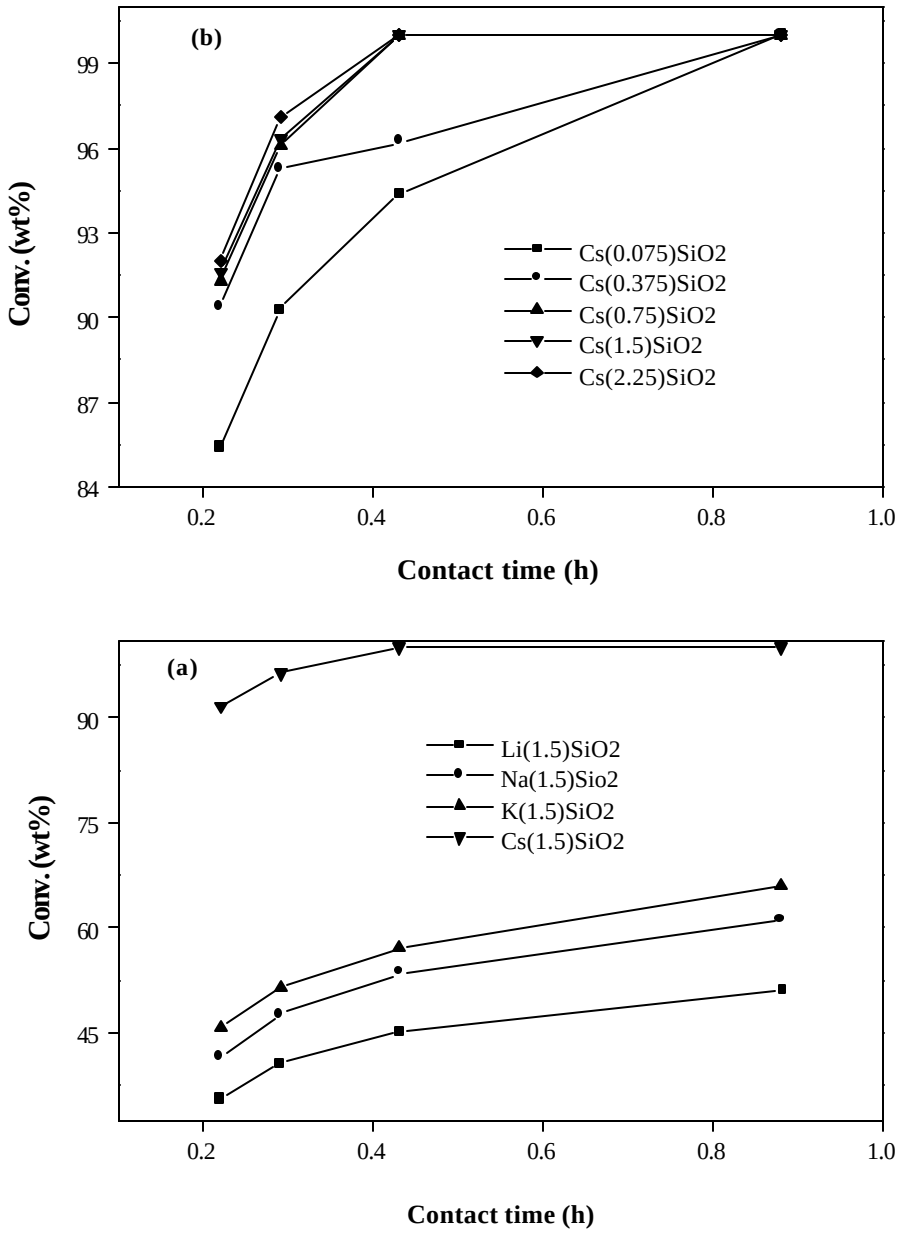

Fig. 4.33 Influence of contact time on conversion over different catalysts (a) alkali loaded SiO_2 and (b) Cs-SiO_2 with different Cs contents (Conditions: Temperature = 673K, time on stream = 1h, methanol / 2-naphthol (mole) = 10, N_2 = 45 ml/min).

The mechanism of the reaction probably is similar to that already discussed. It involves the formation of a transient 2-naphtholate species on the basic O^{2-} sites on the surface of alkali metal-loaded silica and Cs-loaded MCM-41and its reaction with $(CH_3)^{\delta+}(OH)^{\delta-}$ species adsorbed on the adjacent alkali ions as shown below. When the activation of the phenolic groups is relatively less (as in the case of the less basic catalysts), C-alkylation of the ring can also occur producing 1-methyl-2-hydroxynaphthalene.

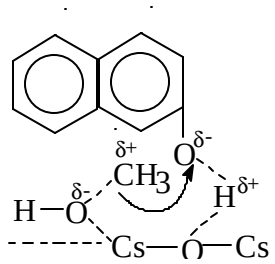

4.4 CONCLUSIONS

The study reveals that alkali supported SiO_2 samples are good catalysts for the alkylation of phenol with methanol, ethanol, n-propanol and n-butanol in the vapour phase. The most active catalyst is Cs-SiO_2. Methanol is more active compared to the other three alcohols in the O-alkylation of phenol. At lower temperatures, deactivation is less and decreases with increasing basicity of the catalyst. Deactivation is less when the methanol to phenol mole ratio is small. Deactivation rate (calculated on the basis of unit conversion) decreases with increase in basicity of the catalyst and with the size of the alcohol.

It is found that alkali loaded fumed silica samples are also excellent catalysts for the o-aklylation of cresols and dihydroxybenzenes in the vapour phase. High

conversions and high O-alkylation selectivities are obtained over these catalysts. The most active and selective catalyst is Cs-SiO_2 with about 1.5 mmole of Cs / g of catalyst. The order of reactivity of the cresols is p-cresol > m-cresol > o-cresol. The catalyst deactivation rate is in the reverse order: o-cresol > m-cresol > p-cresol.

Resorcinol is more reactive than the other two dihydroxy benzenes. The trend in reactivities of the dihydroxy benzenes can be explained if a [HO-C_6H_4-$O^{\delta-}$] adsorbed intermediate is postulated to be formed on the catalyst surface. Catalyst deactivation is more for catechol than for resorcinol and hydroquinone and decreases with increasing basicity of the catalyst. Similarities in basicity (as measured by TPD of CO_2 and FTIR) and activity trends are seen for the different catalysts. In the case of Cs-SiO_2 catalysts, basicity and activity are found to be related to the Cs available at the surface (as estimated by ESCA).

The mono methoxy phenols appear to be more reactive than the dihydroxy benzenes. Studies using p-methoxy phenol reveal that it causes less catalyst deactivation than hydroquinone.

The studies also reveal that Cs supported SiO_2 and MCM-41 are good catalysts for the O-alkylation of 2-naphthol in the vapour phase. Nearly 95% yield of 2-methoxynaphthalene is obtained. The small amount of 1-methyl-2-methoxy naphthalene formed over Cs-catalysts is a result of the further alkylation of 2-methoxynaphthalene.

4.4 REFERENCES

1. R. A. Sheldon, Chem. & Ind., 6th Jan. 1997, p13.
2. T. Yashima, K. Sato, T. Hayasaka, and N. Hara, *J. Catal*. **26**, 303 (1972).
3. M. Onaka, K. Ishikawa and Y. Izumi, *Chem. Lett*. 1783 (1982).
4. A. Corma, V. Fornes, R.M. Martin-Aranda, H. Garcia and Primo, *J. Appl. Catal*. **59**, 237 (1990).
5. P.E. Hathaway and M.E. Davis, *J. Catal*. **116**, 263 (1989).
6. P.E. Hathaway and M.E. Davis, *J. Catal*. **119**, 497 (1989).
7. H. Tsuji, F. Yagi and H. Hattori, *Chem. Lett*. 1881 (1991).
8. J.C. Kim, H.-X. Li, C.-Y. Chen, and M.E. Davis, *Microporous Mater*. **2**, 412 (1994).
9. D. Barthomeuf, *Catal. Rev*. *Sci. Eng*. **38**, 521 (1996).
10. H. Hattori, *Chem. Rev*. **95**, 537 (1995).
11. Y. Ono and T. Baba, *Catal. Today* **38**, 32 (1997).
12. K.R. Kloetstra, M. Van Laven and H. Van Bakkum, *J. Chem. Soc. Faraday Trans* **93**, 1211 (1997).
13. E.J. Doskocil, S.V. Bordawekar and R.J. Davis, *J. Catal*. **169**, 327 (1997).
14. R. Pierantozzi and F. Nordquist, *Appl. Catal*. **21**, 263 (1986).
15. M. Renaud, P.D. Chantal and S. Kaliaguine, *Can. Chem. Eng*. **64**, 787 (1986).
16. V. Durgakumari and S. Narayanan, *Catal. Lett*. **5**, 377 (1990).
17. V.V. Rao, V. Durgakumari and S. Narayanan, *Appl. Catal*. **49**, 165 (1989).

18. V.V. Rao, K.V.R. Chary, V. Durgakumari and S. Narayanan, *Appl. Catal.* **61**, 89 (1990).

19. P. Tundo, F. Trotta, G. Molaglio and F. Ligorati, *Ind. Eng. Chem. Res.* **27**, 1565 (1988).

20. C. Bezouhanova and M.A. Al-Zihari, *Appl. Catal.* **83**, 45 (1992).

21. E. Santacesaria, D. Grasso, D. Gelosa, and S. Carra, *Appl. Catal.* **64**, 83 (1990).

22. J. Xu, Ai-zhan Yan and Qin-Hua Xu, *Reac. Kinet.. Catal. Lett.* **62 (1),** 71 (1997).

23. M.C. Samolada, E. Grigoriadou, Z. Kiparissides and I.A. Salos, *J. Catal.* **152**, 52 (1995).

24. S. Balsama, P. Beltrame, P.L. Beltrame, P. Carniti, L. Forni and G. Zuretti, *Appl. Catal.* **13**, 161 (1984).

25. P.D. Chantal, S. Kaliaguine and J.L. Grandmaison, *Appl. Catal.* **10**, 317 (1984).

26. P. D. Chantal, S. Kaliaguine and J.L. Grandmaison, *Appl. Catal*. **18**, 133 (1985).

27. M. Renaud, P.D. Chantal and S. Kaliaguine, *Can. J. Chem. Eng.* **64**, 787 (1986).

28. V. Durgakumari, S. Narayanan and L. Guczi, *Catal. Lett*. **5**, 377 (1990).

29. Zi - Hua Fu and Y. Ono, *Catal. Lett*. **21**, 43 (1993).

30. M.C. Samolada, E. Grigoriadou, Z. Kiparissides and I.A. Vasalos, *J. Catal.* **152**, 52 (1995).

31. J. Xu, A.Z. Yan and Q. H. Xu, *Reac. Kinet. Catal. Lett*. **62(1)**, 71 (1997).

32. T. Beutel, *J. Chem. Soc., Faraday Trans.* **94(7)**, 985 (1998).

33. F. M. Bautista, J. M. Campelo, A. Garcia, D. Luna, J.M. Marinas and A.A. Romeo, *Reac. Kine. Catal. Lett.* **63(2)**, 261 (1998).

34. S.C. Lee, S.W. Lee, K.S. Kim, T.J. Lee, D.H. Kim, J.C. Kim, *Catal. Today* **44**, 253 (1998).

35. G. Dorothea in: E. Barbara, H. Stephen, S. Gail (Eds) Phenol Derivatives, Ulmann's Encyclopedia of Industrial Chemistry, A19, VCH Verlagsgere Mschaft, Weiteim, 354 (1991).

36. Y. Fu, T. Baba and Y. Ono, *Appl. Catal. A: Gen.* **166**, 419 (1998).

37. Y. Fu, T. Baba and Y. Ono, *Appl. Catal. A: Gen*. **166**, 425 (1998).

38. Y. Fu, T. Baba and Y. Ono, *Appl. Catal. A: Gen.* **176**, 201 (1999).

CHAPTER - V

N-ALKYLATION

N-ALKYLATION OF ANILINE WITH METHANOL AND DIMETHYL CARBONATE

5. 1 INTRODUCTION

N-alkylation of aniline is an industrially important reaction due to the fact that alkylanilines form the basic raw materials for the manufacture of many organic chemicals, dyes, explosives, herbicides, and pharmaceuticals [1]. Vapour phase aniline alkylation over environmentally safe solid catalysts is a superior method than the conventional commercial routes to the production alkylanilines using mineral acids and MeOH [2]. Several types of catalysts based on oxides and supported oxides [3-11], zeolites [12-24] and microporous aluminophosphates [24-26] have been tested for vapour phase aniline methylation. The main factors influencing activity and selectivity (N- and/or C-alkylation) are acid-base properties (number and strength) and shape selectivity in the solid acid catalyst as well as reaction conditions (temperature, feed composition and rate). Rao et al. [24] reported the alkylation of aniline with methanol over $AlPO_4$-5 molecular sieve. They observed that in aniline methylation N-methylaniline appears to be favoured at low temperatures (less than 598K). This is subsequently converted to N,N-dimethylaniline (NNDMA), which itself isomerises to N-methyl toluidine. Campelo et al. [27-29] reported the N-alkylation of aniline with methanol over $CrPO_4$ and $CrPO_4$-$AlPO_4$. They found > 90 mole % selectivity for N-alkylated products in 573-673 K temperature range. Varying the feed rates indicated that low contact time and

low temperature promoted the N-mono methylation reaction. Moreover, N,N-dimethyltoluidines (p- > o-) were present only in very small quantities even at the highest temperatures and/or contact times. On the other hand, the addition of $AlPO_4$ to $CrPO_4$ did not cause any significant change in the selectivity pattern exhibited by the $CrPO_4$ catalyst. This behaviour could indicate that similar adsorbed active species are formed on $CrPO_4$ and $CrPO_4$-$AlPO_4$ catalysts. Furthermore, there is no simple relationship between aniline alkylation activity and surface acidity measured by pyridine and 2,6-dimethylpyridine adsorption at 573 - 673K. Bautista et al. [28-29] also reported that N-alkylated products (NMA and NNDMA) are formed by a stepwise first order reaction process.

Ono et al. [30,31] reported the alkylation of aniline with methanol and dimethyl carbonate (DMC) over zeolites X and Y. They showed that faujasite (X and Y) is a better catalyst than ZSM-5, KL and Na-mordenite with regard to activity and selectivity. In particular, at the experimental conditions used (453 K), KY is a very good catalyst giving up to 99.6% conversion with 93.5% N-methylaniline (NMA) selectivity, the other products being N,N-dimethyl aniline (NNDMA). In N-methylation, DMC is a better methylating agent than methanol.

Selva et al. [32] reported the monomethylation of primary amines by DMC over X and Y type zeolites. According to them the unusual mono N-alkyl selectivity observed is likely to be due to synergistic effects between the double reactivity of DMC (acting both as a methylating and as a reversible methoxy carboxylating agent) and the dual acid base properties of zeolites along with the

steric demand by their cavities. Besides, the high selectivity, which allows high purity mono NMA to be prepared, the reaction also has remarkable environmentally benign features: it uses non toxic DMC, no inorganic wastes are produced (except CO_2) and no solvent is required.

The N-alkylation of aniline with MeOH and DMC over different Cs loaded molecular sieves is presented in this chapter. The reaction is shown below

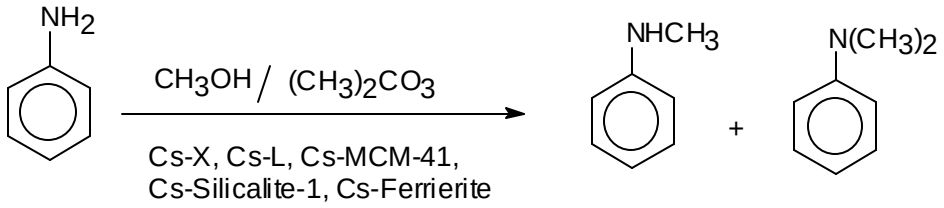

5.2 EXPERIMENTAL

5.2.1 Materials and catalyst

Aniline, methanol and dimethyl carbonate (> 99% purity) were obtained from S.D. Fine-chem Ltd., India. The catalysts used in the studies were CsX(OH), CsL, Cs(0.225)MCM-41, Cs-silicalite and Cs-ferrierite (preparation details given in Chapter II).

5.2.2 Reaction procedure

The catalytic experiments were carried out in a vertical downflow glass reactor (15mm i.d.). The catalyst (2g) was used in the form of granules (10-22 mesh) prepared by pelleting of the powders and crushing into the desire size. The reactor was placed inside a temperature controlled furnace (Geomecanique,

France) with a thermocouple placed at the center of the catalyst bed for measuring the reaction temperature. The catalyst was activated in flowing air (20 ml. min^{-1}) at 773K for 3h prior to flushing in N_2 and adjustment of temperature for start of the experiment. The feed (mixture of the methanol or DMC and aniline) was passed using a syringe pump (Braun, Germany) along with N_2 gas (18ml / min). The product was cooled in a water-cooled (ice-cold) condenser, collected in a receiver and analyzed in a gas chromatograph (HP5880A; capillary column HP1, 50m X 0.2mm; FID detector). Product identification was done by GC-MS and GC-IR.

5.3 RESULTS AND DISCUSSION

5.3.1 N-Alkylation with methanol

5.3.1.1 Activities of the catalysts

The activities of the catalysts in the alkylation of aniline with MeOH are presented in Table 5.1. Catalyst activity increases in the order: Cs-ferrierite < Cs-silicalite < Cs-MCM-41 < Cs-L < Cs-X. The selectivities for N-methylation, N-methyl aniline (NMA) and N,N-dimethyl aniline (NNDMA) also follow the same order. The N-methylation selectivity increases with the basicity of the catalyst. Over MCM-41, ferrierite and silicalite-1, some C-alkylated products, o-toluidine, p-toluidine and N,N-dimethyl toluidine were also found.

The following observations can be made in connection with the above results. 1) The Cs contents of the catalysts are different, being ~ 30% in CsX, ~

20% in CsL and only ~ 3% in the other three catalysts. 2) The experimentally observed basicity (by FTIR of adsorbed CO_2) is found to be related to the Cs content (Table 5.1). For catalysts with the same Cs content (Cs-MCM-41, Cs-silicalite and Cs-ferrierite), basicity decreases with decrease in pore size (or surface area). The basicity decrease with decreasing surface area / pore size is probably due to the poor dispersion of the alkali metal oxides. 3) The larger conversions, observed over the CsX and CsL are due to larger Cs content and basicity. The lowest activity of the Cs-ferrierite sample is due to lower Cs content and smaller pore dimensions, which may cause greater diffusion resistance for the reactants and products. 4) The lower basicity of Cs-MCM-41, Cs-ferrierite and Cs-silicalite (and the presence of weak acidity) is responsible for the formation of C-alkylated products over these catalysts. A surprising result is the absence of shape-selectivity effects over Cs-silicalite and Cs-ferrierite, which possess narrow pores (about 5.5Å for silicalite and 4.2 x 5.4 Å for ferrierite); the NMA / NNDMA ratios observed over these zeolites are 5.1 and 4.1 compared to 5.6 over Cs-MCM-41 and 6 over CsX. One would have expected the ratio to be larger over Cs-silicalite and Cs-ferrierite.

5.3.1.2 Effect of time on stream

The influence of time on stream (TOS) on the conversion of aniline is presented in Fig. 5.1(a). The product distribution over CsX is presented in Fig. 5.1(b). It is observed that all the catalysts deactivate slowly with TOS and N-methyl aniline (NMA) formation decreases, while N,N-dimethyl aniline (NNDMA) formation increases with TOS. The yields of the C-alkylated

products also decrease with time (not shown in figure). The NMA / NNDMA ratio decreases with time on stream over all the catalysts (Fig.5.2). The decrease in the ratios with time is not surprising as the reactivity of NMA is more than that of aniline. The average deactivation rates calculated over a six hour period are presented in Fig.5.3. The deactivation rate is defined as the average deactivation per hour between the first and sixth hours divided by the average conversion during this period. Deactivation rate increases in the order CsX < CsL < Cs-MCM-41< Cs-silicalite-1 < Cs-ferrierite. The rate of deactivation is very large for the medium pore zeolites, the deactivation rate being more for ferrierite with a unidimentional 10 membered ring pore system than for silicalite with a 2-dimentional 10 membered pore system.

5.3.1.3 Effect of temperature

The activities of the different catalysts on conversion of aniline at different temperatures (498-573K) are presented in Fig. 5.4(a). The product distribution over CsX at different temperatures is presented in Fig. 5.4(b). Conversion increases and yields of N-methyl and N,N-dimethyl aniline increase with temperature. In the case of the less basic catalysts, Cs-MCM-41, Cs-silicalite and Cs-ferrierite, C-alkylation products also increase with temperature (not presented). The NMA / NNDMA ratio decreases with increase in temperature (Fig. 5.5).

5.1. Activities of the catalyst in aniline methylation with methanol

Catalyst	Relative basicity[a] (FTIR)	Conv. (wt%)	Yield (wt%)			NMA / NNDMA
			NMA	NNDMA	Others	
CsX	182	69.3	59.4	9.9	-	6
CsL	130	63.8	51.5	11.3	-	4.6
Cs-MCM-41	83	48.9	33.1	5.9	9.9	5.6
Cs-silicalite-1	64	38.0	20.3	4.0	13.7	5.1
Cs-ferrierite	49	25.0	11.7	2.8	9.3	4.1

a: The relative basicities of the catalysts are the relative intensities of the bands of adsorbed CO_2 (at 0.4 mm) in the region 1200 cm^{-1} to 1750 cm^{-1} (Chapter II).
NMA = N-methyl aniline, NNDMA = N,N-dimethyl aniline, Others = o-Toluidine + p-Toluidine + N,N-dimethyl-p-toluidine (Conditions: Temperature = 548K, time on stream = 1h, contact time (h) = 0.58, methanol / aniline (mole) = 5, N_2 = 18 ml/min).

5.3.1.4 Effect of contact time

Conversion increases with increase in contact time for all the catalysts (Fig. 5.6(a)). The yield of NNDMA increases and that of NMA decreases with contact time (Fig. 5.6(b)). The NMA / NNDMA ratios decrease with increase in contact time (Fig. 5.7).

5.3.1.5 Effect of methanol / aniline mole ratios

Conversion increases for all the catalysts with increase in methanol / aniline mole ratio (Fig. 5.8(a)). The product distributions obtained at different MeOH / aniline feed ratios over CsX is presented in Fig. 5.8(b). With the increase in

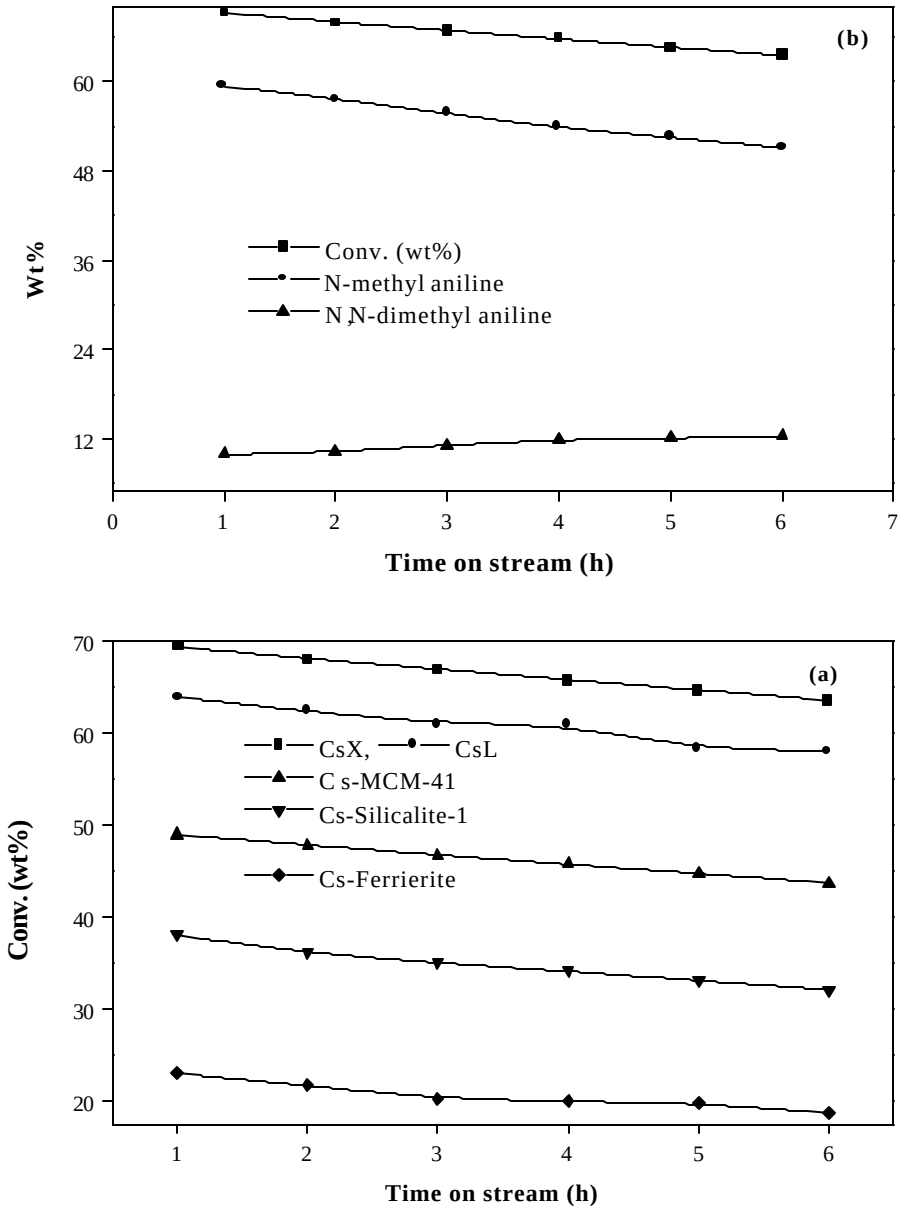

Fig. 5.1 Influence of time on stream on methylation of aniline with methanol (a) conversion over different catalysts; (b) product yields over CsX (Conditions: Temperature = 548K, contact time (h) = 0.58, methanol / aniline (mole) = 5, N_2 = 18 ml/min).

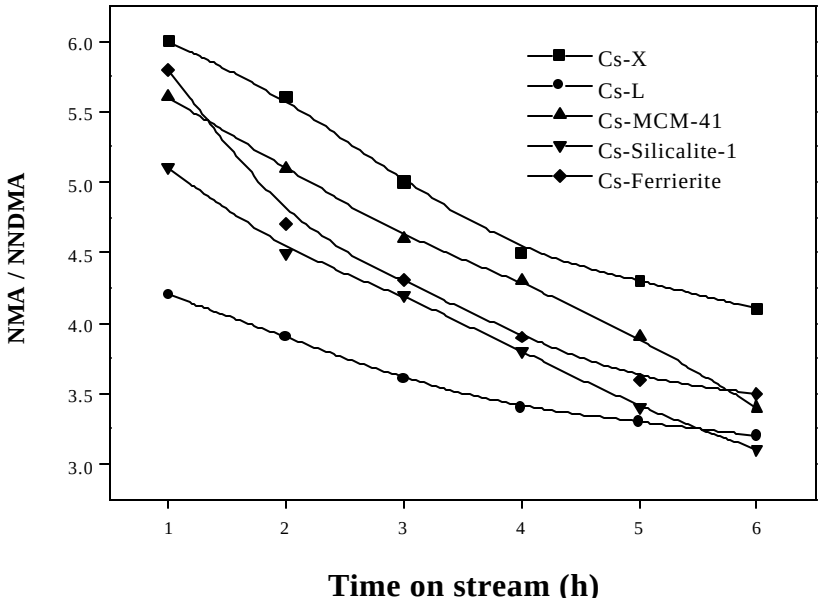

Fig. 5.2 Influence of time on stream on NMA/NNDMA product ratios over different catalysts (Conditions: Temperature = 548K, contact time (h) = 0.58, methanol / aniline (mole) = 5, N_2 = 18 ml/min).

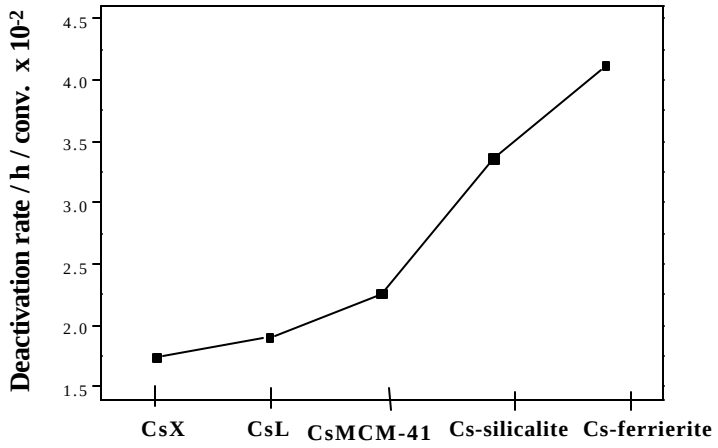

Fig. 5.3 Deactivation rate for various catalysts in aniline methylation with methanol (Conditions: Temperature = 548K, contact time (h) = 0.58, methanol / aniline (mole) = 5, N_2 = 18 ml/min, deactivation rate / h = $2(C_1 - C_6) / 5(C_1 + C_6)$, where C_1 and C_6 are conversions at 1h and 6h respectively.

methanol content of the feed, the selectivity for NMA decreases and that for NNDMA increases. The NMA / NNDMA ratio decreases rapidly with increase in MeOH / aniline (mole) ratio (Fig. 5.9)).

5.3.1.6 Reaction pathway

A plot of product yields against conversions of aniline over CsX is presented in Fig. 5.10. The plot for NMA is extrapolatable to origin suggesting that it is the primary product. The zero slopes at the origin and the upward deviation of the NNDMA plot with conversion suggest NNDMA to be a secondary product formed from NMA.

From the data on feed rate, temperature and the yield vs. conversion curves, it can be concluded that aniline methylation on various Cs-loaded zeolites follows a sequential reaction pathway. NMA is the primary product, which is subsequently converted to NNDMA. The driving force here is the greater nucleophilicity of the N-atom over the C-atom. Besides, NMA reacts faster than aniline due to its greater negative charge on the N-atom associated with the electron donating effect the methyl group. Moreover, dimethyl substitution on N-atoms makes ring alkylation at o- and p- position easy through electron donation to the benzene ring. This leads to increasing amounts of C-alkylated products with increasing NNDMA content. The formation of NNDMA via disproportionation of NMA is less favourable than its formation via successive alkylation [24].

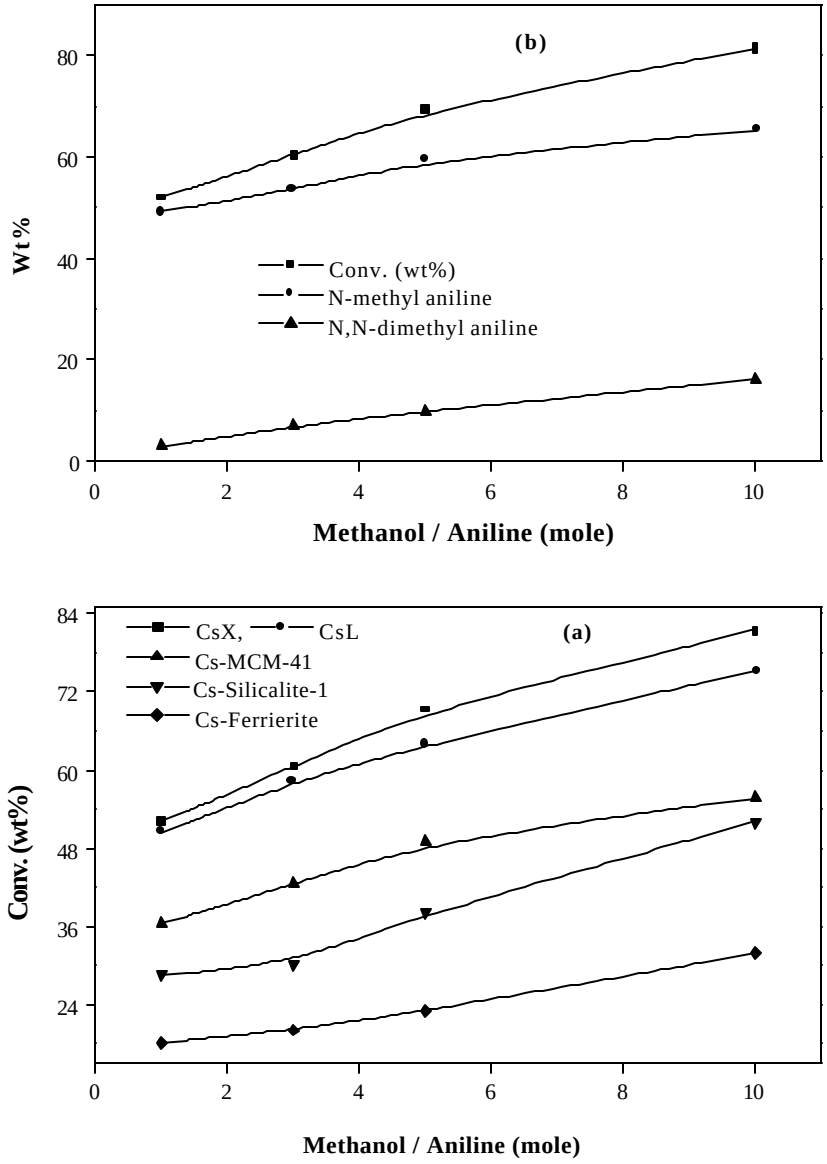

Fig. 5.4 Influence of temperature: (a) aniline conversion; (b) product yields over CsX (Conditions: Time on stream = 1h, contact time (h) = 0.58, methanol / aniline (mole) = 5, N_2 = 18 ml/min).

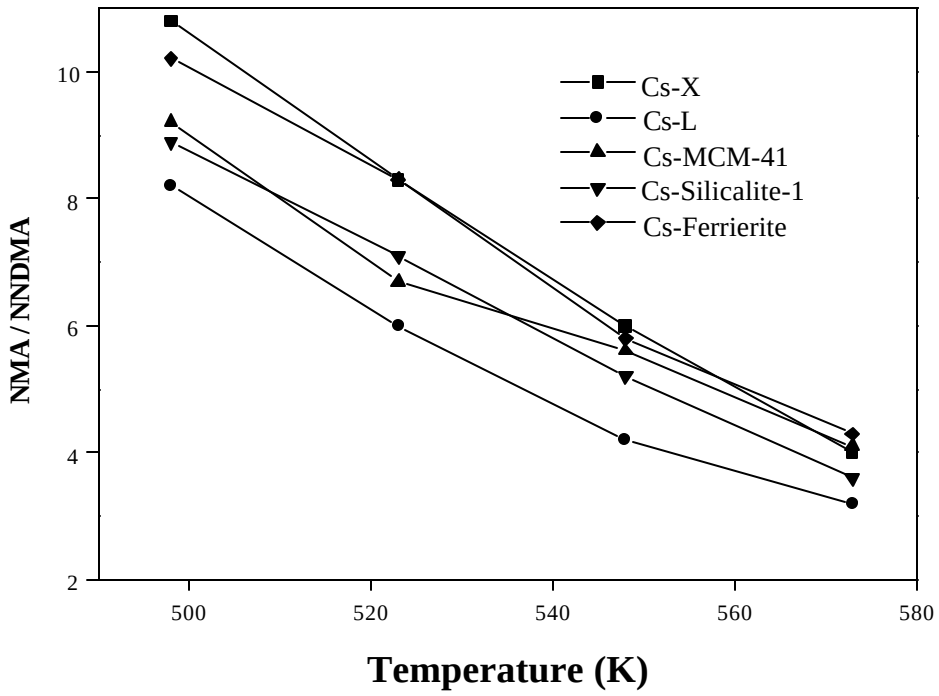

F

ig. 5.5 Influence of temperature on NMA / NNDMA product ratios (Conditions: Time on stream = 1h, contact time (h) = 0.58, methanol / aniline (mole) = 5, N_2 = 18 ml/min).

5.3.2 N-Alkylation with dimethyl carbonate

5.3.2.1 Activities of the catalysts

The activities of the catalysts are presented in the Table 5.2. The activity increases in the order: Cs-ferrierite < Cs-silicalite < Cs-MCM-41 < Cs-L < Cs-X. The selectivities for N-alklation, N-methyl aniline (NMA) and N,N-dimethyl aniline (NNDMA) follow the same order. The N-methylation selectivity increases with the basicity of the catalyst. Over Cs-MCM-41, Cs-ferrierite and

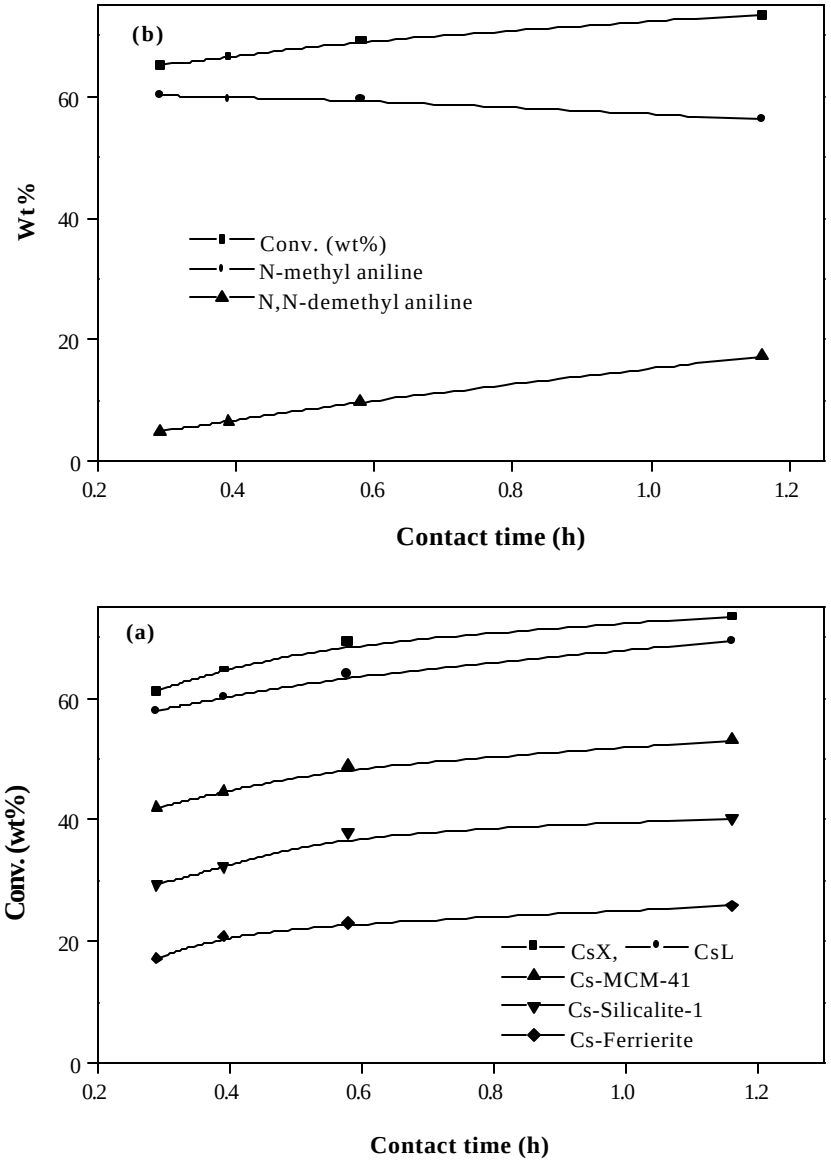

Fig. 5.6 Influence of contact time: (a) aniline conversion over different catalysts; (b) product yields over CsX (Conditions: Time on stream = 1h, temperature = 548K, methanol / aniline (mole) = 5, N_2 = 18 ml/min).

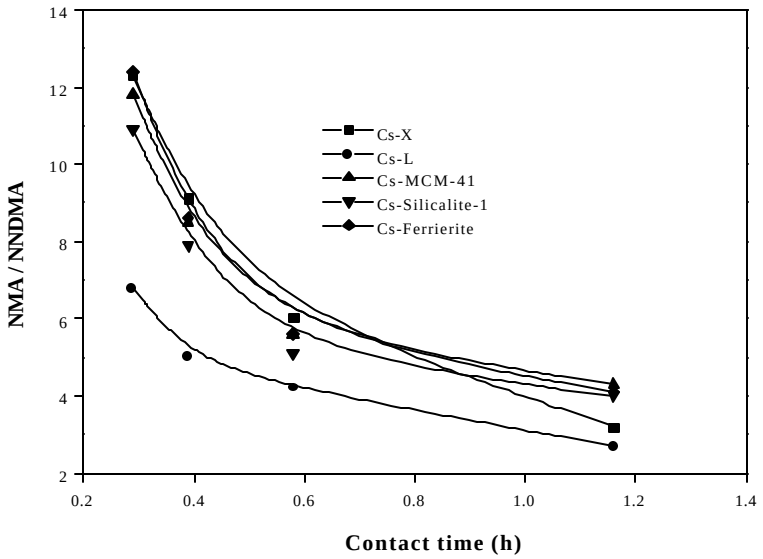

Fig. 5.7 Influence of contact time on NMA / NNDMA product ratios over different catalysts (Conditions: Temperature = 548K, time on stream = 1h, methanol / aniline (mole) = 5, N_2 = 18 ml/min).

Cs-silicalite-1 some C-alkylated products o-toluidine, p-toluidine and methyl phenyl carbamate, N-methyl-N-phenyl carbamate are also found.

In general, the conclusions are similar to those made in the case of methylation with MeOH (Table 5.1; section 5.3.1.1). It is to be noticed that eventhough MeOH / aniline ratio was 5 in the earlier experiments (Table 5.1) and the DMC / aniline ratio is 2.5 in the present experiments, the amount of effective alkylating agent used in both sets of experiments is the same as DMC contains two equivalents of MeOH (2 MeOH + CO_2 $\rightarrow$ Me_2CO_3 + H_2O). Comparing the alkylations with DMC and MeOH (Table 5.1 and 5.2), it is noticed that DMC is a more effective alkylating agent than MeOH as the conversions are larger with DMC compared to MeOH. This is probably due to

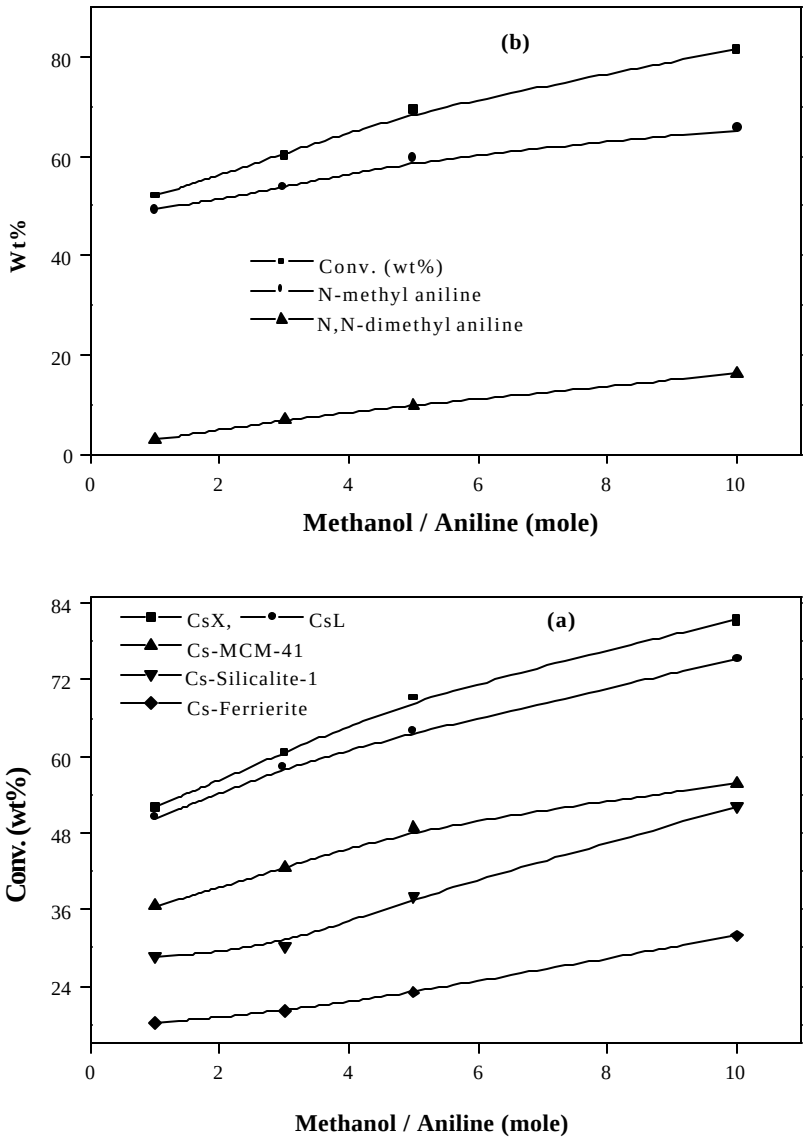

Fig. 5.8 Influence of methanol / aniline molar ratios of feed: (a) aniline conversion over different catalysts; (b) product yields over CsX (Conditions: Time on stream = 1h, temperature = 548K, contact time (h) = 0.58, N_2 = 18 ml/min).

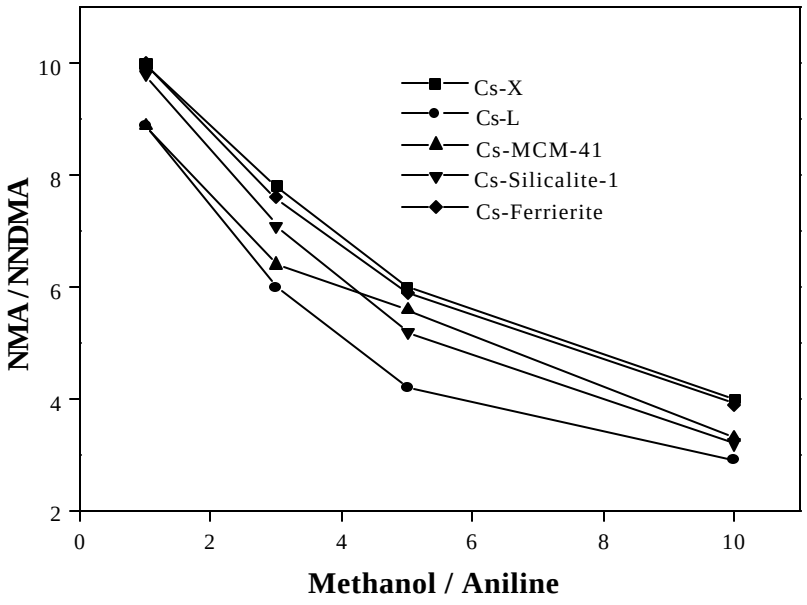

Fig. 5.9 Influence of methanol / aniline mole ratios on NMA / NNDMA product ratios (Conditions: Temperature = 548K, contact time (h) = 0.58, time on stream = 1h, N_2 = 18 ml/min).

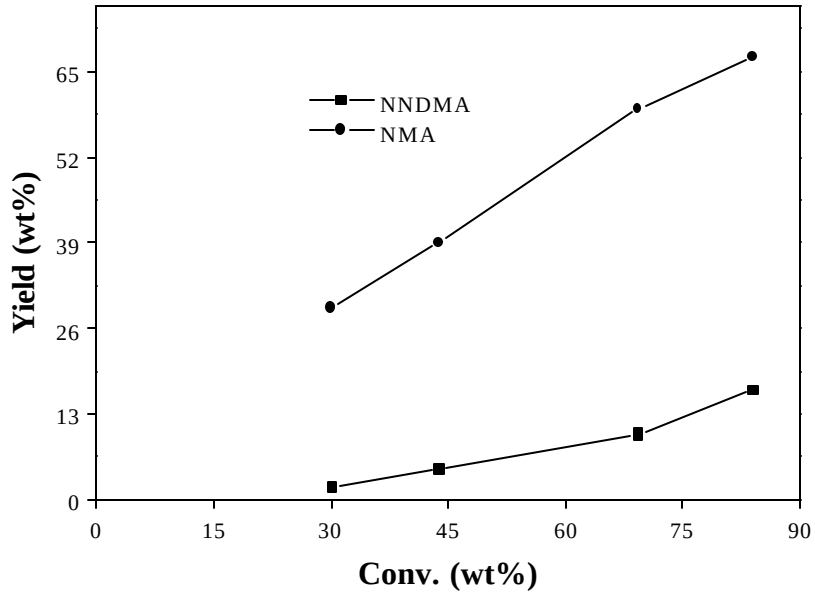

Fig. 5.10 Product yield vs. conversion curves in aniline conversion with methanol over CsX at different temperatures (Conditions: Time on stream = 1h, methanol / aniline (mole) = 5, N_2 = 18 ml/min).

the absence of H_2O and the suppression of the reverse hydrolysis reaction that could occur when MeOH is used. Besides, it is likely that CO_2 (formed when DMC is used) is less damaging to the catalyst than water (formed when MeOH is used). Another observation is that NMA / NNDMA ratios are smaller when DMC is used than when MeOH is used. The NMA / NNDMA values for the different catalysts are in the range 1.5 to 2.5 when DMC is used while it is in the range 4.1 to 6 when MeOH is used. Thus, DMC is a better methylating agent than MeOH. The larger amounts of NNDMA formed with DMC may also be due to simultaneous dimethylation of aniline with DMC though there is no direct proof for its occurrence.

5.3.2.2 Effect of time on stream

The influence of time on stream (TOS) on the conversion of aniline is presented in Fig. 5.11(a). The product distribution over CsX is presented in Fig. 5.11(b). It is observed that all the catalysts deactivate with TOS and N-methyl aniline (NMA) formation decreases while N,N-dimethyl aniline (NNDMA) formation increases. The NMA / NNDMA ratio decreases with time on stream over all the catalysts and is presented in Fig. 5.12. The average deactivation rates calculated over a six hour period are presented in Fig. 5.13. Deactivation rate increases in the order CsX < CsL < Cs-MCM-41< Cs-silicalite-1 < Cs-ferrierite. These observations are similar to those made in the case of MeOH (Section 5.3.1.2.). Comparing the deactivation rates in the presence of MeOH and DMC (Fig. 5.3 and Fig. 5.13), it is noticed that the deactivation rate with DMC is nearly

half of that observed in the case of MeOH. The lower deactivation rate with DMC is probably due to the absence of water which might act as poison. Besides, in the case of MeOH, it might undergo dehydrogenation and condensation reactions on the surface leading to carbonaceous products. The formation of these products is less likely when DMC is used.

Table 5.2. Activities of different catalysts in aniline methylation with dimethyl carbonate

Catalyst	Conv. (wt%)	Yield (wt%)			NMA / NNDMA
		NMA	NNDMA	Others	
CsX	79.5	53.7	25.8	-	2.1
CsL	67.5	40.6	26.9	-	1.5
Cs-MCM-41	53.9	29.9	17.1	6.9	1.8
Cs-silicalite-1	47.5	20.7	12.5	14.3	2.3
Cs-ferrierite	30.1	12.2	5.9	12.0	2.5

NMA = N-methyl aniline, NNDMA = N,N-dimethyl aniline, Others = o-Toluidine + p-Toluidine + methyl phenylcarbamate + N-methyl-N-phenylcarbamate.
(Conditions: Temperature = 548K, time on stream = 1h, contact time (h) = 0.58, dimethyl carbonate / aniline (mole) = 2.5, N_2 = 18 ml/min)

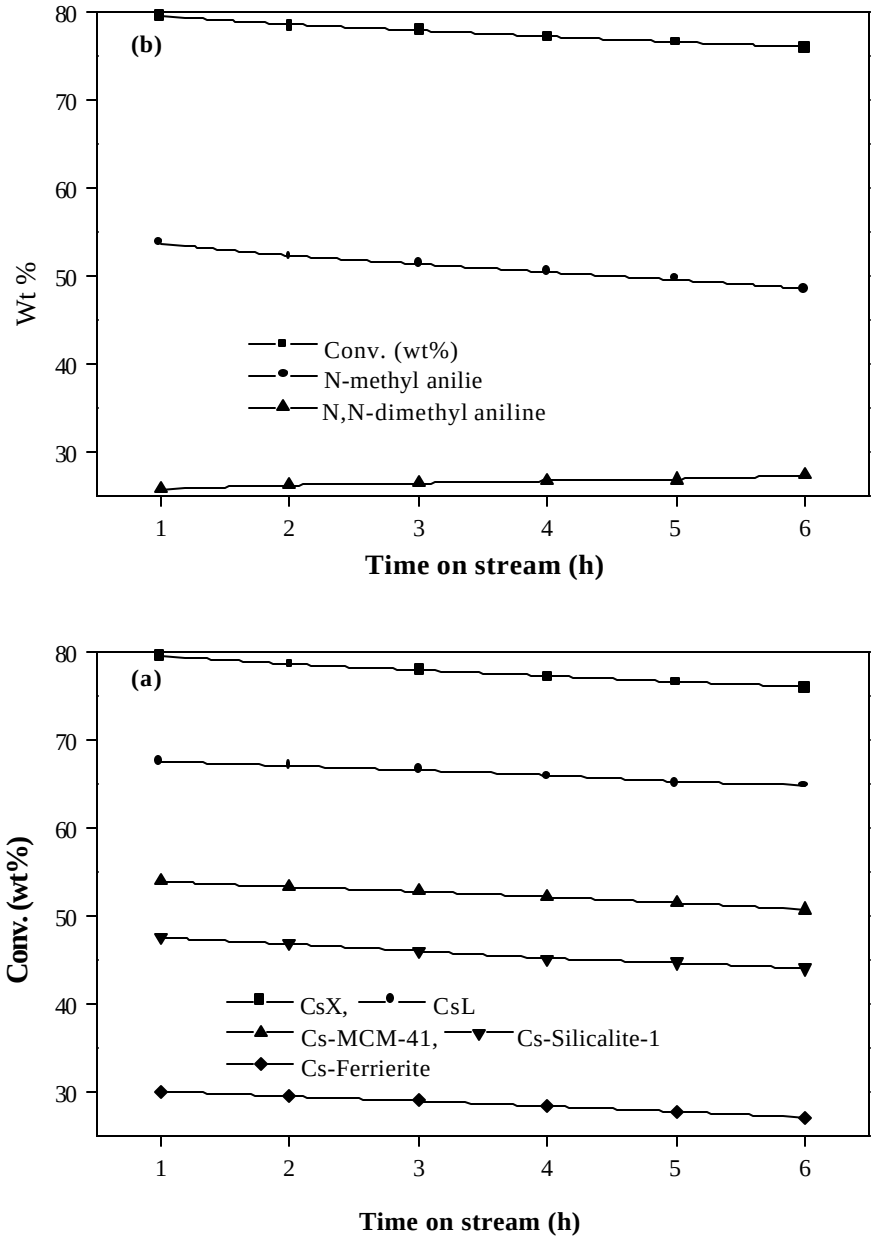

Fig. 5.11 Influence of time on stream: (a) aniline conversion over different catalysts; (b) product yields over CsX (Conditions: Temperature = 548K, contact time (h) = 0.58, DMC / aniline (mole) = 2.5, N_2 = 18 ml/min).

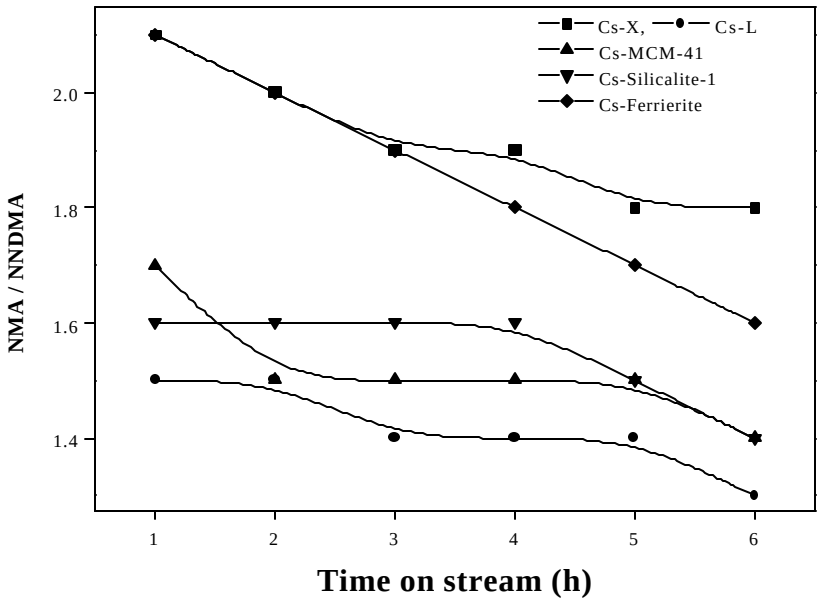

Fig. 5.12 Influence of time on stream on the NMA / NNDMA product ratios (Conditions: Temperature = 548K, contact time (h) = 0.58, DMC / aniline (mole) = 2.5, N_2 = 18 ml/min).

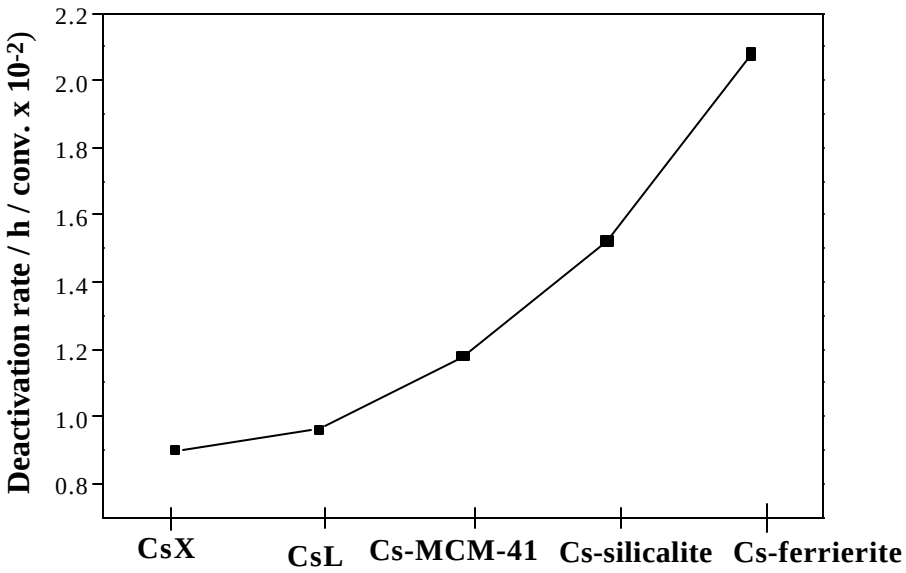

Fig. 5.13 Deactivation rate for various catalysts in aniline methylation with DMC (Conditions: Temperature = 548K, contact time (h) = 0.58, DMC / aniline (mole)= 2.5, N_2 = 18 ml/min).

5.3.2.3 Effect of temperature

The reactivities of aniline at different temperatures (498-573K) are presented in Fig. 5.14(a). Conversion increases with temperature. The product distribution over CsX at different temperatures is shown in Fig. 5.14(b). The yields of both NMA and NNDMA increase with temperature, the increase in yield of NNDMA being more rapid.

Due to the more rapid increase in NNDMA yield, the NMA / NNDMA ratio decreases with increase in temperature (Fig. 5.15).

5.3.2.4 Effect of contact time

Conversion increases with increase in contact time for all the catalysts. The conversion of aniline observed at different contact times over different catalysts is plotted in 5.16(a). The product distribution obtained over CsX at different contact times is shown in Fig. 5.16(b). With increase in contact time, the selectivity for NMA decreases and that for NNDMA increases; the NMA / NNDMA ratios decrease (Fig. 5.17).

5.3.2.5 Effect of DMC / aniline mole ratios

The conversions at different DMC / aniline mole ratios are presented in Fig. 5.18(a). The product distributions over CsX are also given in Fig. 5.18(b). With the increase in DMC / aniline mole ratios the conversion increases for all the catalysts. With the increase in DMC / aniline mole ratio the selectivity for NMA decreases and the selectivity for NNDMA increases (Fig. 5.19). The NMA / NNDMA ratio is plotted as a function of DMC / aniline (mole ratio) in Fig. 5.19. The ratio decreases steeply with increasing DMC content.

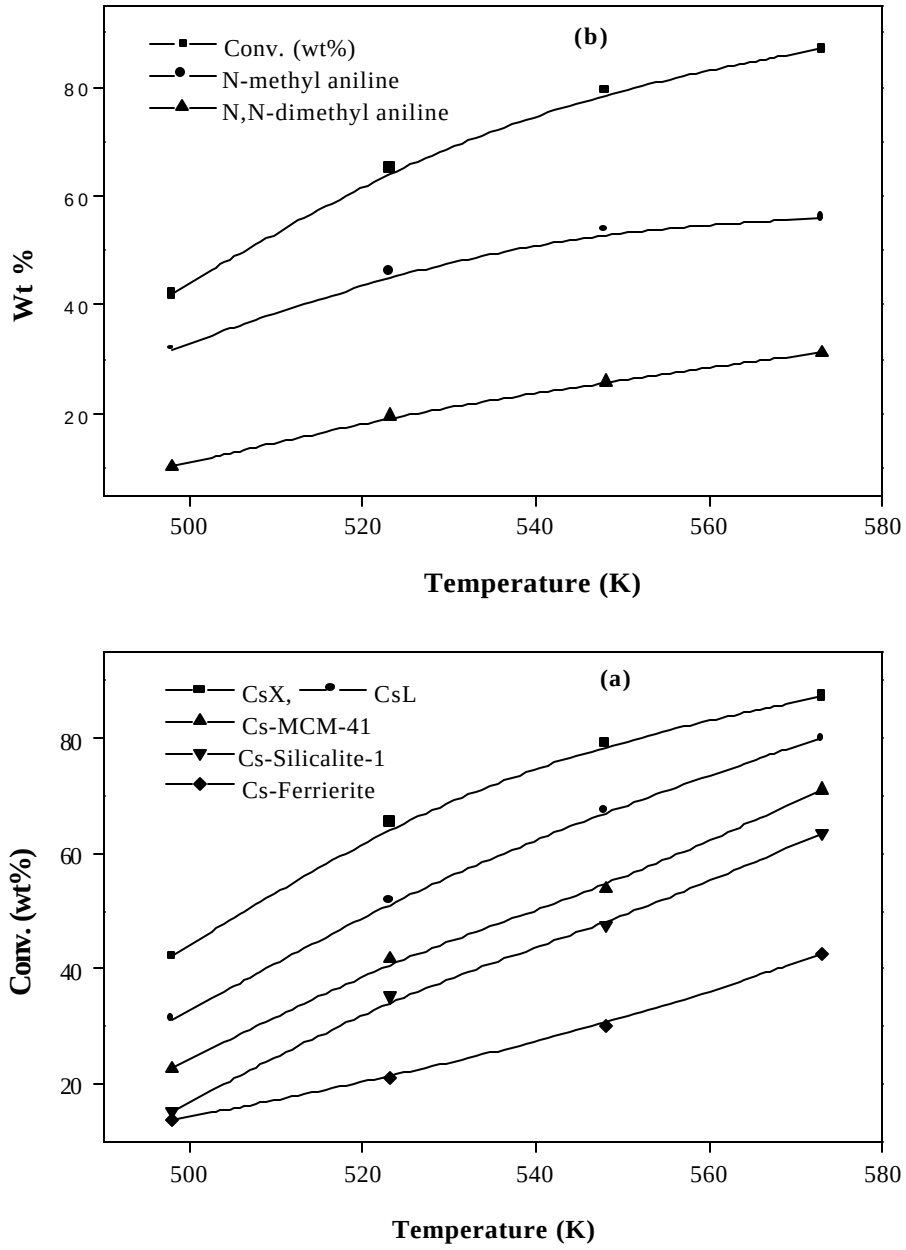

Fig. 5.14 Influence of temperature: (a) aniline conversion over different catalysts; (b) product yields over CsX (Conditions: Time on stream = 1h, DMC / aniline (mole) = 2.5, contact time (h) = 0.58, N_2 = 18 ml/min).

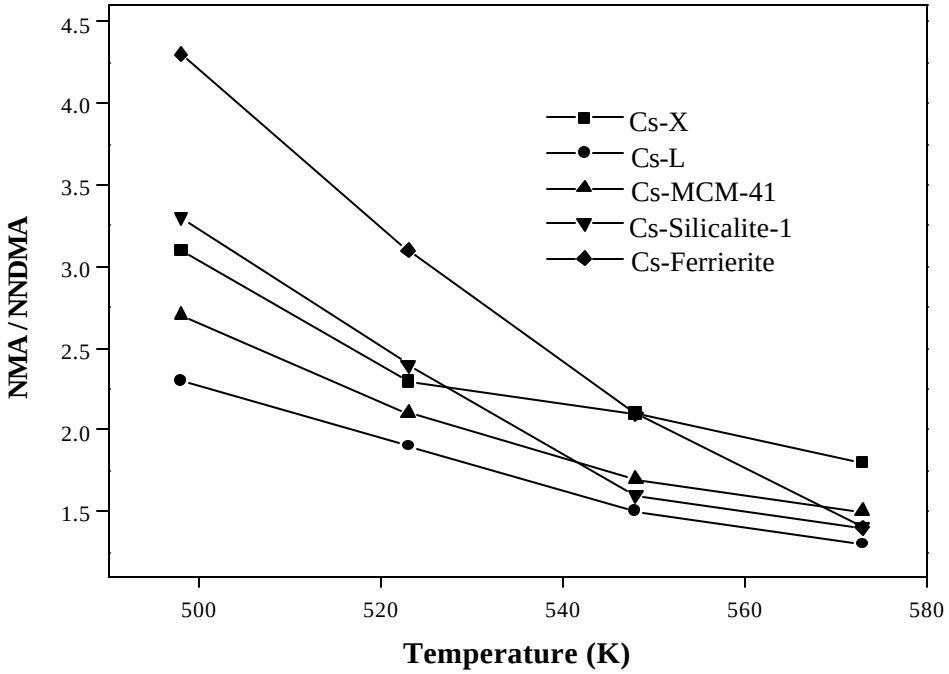

Fig. 5.15 Influence of temperature on NMA / NNDMA product ratios (Conditions: Time on stream = 1h, contact time (h) = 0.58, DMC / aniline = 2.5, N_2 = 18 ml/min).

5.3.2.6 Reaction pathway

From the data on feed rate, temperature and feed composition it can be concluded that aniline methylation with DMC on various Cs-loaded zeolites also follows a sequential reaction pathway as already pointed out in the case of MeOH. NMA is formed first, which is further converted to NNDMA, which then, undergoes C-methylation to give toluidines.

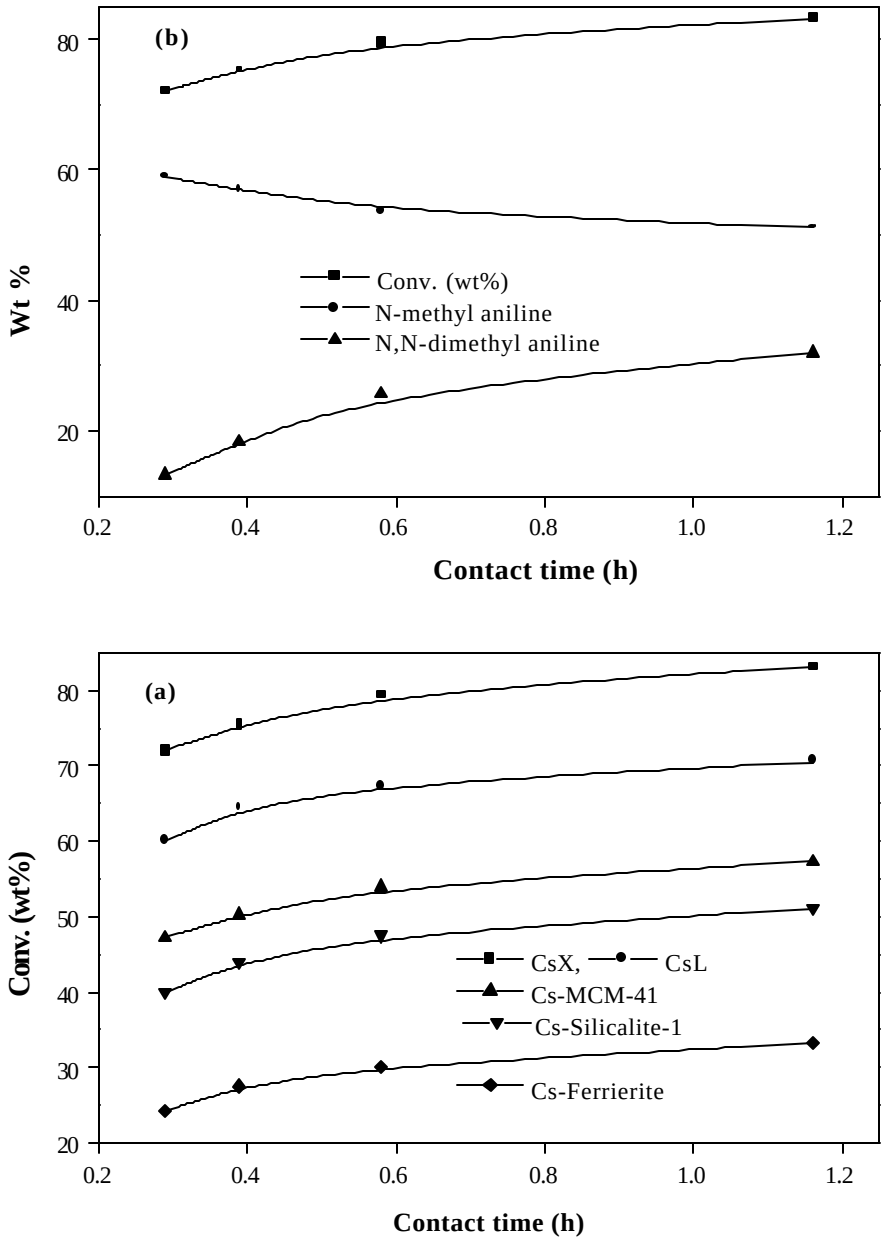

Fig. 5.16 Influence of contact time: (a) aniline conversion over different catalysts; (b) product yields over CsX(OH) (Conditions: Time on stream = 1h, temperature = 548K, DMC / aniline (mole) = 2.5, N_2 = 18 ml/min).

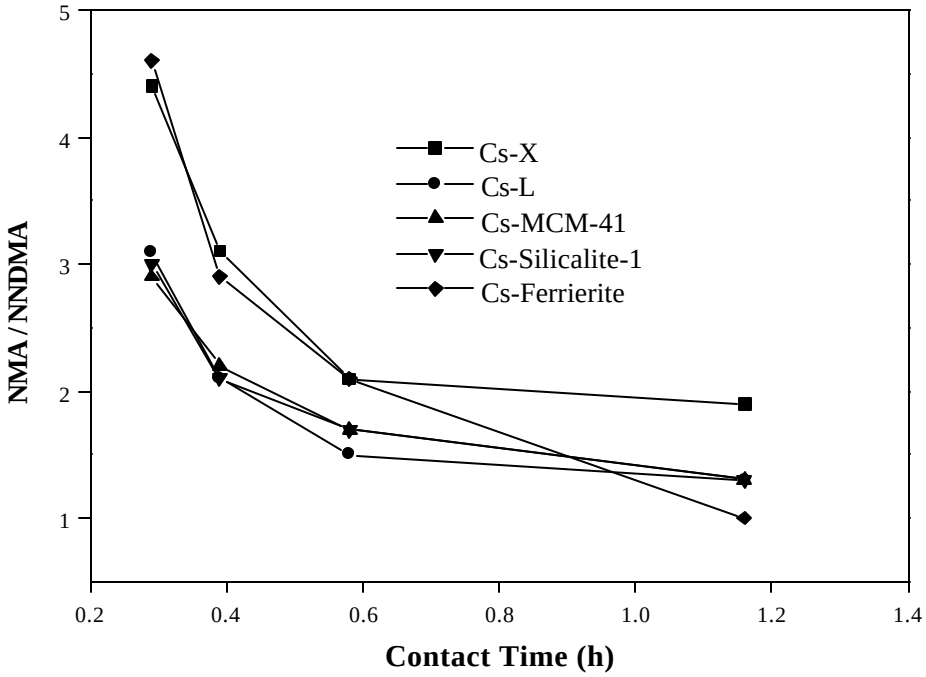

Fig. 5.17 Influence of contact time on NMA / NNDMA product ratios (Conditions: Temperature = 548K, time on stream = 1h, DMC / aniline (mole) = 2.5, N_2 = 18 ml/min).

5.4 CONCLUSIONS

CsX, CsL and Cs-MCM-41, Cs-silicalite, Cs-ferrierite are good catalysts for N-methylation of aniline with methanol and dimethyl carbonate as the methylating agents. Over CsX and CsL, only N-alkylation takes place producing N-methyl aniline and N,N-dimethyl aniline. Over Cs-MCM-41, Cs-silicalite and Cs-ferrierite small amounts of C-alkylated products are also formed. Dimethyl carbonate is a better methylating agent compared to methanol. Conversions are higher and NMA / NNDMA ratios are lower when DMC is used as the alkylating agent instead of MeOH.

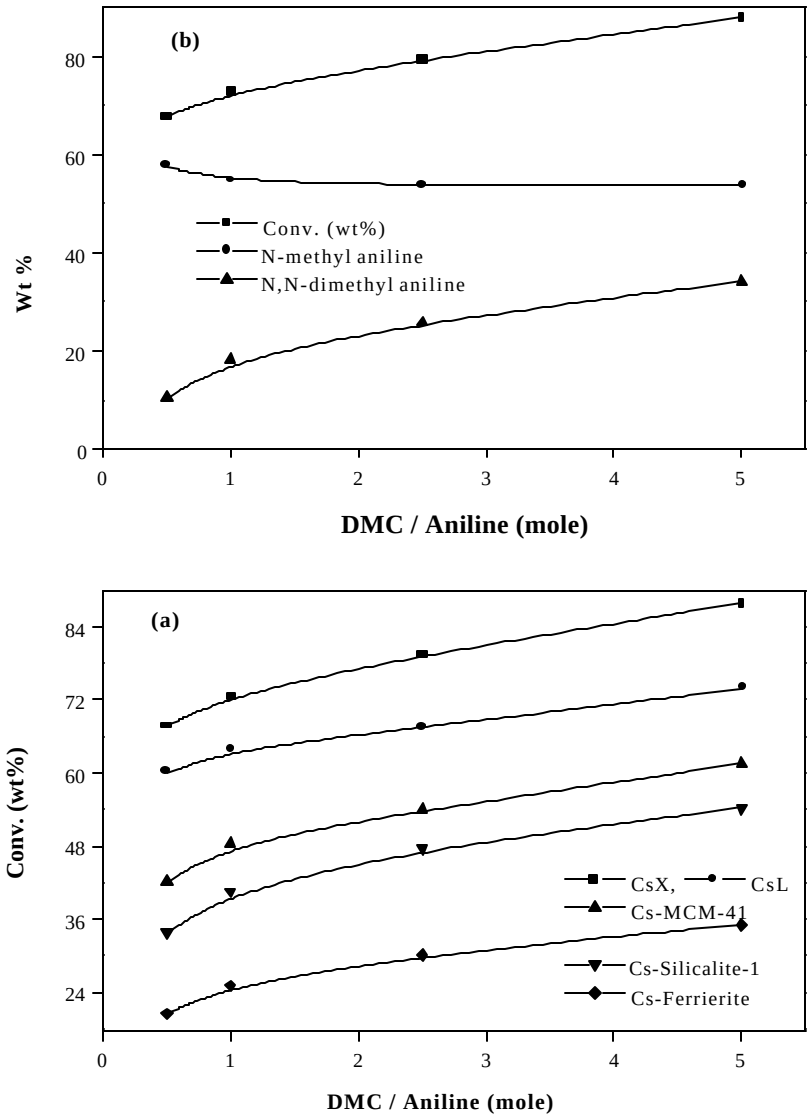

Fig. 5.18 Influence of DMC / aniline molar ratios of feed: (a) = aniline conversions over different catalysts; (b) product yields over CsX (Conditions: Time on stream = 1h, temperature = 548K, contact time = 0.58, N_2 = 18 ml/min).

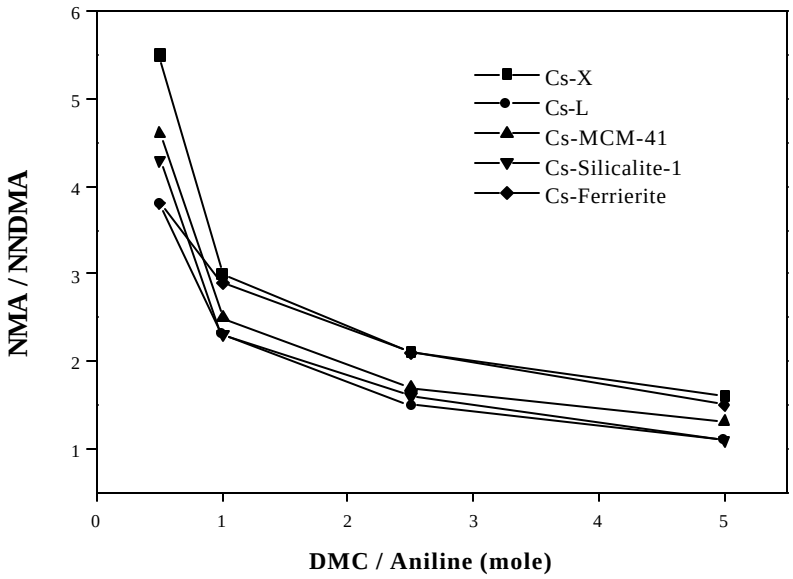

Fig. 5.19 Influence of DMC / aniline mole ratios on the NMA / NNDMA product ratios (Conditions: Temperature = 548K, contact time (h) = 0.58, time on stream = 1h, N_2 18 ml/min).

5.5 REFERENCES

1. Kirk-Othmer, in "*Encyclopodia of Chemical Technology", Wiley, New York, 3rd edn.* **2,** 309 (1978).
2. A. K. Bhattacharya and D.K. Nandi, *Ind. Eng. Chem. Prod. Res. Dev.* **14**, 162 (1975).
3. A.G. Hill, J.H. Shipp and A.J. Hill, *Ind. Eng. Chem.* **43**, 1579 (1951).
4. T. H. Evans and A.N.Bourns, *Can. J. Tech*. **29**, 1 (1951).
5. J.M. Parera, A. Gonzalez and A. Barral, *Ind. Eng. Chem. Prod. Res.* Dev. **7**, 259 (1968).
6. C. M. Naccache and Y.B. Taarit, *J. Catal.* **22**, 171 (1971).

7. N. Takamiya, Y. Koinuma, K. Ando and S. Murai, *Nippon Kagaku Kaishi*, 1452 (1979).

8. N. Kakamiya, H. Yamabe, K. Ando and S. Murai, *Nippon Kagaku Kaishi*, 1316 (1980).

9. L.K. Doraiswamy, G.R.V. Krishnan and S.P. Mukherjee, *Chem. Eng.* **88**, 78 (1981).

10. H. Matsuhashi and K. Arata, *Bull. Chem. Soc. Jp*. **64**, 2605 (1991).

11. A. N. Ko, C. L. Yang, W. Zhu and H. Lin, *Appl. Catal. A: Gen.* **134**, 53 (1996).

12. M. Onaka, K. Ishikawa and Y. Izumi, *Chem. Lett*. 1783 (1982).

13. O. Mokoto, I. Koji and I. Yusuke, *J. Inclusion Phenom.* **2**, 359 (1984).

14. G.O. Chivadze and L.Z. Chkheidze, *Iz. Akad. Nauk. Gruz. SSR, Ser. Khim.* **10,** 232 (1984).

15. P.Y. Chen, M.C. Chen, H.Y. Chu, N.S. Chang and T.K. Chuang, in "New Developments in Zeolite Science and Technology" (Y. Murakami, A. Iijima and J.W. Ward, Eds.), p. 739, Elsevier, Amsterdam.

16. K.G. Ione and O.V. Kikhtyanin, in "Zeolites: Facts, Figure, Fiture" (P.A. Jacobs and R.A. van Santen, Eds.), p. 1073, Elsevier, Amsterdam, 1989.

17. S.I. Woo, J.K. Lee, S.B. Hong, Y.K. Park and Y.S. Hu, in "Zeolites: Facts, Figure, Fiture" (P.A. Jacobs and R.A. van Santen, Eds.), p. 1095, Elsevier, Amsterdam, 1989.

18. P.Y. Chem, S.J. Chu, N.S. Chuang and T.K. Chuang, in "Zeolites: Facts, Figure, Fiture" (P.A. Jacobs and R.A. van Santen, Eds.), p. 1105, Elsevier,

Amsterdam, 1989.

19. O.V. Kikhtyanin, K.G. Ione, L.V. Malysheva and A.V. Toktarev, in " Chemistry of Microcrystals" (T. Inui, S. Namba and T. Tatsumi, Eds.), p. 319, Elsvier, Amsterdam, 1991.

20. Y.K. Park, K.Y. Park and S. I. Woo. *Catal. Lett*. **26**, 169 (1994).

21. B.L.Su and D. Barthomeuf, *Appl. Catal. A: Gen.* **124**, 73 (1995).

22. B.L.Su and D. Barthomeuf, *Appl. Catal. A: Gen*. **124**, 81 (1995).

23. P.R.H.P. Rao, P. Massiani and D. Barthomeuf, in "Zeolite Science 1994: Recent Progress and Discussions (H.G. Karge and J. Weitkamp, Eds.), p. 287, Elsvier, Amsterdam, 1985.

24. P.S. Sing, R. Bandyopadhyay and B.S. Rao, *Appl. Catal. A* **136,** 177(1996).

25. S. Prasad and B.S. Rao, *J. Mol. Catal.* **62**, L17 (1990).

26. S.M. Yang and T.W. Pan, *J. Chin. Chem. Soc.* **42,** 935 (1995).

27. F. M. Bautista, J. M. Campelo, A. Garcia, D. Luna, J. M. Marina, A.A. Romero and M.R. Urbano, *J. Catal.* **172**, 103 (1997).

28. F. M. Bautista, J. M. Campelo, A. Garcia, D. Luna, J. M. Marina and A.A. Romero, *Appl. Catal. A: Gen.* **166**, 39 (1998).

29. F. M. Bautista, J. M. Campelo, A. Garcia, D. Luna, J.M. Marinas and A.A. Romero, *Stud. Surf. Sci. Catal*. **108**,123 (1997).

30. Z.H. Fu and Y. Ono, C*atal. Lett*. **18**, 59 (1993).

31. Z.H. Fu and Y. Ono, *Catal. Lett*. **22**, 277 (1993).

32. M. Selva, A. Bomben and P. Tuldo, *J. Chem. Soc., Perkin. Trans*. **1**, 1041 (1999).

CHAPTER - VI

SUMMARY AND CONCLUSIONS

The thesis is a study of C-, O- and N- alkylation reactions over a number of solid basic catalysts. The basic catalysts investigated are various alkali metal (Li, Na, K and Cs) exchanged X and L zeolites, Cs_2O impregnated MCM-41, silicalite-1 and ferrierite and various alkali metal (Li, Na, K and Cs) oxides deposited on fumed SiO_2. The reactions investigated are the side chain (C-) alkylation of toluene and ethylbenzene (over alkali exchanged X), O-alkylation of phenol, cresols, dihydroxy benzenes, p-methoxy phenol and 2-naphthol (over alkali loaded SiO_2 and Cs loaded MCM-41) and the N-alkylation of aniline (over Cs exchanged X and L, and Cs_2O deposited MCM-41, silicalite-1 and ferrierite).

The various zeolites have been prepared by hydrothermal methods, calcined and ion-exchanged with the desired metal ions using chlorides, acetates and hydroxides. The loading of Cs_2O on SiO_2, MCM-41 and the medium pore silicalites was carried out by simple impregnation methods using salt solutions. The zeolites and molecular sieves were characterized by XRD for structural purity and intergrity. All the catalysts have been characterized by surface area and pore volume measurements. Surface area loss is noticed in the case of all the catalysts when alkali metal ions are loaded either by ion exchange or impregnation methods. The surface area loss (especially in alkali loaded SiO_2) increases with metal loading and basicity of the alkali metal. When the areas are calculated on pure SiO_2 basis (excluding the deposited oxides), they are reasonably similar (155 ± 10 m^2 / g) to that of the parent SiO_2 (166 m^2 / g) for most of the samples suggesting a reasonably good dispersion of the supported alkali metal oxides on the SiO_2 surface and absence of significant pore blockage.

^{29}Si-NMR of Cs-MCM-41 reveales that the surface silanol groups (Si-OH) are progressively replaced by Si-O-Cs groups. Progressive changes in ^{133}Cs NMR spectra of Cs-SiO_2 and Cs-MCM-41 samples on Cs loading suggest that Cs ions are more mobile at higher loadings and agglomeration of Cs_2O species could occur at higher metal loading. ESCA measurements also suggest saturation of the surface by Cs ions at high loading.

The basicity of all the catalysts have been characterized by temperature programmed desorption and FTIR spectra of adsorbed CO_2. In the case of the TPD experiments, it is found that most of the adsorbed CO_2 desorbs below 623K. The amount of desorbed CO_2 increases with increasing basicity of the alkali ions (Cs > K > Na > Li) and with increasing metal loading. The intensity of the absorption bands of adsorbed CO_2 in the region 1200 cm^{-1} to 1750 cm^{-1} has been used to estimate the relative basicities of the various catalysts. The spectra of CO_2 adsorbed at two different equilibrium pressures (0.4 mm and 5 mm) are used for the analysis of the data. The FTIR spectra reveal that on alkali oxide loaded SiO_2, $CO_2^{\delta-}$ species are formed giving rise to characteristic pairs of adsorption bands. At ambient temperature, the surface complex transforms into more stable bidentate carbonate species with increasing basicity of the alkali oxides.

Adsorption of CO_2 on alkali metal incorporated zeolites reveals that the energetics of adsorption depends on the basicity of cation, anionic charge on the zeolite framework and pore size of the zeolite. It also shows that CO_2 adsorbs on all the zeolites except NaX as bidentate species. In the case of NaX, symmetrical

carbonate species are also identified. Overall, two types of adsorption sites can be identified, one near the wall of the pore and another in the bulk of the pore (cage).

The summary and conclusions of the studies of different alkylation reactions are given below.

1) C-alkylation

a) Side chain alkylation of ethylbenzene

Side chain C-alkylation of ethylbenzene (EB) with dimethylcarbonate (DMC) is promoted by alkali exchanged zeolite-X. Propylbenzenes (n- and i-) are the major products besides styrene and o-xylene. Side chain alkylation activity increases with increasing basicity of the exchanging cation. The catalysts prepared by exchanging with alkali hydroxides are more active than those prepared from chlorides. Conversion of EB and the yield of the products are maximum at a process time of 2 h. Maximum EB conversion and side chain alkylation product formation are observed at ~733K at an EB/DMC mole ratio of 5 and a W/F ($g.h.mole^{-1}$) of 60.

b) Side chain alkylation of toluene

Side chain C-alkylation of toluene with dimethylcarbonate (DMC) over alkali exchanged zeolite-X produces ethylbenzene as the major product besides i-propylbenzene as the doubly methylated product. Maximum toluene conversion and side chain alkylation product formation are observed at ~698K at toluene/DMC mole ratio of 5 and a W/F ($g.h.mole^{-1}$) of 30 at a process time of 2 h.

2) O-alkylation

a) O-alkylation of phenol

O-alkylation was carried out using methanol, ethanol, n-propanol and n-butanol as the alkylating agents to get aryl alkyl ethers. The study reveals that alkali supported SiO_2 samples are good catalysts for this O-alkylation reaction in the vapour phase. The most active catalyst is Cs-SiO_2. Methanol is more active compare to other three alcohols in the O-alkylation of phenol. At lower temperatures deactivation is less and decreases with increasing basicity of the catalyst. Deactivation decreases with decrease in methanol to phenol mole ratio and increase in carbon number of the alcohols. Deactivation rate (calculated on the basis of unit conversion) decreases with the increase in basicity of the catalyst.

b) O-methylation of cresols

O-methylation of cresols (o-cresol, m-cresol and p-cresol) was carried out with methanol in the vapour phase over alkali loaded SiO_2 catalysts to get methyl anisoles. High conversions and high O-alkylation selectivities are obtained over these catalysts. The reactivity of the cresols is in the order: o-cresol < p-cresol ~ m-cresol. Here the deactivation rate (calculated on the basis of unit conversion) decreases with the increase in basicity of the catalyst. Activity and selectivity increase with basicity of the catalyst, Cs-SiO_2 being the most active and selective catalyst.

c) O-methylation of dihydroxy benzenes

The study also reveals that alkali supported SiO_2 samples are good catalysts for the O-methylation of catechol, resorcinol and hydroquinone in the vapour phase. The most active and selective catalyst is Cs-SiO_2 with about 1.5 mmole of Cs / g of catalyst. Resorcinol is more reactive than the other two dihydroxy benzenes. The

trend in reactivities of the dihydroxy benzenes can be explained if a [HO-C_6H_4-$O^{\delta-}$] adsorbed intermediate is postulated to be formed on the catalyst surface. Catalyst deactivation is more for catechol than for resorcinol and hydroquinone and decreases with increasing basicity of the catalyst.

d) O-methylation of p-methoxy phenol

Studies on the methylation of p-methoxy phenol with methanol over different alkali loaded SiO_2 catalysts reveal that p-methoxy phenol is more reactive than hydroquinone. Besides it also causes less catalyst deactivation than hydroquinone.

e) O-methylation of 2-naphthol

Cs supported SiO_2 and MCM-41 are good catalysts for the O-alkylation of 2-naphthol with methanol in the vapour phase. Increase in conversion with Cs-loading is not as pronounced as for the other substrates. Nearly 95% yield of 2-methoxynaphthalene is obtained over Cs-SiO_2 at 673K, contact time (h) = 0.58 and a methanol / 2-naphthol (mole) = 10. The small amount of 1-methyl-2-methoxy naphthalene formed over Cs-catalysts is a result of the further alkylation of 2-methoxynaphthalene.

3) N-alkylation

a) N-methylation of aniline with methanol

Vapour phase N-methylation of aniline with methanol over Cs exchanged X and L and Cs loaded MCM-41, silicalite-1 and ferrierite reveals that they are good catalysts for N-methylation. Over CsX and CsL, only N-alkylation takes place producing N-methyl aniline (NMA) and N,N-dimethyl aniline (NNDMA). Over Cs-

MCM-41, Cs-silicalite and Cs-ferrierite small amounts of C-alkylated products are also formed along with NMA and NNDMA. This may be mainly due to the lower Cs content (~ 3wt%) in the catalysts compared to CsX (~30%) and CsL (~20%). NMA is the primary product and NNDMA is the secondary product. Due to the different pore size and structure, the activities of the three catalysts Cs-MCM-41, Cs-silicalite-1 and Cs-ferrierite are different eventhough their Cs content is the same (~ 3%). Conversion increases with increase in methanol / aniline mole ratio for all the catalysts.

b) N-methylation of aniline with dimethyl carbonate

N-methylation of aniline with dimethyl carbonate (DMC) reveals that DMC is a better methylating agent than methanol. DMC produces more NNDMA compare to methanol. Deactivation rate (calculated on the basis of unit conversion) is less when DMC is used instead of methanol.

The studies reveal that alkali metal (especially Cs) exchanged zeolite X can alkylate ethylbenzene and toluene with dimethyl carbonate to i- (and n-) propylbenzene and ethylbenzene, respectively. Similarly alkali metal (especially Cs) loaded SiO_2 and MCM-41 is excellent basic catalysts for the selective O-alkylation of hydroxy aromatic compounds with methanol. Similarly, CsX is a good catalyst for the N-alkylation of aniline.

List of publication

1. Side chain methylation of toluene and ethylbenzene with dimethyl carbonate over alkaline X-zeolite
   Rajaram Bal and S. Sivasanker, **Stud. Surf. Sci. Catal., 130 (2000) 2645.**

2. Selective O-alkylation of cresols with methanol: catalysis by Cs loaded silica, a solid base
   Rajaram Bal and S. Sivasanker, **Green Chemistry, 2 (2000) 106.**

3. Vapour phase O-methylation of 2-naphthol over the solid bases: alkali loaded silica and Cs-loaded MCM-41
   Rajaram Bal, K. Choudhari and S. Sivasanker, **Catalysis Letters, 70 (2000) 75.**

4. Redox and catalytic chemistry of Ti in Titanosilicate molecular sieves: an EPR investigation
   Rajaram Bal, K. Choudhari, D. Srinivas, S. Sivasanker and P. Ratnasamy, **Journal of Molecular Catalysis A: Chemical, 162 (2000) 199.**

5. Electron Spin Resonance Investigations on the location and reducibility of Zirconium in mesoporous Zr-MCM-41 molecular sieves
   K. Choudhari, **Rajaram Bal,** T. K. Das, A. Chandawadkar, D. Srinivas and S. Sivasanker, **J. Phys. Chem. B, 104 (2000) 11066.**

6. Vapour phase O-methylation of dihydroxy benzenes with methanol over cesium loaded silica, a solid base
   Rajaram Bal, B.B. Tope and S. Sivasanker, **Journal of Molecular Catalysis: A Chemical, (accepted).**

7. Vapour phase O-alkylation of phenol over alkali loaded silica
   Rajaram Bal and S. Sivasanker, **Journal of Catalysis, (Communicated).**

8. Alkali loaded silica, a solid base: Investigation by Infrared Spectroscopy and its catalytic activity
   Rajaram Bal, B.B.Tope, T.K. Das, S.G.Hegde and S. Sivasanker, **Journal of Catalysis, (Communicated).**

9. Cs-loaded on Cs-X, Cs-L, Cs-MCM-41, Cs-Silicalite, Cs-Ferrierite: Investigation by Infrared Spectroscopy and catalytic activity
   Rajaram Bal, B.B. Tope, S.G. Hegde and S. Sivasanker, **Journal of Catalysis, (Communicated)**.

10. N-alkylation of aniline with methanol and dimethyl carbonate over Cs-loaded on Cs-X, Cs-L, Cs-MCM-41, Cs-Silicalite, Cs-Ferrierite
    Rajaram Bal and S. Sivasanker, **Microporous and Mesoporous Material (To**

be communicated).

11. Gallosilicate, a Faujacite structure: Characterization and its catalytic activity
Rajaram Bal, T.H. Bennur and S. Sivasanker, **Journal of Catalysis, (To be communicated).**

12. Vopour phase Beckmann rearrangement of cyclohexanone oxime over mesoporous
MCM-41 and Al-MCM-41 molecular sieves
K. Chaudhari, **Rajaram Bal,** A.J. Chandwadkar and S. Sivasanker, **Journal of Molecular Catalysis A: Chemical, (accepted).**

13. Redox behaviour and selective oxidation properties of mesoporous titano- and zirconosilicate MCM-41 molecular sieves
K. Choudhari, **Rajaram Bal,** A. Chandawadkar, D. Srinivas and S. Sivasanker, **Microporous and Mesoporous Material, (Communicated)**.

14. Palladium Containing Hydrotalcite: A New Heterogeneous Catalyst for Heck Reaction
T. H. Bennur, A. Ramani, **Rajaram Bal**, B. M. Chanda and S. Sivasanker, **Chemical Communication, (Communicated).**

15. Investigation of the coke formation by ESR spectroscopy.
Rajaram Bal, D. Srinivas and S. Sivasanker (**To be communicated**).

Symposia/Workshop participated and papers presented

1. Side chain methylation of toluene and ethylbenzene with dimethyl carbonate over alkaline X-zeolite
Rajaram Bal and S. Sivasanker, Presented in the 12th International Congress on Catalysis at Granada, Spain (July, 2000).

2. Selective O-methylation of hydroxy aromatic compound with methanol over Alkali loaded silica
Rajaram Bal and S. Sivasanker, Presented in the **ZMPC symposium**, Sendai, Japan (August, 2000).

3. Location, redox behaviour and catalytic activity of zirconium and titanium in MCM-41 molecular sieves
K. Chaudhari, **Rajaram Bal**, A.J. Chandwadkar, D. Srinivas and S. Sivasanker, Presented in the **ZMPC symposium**, Sendai, Japan (August, 2000).

4. Side chain alkylation of ethylbenzene with dimethyl carbonate over alkaline X-zeolite
Rajaram Bal and S. sivasanker, Presented in the **Golden Gubilee Symposiun on Catalysis**, National Chemical Laboratory, Pune, India (January, 1999).

5. Vapour phase O-methylation of dihydroxy benzenes with methanol over cesium loaded silica, a solid base
   Rajaram Bal, B.B. Tope and S. Sivasanker, Presented in Indo-Pacific Catalysis Symposium and **National Catalysis Symposium (IPCAT-2 & CATSYMP-15**) at National Chemical Laboratory,Pune (January, 2001).
6. Location, redox behaviour and catalytic activity of zirconium and titanium in MCM-41 molecular sieves
   K. Chaudhari, **Rajaram Bal**, A.J. Chandwadkar, D. Srinivas and S. Sivasanker
   Presented in **Indo-Pacific Catalysis Symposium and National Catalysis Symposium (IPCAT-2 & CATSYMP-15**) at National Chemical Laboratory,Pune (January, 2001).